Application of the Stereodivergent Oxy-Michael Cyclisation to the Synthesis of Natural Products

and

Organocatalytic Asymmetric Aldol Reactions in Water

Yin-Ting Hsiao

PhD

University of York

Chemistry

September 2017

Abstract

This work outlines two different projects. The first project was the study of a stereodivergent oxy-Michael cyclisation and its application towards the synthesis of natural products, diospongin A, diospongin B and psymberin/ircinistatin A.

The *α*,*β*-unsaturated thioesters under TBAF-mediated conditions gave the 2,6-*trans*-tetrahydropyran; under acid-mediated conditions gave the 2,6-*cis*-tetrahydropyran. The 4-hydroxyl group is crucial for the stereodivergence; when the hydroxyl group was removed or protected the stereodivergence vanished.

The second project was the study of (*L)*-proline benzyl ester-catalysed asymmetric aldol reactions in water. The reaction was carried out in a pH 7 buffered aqueous solution of cyclohexanone and a series of aryl aldehydes to provide *anti* aldol products in 7-89% *ee*.

The aldol reaction between various ketone donors with 4-nitrobenzaldehyde under the same conditions were also developed to provide products in 13-61% *ee*.

List of Contents

List of Figures

List of Schemes

Lists of Tables

Acknowledgements

I would like to thank my supervisoir, Dr. Paul Clarke for providing me with the opportunity to work as part of his research group, as well as his support and advice during my PhD.

I would also like to thank the analytical services at the University of York, in particular Heather Fish for her assistance in NMR data and the MS service run by Karl Hale.

I would also like to acknowledge all members of the PAC group expecially Ian and Chris for proof reading my thesis.

I am grateful to the Department of Chemistry, University of York Wild Fund for financial support.

Finally, I would like to especially thank my family for providing endless support and encouragement throughout my studies, for which I am extremely grateful.

Author's Declaration

I declare that this thesis is a presentation of original work and I am the sole author. This work has not previously been presented for an award at this, or any other, University. All sources are acknowledged as references.

Part of this work has been reproduced in a published paper, a copy of which can be found in Appendices: Kristaps Ermanis, Yin-Ting Hsiao, Ugur Kaya, Alan Jeuken and Paul A. Clarke*; The stereodivergent formation of 2,6-*cis* and 2,6-*trans*-tetrahydropyrans: experimental and computational investigation of the mechanism of a thioester oxy-Michael cyclization; *Chem. Sci*., 2017, **8**, 482.

1. Studies Towards the Total Synthesis of (±)-Diospongin A and B *via* a Stereodivergent Oxy-Michael Cyclisation

1.1. Introduction

1.1.1. General approaches towards the synthesis of tetrahydropyrans

Tetrahydropyrans are important structural motifs that are found in many natural products, including diospongin A **1** and B **2**, psymberin/ircinistatin A **3**, phorboxazole A **4** and phorboxazole B **5** (**Figure 1**).

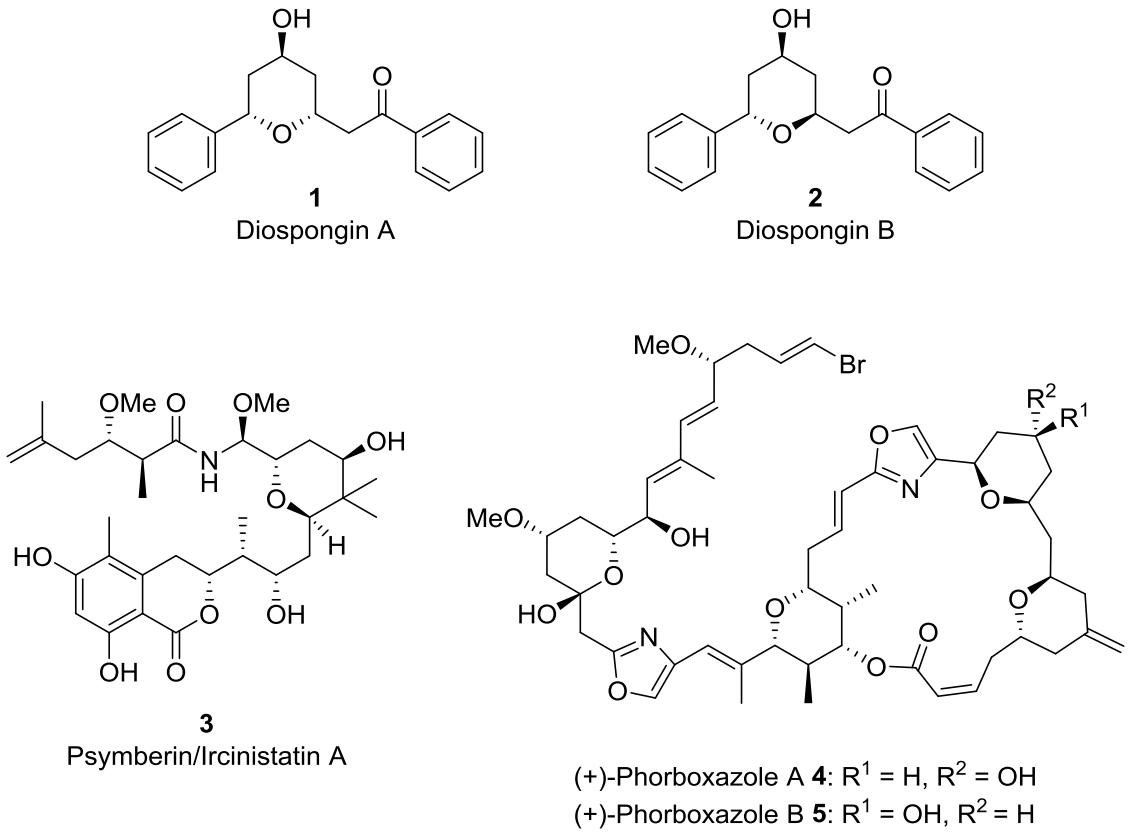

Figure 1 Tetrahydropyran-containing natural products.

In recent years, interest in the development of robust strategies for synthesising tetrahydropyrans has significantly increased due to the intriguing biological

properties that many tetrahydropyran-containing natural products possess.[1, 2] Phorboxazoles A **4** and B **5** have been reported to have anticancer properties,[1, 3] whereas diospongin B **2** has been reported to have anti-osteoporotic activities.[2]

For the synthesis of tetrahydropyran derivatives, several approaches have been established, including Prins cyclisation,[4] oxy-Michael reactions,[5] transition metal catalysed cyclisations,[6] nucleophilic addition to cyclic oxocarbenium ions[7] and hetero-Diels–Alder cycloadditions.[8] In a recent study, the Clarke group developed a novel and efficient synthetic route to construct tetrahydropyrans *via* a stereodivergent oxy-Michael cyclisation, which was then applied to synthesise the C-20–C-32 core of phorboxazole B **7** (**Scheme 1**).[9]

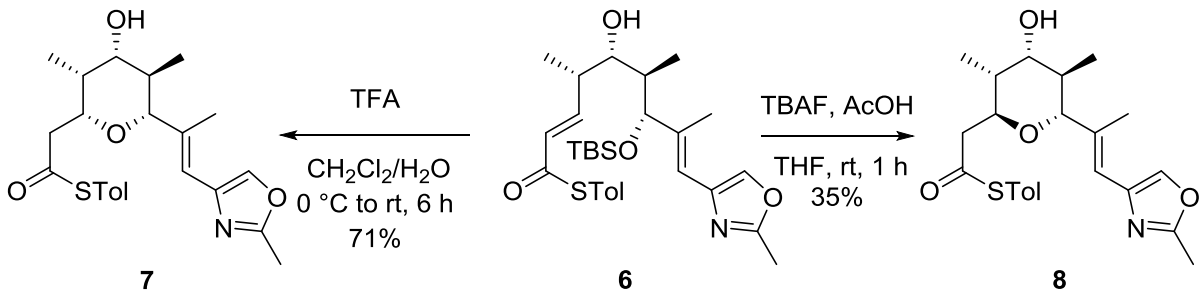

Scheme 1 Synthesis of C-20–C-32 core of phorboxazole B **7**.[9]

1.1.2. Isolation and structure elucidation of diospongin A and B

In 2003, diospongin A **1** along with its diastereomer diospongin B **2** were initially isolated from the rhizomes of *Dioscorea spongiosa via* bioassay-guided fractionation by Kadota and co-workers.[2] As shown in **Figure 2**, both diospongin A **1** and B **2** have a

six-membered tetrahydropyran core with two aromatic side chains, and only differ in their 3,7 stereochemical configuration.

Figure 2 Structure of diospongin A **1** and B **2**.

In diospongin A **1** C-3 has an *R* configuration whereas in diospongin B **2** it has an *S* configuration. Kadota and co-workers were the first to elucidate the absolute configuration of diospongin A **1** and B **2**.[2]

As shown in **Figure 3**, diospongin A **1** is presented as (3*R**,5*S**,7*S**)-1,7-diphenyl-3,7-epoxy-5-hydroxy-1-heptanone and diospongin B **2** is presented as (3*S**,5*S**,7*S**)-1,7-diphenyl-3,7-epoxy-5-hydroxy-1-heptanone.

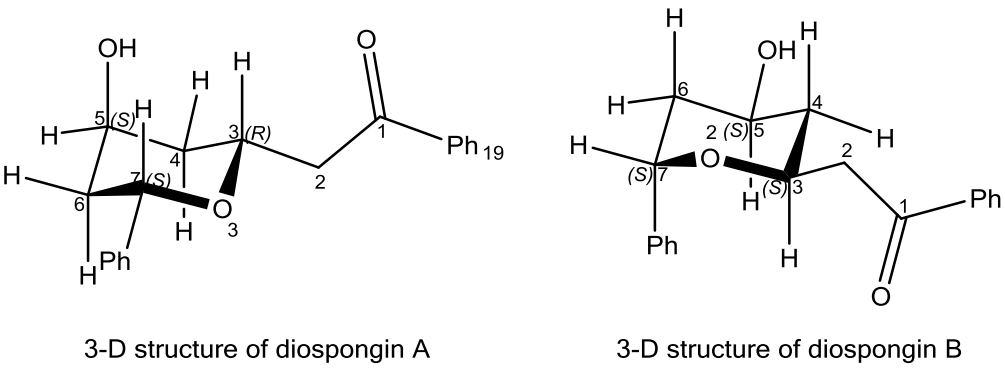

Figure 3 3-D structure of diospongin A **1** and B **2**.

Despite the structural similarities between diospongin A **1** and B **2**, their biological activities are remarkably different. Diospongin B **2** has anti-osteoporotic activity whereas diospongin A **1** does not.[2]

Osteoporosis is a skeletal disease which is often called a silent disease. This is due to the challenges of diagnosing bone loss in the early stages. Diospongin B **2** has shown to have effective inhibitory activities of ^{45}Ca release at 200 μM (30.5%) and 20 μM (18.2%).[2] Due to their promising activities in the treatment of osteoporosis, the diospongins have proven to be popular synthetic targets and have therefore been widely reported.

1.1.3. Previous synthesis of diospongin A and B

Various approaches to synthesise diospongin A **1** and B **2** have been published. To date, the total synthesis of diospongin A **1** has been reported by 21 groups,[10-30] whereas diospongin B **2** synthesis has been reported by 12 groups.[12, 16-19, 22, 28, 30-34] The most important step in the synthesis of diospongin A **1** and B **2** is the construction of the tetrahydropyran core. The strategies used include intramolecular oxy-Michael reaction,[10, 11, 13, 26] Prins cyclisation,[14, 15] intramolecular Pd(II)-catalysed cyclisations,[16] hetero-Diels–Alder (HDA) reactions,[19, 21, 22] nucleophilic addition to a cyclic oxocarbenium ion[12] and palladium(II)-catalysed hydroxycarbonylation of hexenols.[23]

In 2006, the first synthesis of diospongin A **1** was reported by Chandrasekhar and co-workers. The tetrahydropyran formation step, which is key in this process, is shown in **Scheme 2**.[10]

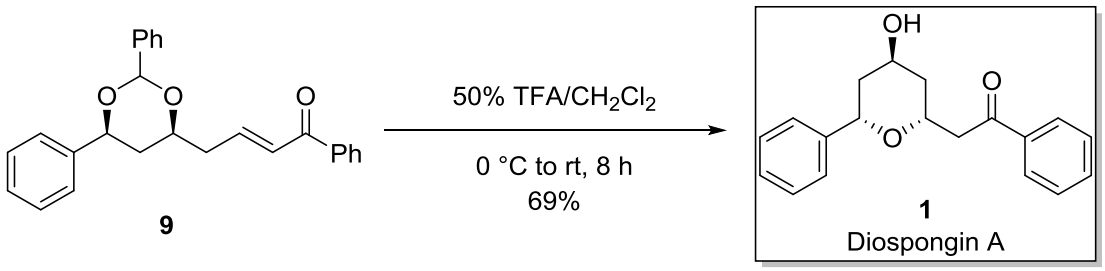

Scheme 2 Synthesis of diospongin A **1** as reported by Chandrasekhar and co-workers.[10]

Diospongin A **1** was obtained by hydrolysis of the benzylidene acetal group and subsequent intramolecular oxy-Michael addition of **9** in the presence of TFA in a one-pot process.

Surprisingly, Chandrasekhar claimed that the compound that was generated was diospongin B. However, the NMR spectroscopic data of their diospongin "B" did not correspond to the findings reported by Kadota (**Table 1**).[2] In a subsequent study, Jennings and co-workers, confirmed that this compound was in fact diospongin A **1**.[12]

Table 1 Comparison of ^{1}H NMR spectroscopic data of diospongin A **1** and B **2** as reported by the Kadota and Chandrasekhar groups.[2, 10]

Diospongin A (Kadota)[2]	**Dioaspongin B (Kadota)[2]**	**Chandrasekhar[10]**
δH ($CDCl_3$)	**δH ($CDCl_3$)**	**δH ($CDCl_3$)**
3.41 dd (16.0, 6.0 Hz)		
3.07 dd (16.0, 6.8 Hz)	3.45 dd (15.8, 6.8 Hz)	3.38 dd (16.2, 6.03 Hz)
4.65 dddd (11.2, 6.8, 6.0, 1.7 Hz)	3.17 dd (15.8, 6.8 Hz)	3.38 dd (16.2, 6.4 Hz)
1.97 ddd (14.0, 3.0, 1.7 Hz)	4.23 dddd (9.5, 6.8, 5.8, 3.0 Hz)	4.50 dddd (11.8, 6.4, 6.0, 2.8 Hz)
1.67 ddd (14.0, 11.2, 3.0 Hz)	2.05 ddd (12.4, 5.2, 3.0 Hz)	2.12 ddd (14.5, 2.8, 1.8 Hz)
4.35 quint (3.0 Hz)	1.50 dt (12.4, 9.5 Hz)	1.74 ddd (14.5, 11.8, 1.0 Hz)
	4.02 dddd (9.8, 9.5, 5.2, 3.9 Hz)	4.75 ddd (11.7, 2.5, 1.0 Hz)
1.94 ddd (14.0, 3.0, 1.7 Hz)	2.51 ddd (13.3, 4.1, 3.9 Hz)	2.08 ddd (14.5, 2.8, 2.5 Hz)
1.75 ddd (14.0, 12.0, 3.0 Hz)	1.92 ddd (13.3, 9.8, 4.1 Hz)	1.84 ddd (14.5, 11.8, 2.8 Hz)
4.95 dd (12.0, 1.7 Hz)	5.19 t (4.1 Hz)	5.46 t (2.8 Hz)
7.97 dd (7.8, 1.0 Hz)	7.98 dd (7.8, 1.0 Hz)	7.90 m
7.44 t (7.8 Hz)	7.47 t (7.8 Hz)	7.40 m
7.55 t (7.8 Hz)	7.57 t (7.8 Hz)	7.47 m
7.30 m	7.35 m	7.24 m
7.30 m	7.32 m	7.22 m
7.28 m	7.23 t (6.8 Hz)	7.20 m

Later in 2006, an alternative synthetic approach towards diospongin A **1** and B **2** was presented by Jennings and coworkers (**Scheme 3** and **Scheme 4**).[12] The key reaction involved nucleophilic addition to a cyclic oxocarbenium ion.

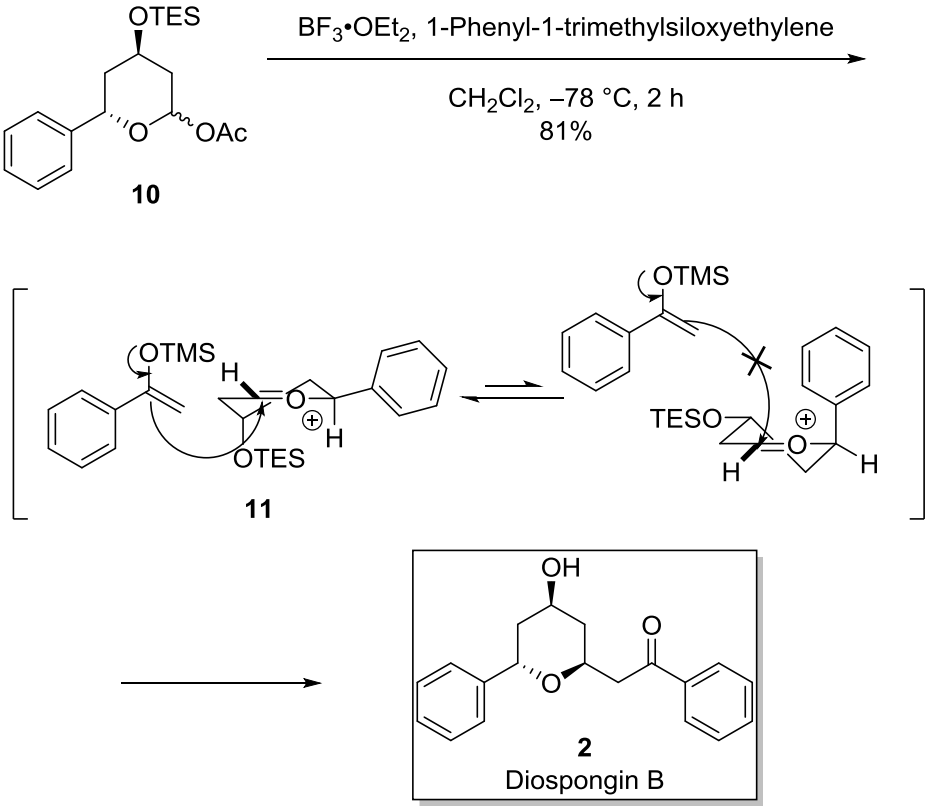

Scheme 3 Synthesis of diospongin B **2** as reported by the Jennings group.[12]

Addition of boron trifluoride diethyl etherate to lactol **10** allowed for the formation of oxocarbenium cation **11**. Synthesis was completed *via* nucleophilic attack of the trimethylsilyl enol ether, which was followed by deprotection. In the favoured conformer of **11**, the phenyl ring was placed in an equatorial position and the triethylsiloxy enol ether attacked from a *pseudo*-axial trajectory to generate diospongin B **2** (**Scheme 3**).[12]

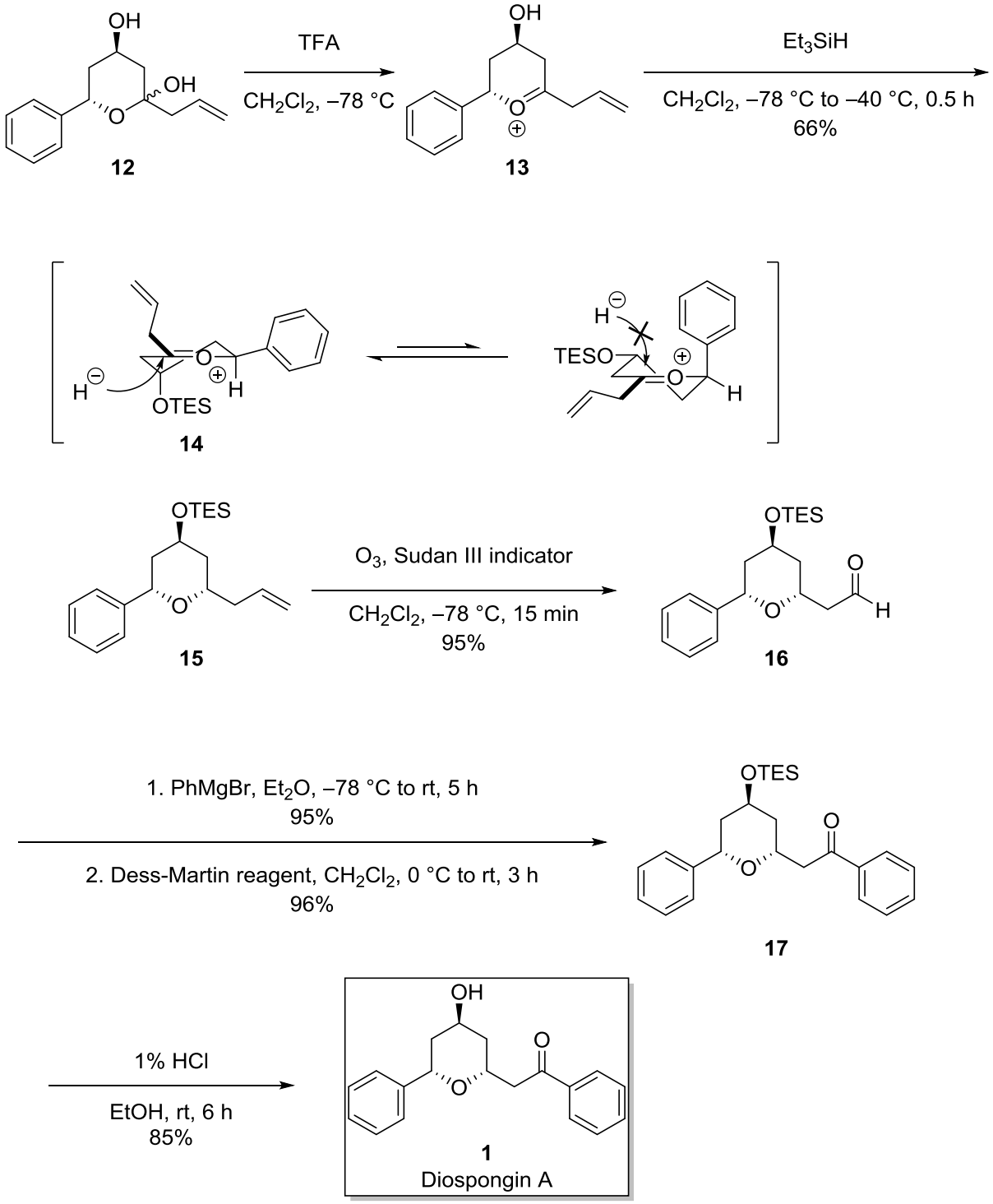

Scheme 4 Synthesis of diospongin A **1** as reported by the Jennings group.[12]

The synthesis of diospongin A **1** is presented in **Scheme 4**. The dehydration of **12** using TFA provided the key oxocarbenium cation intermediate **13** which was subsequently reduced with triethylsilane. In a similar fashion to the synthesis of diospongin B **2**, the phenyl ring was in the *pseudo*-equatorial position whereas the silyl ether group was in the axial position **14**. This chair-like transition state allowed for the stereoselective axial nucleophilic attack by hydride to generate **15** with 2,6-*cis* stereochemistry in the tetrahydropyran ring. Synthesis was completed after ozonolysis, Grignard addition, oxidation and deprotection.

Jennings and co-workers presented the synthesis of both diospongins A **1** and B **2** and verified the structures involved,[12] which were in agreement with the configuration as proposed by Kadota.[2]

1.1.3.1. Synthesis of tetrahydropyrans *via* the intramolecular oxy-Michael reaction

In 2006, Cossy and co-workers demonstrated the synthesis of diospongin A **1** *via* deprotection and an intramolecular oxy-Michael reaction of 1,7-diarylheptanoid **18** in a one-pot process to generate diospongin A **1** in a yield of 60% (**Scheme 5**).[11]

Moreover, Bates and co-workers also reported the synthesis of diospongin A **1** with a similar strategy, however resin was used to generate diospongin A **1** in a yield of 83%.[13]

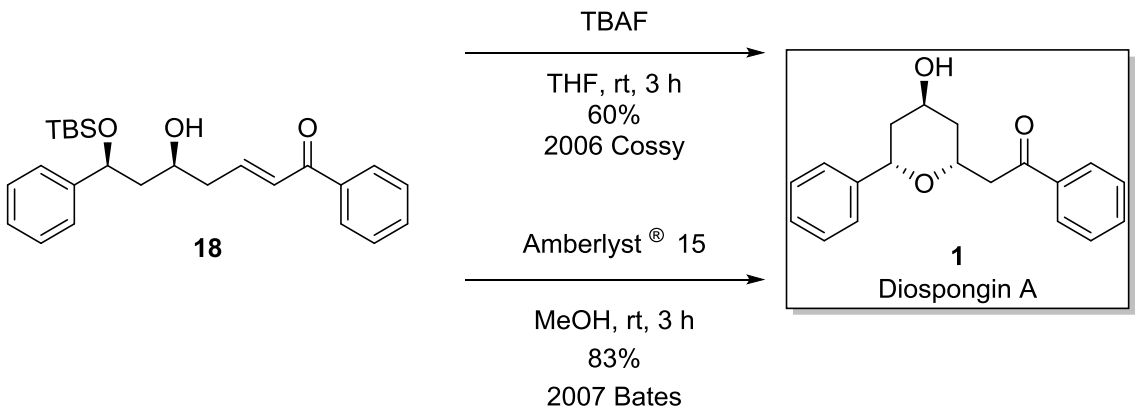

Scheme 5 Synthesis of diospongin A **1** as reported by the Cossy group[11] and the Bates group.[13]

In 2011, Meshram proposed the stereoselective synthesis of diospongin A **1** *via* intramolecular oxy-Michael addition (**Scheme 6**).[26]

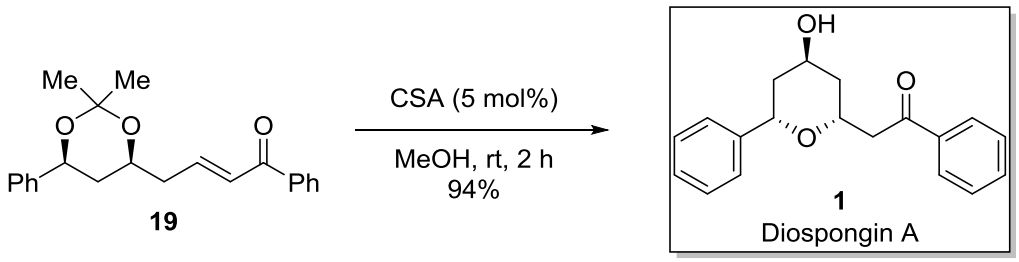

Scheme 6 Synthesis of diospongin A **1** as reported by Meshram and co-workers.[26]

Deprotection and cyclisation of **19** was successfully achieved by using a one-pot process by adding of CSA (5 mol%) in methanol to give the target molecule, diospongin A **1** in high yield (94%).[26]

1.1.3.2. Synthesis of tetrahydropyrans *via* the Prins reaction

Tetrahydropyran rings can also be formed by the Prins reaction as reported in a study by the Yadav[14] (**Scheme 7**) and Piva[15, 24] groups (**Scheme 9**).

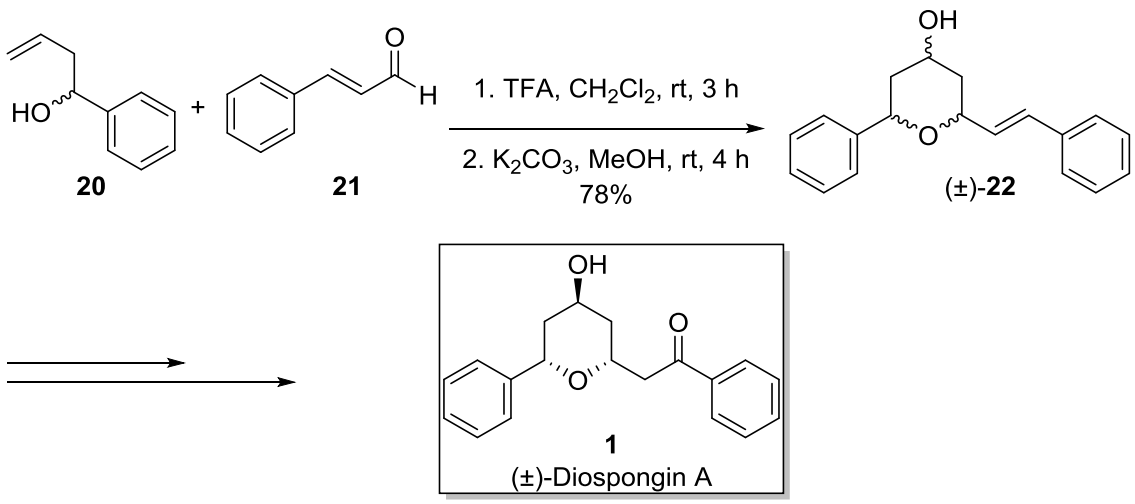

Scheme 7 Synthesis of diospongin A **1** *via* the Prins reaction as reported by Yadav and co-workers.[14]

The synthesis of diospongin A **1** as reported by Yadav and co-workers began with a Prins cyclisation reaction, which provided **22** from cinnamaldehyde **21** and 1-phenylbut-3-en-1-ol **20** in 78% yield as a single diastereomer. The mechanism involved is shown in **Scheme 8**.

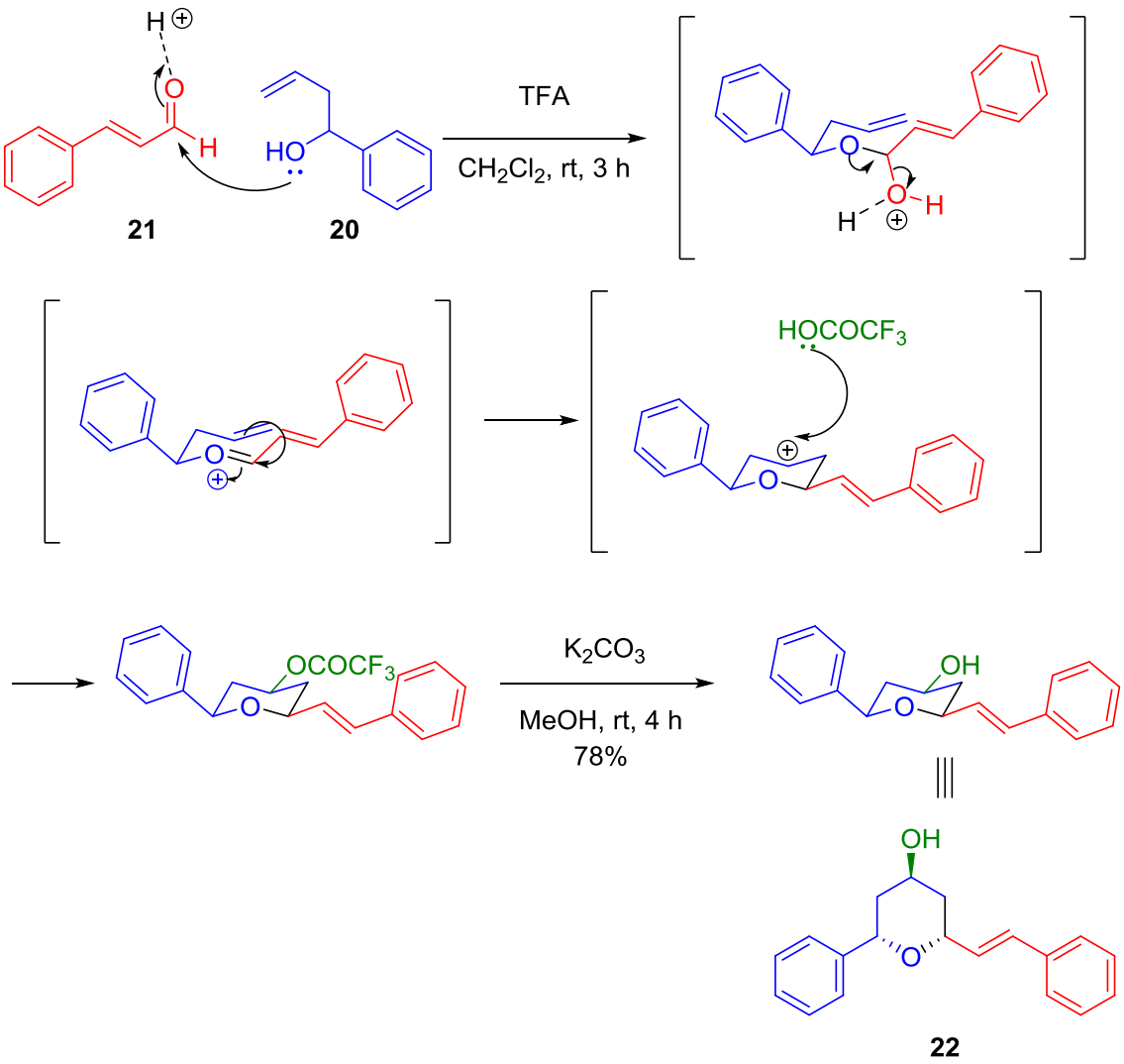

Scheme 8 Mechanism of the Prins reaction as reported by the Yadav group.[14]

In Piva's synthesis, the key step in the formation of the tetrahydropyran ring also involved a Prins reaction.[15] The homoallylic alcohol **20** with benzaldehyde **23** gave **24** in 83% yield. Inversion of the hydroxyl group at the C-4 position was carried out *via* the Mitsunobu reaction to generate diospongin A **1** (**Scheme 9**).

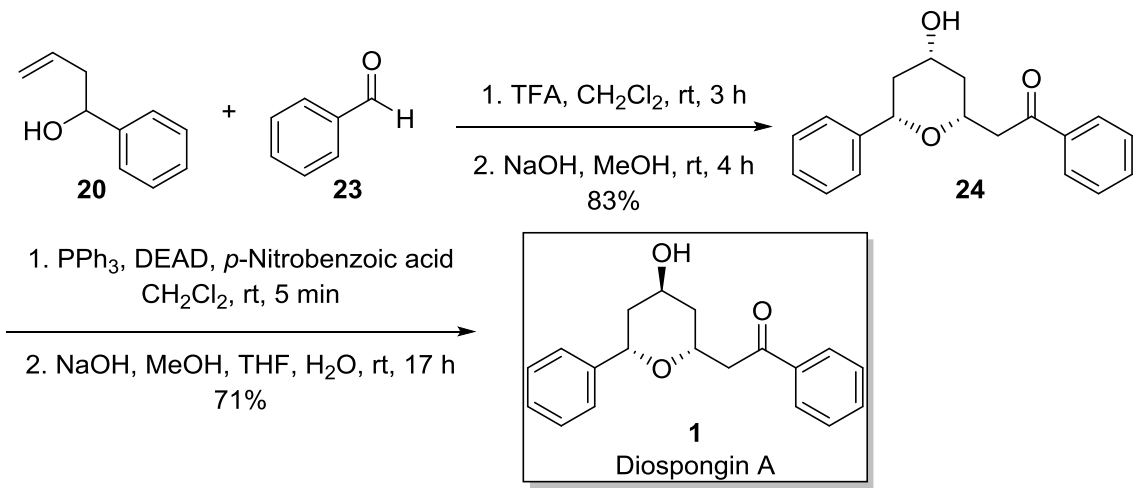

Scheme 9 Synthesis of diospongin A **1** *via* a Prins reaction as reported by the Piva group.[15, 24]

1.1.3.3. Synthesis of tetrahydropyrans *via* Pd(II)-catalysed cyclisation

In a previous study, Uenishi and co-workers demonstrated a novel synthetic approach towards the synthesis diospongin A **1** and B **2** by using a Pd(II) catalyst to promote cyclisation, followed by a Wacker oxidation reaction (**Scheme 10**).[16, 35-38]

When triol **25** was treated with bis(acetonitrile)dichloropalladium(II), the desired *cis*-tetrahydropyran **26** was obtained in 92% yield, along with *trans*-tetrahydropyran **28** in 6% yield. This was followed by Wacker oxidation to generate diospongin A **1** in 56% yield. The triol **27**, under the same reaction conditions, formed *trans*-tetrahydropyran **28** in 86% yield, along with *cis*-tetrahydropyran **26** in 5% yield. Compound **28** was then protected with MOMCl, followed by Wacker oxidation and deprotection to give diospongin B **2** in 91% yield.

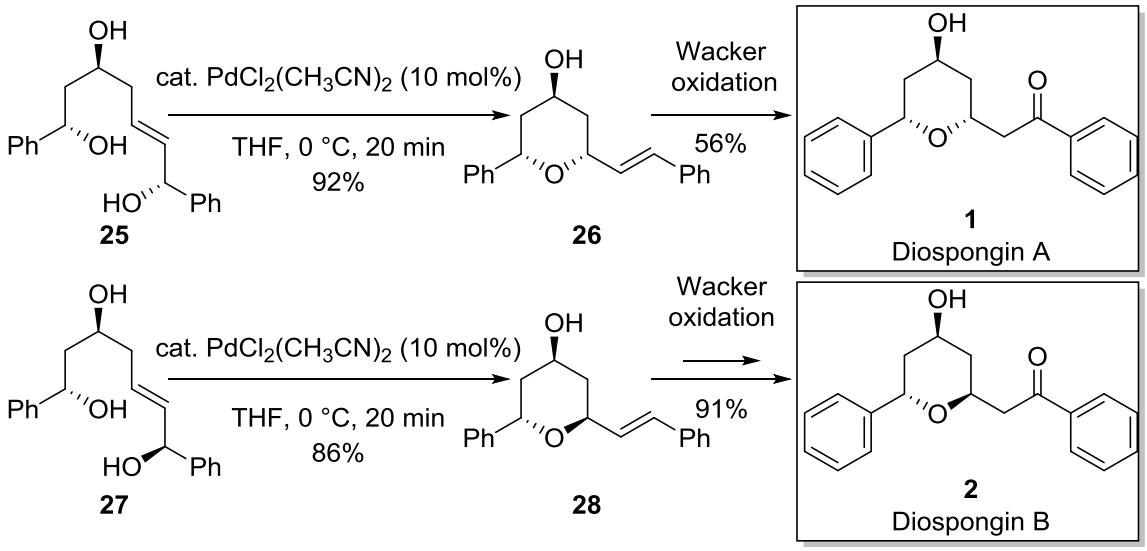

Scheme 10 Synthesis of diospongin A **1** and B **2** as reported by Uenishi and co-workers.[16]

Gracza and co-workers have developed a diastereoselective synthesis of 2,6-*cis*-tetrahydropyranyl carboxylic acids based on intramolecular hydroxycarbonylation by using palladium(II) as a catalyst (**Scheme 11**).[23]

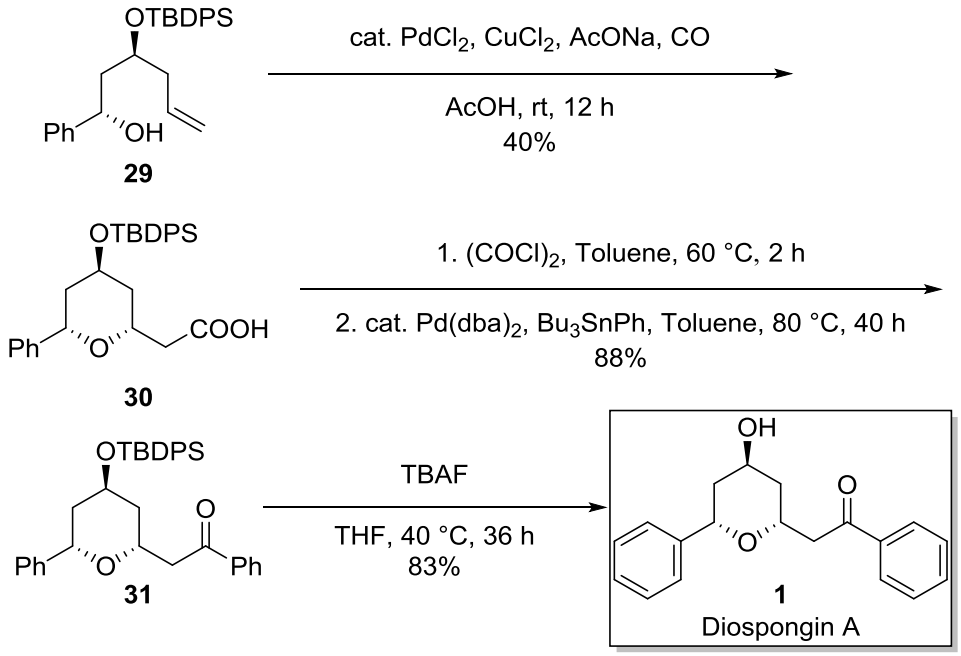

Scheme 11 Synthesis of diospongin A **1** as reported by Gracza and co-workers.[23]

The synthesis of 2,6-*cis*-diastereomer **30** was achieved by the treatment of protected diol **29** under hydroxycarbonylation with carbon monoxide in acetic acid in the presence of palladium(II) chloride. Next, the 2,6-*cis*-tetrahydropyranyl carboxylic acid **30** was converted to **31** in 2 steps. The reaction started with treatment of **30** with oxalyl chloride to give acid chloride, followed by Stille coupling[39] with tributylphenyltin and bis(dibenzylideneacetone)palladium(0) to generate **31** in 88% yield over two steps. Finally, after deprotection gave the target molecule **1** in 83% yield.

1.1.3.4. Synthesis of tetrahydropyrans *via* dihydropyranone

In 2016, the Clarke group also reported the synthesis of diospongin B **2**.[32] The *trans*-tetrahydropyran core was obtained *via* conjugate addition of Gilman cuprates to dihydropyran-4-one **32**. Decarboxylation of **33** and followed by reduction to give **34** in 66% yield. Protection of **34** with MOMCl, followed by a Wacker oxidation gave **35**. Finally, deprotection of **35** using hydrochloric acid in THF to complete the synthesis of diospongin B **2** (**Scheme 12**).

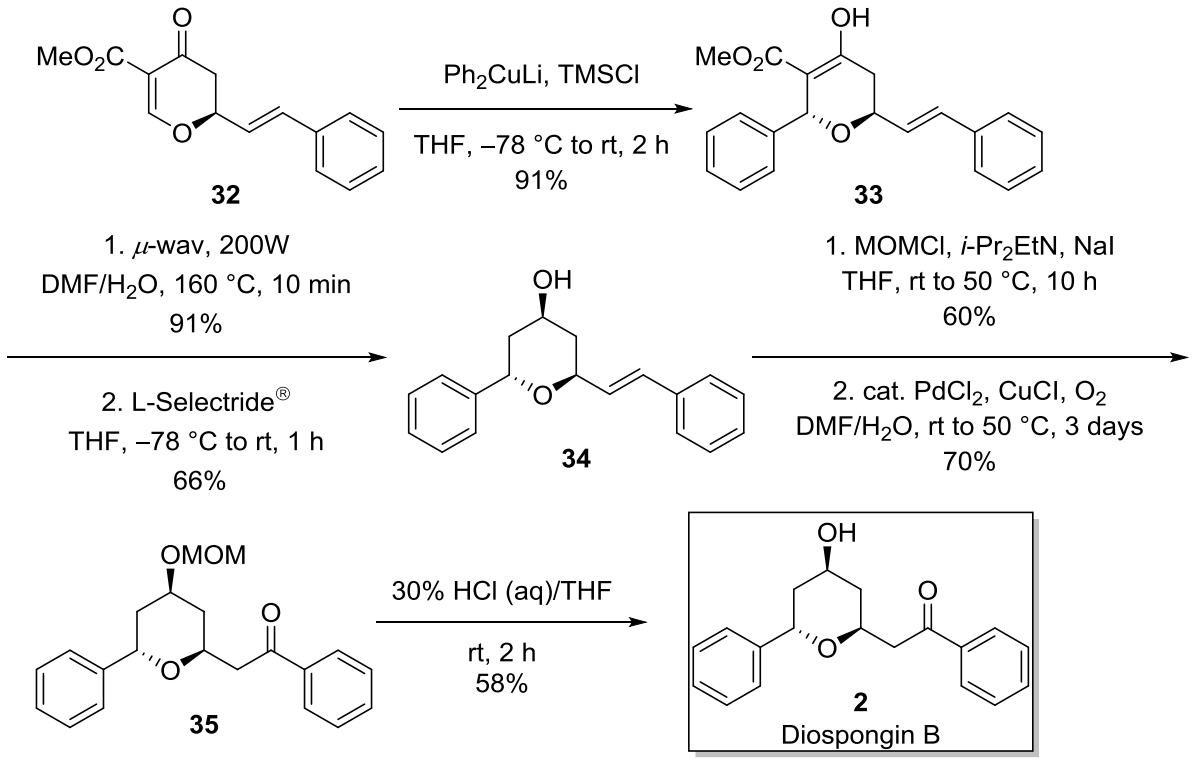

Scheme 12 Synthesis of diospongin B **2** as reported by the Clarke group.[32]

1.1.3.5. Synthesis of tetrahydropyrans *via* the Diels–Alder reaction

In addition to other reactions, the hetero-Diels–Alder reaction has also been used to form the tetrahydropyran core. In 2010, groups led by More[21] and Hashimoto[22]

accomplished the synthesis of diospongin A **1** and B **2** by using a hetero-Diels–Alder reaction (**Scheme 13**).

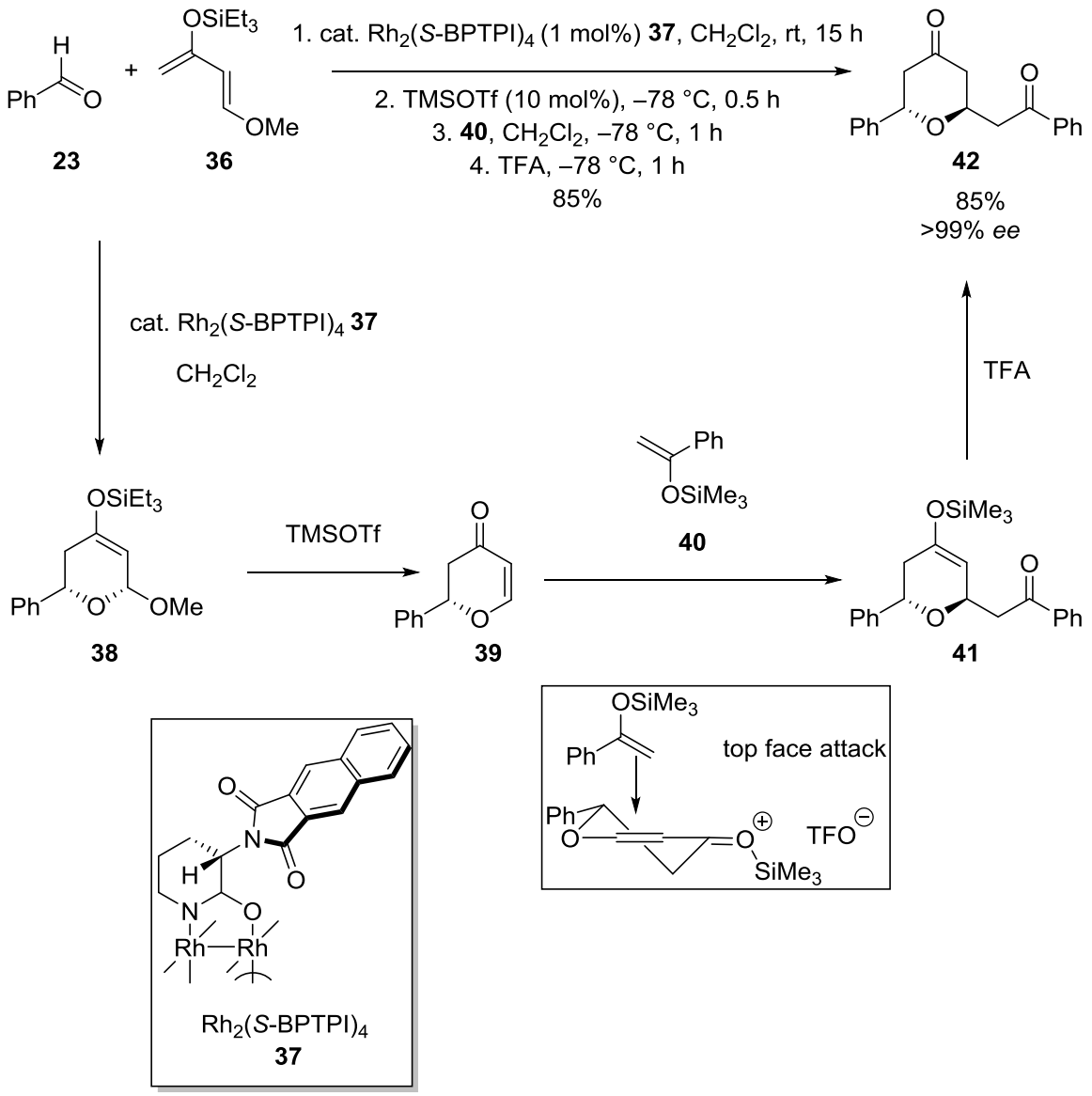

Scheme 13 Synthesis of compound **42** as reported by Hashimoto and co-workers.[22]

The synthesis of diospongin A **1** and B **2** reported by Hashimoto and co-workers was shown in **Scheme 13**. The synthesis began with an enantioselective

hetero-Diels–Alder reaction between Danishefsky-type diene **36** and benzaldehyde **23** using 1 mol% Rh_2(*S*-BPTPI)$_4$ **37** as a catalyst to give **38**. Then, 10 mol% of TMSOTf was used to give dihydropyranone **39**, after which the Mukaiyama–Michael addition was immediately performed with silyl enol ether **40** to give **41**. Addition of TFA resulted **42** in 85% yield with >99% *ee*. Diospongin B **2** was obtained as a single diastereomer in 86% from **42** *via* a chemo and stereoselective reduction with K-selectride®. Diospongin A **1** was synthesised from diospongin B **2** using 30% hydrochloric acid in THF (**Scheme 14**).

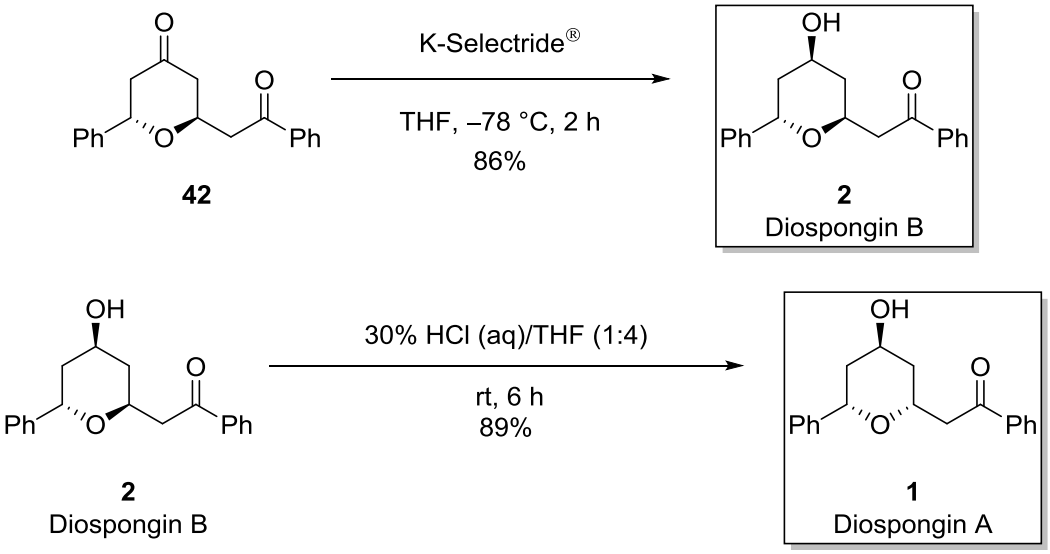

Scheme 14 Synthesis of diospongin A **1** and B **2** as reported by Hashimoto and co-workers.[22]

1.1.4. Stereodivergent oxy-Michael reaction

In 2011, Fuwa and co-workers reported an oxy-Michael cyclisation of *α*,*β*-unsaturated thioesters to form tetrahydropyrans.[40] Treatment of *α*,*β*-unsaturated thioesters **43** with a Brønsted acid catalyst, leads to high diastereoselectivity for the 2,6-*cis*-tetrahydropyran product **44**; under basic

conditions using potassium *tert*-butoxide the cyclisation favoured the formation of 2,6-*trans* product **45** (**Scheme 15**).

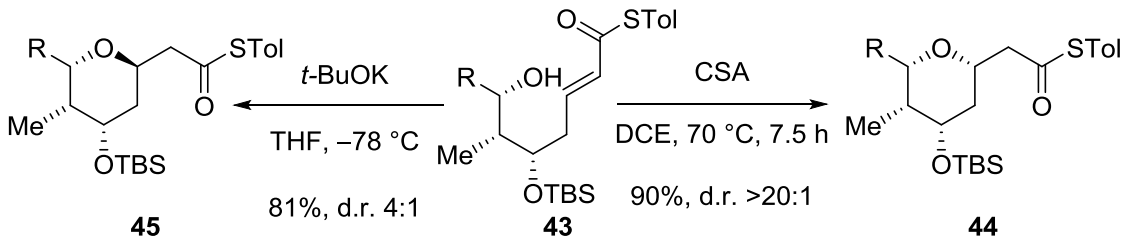

Scheme 15 Synthesis of *cis*- and *trans*-tetrahydropyran ring through an oxy-Michael reaction as reported by Fuwa and co-workers.[40]

The transition state model proposed by Fuwa and co-workers showed that the 2,6-*cis* product possibly went through the chair-like transition state **46a** *via* an allylic carbocation mechanism (**Scheme 16**). The *cis*-product **44** was formed because this conformation showed the minimum steric interactions between its substituents.

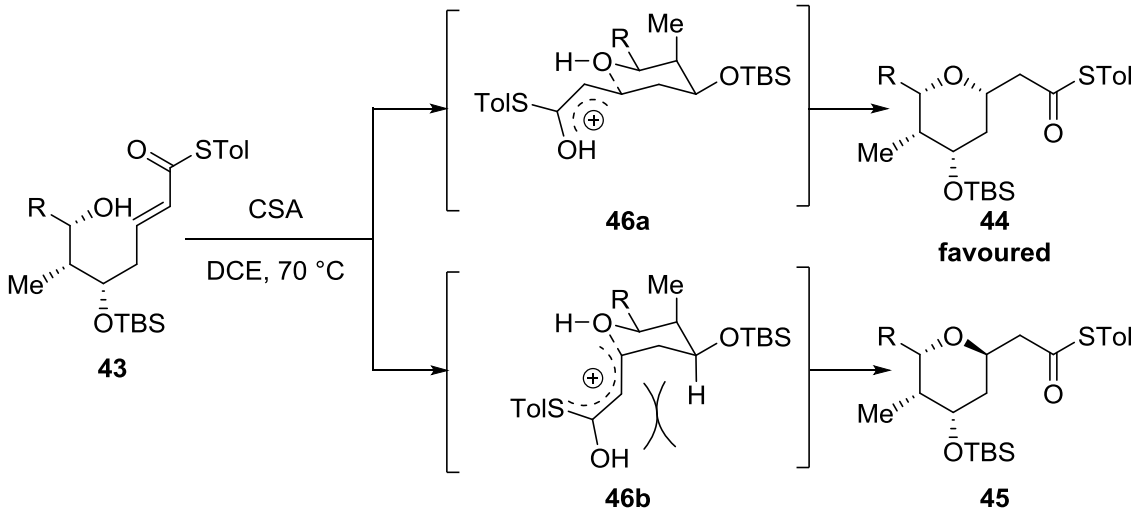

Scheme 16 Mechanistic studies of the *cis*-tetrahydropyran as proposed by Fuwa.[40]

The preferential formation of the 2,6-*trans* tetrahydropyran ring under potassium *tert*-butoxide-catalysed reaction condition could be explained by the chelation-controlled model (**Scheme 17**).

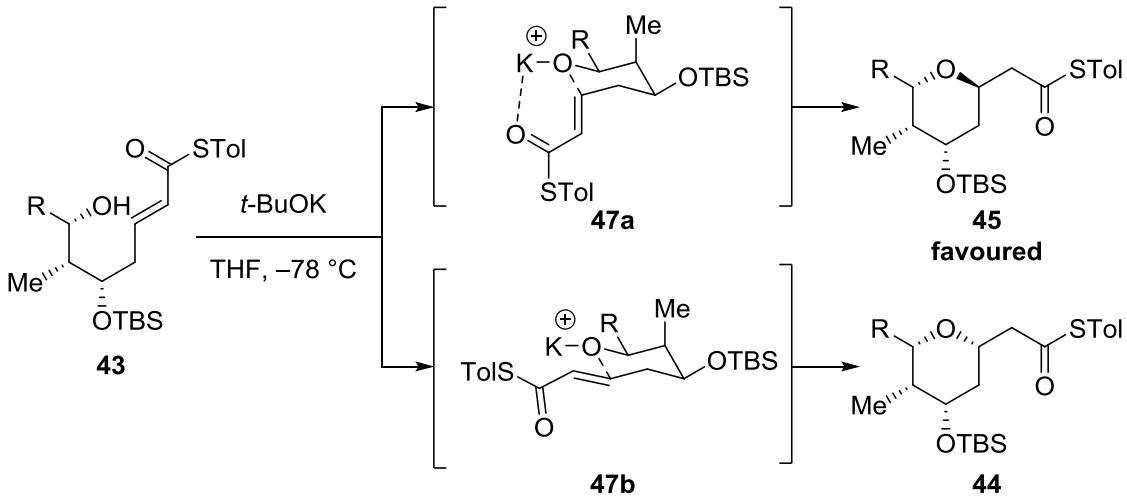

Scheme 17 Mechanistic studies of the *trans*-tetrahydropyran as proposed by Fuwa and co-workers.[40]

The potassium ion was coordinated with the thioester oxygen atom and hydroxyl group to form the transition state **47a** and **47b**. However, for the **47b** transition state, the thioester oxygen atom would be more difficult to chelate with the potassium ion as it would be too far away. Therefore, under potassium *tert*-butoxide condition, *trans*-tetrahydropyran was preferentially formed.

The Clarke group discovered a similar reaction as the sterodivergent reaction described above; the *α*,*β*-unsaturated thioesters **6** under acetic acid-buffered TBAF conditions produced 2,6-*trans*-tetrahydropyran rings **8** in 35% yield and in >20:1 diastereoselectivity, however, under TFA conditions the formed tetrahydropyran had

a 2,6-*cis* configuration **7** in 71% yield and in >13:1 diastereoselectivity (**Scheme 18**).[9] In order to explain this diastereoselectivity, computational studies were carried out.[41, 42]

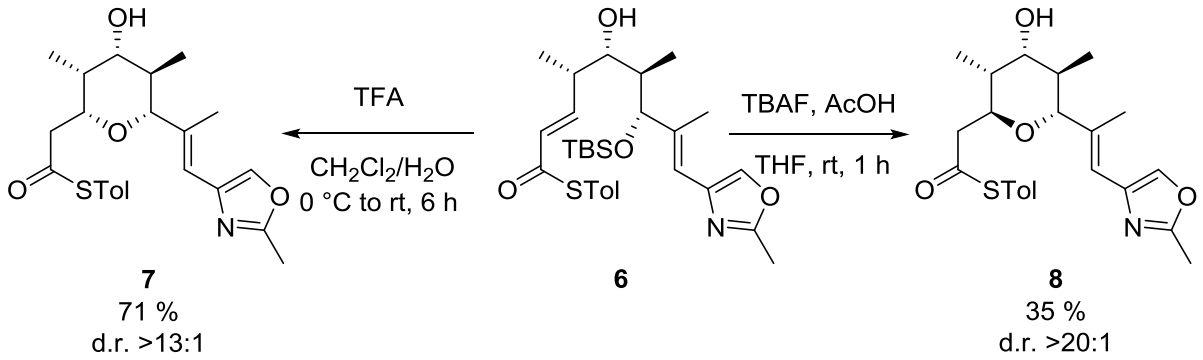

Scheme 18 Stereodivergent oxy-Michael reaction.[9]

The computational studies showed that under acidic conditions the TFA plays a dual role to protonate the thioester and to deprotonate the alcohol (transition state **49**). With this coordination, the electrophilicity and nucleophilicity of the thioester and alcohol were increased, respectively and only two possible *(E)*-thioenols **50** and **51** were formed (**Scheme 19**).

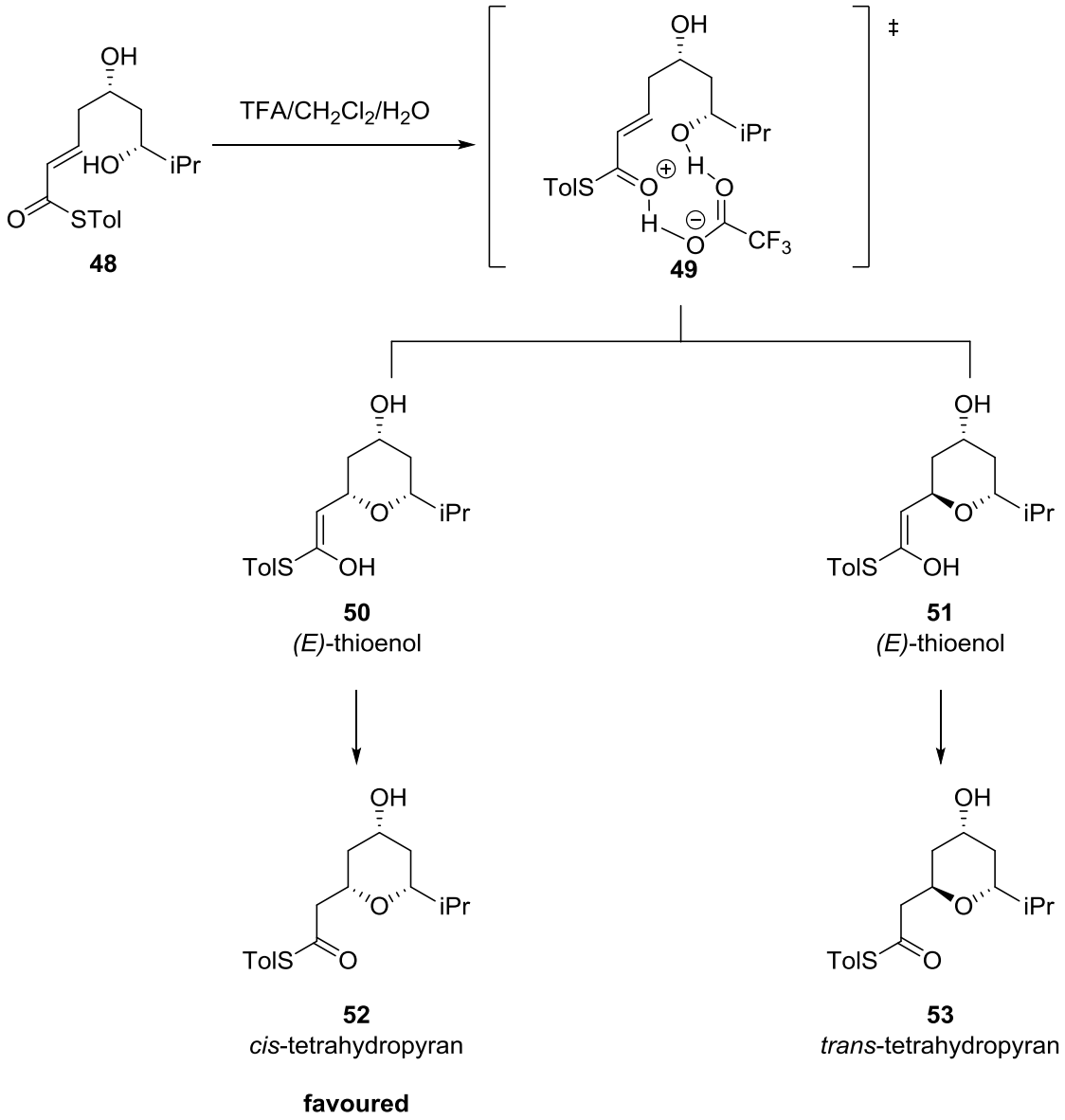

Scheme 19 Mechanistic studies of TFA-mediated cyclisation.[41]

Several transition states may lead to the formation of two possible*(E)*-thioenols **50** and **51**. Using DFT calculations (B3LYP/6-31G*), four lowest energy transition states with both chair (**50a** and **51a**) and boat (**50b** and **51b**) conformations were shown in **Figure 4**.

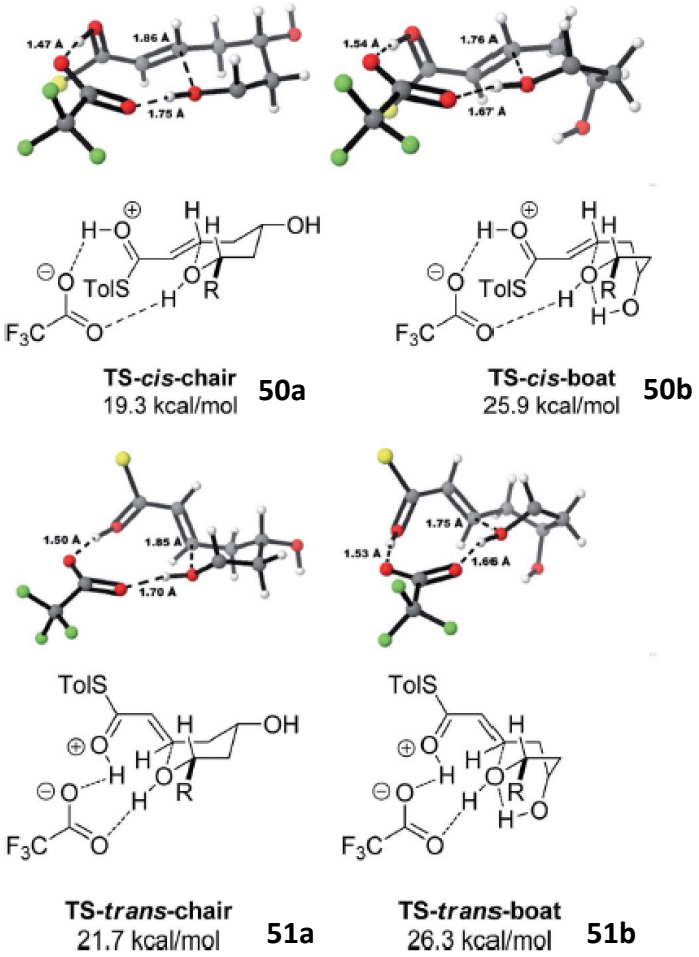

Figure 4 Transition states for the TFA-mediated cyclisation. Activation enthalpies calculated in dichloromethane implicit solvent model and were relative to the ground state conformation of diol **53** complex with TFA. Tolyl and *i*-Pr groups were omitted for clarity.[41]

The transition state leading to the *cis*-product with chair configuration **50a** was calculated to have the lowest activation enthalpies and was 2.4 kcal/mol lower in energy when compared to the *trans*-chair-like transition state **51a**. Compared to the *trans*-configuration, fewer steric interactions were found between the 6-proton and the 2-thioester substituent in *cis*-configuration, therefore the formation of the *cis*-product was favoured, supporting the results seen in our synthetic studies.

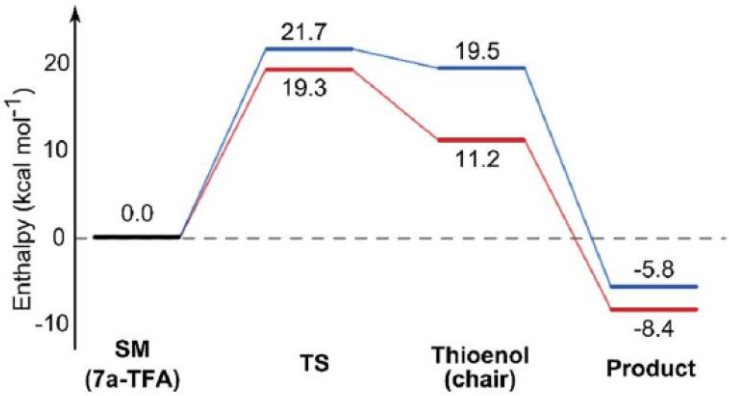

Figure 5 Energy diagram for the TFA-mediated lowest energy pathways for the 2,6-*cis* **52** (red) and 2,6-*trans* **53** (blue). Enthalpies calculated in dichloromethane implicit solvent model and were relative to the ground state conformation of **53** complex with TFA.[41]

Moreover, these calculations also confirmed that the reaction was kinetically controlled, because the activation energy of the reverse reaction was higher compared to the forward reaction (**Figure 5**). In contrast, the 2,6-*trans*-configuration was obtained under buffered TBAF conditions.

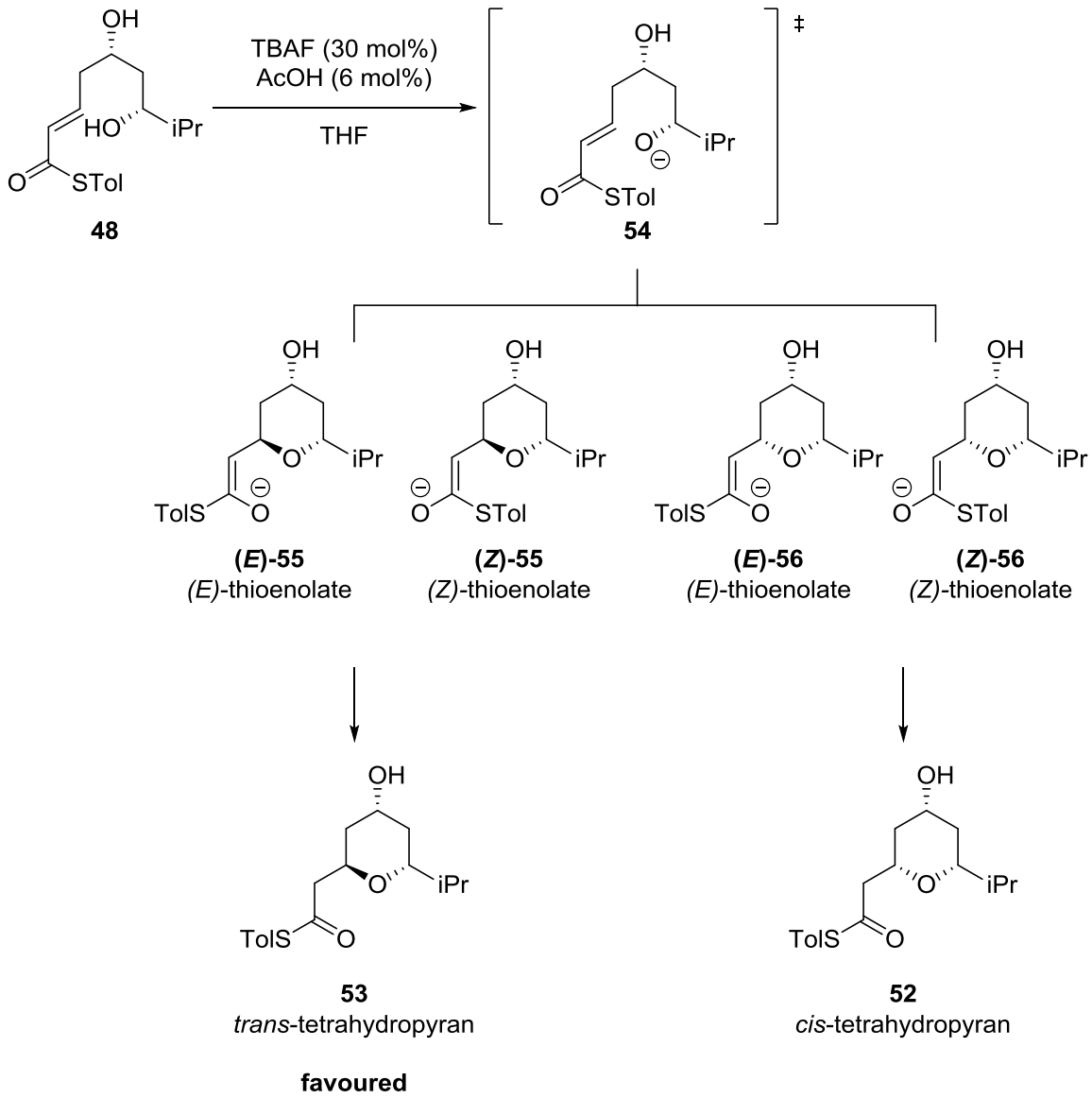

Figure 6 Mechanistic considerations of TBAF-mediated cyclisation.

It was assumed that the alkoxide attacked the conjugate double bond to form the 4 possible thioenolates : both (*E*) and (*Z*)-thioenolate of the *trans*-tetrahydropyran **55** and both (*E*) and (*Z*)-thioenolate of the *cis*-tetrahydropyran **56** (**Figure 6**). Several transition states may lead to the formation of four possible thioenolates **(*E*)-55**, **(*Z*)-55**, **(*E*)-56** and **(*Z*)-56**. As shown in **Figure 7**, 6 possible transition states are

presented with lowest in energy to form the (*E*) and (*Z*)-thioenolates.

It was found that the **(*E*)-55a** had the lowest energy and with a boat-like conformation. The unusual boat-like transition state might be due to a strong hydrogen-bonding interaction between the 4-hydroxyl and the alkoxide to stabilise the conformation.[43, 44] In contrast with the TFA case, the 4-hydroxyl group was directly involved in stabilization of the transition state, which might be involved in the stereodivergence.

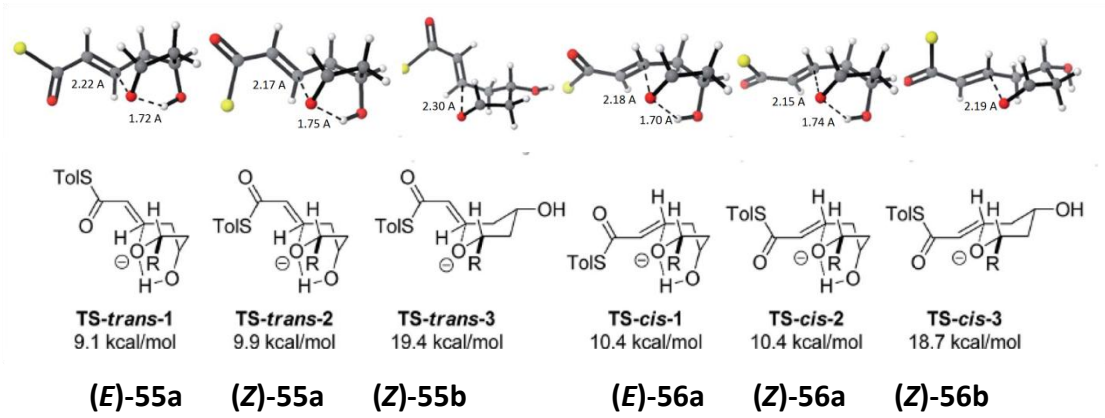

Figure 7 Transition states for the TBAF-mediated cyclisation.[41] Activation enthalpies calculated in the THF implicit solvent model and were relative to the ground state conformation of alkoxide **54**. Tolyl and *i*-Pr groups were omitted for clarity.

As demonstrated in energy diagram (**Figure 8**), the energy barrier of *trans*-tetrahydropyran **(*E*)-55a** was 9.1 kcal/mol and that of *cis*-tetrahydropyran **(*E*)-56a** was 10.4 kcal/mol. These two energy barriers were small, which may account for the rapid product formation (usually fewer than 10 minutes at room temperature). **(*E*)-55a** was 1.3 kcal/mol lower in energy compared to **(*E*)-56a**, which were consistent with the diastereoselectivity results obtained in our synthetic studies.

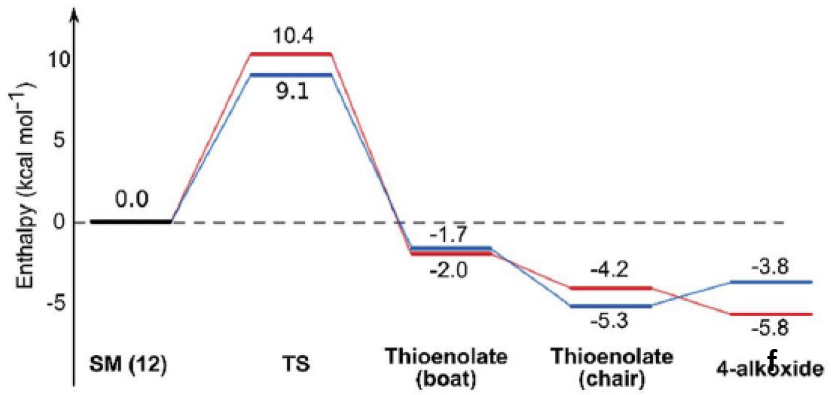

Figure 8 Energy diagram for theTBAF-mediated lowest energy pathways to the 2,6-*trans* **53** (blue) and 2,6-*cis* **52** (red). Enthalpies calculated in THF implicit solvent model and were relative to the ground state conformation of alkoxide **54**.

The reaction is likely under kinetic control if the energy barrier in the forward direction is much smaller than in the reverse reaction. The total energy barrier of the *cis*-tetrahydropyran in the reverse direction was 14.4 kcal/mol (**Figure 8**), which supported the hypothesis that the reaction under TBAF conditions was kinetically controlled.

1.1.5. Synthetic investigation of the role of the 4-OH group in the stereodivergent oxy-Michael cyclisation

Based on the computational studies described in chapter **1.1.4**, it was deduced that the 4-hydroxl group was an important functional group that was essential for stereodivergence. To confirm this, synthetic studies were performed by using compounds **57**, **58**, **59** and **60** as the substrates. Compounds **57**, **58** and **59** which did not have the hydroxyl group at the C-4 position, and the 4-hydroxl group in compound **60** was protected as a methyl ether (**Figure 9**).

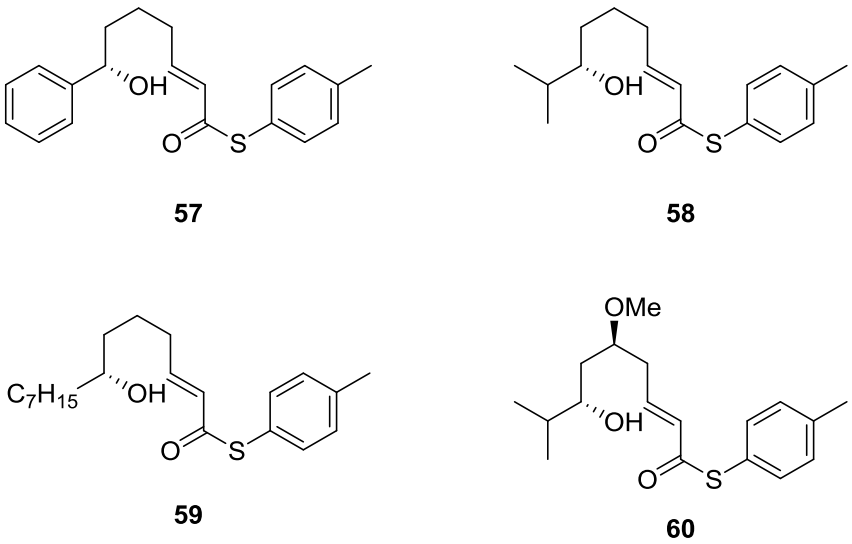

Figure 9 Structure of compounds **57**, **58**, **59** and **60**.

The general synthetic routes to synthesis **57**, **58** and **59** are depicted in **Scheme 20**.

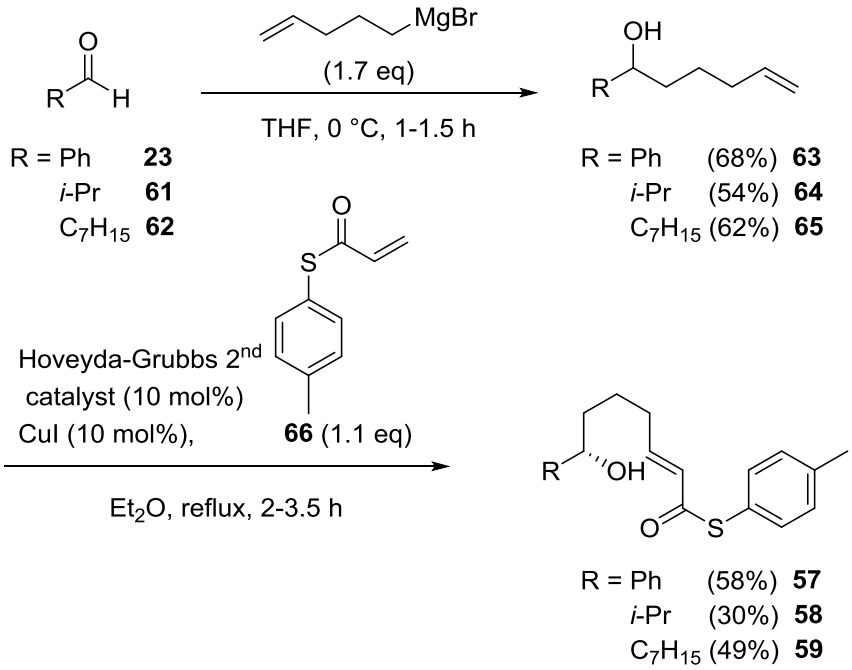

Scheme 20 Overview of the synthesis of compounds **57**, **58** and **59**.

The synthesis started with Grignard addition to aldehydes **23**, **61** and **62** to provide corresponding products **63** (68%), **64** (54%) and **65** (62%). Next, the alcohols **63**, **64** and **65** underwent the cross-metathesis reaction with S-*p*-tolyl prop-2-enethioate **66** in the presence of 10 mol% of 2nd generation of Hoveyda-Grubbs catalyst and 10 mol% of copper(I) iodide to generate the thioesters **57** (58%), **58** (30%) and **59** (49%).

After successful synthesis of the cyclisation precursors **57**, **58** and **59**, evaluation of the stereodivergent oxy-Michael cyclisation was performed.

Table 2 The evaluation of stereodivergent oxy-Michael cyclisation to **57**, **58** and **59** substrates.

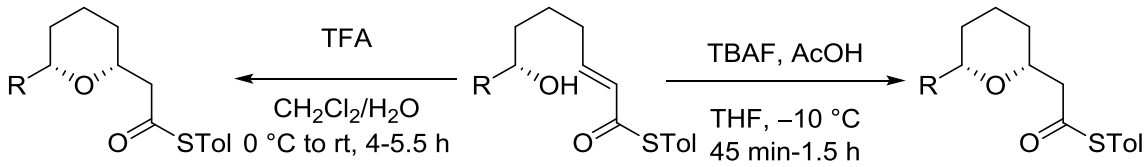

Entry	Ratio *cis*:*trans*	TFA Yield/%	R	TBAF Yield/%	Ratio *cis*:*trans*[1]
1	8:1	56 **67**	Ph **57**	53 **67**	>20:1
2	4:1	27 **68**	*i*-Pr **58**	27 **68**	>20:1
3	5:1	36 **69**	C_7H_{15} **59**	25 **69**	>20:1

1. [1]Determined by ^{1}H NMR.

When thioesters **57**, **58** and **59** were submitted to the acid cyclisation conditions, the cyclisation smoothly proceeded to form the *cis*-products **67** (56%), **68** (27%) and **69**

(36%) with 8:1, 4:1 and 5:1 of diastereoselectivities for **67**, **68** and **69**, respectively. Treatment of thioesters **57**, **58** and **59** under buffered TBAF conditions also lead to the formation of *cis*-products **67** (53%), **68** (27%) and **69** (25%) with more than 20:1 diastereoselectivity (**Table 2**).

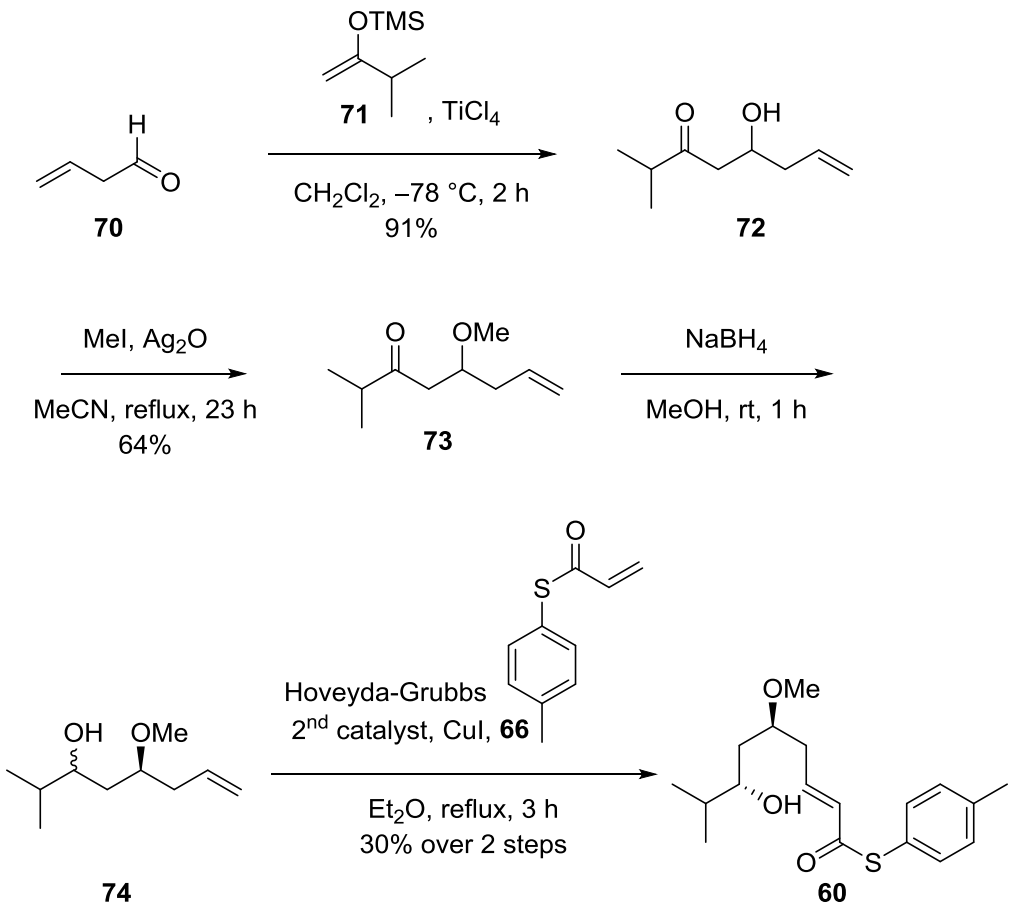

Scheme 21 Synthesis of thioester **60**.

The synthesis of cyclisation precursor **60**, which had the 4-hydroxyl group protected as a methyl ether, began with an aldol reaction. Aldehyde **70** could be synthesised in two steps from a tin metal mediated[45] Barbier-type reaction[46] and subsequent cleavage of diol. Aldehyde **70** was then treated with silyl enol ether **71** to give **72** in 91% yield. This was methylated to give **73** in 64% yield. Compound **73** was then

converted into **74** *via* reduction with sodium borohydride to give both *syn*- and *anti*-products. Without the separation of these two diastereoisomers, cross-metathesis was carried out to give product **60** in 30% yield after purification (**Scheme 21**).

Next, the protected thioester **60** was also submitted to both the acid and the buffered TBAF reaction conditions (**Scheme 22**).

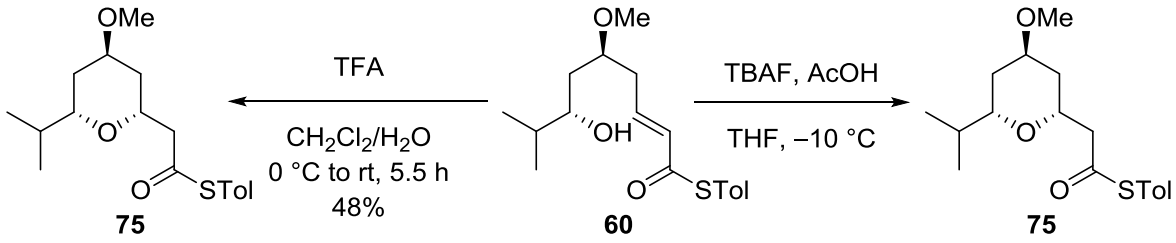

Scheme 22 Investigating of stereodivergent oxy-Michael cyclisation to substrates **60**.

Treating **60** under TFA conditions gave the *cis*-product in 48% yield. Under buffered TBAF conditions a hydrolysis product was the major product, detected the *cis*-cyclised product peak was identified in the crude reaction mixture (**Scheme 22**).

The above results indicated that the formation of the *trans*-tetrahydropyrans under buffered TBAF condition was dependent on the presence of the 4-hydroxyl group. This was consistent with the computational studies, which was showed that the 4-hydroxyl group was a hydrogen-bond donor in the stereodivergent oxy-Michael cyclisation.

Interconversion experiments were performed, to prove that the formation of both *cis*- and *trans*-products were under kinetic control. The *cis*-product **76** was treated with buffered TBAF conditions, while the *trans*-product **77** was submitted to acidic cyclisation conditions (**Scheme 23**).

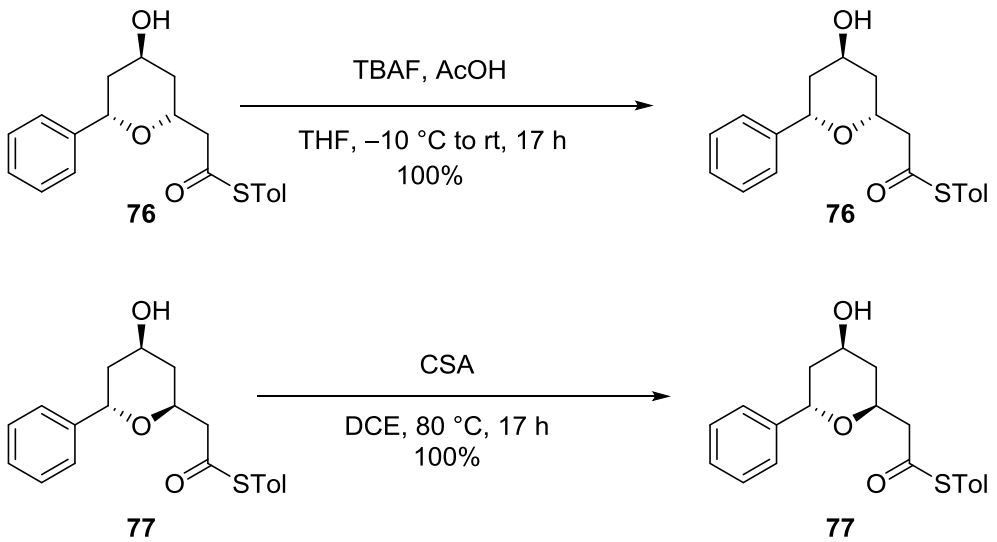

Scheme 23 Interconversion studies for the *cis*-product **76** and *trans*-product **77**.

The reaction was monitoring by TLC and by analysis of the ^{1}H NMR spectrum. Interestingly, no interconversion was observed. Therefore it was deduced that the formation of the *cis* and *trans* cyclisation products **76** and **77** were under kinetic control, as indicated by the computational studies.

The stereoselective oxy-Michael addition was successfully applied to form the tetrahydropyran ring of phorboxazole B **7**. The aim was to apply this remarkable reaction towards the synthesis of both (±)-diospongin A **1** and B **2** from a single acyclic precursor.

1.2. Results and discussion

1.2.1. Background and previous results

Previous work by the Clarke group showed that the C-20–C-32 penta-substituted tetrahydropyran core of phorboxazole B **7** could be accessed by the use of thioesters as electophiles in the stereodivergent oxy-Michael reaction (**Scheme 24**).[9] The deprotection of TBS-ether **6** under acetic acid-buffered TBAF conditions, resulted in formation of the 2,6-*trans*-tetrahydropyran ring **8** in which no traces of the 2,6-*cis*-tetrahydropyran ring **7** were detected. However, under TFA conditions, the tetrahydropyran formed had the 2,6-*cis* configuration **7**. Because of this unique stereodivergence, it was envisaged that the oxy-Michael reaction could be applied for the synthesis of diospongin A **1** and B **2**.

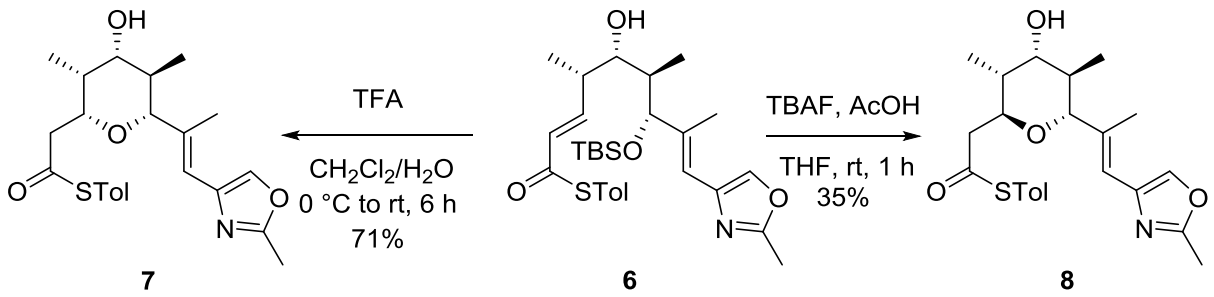

Scheme 24 Synthesis of C-20–C-32 fragment of the phorboxazole B **7** *via* stereodivergent oxy-Michael reaction.[9]

1.2.2. Retrosynthetic approaches

The retrosynthetic analysis of diospongin A **1** and B **2** is illustrated in **Scheme 25**.

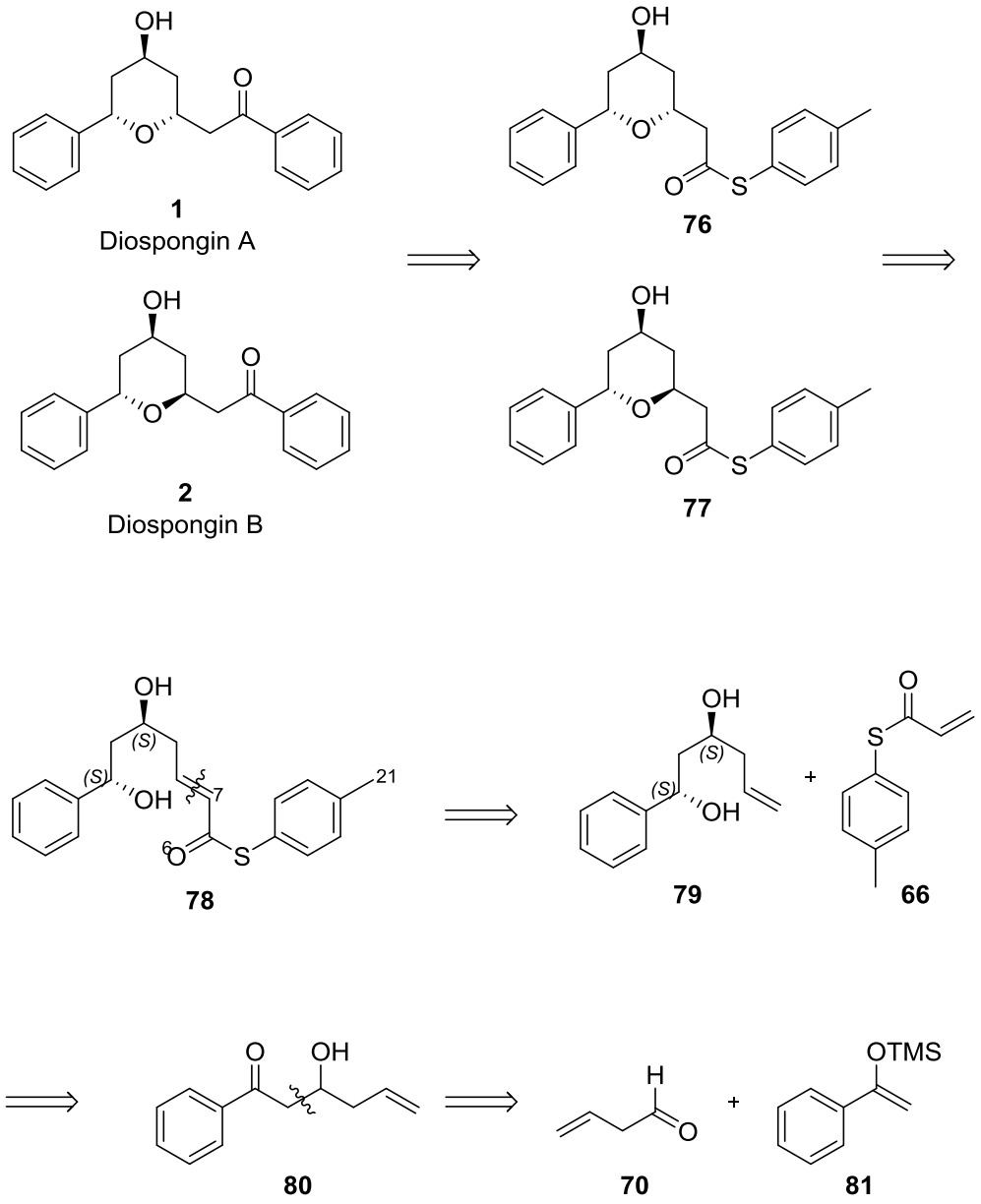

Scheme 25 Retrosynthetic analysis of diospongin A **1** and B **2**.

We envisioned that the synthesis of diospongin A **1** and B **2** could be achieved in one step from the thioesters **76** and **77** by a Liebeskind–Srogl type coupling reaction.[47] The key tetrahydropyran forming step to generate both diastereomeric,

cis-tetrahydropyran **76** and *trans*-tetrahydropyran **77** was proposed *via* a stereoselective oxy-Michael addition onto an *α,β*-unsaturated thioester **78**. Additional disconnection at the C-6 and C-7 bond of *α,β*-unsaturated thioester **78** resulted in diol **79** and S-*p*-tolyl prop-2-enethioate **66**. Diol **79** was accessible through diastereoselective reduction of the Mukaiyama aldol product **80**. The aldol product **80** could be obtained by coupling the silyl enol ether **81** and 3-butenal **70**.

1.2.3. Total synthesis of (±)-diospongin A and B

Preparation of the key cyclisation precursor **78** for the synthesis of diospongin A **1** and B **2** is presented in **Scheme 26**.

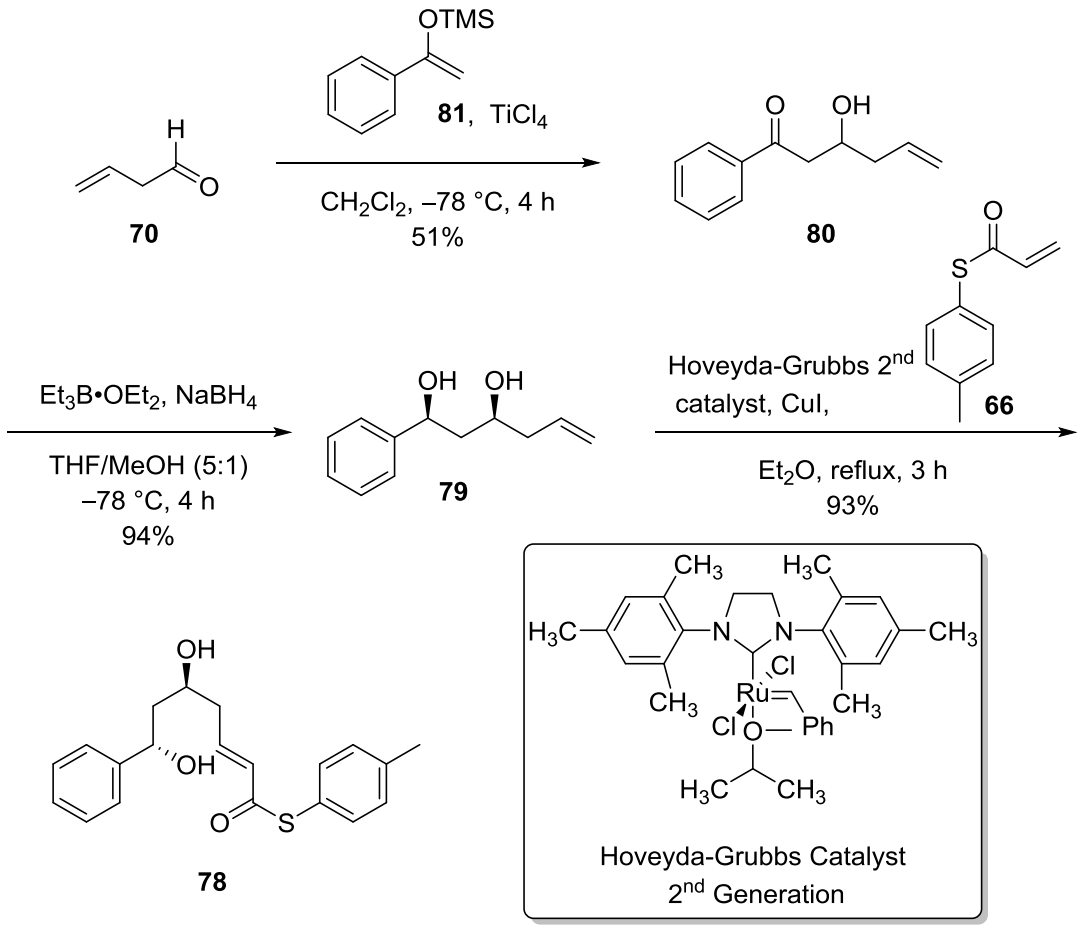

Scheme 26 Synthesis of *α,β*-unsaturated thioesters **78**.

It was anticipated that the C-4 hydroxyl group could be installed *via* a Mukaiyama aldol reaction. Therefore, the proposed synthetic route to diospongin A **1** and B **2** began with the coupling reaction between freshly-made of 3-butenal **70** and trimethyl((1-phenylvinyl)oxy) silane **81** to form the *β*-hydroxy ketone **80**.

The preparation of 3-butenal **70** originated from a tin metal-mediated[45] Barbier-type reaction[46] between commercially available glyoxal **82** and allyl bromide **83** to form 1,7-octadiene-3,4-diol **84** in 72% yield.[48] Subsequent cleavage of the diol **84** with sodium (meta)periodate in a biphasic dichloromethane-water system generated 3-butenal **70** (**Scheme 27**).[49]

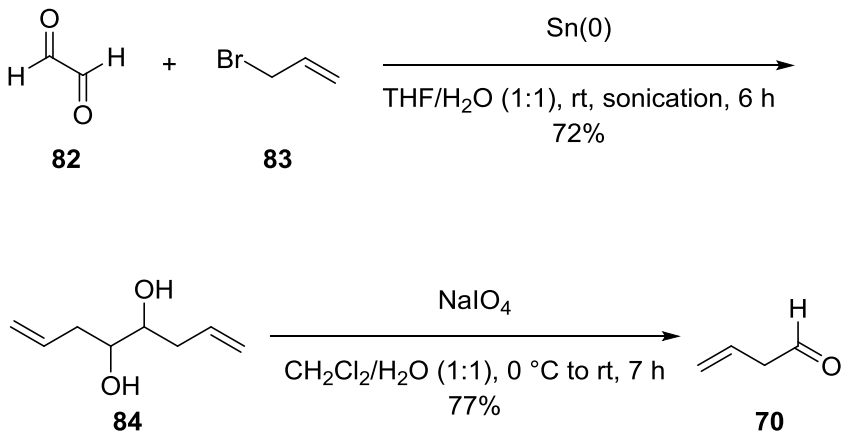

Scheme 27 Synthesis of 3-butenal **70**.

Treatment of commercially available acetophenone **312** with trimethylchlorosilane in the presence of triethylamine and sodium iodide in acetonitrile resulted in the formation of trimethyl ((1-phenylvinyl)oxy) silane **81** in high yield (97%) (**Scheme 28**).[50-52]

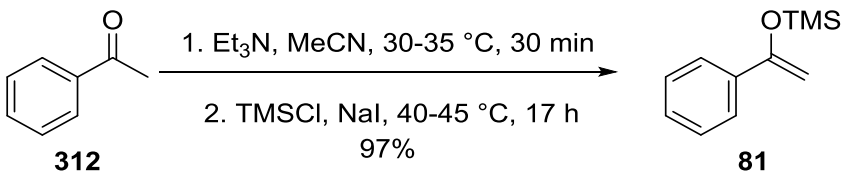

Scheme 28 Synthesis of trimethyl ((1-phenylvinyl)oxy) silane **81**.

After having successfully synthesised of both aldehyde **70** and silyl enol ether **81**, the Mukaiyama aldol reaction was carried out. The reaction was completed using a standard procedure,[53] in which the aldehyde **70** was coupled with the silyl enol ether **81** in the presence of titanium tetrachloride at −78 °C in dichloromethane. The desired aldol product, *β*-hydroxy ketone **80** was obtained in a moderate yield (51%) (**Scheme 26**).

The next step in the synthetic sequence involved the diastereoselectivity reduction of *β*-hydroxy ketone **80** to *syn*-diol **79**.

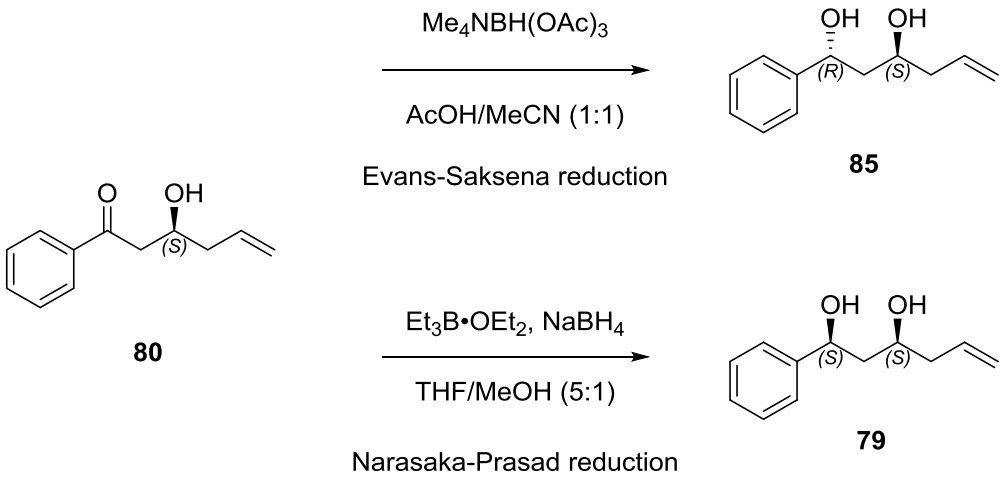

Scheme 29 Diastereoselective reduction to reduce *β*-hydroxy ketone **80**.

According to the literature,[54-58] under different reaction conditions, both *syn*- and *anti*-1,3-diols can easily be synthesised from the same *β*-hydroxy ketone. The formation of *syn*-diols was favoured under Narasaka–Prasad conditions,[57, 58] whereas when using Evans–Saksena conditions,[54-56] the formation of *anti*-1,3-diols was favoured (**Scheme 29**).

In the Evans–Saksena reduction, tetramethylammonium triacetoxyborohydride reducing agent was used in a 1:1 acetic acid and acetonitrile solvent system, and resulted in the formation of *anti*-1,3-diols. This reaction proceeded through an intramolecular hydride delivery to ketone with the hydroxyl directing the reduction in the transition state. Two possible competing chair-like transition states **86** and **87** were proposed to account for the diastereoselectivity (**Scheme 30**).

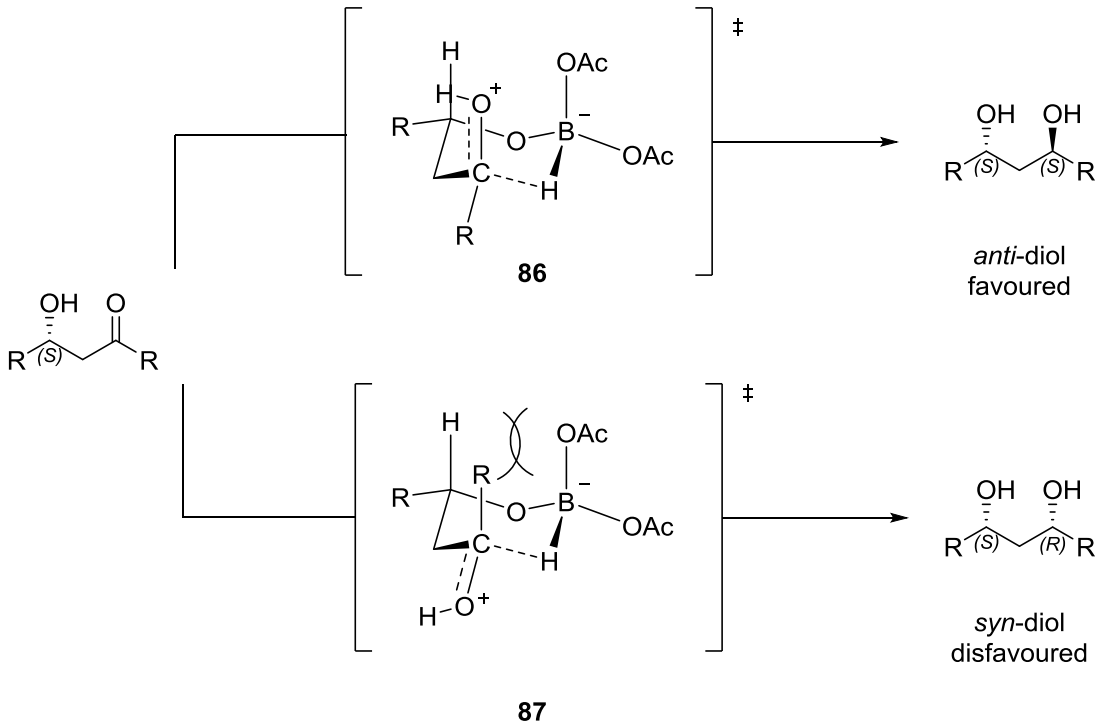

Scheme 30 Transition state of the Evans–Saksena reduction.[54-56]

Given the 1,3-diaxial interactions presented in the transition states **87**, the transition state **86** is more favourable. Therefore, under Evans–Saksena reduction, *anti*-diol was preferentially formed.

In contrast, to gain access to the *syn*-diol **79** the approach as reported by Narasaka[58] and Prasad[57] was used. In brief, *β*-hydroxy ketone **80** was treated with sodium borohydride and triethyl borane in a solvent mixture of THF and methanol at −78 °C to generate the desired *syn*-diol **79** in a high yield (94%) (**Scheme 26**). Triethylborane may acts as a chelating agent that coordinated with *β*-hydroxy ketone **80** to form diethylborinic ester through a chelated 6-membered transition state in a half-chair-like conformation **88a** and **88b** (**Scheme 31**).

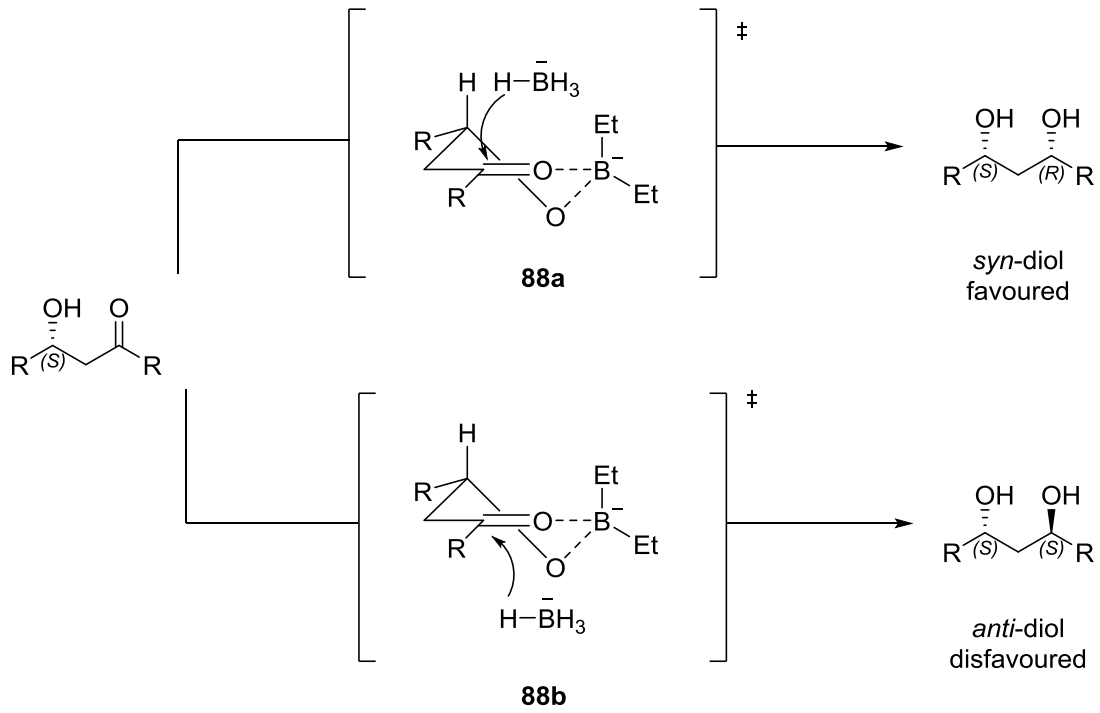

Scheme 31 Transition state of the Narasakand–Prasad reduction.[57, 58]

The approach of a reducing agent is through an external hydride delivery. Addition of hydride from the bottom face **88b**, leading to an initial conformation and formation of a twist-boat intermediate. On the other hand, hydride addition from the top face (*pseudo*-axial attack) **88a**, resulting in an initial conformation of a product being in the chair conformation.

The chair conformation would be lower in energy compared to that of the twist-boat, therefore the addition of hydride reagents showed a preference in attacking from the top face (*pseudo*-axial attack) **88a** to form *syn*-diol as the major product.

Following the successful synthesis of *syn*-diol **79**, the next step involved synthesis of the cyclisation precursor **78** *via* olefin cross-metathesis.

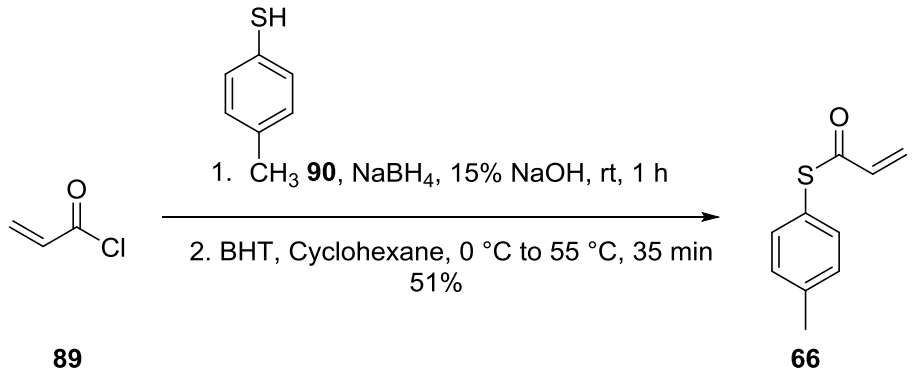

Scheme 32 Synthesis of S-(4-methylphenyl) 2-propenthioate **66**.

The S-(4-methylphenyl) 2-propenthioate **66** was prepared by following the procedure described by Fuwa (**Scheme 32**).[40] Treatment of 4-methylbenzenethiol **90** with sodium borohydride resulted in sodium thiolate formation. Subsequently, acryloyl chloride **89** was added in the presence of BHT and the desired

S-(4-methylphenyl) 2-propenthioate **66** was obtained in 51% yield. The sodium thiolate was a harder nucleophile and prone to react with the acid chloride. In this reaction, sodium borohydride will also reduce disulfide **91** back to thiol (**Figure 10**).

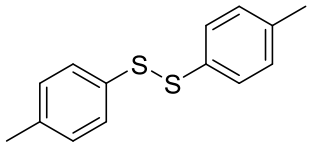

Figure 10 Structure of disulfides **91**.

To prevent polymerization of both acrolyl chloride **89** and S-(4-methylphenyl) 2-propenthioate **66**, BHT was added into the reaction.

The metathesis reaction that was used to form the *α,β*-unsaturated thioester **78** was a variation of the conditions reported by Lipshutz.[59] Treatment of *syn*-diol **79** with excess S-(4-methylphenyl) 2-propenthioate **66**, used 10 mol% of 2nd generation of Hoveyda-Grubbs catalyst and copper(I) iodide as a co-catalyst allowed for the formation of *α,β*-unsaturated thioester **78** in a high yield (93%) (**Scheme 26**). In the absence of copper(I) iodide co-catalyst, lower yields were obtained.[42] After completion of the synthesis of *α,β*-unsaturated thioester **78**, the oxy-Michael reaction was performed (**Scheme 33**).

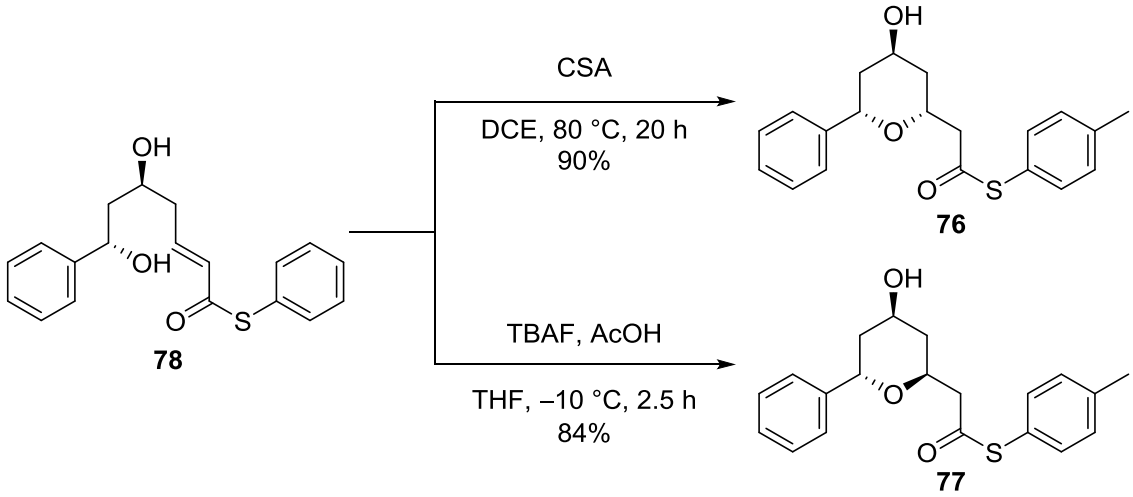

Scheme 33 Stereoselective oxy-Michael addition to form di-substituted tetrahydropyran rings **76** and **77**.

Treatment of *α,β*-unsaturated thioester **78** with CSA formed the corresponding *cis*-tetrahydropyran product **76** in 90% yield. While, cyclisation of thioester **78** under buffered fluoride conditions resulted in *trans*-tetrahydropyran product **77** in 84% yield (**Scheme 33**). The products were confirmed by both 1-D, 2-D NMR spectroscopy and mass spectrometry and the data were consistent with previous findings of stereodivergent reactions reported by our group. Under TBAF-mediated conditions gave the 2,6-*trans*-tetrahydropyran, however under acid-mediated conditions 2,6-*cis*-tetrahydropyran was obtained. Giving access to both *cis*- and *trans*-tetrahydropyran rings from the same starting material.[41]

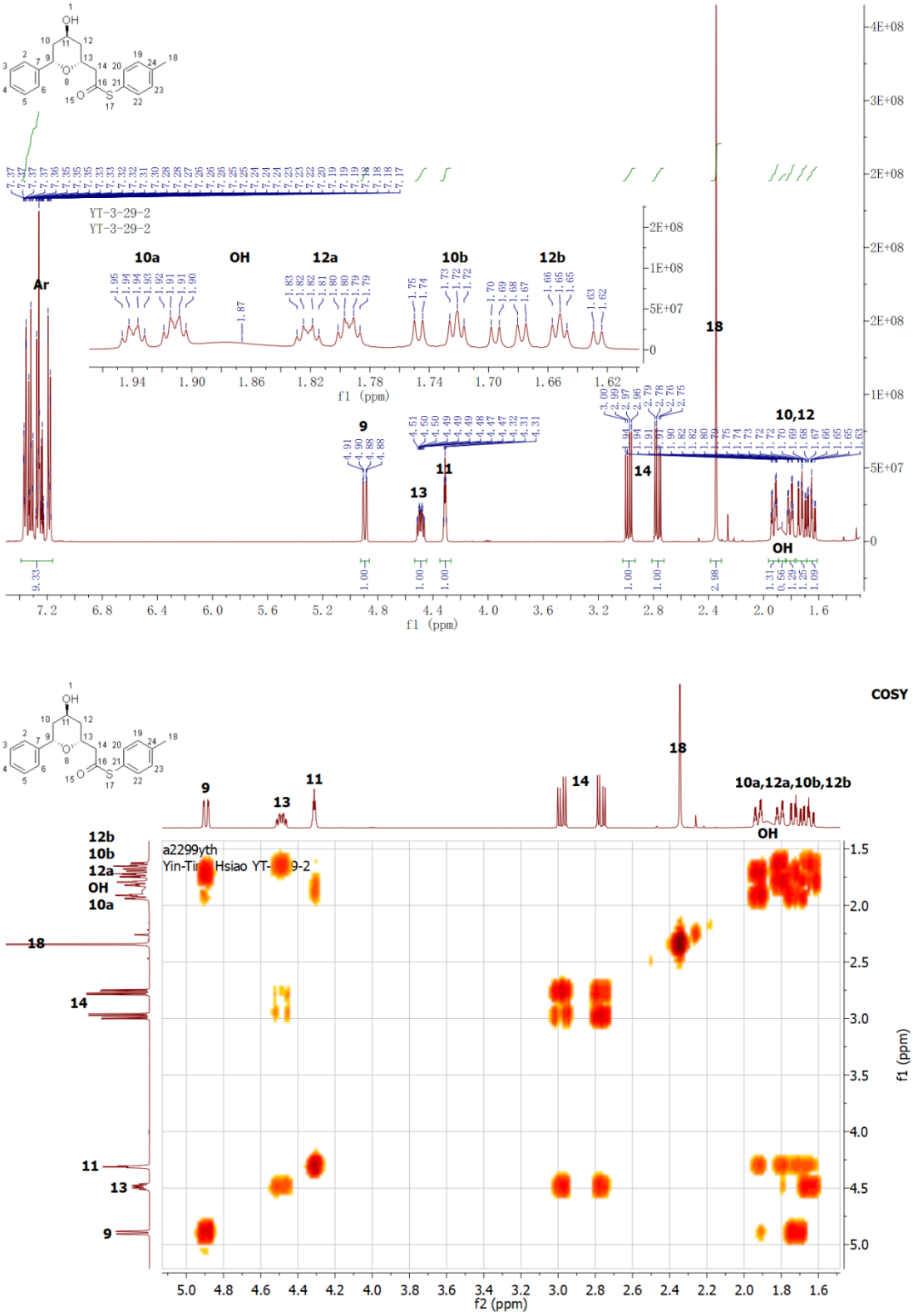

Figure 11 ^{1}H and ^{1}H-^{1}H COSY NMR spectra of the *cis*-tetrahydropyran product **76**.

The ^{1}H NMR spectrum peaks at 7.37-7.17 ppm, which were assigned as the aromatic protons. A double-doublet peak at 4.89 ppm was assigned as H-9. Correlation of H-9 in the COSY spectrum was shown with peaks at 1.95-1.90 ppm and 1.72 ppm, which were assigned as H-10a and H-10b with the coupling constants of 2.2 Hz and 11.8 Hz, respectively. Both H-10a and H-10b correlated with the peak at 4.31 ppm, which was assigned as H-11 with a coupling constant of 2.8 Hz. Correlation of H-11 in the COSY spectrum was shown with peaks at 1.83-1.79 ppm and 1.65 ppm and were assigned as H-12a and H-12b with a coupling constant of 2.8 Hz. Correlation of H-12a and H-12b in the COSY spectrum was shown with peaks at 4.49 ppm, which were assigned as H-13 with the coupling constants of 2.1 and 11.7 Hz. H-13 correlated with H-14a and H-14b at 2.98 and 2.77 ppm with the coupling constants of 6.9 and 6.0 Hz (**Figure 11** and **Figure 12**).

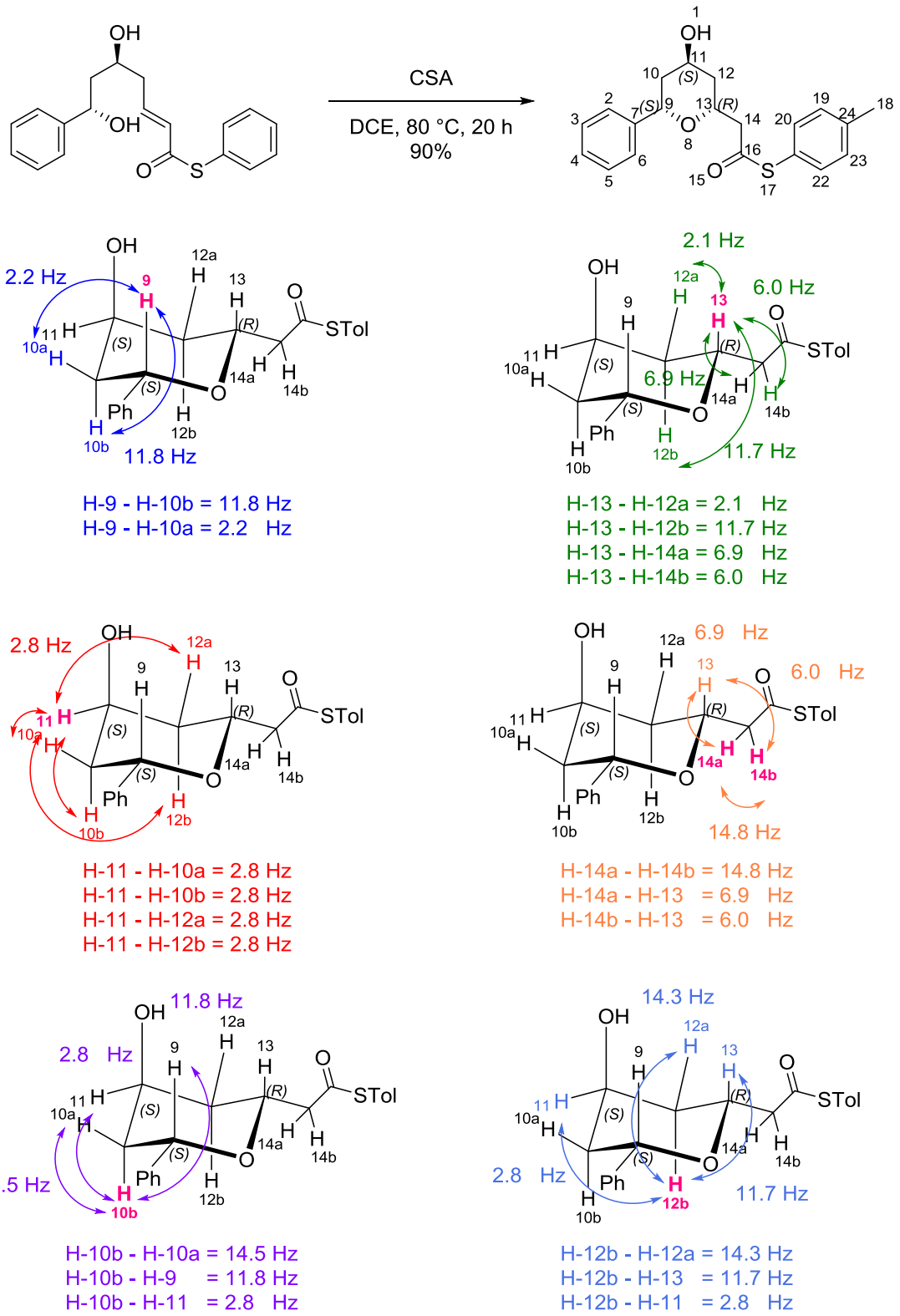

Figure 12 Coupling constants of the *cis*-tetrahydropyran product **76**.

The structure of *trans*-tetrahydropyran product **77** was also elucidated by the same method (**Figure 13** and**Figure 14**).

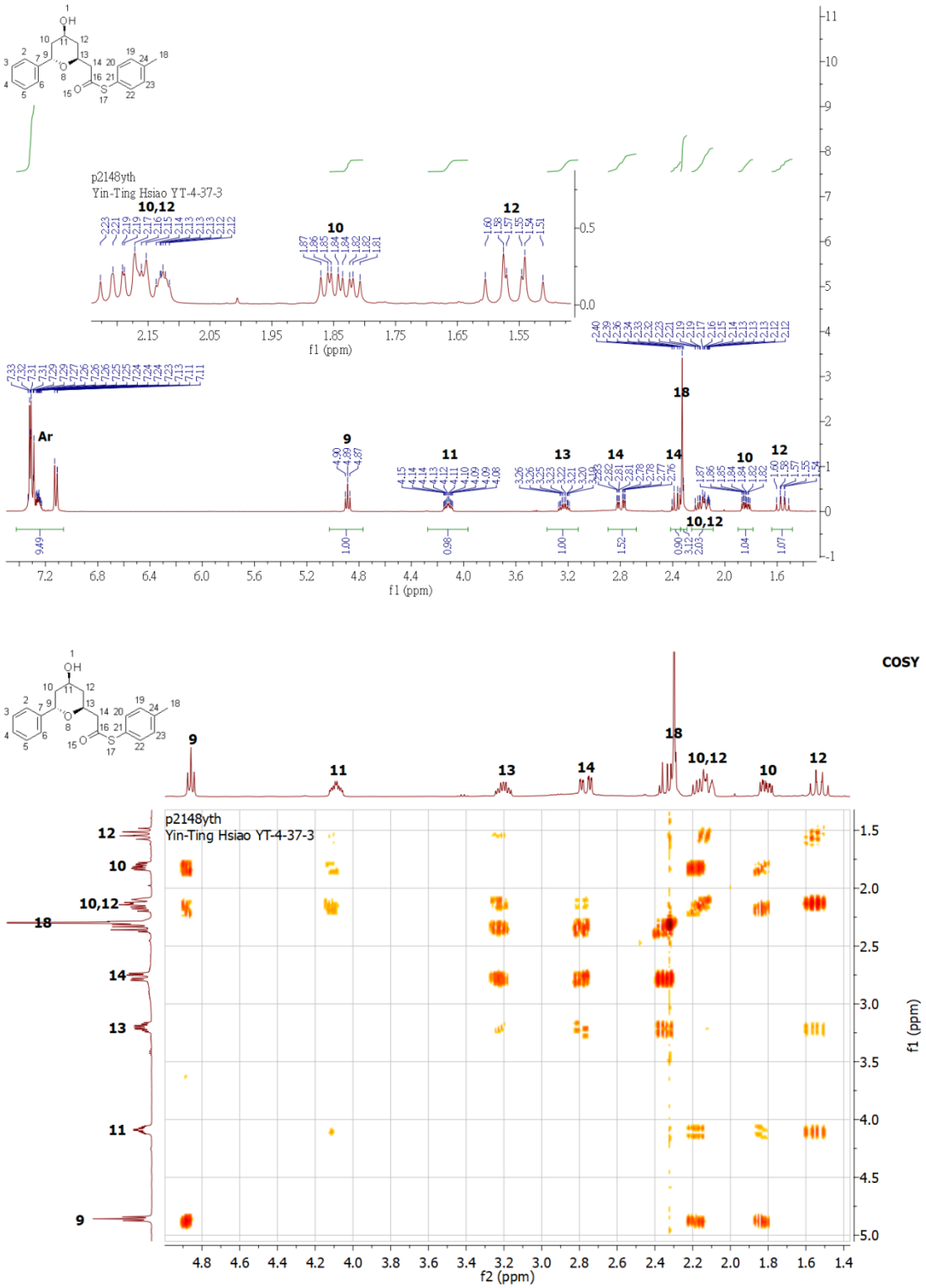

Figure 13 ^{1}H and ^{1}H-^{1}H COSY NMR spectra of the *trans*-tetrahydropyran product **77**.

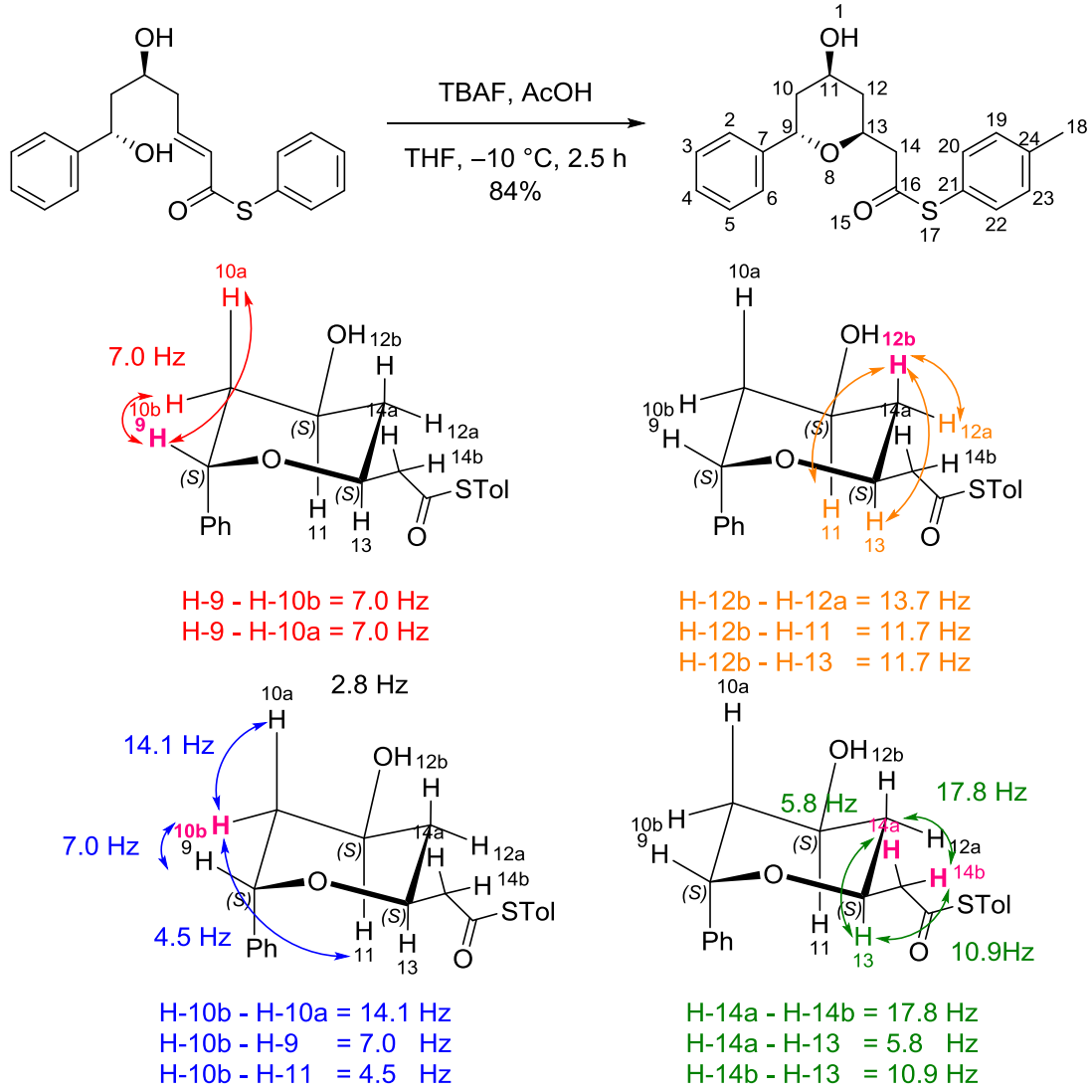

Figure 14 Coupling constants of the *trans*-tetrahydropyran product **77**.

The ^{1}H NMR spectrum exhibited peaks at 7.33-7.11 ppm range which referred to the aromatic protons. A double-doublet peak at 4.89 ppm was assigned as H-9. Correlation of H-9 in the COSY spectrum was shown with peaks at 2.23-2.21 ppm and 1.84 ppm, and were assigned as H-10a and H-10b with a coupling constant of 7.0 Hz for both. Both H-10a and H-10b correlated with the peak at 4.15-4.08 ppm, which was assigned as H-11. H-10b and H-11 had a coupling constant of 4.5 Hz. In the COSY

spectrum, H-11 correlated with peaks at 2.23-2.21 ppm and 1.56 ppm, which were assigned as H-12a and H-12b, respectively. H-11 and H-12b had a coupling constant of 11.7 Hz. Correlation of H-12a and H-12b was shown with peaks at 3.29-3.19 ppm and were assigned as H-13. H-12b and H-13 had a coupling constant of 11.7 Hz. H-13 correlated with H-14a and H-14b at 2.80 ppm and 2.36 ppm, respectively. H-14b and H-13 had a coupling constant of 10.9 Hz. Because the peaks of H-11, H-13, H-10a and H-12a in NMR spectrum were multiplets, corresponding coupling constants could not be obtained.

The stereochemistry of both the *cis*-tetrahydropyran product **76** and *trans*-tetrahydropyran product **77** were confirmed by NOE correlation. It was presumed that the H-9 should have the NOE correlation to H-13 in the *cis*-tetrahydropyran **76** product.

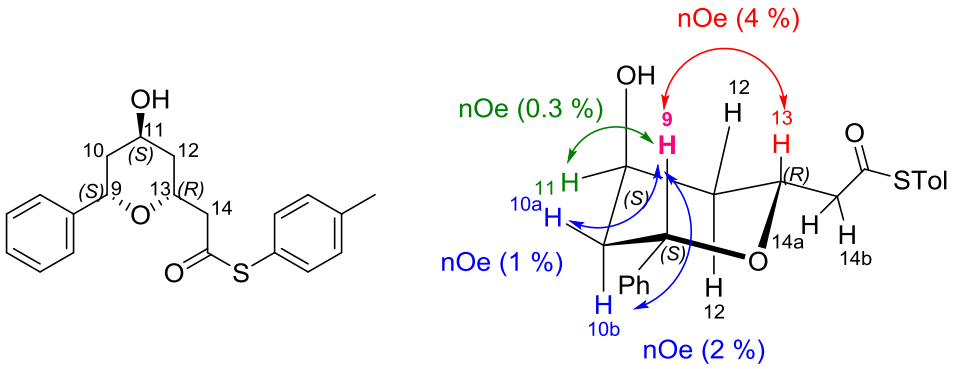

76 **92**

Figure 15 NOE correlation of the *cis*-tetrahydropyran **76**.

As expected, irradiation of H-9 was found to have large correlation (4%) with H-13 **92**. These two protons were oriented from the same side in spce. The H-9 also correlated with H-11 (0.3%) and H-10 (2%), which confirmed the stereochemistry of compound

76 as *cis*-tetrahydropyran (**Figure 15**).

It was assumed that the H-9 in the *trans*-tetrahydropyran product **77** would not correlate with H-13, instead a correlation was expected between H-11 and H-13 in the *trans*-tetrahydropyran product **77**, which was not present in the *cis*-tetrahydropyran **76** product.

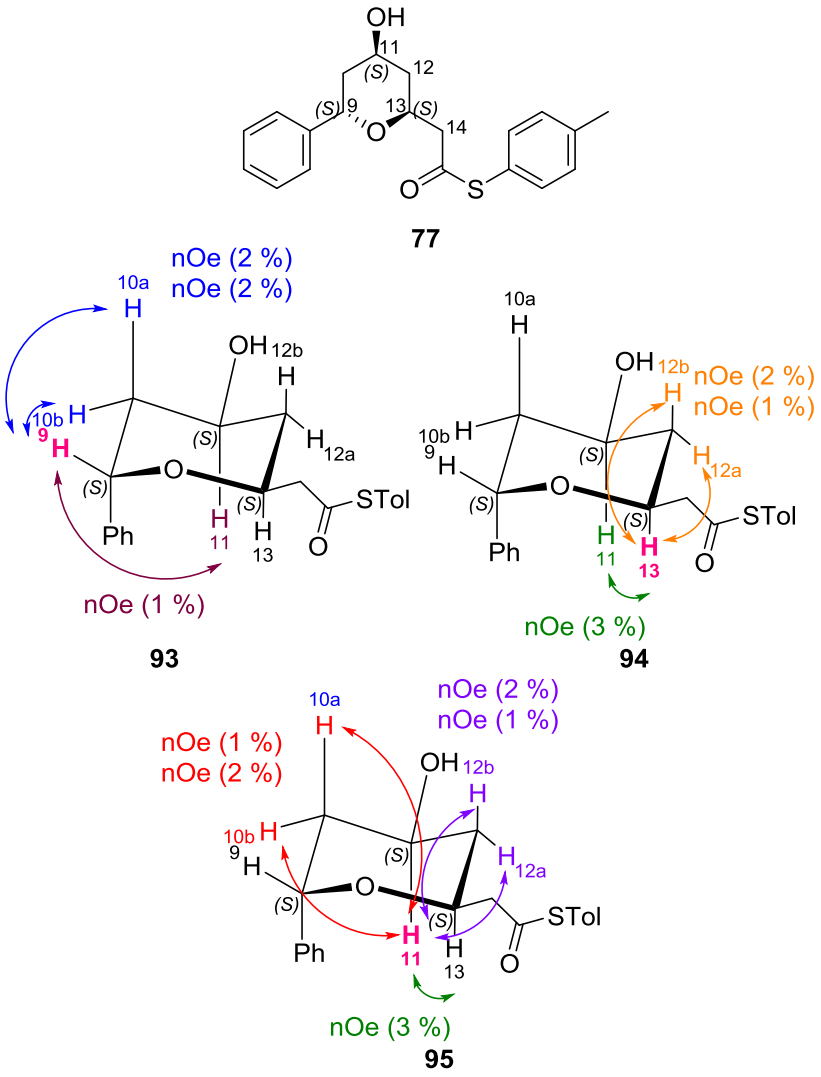

Figure 16 NOE correlation of the *trans*-tetrahydropyran product **93**.

Irradiation of H-9 of the *trans*-tetrahydropyran product **77**, no NOE correlation was observed between H-9 and H-13 (**93**), H-9 only correlated with H-11 (1%) and H-10 (2%). The *trans* configuration was further confirmed by irradiation of H-13 (**94**). H-13 correlated with H-12a (2%), H-12b (1%) and H-11 (3%) which supported the findings that H-13 and H-11 were on the same side. Irradiation of H-11 (**95**), showed a correlation with H-13 (3%), H-12a (2%), H-12b (1%), H-10a (1%) and H-10b (2%) confirming that the compound had the *trans*- stereochemistry (**Figure 16**).

In 2000, Liebeskind and Srogl presented a new reaction for the synthesis of ketones.[47, 60] The palladium-catalysed cross-coupling reaction between a thioesters **96** and a boronic acids **97** proceeded in the presence of a copper co-catalysts to generate the corresponding ketones **98** (**Scheme 34**).

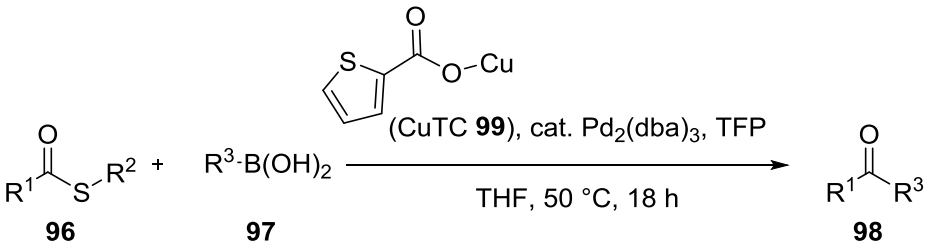

Scheme 34 Ketones synthesis by the Liebeskind–Srogl reaction.[47, 60]

Although the mechanism remains unclear, the ternary complex **100** as the reactive key intermediate was proposed by Liebeskind in 2004 (**Figure 17**).[47] The soft copper (I) **99** reagent was shown to have an important role in the reaction process. This was based on the fact that soft copper (I) **99** favoured to coordinate with sulfur **96**. As a thiophilic agent, CuTC **99** was assumed to help Pd–S bond polarised. The carboxylate group on CuTC **99** was also coordinated to boron **97**, which may help to activate the

boron compound (**Figure 17**).

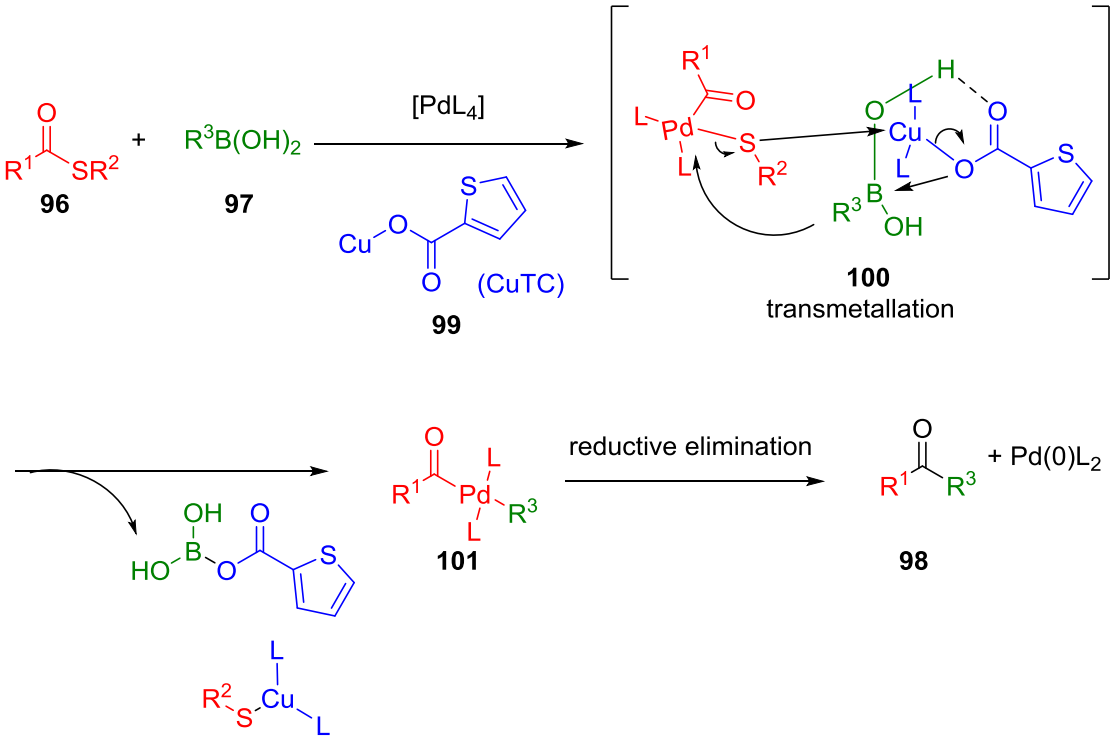

Figure 17 Proposed mechanism for the Liebeskind–Srogl reaction.[47, 60]

The synthesis of diospongin A **1** was carried out *via* a Liebeskind–Srogl reaction[47, 60] by following the procedure reported by Fuwa and co-workers to convert the thioester to the aryl ketone.[40, 61]

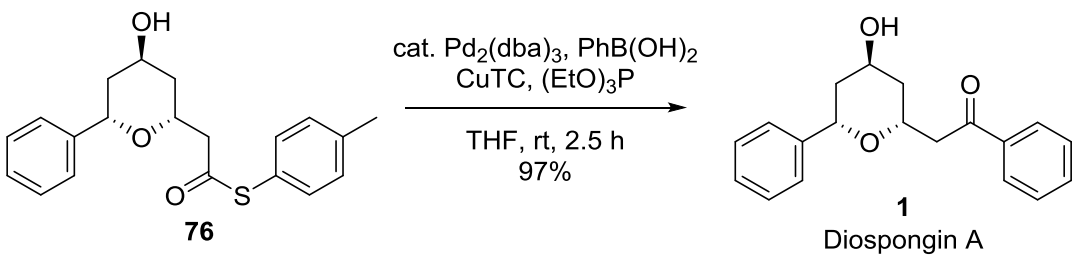

Scheme 35 Synthesis of diospongin A **1** *via* Liebeskind–Srogl reaction.

Treatment of *cis*-tetrahydropyran **76** with phenylboronic acid in the presence of commercially available CuTC, triethyl phosphite ligand and tris(dibenzylideneacetone)dipalladium(0) as a catalyst resulted in the desired diospongin A **1** at an excellent yield (97%) (**Scheme 35**).

The NMR data was consistent with those published in the isolation paper and the recent publication by Hashimoto and coworkers[22] and are presented in **Table 3**.

Table 3 Comparison of NMR data of diospongin A **1** between experimental and published data.[22]

Experimental data (500 MHz, $CDCl_3$)	**Literature[22] (500 MHz, $CDCl_3$)**
7.98 (2H, dd, *J* = 5.2, 3.3 Hz, H-Ar)	7.99 (2H, dd, *J* = 7.4, 1.1 Hz)
7.56 (1H, t, *J* = 7.4 Hz, H-Ar)	7.56 (1H, t, *J* = 7.4 Hz)
7.46 (2H, t, *J* = 7.6 Hz, H-Ar)	7.45(2H, t, *J* = 7.4 Hz)
7.31-7.21 (5H, m, H-Ar)	7.32-7.21 (5H, m)
4.93 (1H, dd, *J* = 11.8, 2.0 Hz, H-6)	4.93 (1H, dd, *J* = 11.5, 1.7 Hz)
4.68-4.62 (1H, m, H-2)	4.65 (1H, dddd, *J* = 11.5, 6.9, 5.7, 1.7 Hz)
4.38 (1H, p, *J* = 2.8 Hz, H-4)	4.37 (1H, quint, *J* = 2.9 Hz)
3.42 (1H, dd, *J* = 16.0, 5.8 Hz, H-1a)	3.42 (1H, dd, *J* = 16.0, 5.7 Hz)
3.07 (1H, dd, *J* = 16.0, 6.8 Hz, H-1b)	3.07(1H, dd, *J* = 16.0, 6.9 Hz)
1.99-1.93 (2H, m, H-3a, H-5a)	1.98-1.94 (2H, m)
1.76 (1H, ddd, *J* = 14.4, 11.8, 2.8 Hz, H-5b)	1.76 (1H, ddd, *J* = 14.3, 12.0, 2.9 Hz)
1.69 (1H, ddd, *J* = 14.2, 11.4, 2.8 Hz, H-3b)	1.68 (1H, ddd, *J* = 13.8, 11.5, 2.3 Hz)

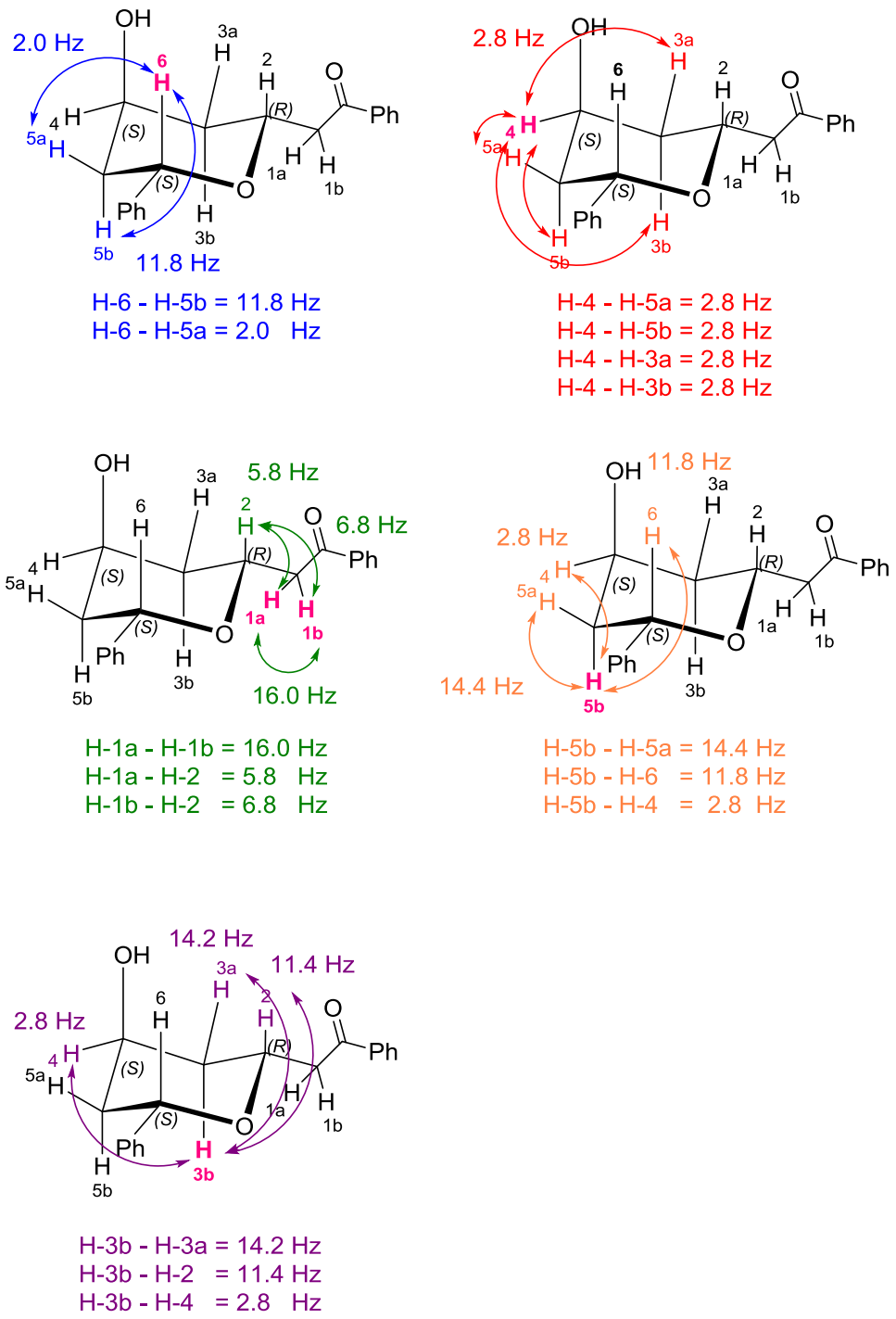

Figure 18 ^{1}H-^{1}H coupling constants of diospongin A **1**.

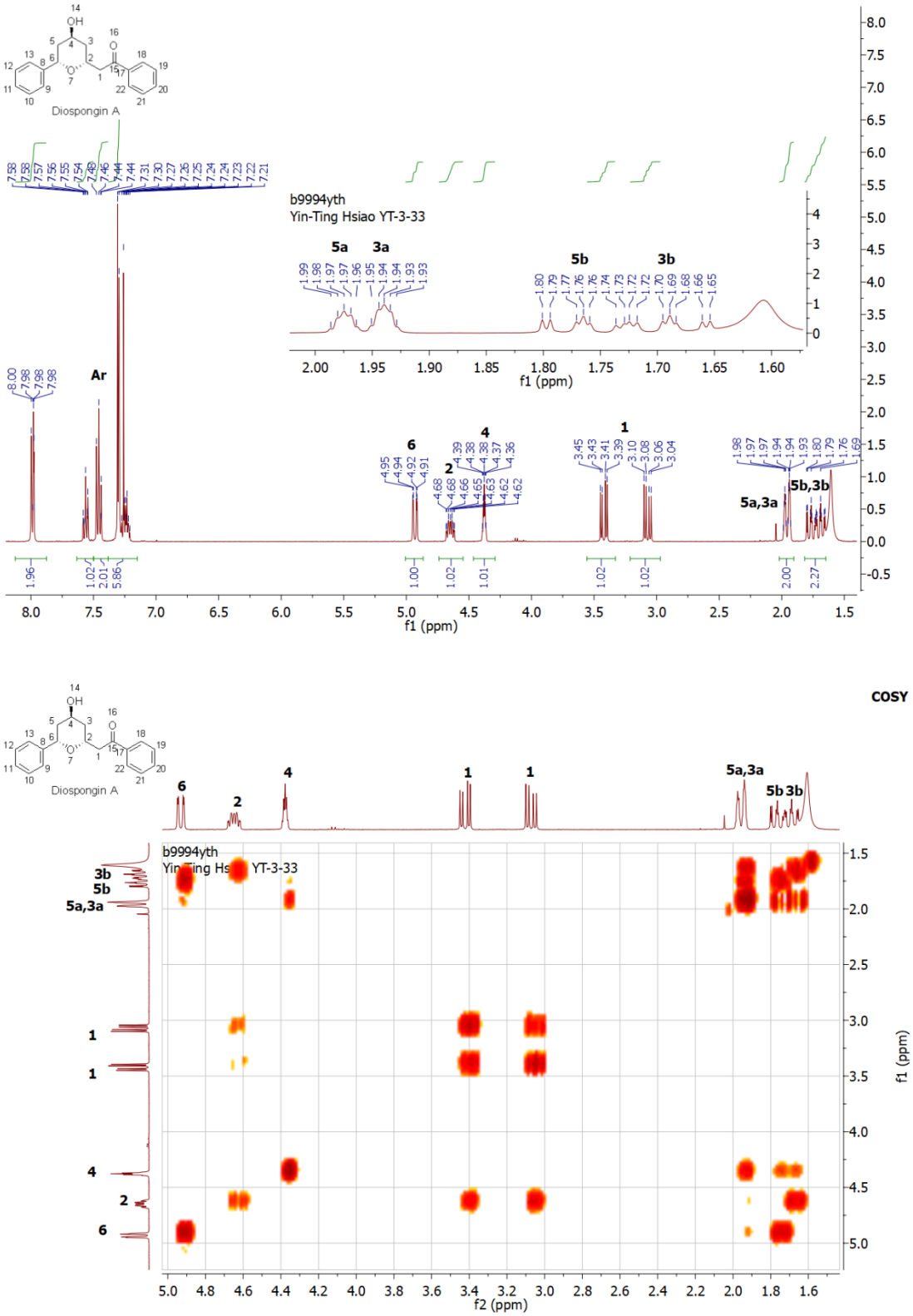

Figure 19 ^{1}H and ^{1}H-^{1}H COSY NMR spectra of diospongin A **1**.

The ^{1}H NMR spectrum exhibited peaks at 8.00-7.21 ppm which were assigned as aromatic protons. A double-doublet peak at 4.93 ppm was assigned as H-6. Correlation of H-6 was shown with peaks at 1.99-1.96 ppm and 1.76 ppm, and were assigned as H-5a and H-5b with the coupling constants of 2.0 Hz and 11.8 Hz, respectively. Both H-5a and H-5b correlated with the peak at 4.38 ppm, which was assigned as H-4 with a coupling constant of 2.8 Hz. Correlation of H-4 in the COSY spectrum was shown with peaks at 1.95-1.93 ppm and 1.69 ppm, and were assigned as H-3a and H-3b with a coupling constant of 2.8 Hz. Correlation of H-3 in the COSY spectrum was shown with peaks at 4.68-4.62 and was assigned as H-2 with a coupling constant of 11.4 Hz. H-2 showed correlation with H-1 at 3.42 ppm and 3.07 ppm with the coupling constants of 6.8 Hz and 5.8 Hz (**Figure 19**).

Attempts to prepare diospongin B **2** using the same coupling conditions were unsuccessful. Disappointingly, the reaction did not proceed and only starting material was recovered, even when catalyst loadings (**Table 4**, **Entries 1** and **2**), temperature (**Table 4**, **Entries 2** and **5**) and reaction times (**Table 4**, **Entries 1** and **3**) were increased.

Table 4 Conditions applied to the synthesis of diospongin B **2**.

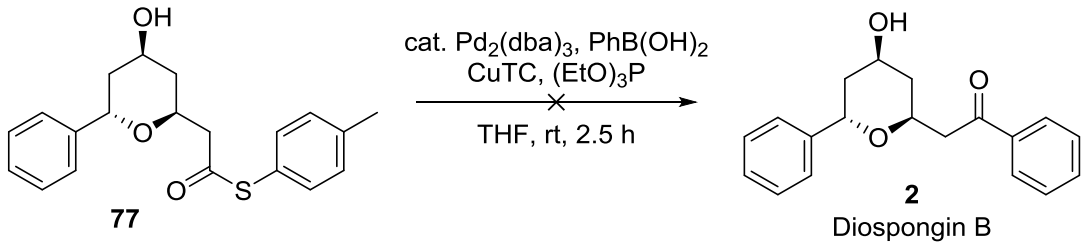

Entry	$Pd_2(dba)_3$ /mol%	$PhB(OH)_2$ /eq.	CuTC /eq.	$(EtO)_3P$ /eq.	Time /h	Temperature	Result
1	5	1.5	1.5	4	24	rt	starting material[1]
2	10	1.5	1.5	8	24	rt	starting material[1]
3	5	1.5	1.5	4	48	rt	starting material[1]
4	10	3.0	3.0	8	24	rt	starting material[1]
5	10	1.5	1.5	8	24	reflux	starting material[1]

1. [1]Fully recovered and characterised

Changing the ligand from triethyl phosphite to Xphos or tri(o-tolyl) phosphine also did not result in a discernible formation of product and only starting material was recovered.

Given that the attempt to use the reaction conditions published by Liebeskind and Srogl.[60] The reaction was instead treated with TFP as a ligand. However, this reaction also failed to generate the desired product **2**.

Next, the conversion of the thioester **77** to the desired phenyl ketone **2** was attempted by using Fukuyama coupling (**Scheme 36**).[62]

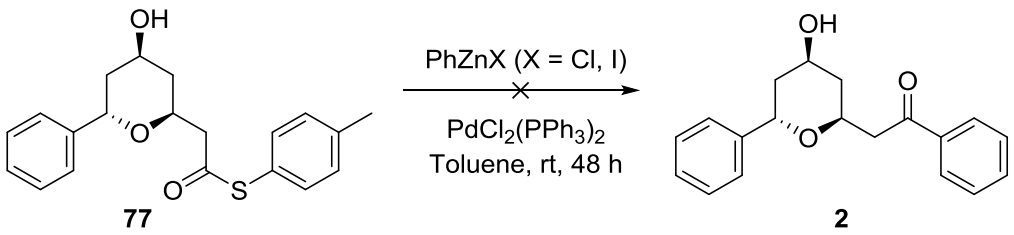

Scheme 36 Attempted synthesis of diospongin B **2** *via* Fukuyama coupling.

Initially, the thioester **77** was coupled with phenylzinc chloride in the presence of bis(triphenylphosphine)palladium(II) dichloride in toluene. The phenylzinc chloride was synthesised by treating zinc chloride with phenyllithium solution. The coupling reaction was monitored by TLC, and after 48 hours the starting material was fully consumed and several products were formed at room temperature. Comparing the crude ^{1}H NMR data to published data,[33] indicated that no diospongin B **2** had been formed. The purification process was challenging; therefore, no identifiable products were isolated. The Fukuyama coupling reaction was also attempted by treating thioester **77** with commercially available 5 M phenylzinc iodide solution. However, the reaction also did not result in any products of interest.

Alternative routes for the synthesis of diospongin B **2** were carried out according to another procedure reported by Liebeskind and Srogl.[63] Cross-coupling the thioesters **102** with organostannanes **103** with CuDPP **109**, tris(dibenzylideneacetone)dipalladium(0) and TFP may provide the corresponding ketones **104** (**Scheme 37**).

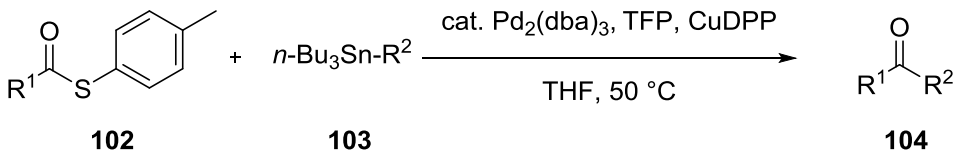

Scheme 37 Ketones synthesis by coupling of thioesters and organostannanes.

A model study was conducted before applying the Liebeskind organostannane conditions to our system. The dodecanethioic acid *S*-*p*-tolyl ester **107** was chosen as the starting material for the model study because this starting was easy to synthesis and was one of examples shown in Liebeskind's paper.[63] The synthesis started with lauric acid **105** and thionyl chloride to generate acid chloride **106**, which was then treated with 4-methylbenzenethiol **90** to provide dodecanethioic acid *S*-*p*-tolyl ester **107** in a two-step sequence in 64% yield (**Scheme 38**).

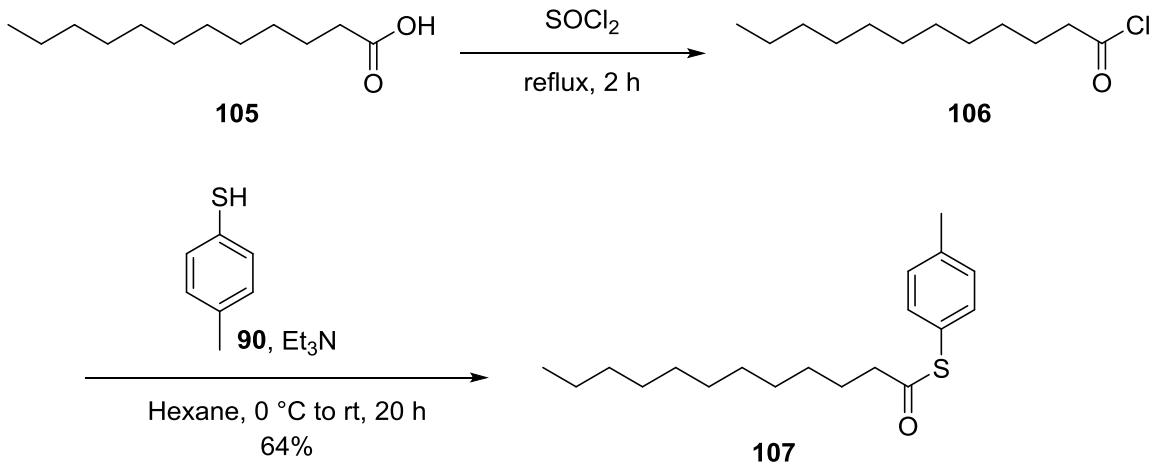

Scheme 38 Synthesis of dodecanethioic acid *S*-*p*-tolyl ester **123**.

The CuDPP **109** catalyst was synthesised by refluxing diphenylphosphinic acid **108** and copper(I) oxide in toluene according to a previously published procedure (**Scheme 39**).[63]

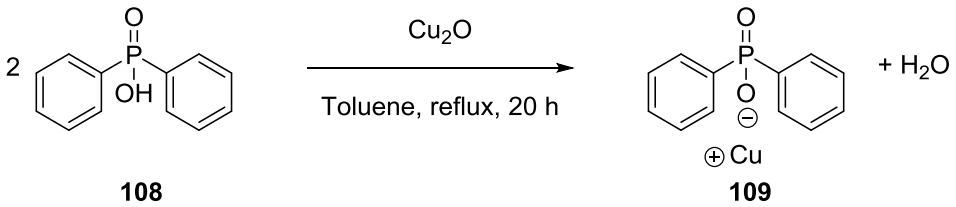

Scheme 39 Synthesis of Cu(I) diphenylphosphinate **109**.

After successful completion of the synthesis of CuDPP **109** and dodecanethioic acid *S*-*p*-tolyl ester **107**, the coupling reaction of dodecanethioic acid *S*-*p*-tolyl ester **107** with 2-(tri-*n*-butylstannyl)furan, which was reported by Liebeskind and Srogl, was attempted (**Scheme 40**).[63]

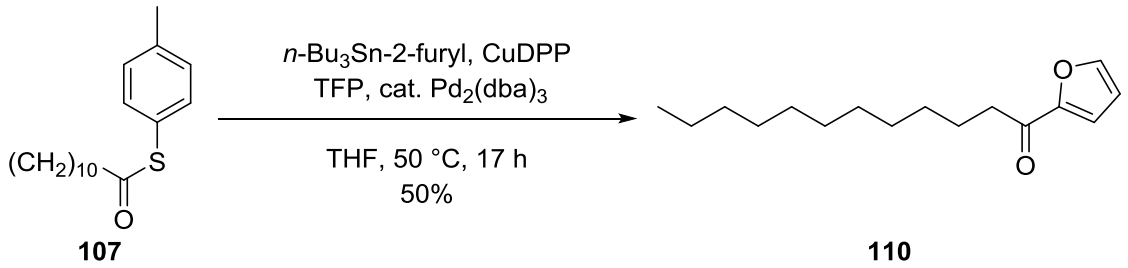

Scheme 40 Synthesis of ketone **110** for the model study.

The results show 1-furan-2-yl-dodecan-1-one **110** was successfully obtained and the ^{1}H NMR data corresponded to the paper.[63] Given that the model study was successful, the same batch of CuDPP **109** was directly used for the reaction system (**Scheme 41**).

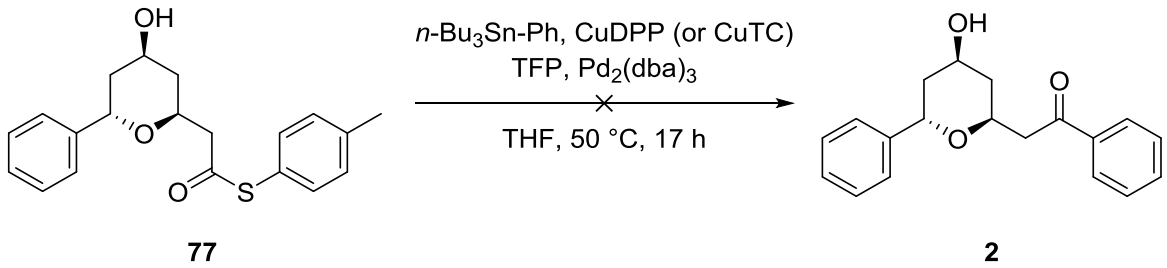

Scheme 41 Attempted synthesis of diospongin B **2** by using organostannane coupling with thioester **77** as reported by Liebeskind and Srogl.[63]

Using the same approach to the reaction with thioester **77** and tributylphenyltin, no observable reaction occurred, only the starting material was recovered. Moreover, the use of commercial sources of Cu(I) (CuTC), did not result in conversion to product (**Scheme 41**). Given the difficulty to direct conversion of **77** into diospongin B **2**, an alternative multi-step approach was adopted (**Scheme 42**).

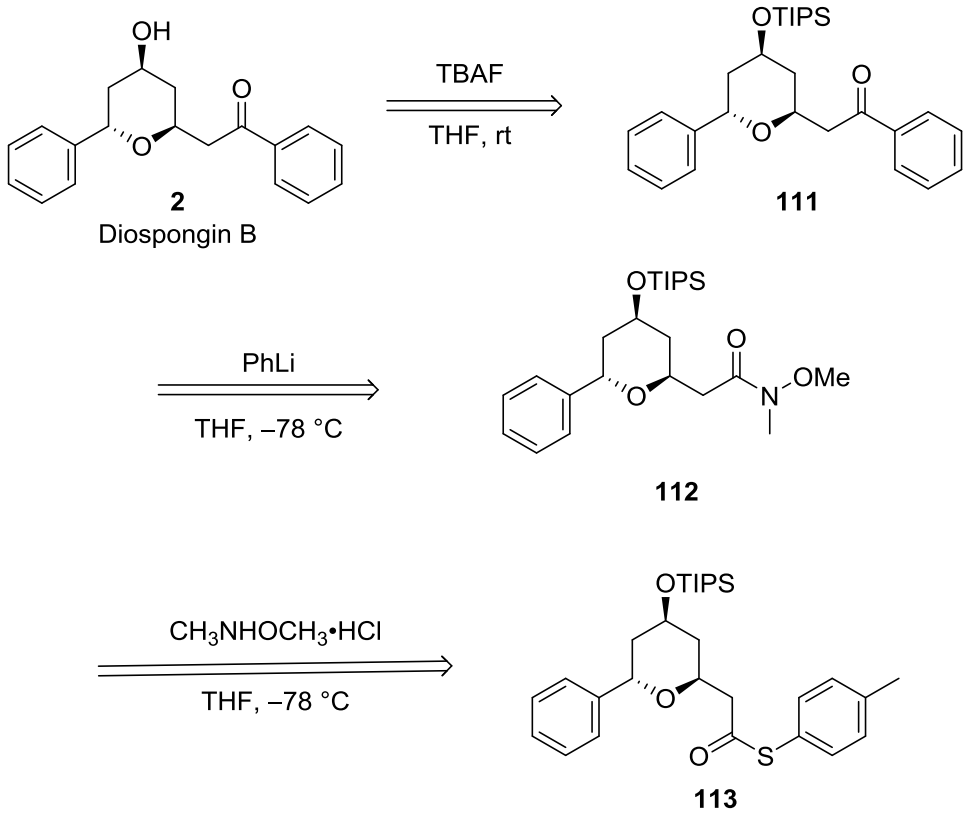

Scheme 42 Alternative routes to the synthesis of diospongin B **2**.

The revised synthesis of diospongin B **2** was proposed with the aim to form the Weinreb amide **112** from the protected thioester **113**, followed by addition of single equivalent of phenyl lithium and deprotection with TBAF to generate diospongin B **2** (**Scheme 42**).

Initially, TIPS protection of the free hydroxyl on **77** was investigated. Unfortunately, no reaction was observed even when using excess TIPSCl, imidazole (**Table 5**, **Entries 1**-**3**) and extended reaction times (**Table 5**, **Entries 2** and **3**).

Table 5 Conditions applied to the synthesis of **113**.

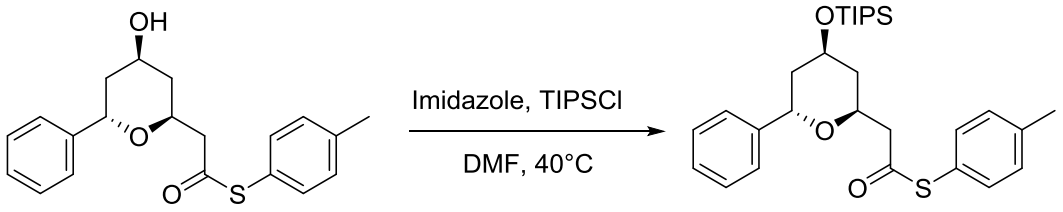

77 **113**

Entry	Im/eq.	TIPSCl/eq.	Times/h	Result
1	1.2	1.1	24	Starting material
2	3.6	3.0	24	Starting material
3	3.6	3.0	48	Starting material
4	10.8	9.0	72	2.3% yield

Only a trace amount (2.3%) of product detected when using 10.8 equivalents of imidazole and 9.0 equivalents of TIPSCl (**Table 5**, **Entry 4**). TLC analysis indicated that the reaction was not complete after being stirred for 3 days.

Attempts to protect the hydroxyl with TBSCl were also unsuccessful, the reaction was very slow and after 4 days, product **114** was only obtained in 15% yield (**Scheme 43**).

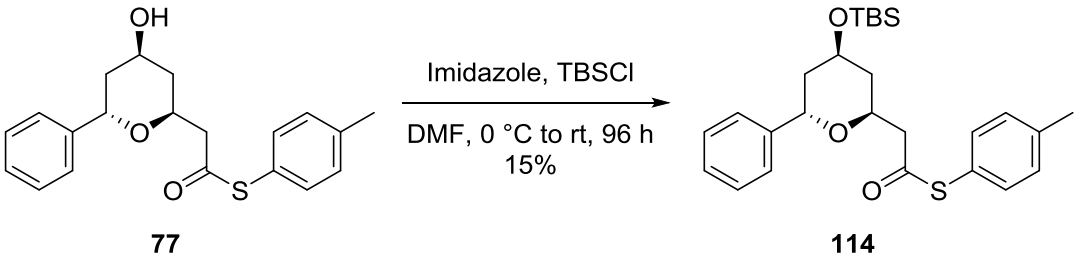

Scheme 43 Synthesis of TBS-protected thioester **114**.

Further studies investigated the use of TIPSOTf with pyridine in an attempt to protect the free hydroxyl group on **77** (**Scheme 44**). Subsequently, it was found that if the reaction was carried out with 2 equivalents of TIPSOTf in pyridine and that the desired product **113** was formed in 57% yield after a reaction time of 24 hours, however trace amounts of starting material were still observed. Attempts to push the reaction to completion with 4 equivalents of TIPSOTf after 24 hours, complete consumption of the starting material was observed, resulting in product **113** in 69% yield.

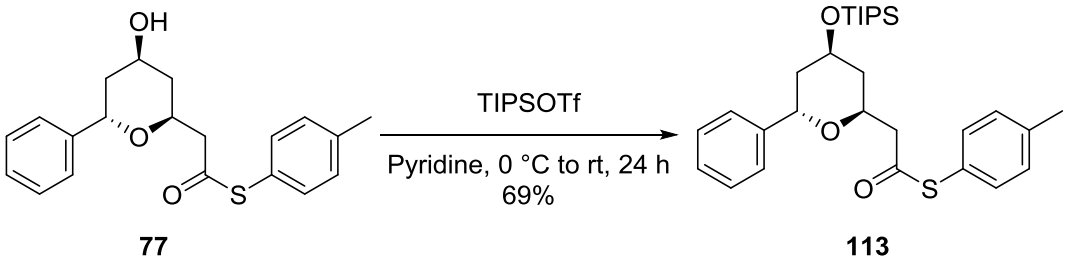

Scheme 44 Synthesis of TIPS-protected thioester **113**.

Weinreb amide **112** formation was attempted by adding N,O-dimethylhydroxyamide to **113** in THF (**Scheme 42**). The reaction mixture was monitored by TLC, and after 24 hours, TLC analysis of the reaction mixture indicated the presence of several different products. Analysis of the crude reaction mixture by ^{1}H NMR spectroscopy

resulted in a complex spectrum with no evidence for the formation of **112**.

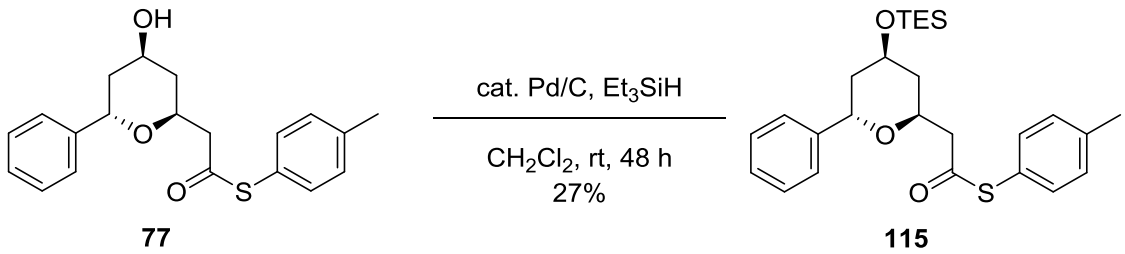

Scheme 45 Attempted synthesis of aldehyde **116** *via* Fukuyama reduction.

Next, the procedure reported by Fuwa was followed and we envisaged that reduction of the thioester **77** to aldehyde **116** may occurred *via* Fukuyama reduction by utilising palladium on carbon and triethylsilane.[40] Disappointingly, after 2 days, no reduction of the thioester was observed (**Scheme 45**). Only the TES-protected thioester was obtained **115**. Due to the failed reduction, alternative routes were sought to reduce the thioester **77** to aldehyde **116** by using DIBAL-H (**Scheme 46**).

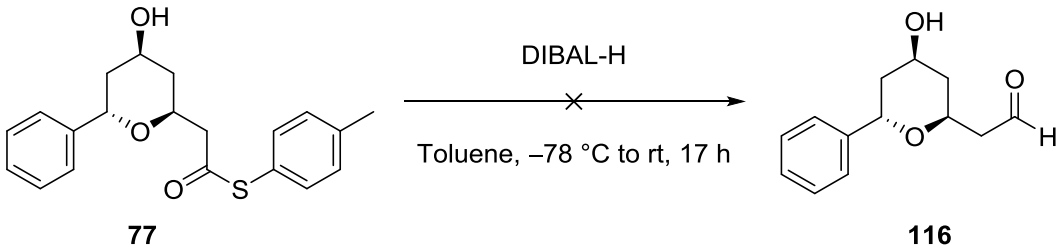

Scheme 46 Attempted synthesis of aldehyde **116**.

Difficulties were also encountered when DIBAL-H was used as the reductant. The reaction resulted in complex mixtures and with no aldehyde peak was observed in the ^{1}H NMR spectrum.

Due to the failed efforts to convert the thioester **77** to aldehyde **116** by using Fukuyama procedure and DIBAL-H reduction, attention was turned to reduction of the thioester **77** to alcohol **118**, followed by a literature procedure reported by Xian[18] to give access to generate diospongin B **2** (**Scheme 47**).

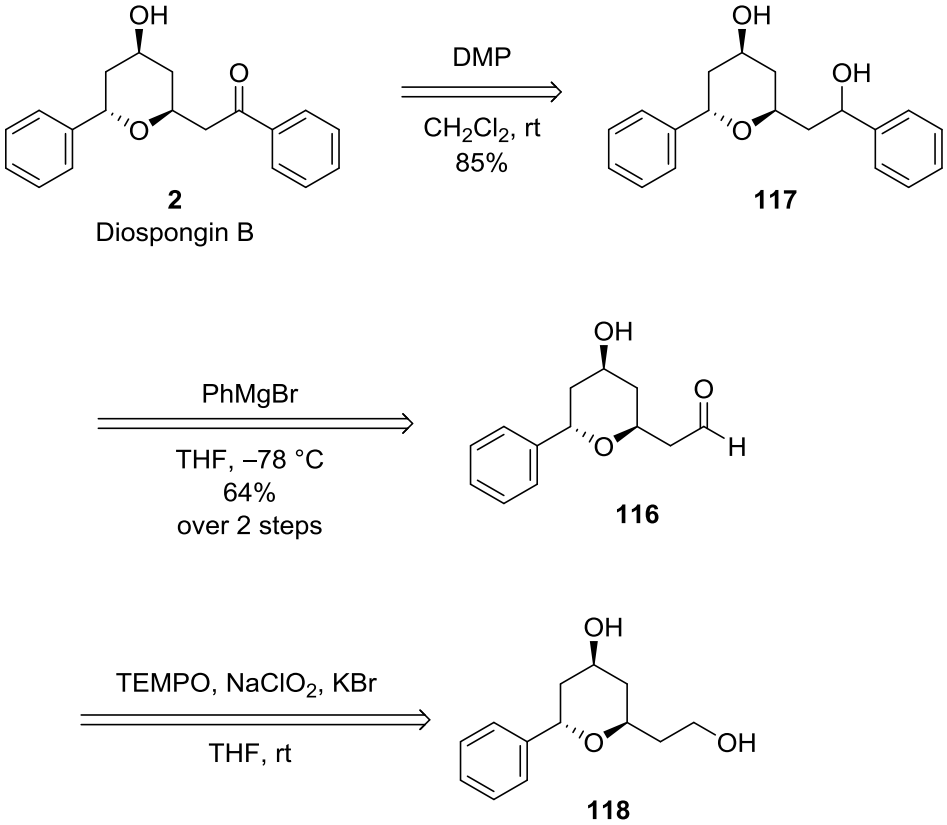

Scheme 47 Synthetic approach towards diospongin B **2** as proposed by Xian and co-workers.[18]

The Xian group proposed that synthesis of diospongin B **2** began with selective oxidation of the primary alcohol **118** by using TEMPO and sodium hypochlorite generated aldehyde **116**. Subsequently, **116** was transferred to **117** under the Grignard reaction. Finally, Dess–Martin oxidation was applied to complete the synthesis of diospongin B **2**.[18]

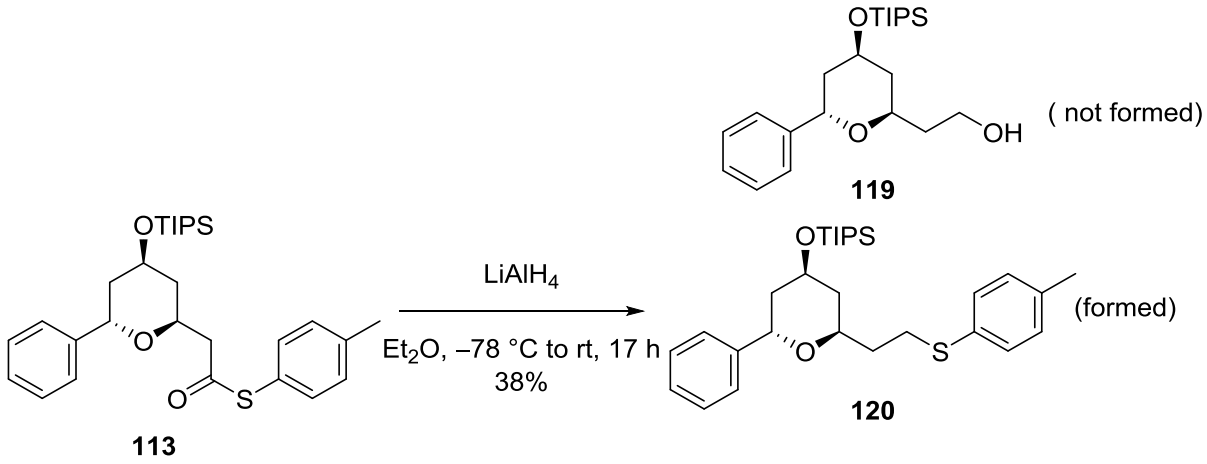

Scheme 48 Attempted synthesis of alcohol **119**.

Initial attempts to prepare alcohol **119** by treating protected thioester **113** with lithium aluminium hydride gave thioether **120** (**Scheme 48**). The structure of **120** was elucidated by using 1D, 2D NMR techniques and ^{1}H-^{1}H COSY spectroscopy (**Figure 20**). The ^{1}H NMR spectrum exhibited peaks in the 7-8 ppm which were assigned as aromatic protons. A triplet peak at 5.06 ppm which was assigned as H-9. Correlation of H-9 in the COSY spectrum was shown with peaks at 2.11-2.03 ppm and 1.78-1.54 ppm, which were assigned as H-10a and H-10b with a coupling constant of 6.8 Hz. Both H-10a and H-10b correlated with the peak at 4.16-4.11 ppm, which was assigned as H-11. H-11 in the COSY spectrum correlated with peaks at 1.78-1.54 ppm for one proton, which was assigned as H-12.The peak at 2.11-2.03 ppm was assigned to another proton of H-12. H-12 in the COSY spectrum correlated with peaks at 3.66-3.60, which was assigned as H-13. H-13 correlated with H-14 at 1.78-1.54 ppm. H-14 correlated with peaks at 3.58-3.51 ppm, and was assigned as H-15.

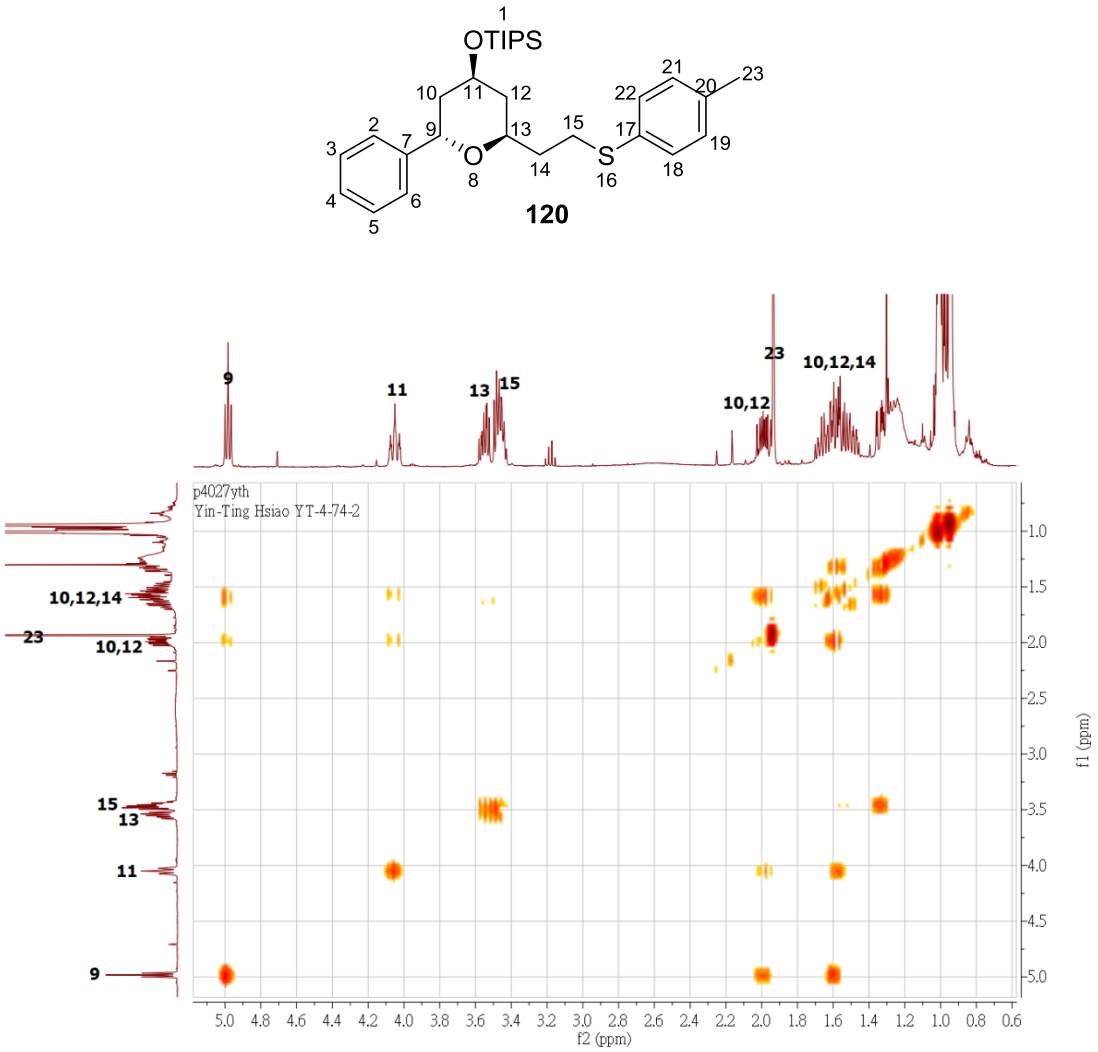

Figure 20 ^{1}H-^{1}H COSY spectrum of compound **120**.

Alternative methods for reducing thioester **113** with L-selectride® and sodium borohydride were considered. Surprisingly, with the use of different reducing reagents also resulted in the formation of thioether **120** (**Scheme 49**).

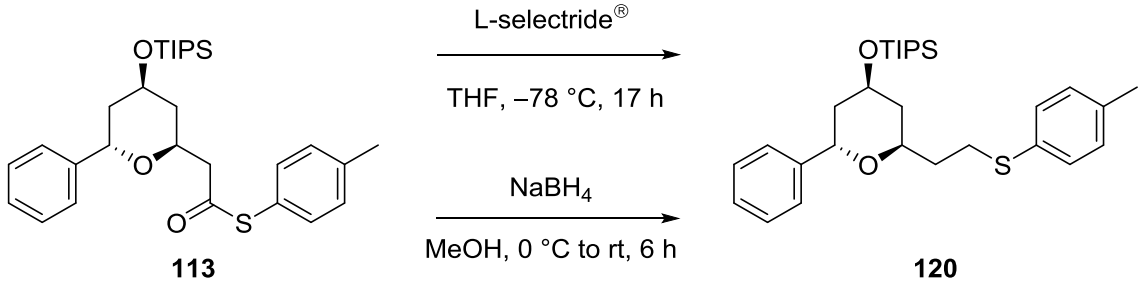

Scheme 49 Reduction of thioester **113**.

An alternative approach to synthesise diospongin B **2** was also attempted. The synthetic approach started with transesterification of the thioester **113** to ether **121**, followed by reduction, Grignard addition, benzylic oxidation with manganese dioxide and finally deprotection to form diospongin B **2** (**Scheme 50**).

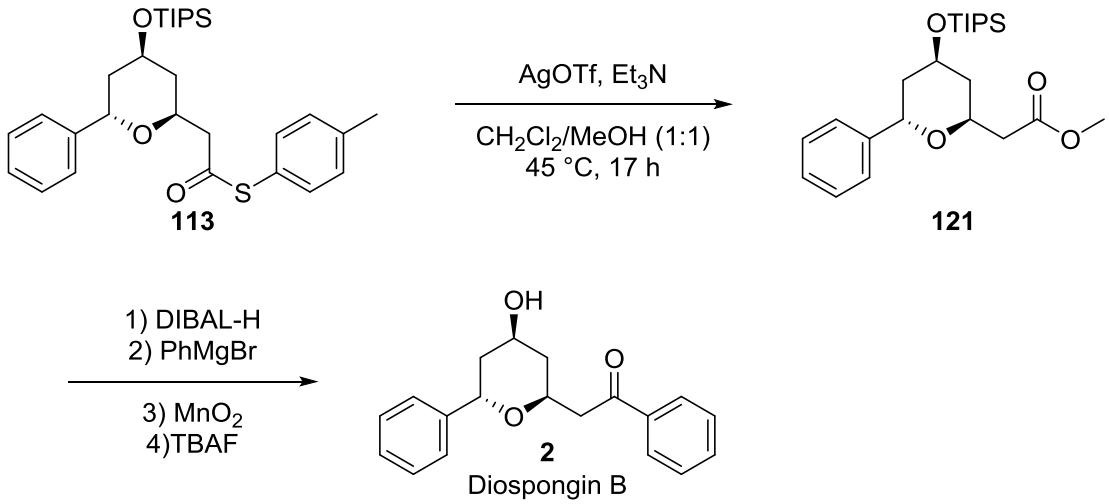

Scheme 50 Alternative approach to the synthesis of diospongin B **2** starting from transesterification of the thioester **113**.

The transesterification was attempted using a procedure reported by Hanessian.[64] The reaction was carried out by treatment of the thioester **113** with silver(I) trifluoromethanesulfonate in a 1:1 dichloromethane and methanol solvent system in the presence of triethylamine. Unfortunately, the reaction failed to provide the desired product **121.** Analysis of the crude reaction mixture by ^{1}H NMR spectrum resulted in a complex mixture, which made it challenging to isolate all the individual products (**Scheme 50**).

Table 6 Conditions applied to the synthesis of **111**.

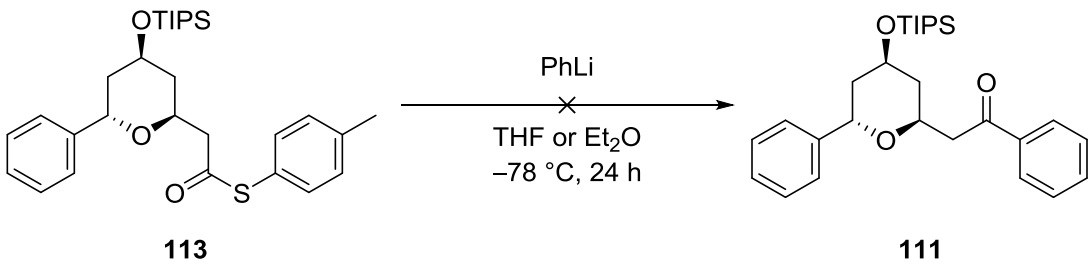

Entry	PhLi/eq.	Solvent	Additive	Result
1	1.1	THF	-	Complex mixture
2	1.5	THF	-	Complex mixture
3	2.0	THF	-	Complex mixture
4	1.1	THF	TMEDA	Complex mixture
5	1.1	Et_2O	-	Complex mixture
6	1.1	Et_2O	TMEDA	Complex mixture

It was assumed that the diospongin B **2** would be synthesised by phenyllithium addition. Several approaches to synthesise **111** *via* phenyllithium to **113** were

attempted. Surprisingly, different amounts of PhLi resulted in a complex mixtures, which was difficult to purify (**Table 6**, **Entries 1**-**3**). Using TMEDA as an additive (**Table 6**, **Entries 4** and **6**) as well as using different solvents (**Table 6**, **Entries 5** and **6**) were also attempted. However, these conditions resulted in the formation of many unknown products but were unsuccessful at generating the desired product **111**.

Finally, the synthesis of diospongin B **2** was completed by treating thioester **77** with phenyllithium (2.2 eq.) at −78 °C, which was warmed up to room temperature overnight to form diospongin B **2** in 55% yield (**Scheme 51**).

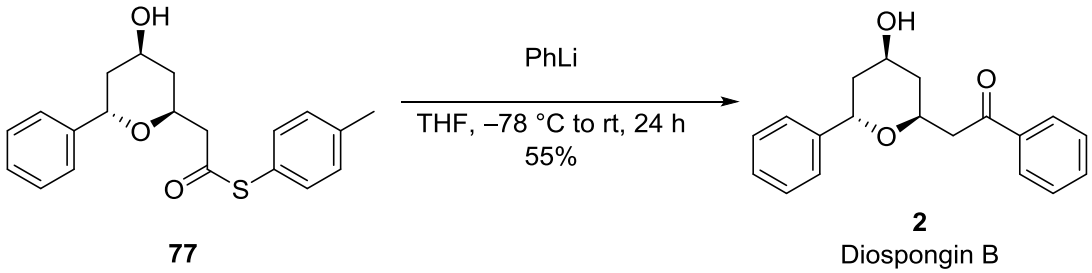

Scheme 51 Synthesis of diospongin B **2** with phenyllithium.

The NMR spectroscopic data of diospongin B **2** was consistent with those presented in the paper published by Tong and co-workers, as shown in **Table 7**.[33]

Table 7 Comparison of NMR data of diospongin B **1**.

Experimental data (500 MHz, $CDCl_3$)	**Literature[33] (500 MHz, $CDCl_3$)**
8.00-7.98 (2H, m, H-Ar)	8.01-7.94 (2H, m)
7.60-7.53 (1H, m, H-Ar)	7.62-7.55 (1H, m)
7.49-7.46 (2H, m, H-Ar)	7.51-7.44 (2H, m)
7.37-7.22 (4H, m, H-Ar)	7.37-7.31 (4H, m)
7.24-7.22 (1H, m, H-Ar)	7.25-7.19 (1H, m)
5.20 (1H, t, *J* = 4.3 Hz, H-6)	5.19 (1H, t, *J* = 4.3 Hz)
4.24 (1H, dddd, *J* = 9.5, 6.6, 7.0, 3.0 Hz, H-2)	4.23 (1H, ddt, *J* = 9.2, 6.6, 3.4 Hz)
4.06-4.00 (1H, m, H-4)	4.02 (1H, tt, *J* = 9.2, 4.2 Hz)
3.46 (1H, dd, *J* = 15.8, 7.0 Hz, H-1a)	3.45 (1H, dd, *J* = 15.7, 7.2 Hz)
3.18 (1H, dd, *J* = 15.8, 6.6 Hz, H-1b)	3.17 (1H, dd, *J* = 15.8, 6.0 Hz)
2.53 (1H, ddt, *J* = 13.8, 4.3, 1.7 Hz, H-5a)	2.52 (1H, dtd, *J* = 13.4, 3.8, 1.7 Hz)
2.09-2.04 (1H, m, H-3a)	2.11-2.01 (1H, m)
1.92 (1H, ddd, *J* = 13.8, 9.9, 4.3 Hz, H-5b)	1.92 (1H, ddd, *J* = 13.4, 9.8, 5.2 Hz)
-	1.73 (1H, br)
1.51 (1H, dt, *J* = 12.5, 9.5 Hz, H-3b)	1.51 (1H, dt, *J* = 12.6, 9.5 Hz)

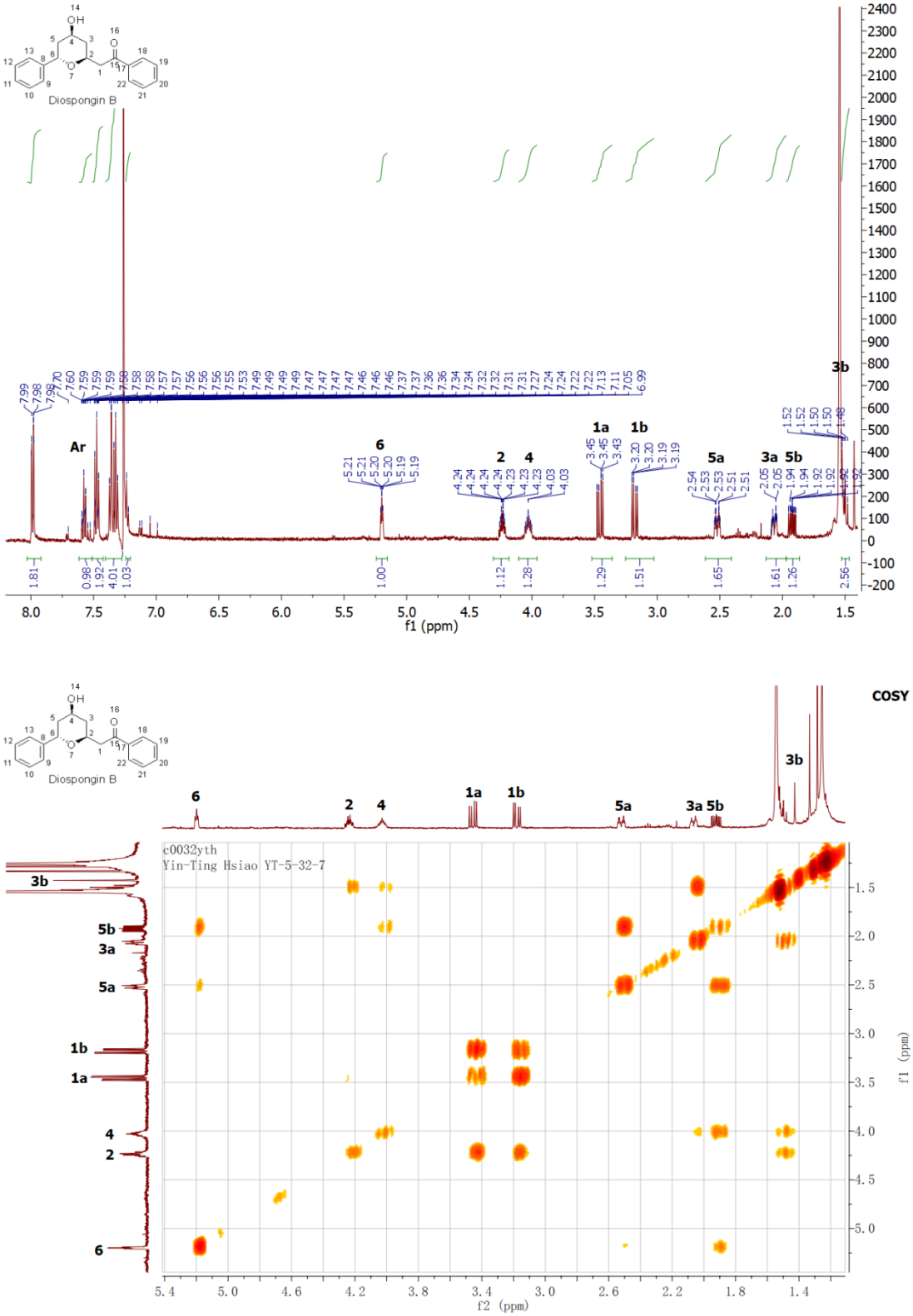

Figure 21 ^{1}H and ^{1}H-^{1}H COSY NMR spectra of diospongin B **2**.

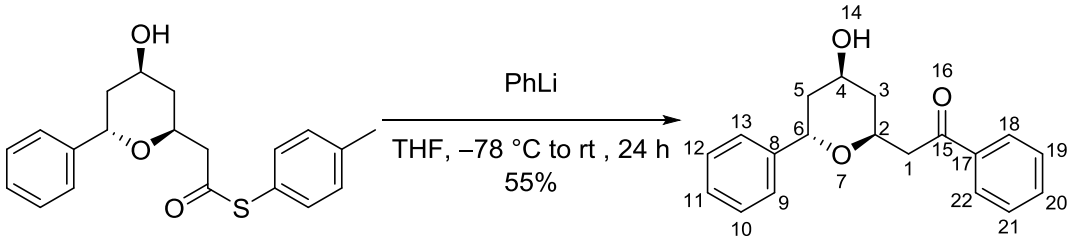

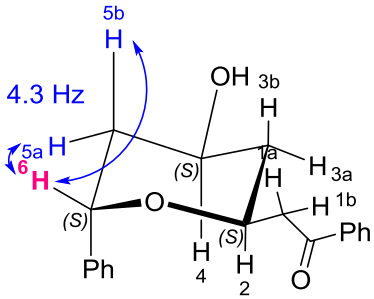

H-6 - H-5a = 4.3 Hz
H-6 - H-5b = 4.3 Hz

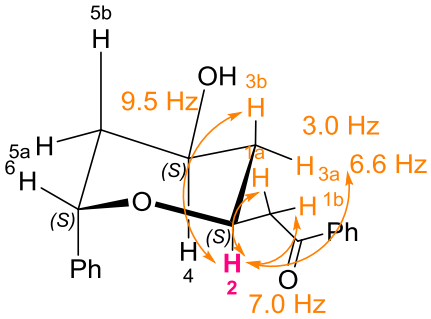

H-2 - H-3a = 3.0 Hz
H-2 - H-3b = 9.5 Hz
H-2 - H-1a = 7.0 Hz
H-2 - H-1b = 6.6 Hz

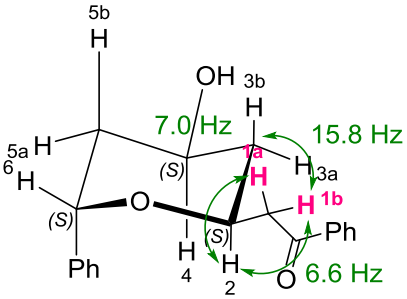

H-1a - H-1b = 15.8 Hz
H-1a - H-2 = 7.0 Hz
H-1b - H-2 = 6.6 Hz

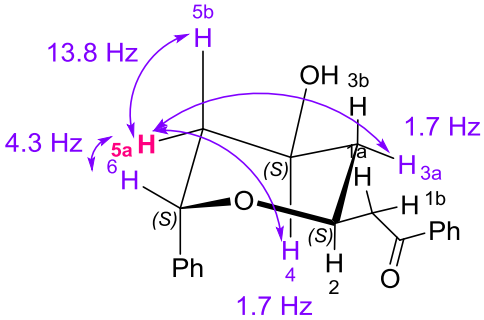

H-5a - H-5b = 13.8 Hz
H-5a - H-4 = 1.7 Hz
H-5a - H-3a = 1.7 Hz
H-5a - H-6 = 4.3 Hz

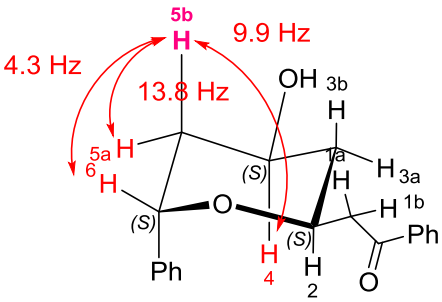

H-5b - H-5a = 13.8 Hz
H-5b - H-4 = 9.9 Hz
H-5b - H-6 = 4.3 Hz

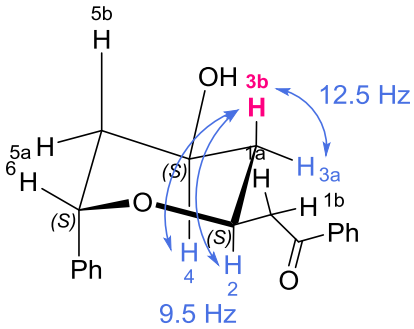

H-3b - H-3a = 12.5 Hz
H-3b - H-4 = 9.5 Hz
H-3b - H-2 = 9.5 Hz

Figure 22 Coupling constants of diospongin B **2**.

The structure of diospongin B **2** was elucidated by 1-D and 2-D NMR techniques with ^{1}H-^{1}H COSY spectroscopy (**Figure 22**). The ^{1}H NMR spectrum exhibited peaks at 8.00-7.22 ppm which were assigned as aromatic protons. A triplet peak at 5.20 ppm was assigned as H-6. Correlation of H-6 in the COSY spectrum were shown with peaks at 2.53 ppm and 1.92 ppm and were assigned as H-5a and H-5b, respectively, with a coupling constant of 4.3 Hz. Both H-5a and H-5b correlated with the peak at 4.06-4.00 ppm, which was assigned as H-4. Correlation of H-4 in the COSY spectrum was shown with peaks at 2.09-2.04 ppm and 1.51 ppm, and were assigned as H-3a and H-3b. H-3b and H-4 had a coupling constant of 9.5 Hz. Correlation of H-3a and H-3b in the COSY spectrum was shown with peaks at 4.24 ppm, whihc was assigned as H-2. H-3a and H-2 had a coupling constant of 3.0 Hz. H-3b and H-2 had a coupling constant of 9.5 Hz. H-2 correlated with H-1 at 3.46 ppm and 3.18 ppm with the coupling a constant of 7.0 Hz with H-1a, and a coupling constant of 6.6 Hz with H-1b (**Figure 22**).

1.2.4. Invesitigating the stereodivergent oxy-Michael cyclisation to *α,β*-unsaturated ketones

Thioesters are shown to be more enone-like compared to oxoesters because the oxygen lone pair of oxoesters has a better orbital overlap with C=O π*.[65] We decided to investigate the possibility of distereo divergence on an enone system. To test this hypothesis, ketones **122** and **123** were used as cyclisation precursors, which underwent both acid and buffered TBAF oxy-Michael cyclisation conditions (**Scheme 52**).

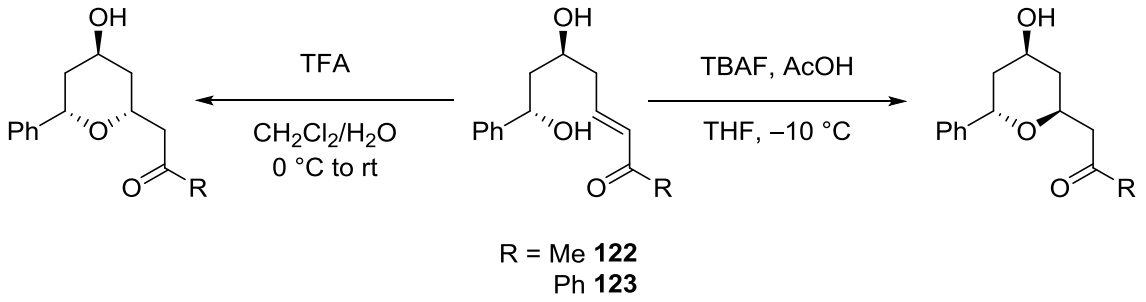

Scheme 52 Invesitigating the stereodivergent oxy-Michael cyclisation to ketones **122** and **123**.

Synthesis of ketones **122** and **123** is presented in (**Scheme 53** and **Scheme 56**).

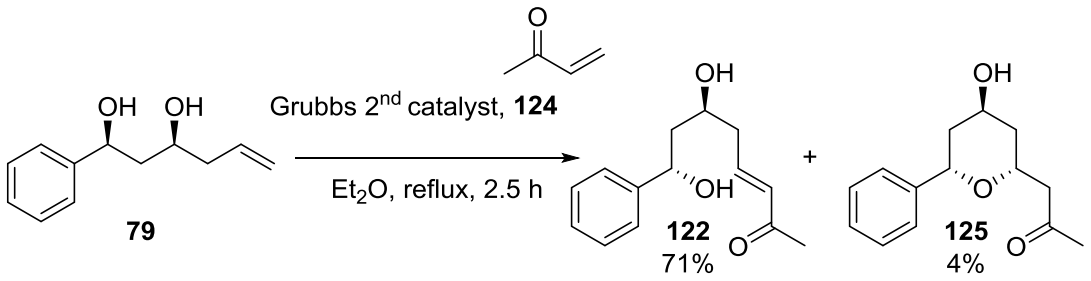

Scheme 53 Synthesis of ketone **122**.

Treatment of *syn*-diol **79** with excess 3-buten-2-one **124** using 10 mol% of 2nd generation of Grubbs catalyst in refluxing diethyl ether gave ketone **122** in a good isolated yield (71%), however the spontaneously cyclised product **125** was also formed in 4% yield. This may be due to the greater reactivity (lower LUMO) of the *α,β*-unsaturated ketone compared to the thioester.

The cross-metathesis substrate **128** was synthesised from acrolein **126** by the Grignard addition to form product **127** in a yields of 42%. Subsequently, manganese(IV) oxide oxidation provided **128** enone with a low yield of 10% (**Scheme 54**).

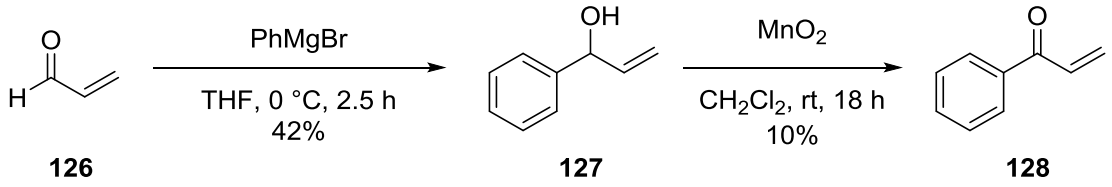

Scheme 54 Synthesis of 1-phenylprop-2-en-1-one **128**.

In order to improve the yield, an alternative reaction as proposed by Iwasa,[66] was considered (**Scheme 55**).

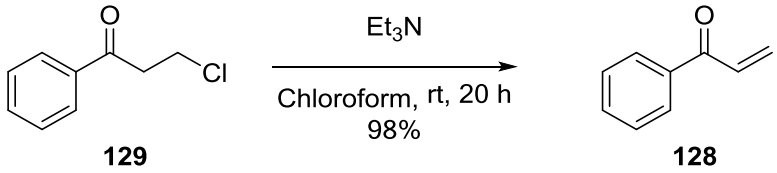

Scheme 55 Synthesis of 1-phenylprop-2-en-1-one **128** by following the procedure as reported by Iwasa and co-workers.[66]

Synthesis of **128** was instead carried out by treating 3-chloropropiophenone **129** with triethylamine in chloroform for 18 hours at room temperature. To our delight, **128** was successfully obtained in a high yield (98%).

Ketone **123** was obtained in a good isolated yield (65%) by treatment of *syn*-diol **79**, with excess of 1-phenylprop-2-en-1-one **128**, in the presence of 10 mol% of 2nd generation of Hoveyda-Grubbs catalyst in refluxing diethyl ether for 5 hours. The spontaneously cyclised product was also obtained in 30% yield. The phenyl enone was even more reactive (had a lower LUMO) compared to methyl enone, which was presumably due to conjugation.

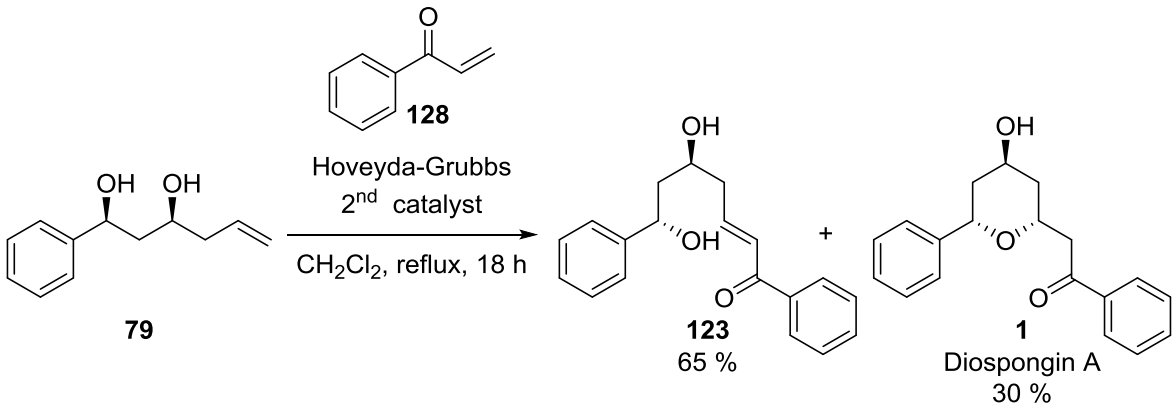

Scheme 56 Synthesis of ketone **123**.

With the cyclisation precursor **122** and **123** being synthesised, investigating the stereodivergent oxy-Michael reaction to ketones were performed under both TFA and buffered TBAF conditions (**Scheme 57** and **Scheme 58**).

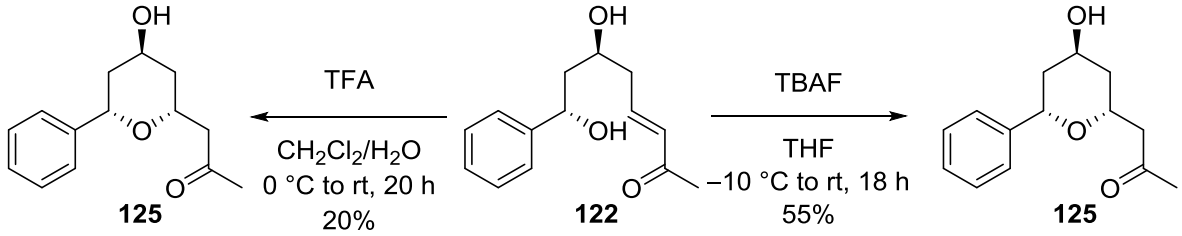

Scheme 57 Invesitigating the stereodivergent oxy-Michael cyclisation to ketone **122** under buffered TBAF and TFA conditions.

Treating ketone **122** with both TFA-mediated and buffered TBAF conditions only generated the *cis*-tetrahydropyran product **125**, where the stereodivergence phenomenon had disappeared.

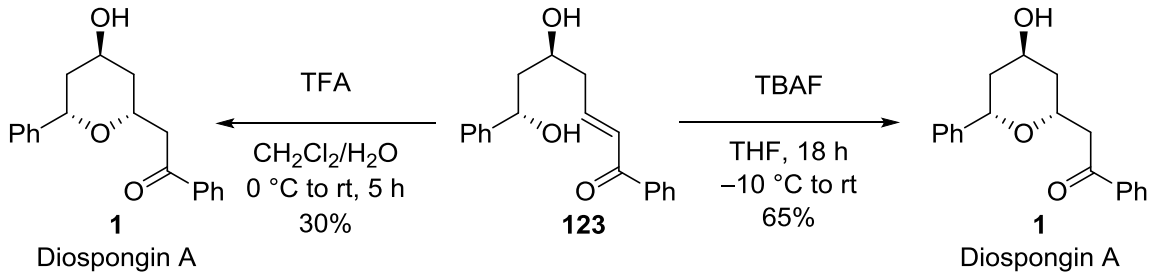

Scheme 58 Invesitiging the stereodivergent oxy-Michael cyclisation to ketone **123** under buffered TBAF and TFA conditions.

By using ketone **123** as a cyclisation precursor, under TFA condition, was provided the expected *cis*-tetrahydropyran in 30% yield. Under TBAF condition the *cis*-tetrahydropyran was also obtained in 65%. Taken together, it can be concluded that by using ketones as cyclisation precursors no stereodivergent formation of *cis*-tetrahydropyran and *trans*-tetrahydropyran could be realised.

1.3. Conclusions and Future work

The stereodivergent oxy-Michael reaction was successfully applied for the synthesis of the natural products, diospongin A **1** and B **2**. The method provides a new synthetic route to produce both diospongin A **1** and B **2** in 6 steps with an overall yield of 24% and 13%, respectively.

The *α*,*β*-unsaturated thioesters were found to be good cyclisation precursors for the stereodivergence to form both *cis*- and *trans*-tetrahydropyrans. The *α*,*β*-unsaturated thioesters under TBAF-mediated conditions gave the 2,6-*trans*-tetrahydropyran, however under acid-mediated conditions 2,6-*cis*-tetrahydropyran was obtained. In contrast, by using ketones as cyclisation precursor no stereodivergence was observed.

Previous computational studies have shown that the 4-hydroxyl group was crucial for the stereodivergence to form both *cis*- and *trans*-tetrahydropyrans.[41] When cyclisation was attempted with the 4-hydroxyl group removed or protected, it was found that the stereodivergence vanished. These findings are in agreement with the data presented in the previous computational studies.

The *α*,*β*-unsaturated thioesters were found to be good cyclisation precursors, however converting the thioesters to other substrates was not always easy.
It was found that by reducing the *α*,*β*-unsaturated thioesters with $NaBH_4$ or $LiAlH_4$ or L-selectride® led to thioether formation. For these interesting results, future work will need to be performed to investigate the thioester reduction by exploring other thioester substrates to verify this type of reaction.

2. Studies Towards the Synthesis of Tetrahydropyran Core of (±)-Psymberin/Ircinistatin A

2.1. Introduction

Psymberin and ircinistatin A **3** were isolated from different sponges and were proven to have an identical structure. Psymberin/ircinistatin A **3** is one of the 36 natural products that is contained in the pederin family; several of these natural products are presented in **Figure 23**.[67] The skeleton of the pederin group generally possesses an N,O-aminal moiety and a 2,6-*trans*-tetrahydropyran core.

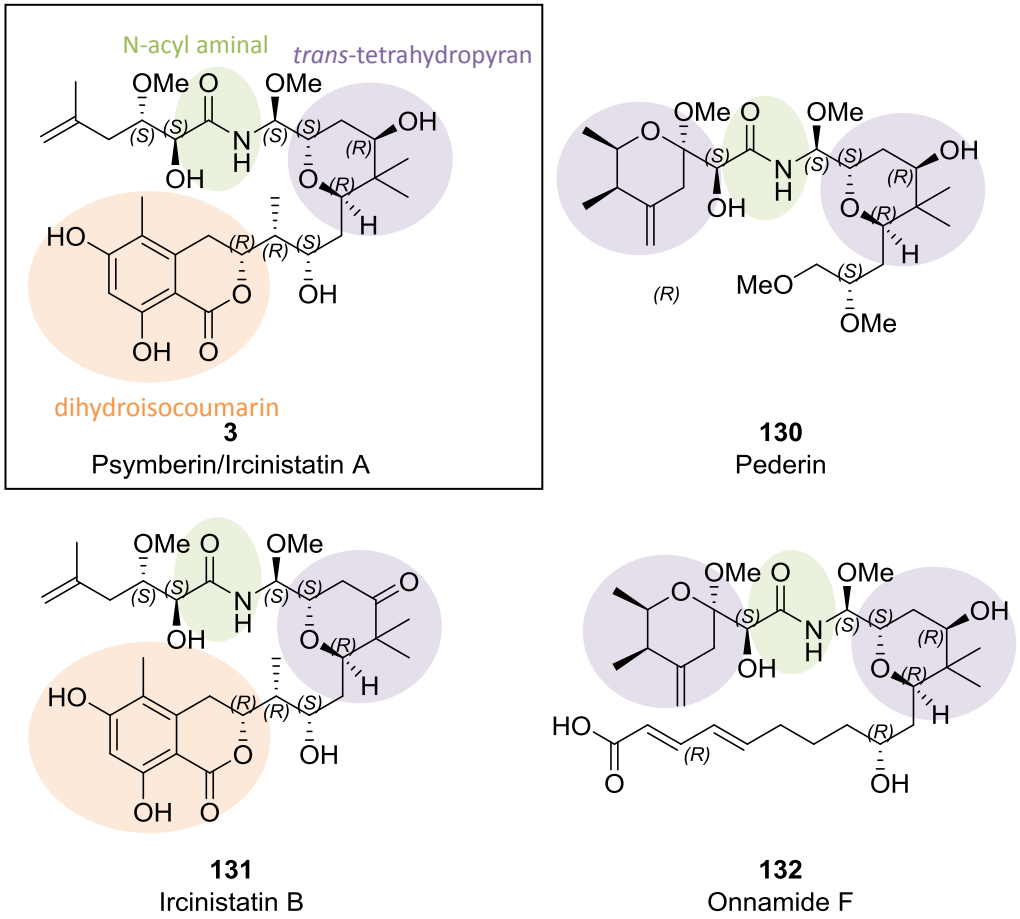

Figure 23 Natural products in the pederin family.

In addition to their structural similarity, many of natural products in the pederin family were found to possess significant antitumor activity.[68, 69] However, in contrast with other natural products in the pederin class, psymberin/ircinistatin A **3** was discovered to have remarkably different biological acitivity when compared to other family members against a wide range of cancer cell lines.[67, 70] It was suggested that the unique structural feature, the dihydroisocoumarin unit resulted in a distinct cytotoxicity in comparison to other members of the pederin family.[71]

2.1.1. Isolation and structure elucidation of Psymberin/Ircinistatin A

In 2004, psymberin and ircinistatin A were discovered by two different research groups, Pettit[70] and Crews.[67] Ircinistatin A was initially isolated by the Pettit group from the Indo-Pacific marine sponge, Ircinia ramose, which had been collected in 1991. Later, the Crews group also extracted the natural product psymberin, which was proven to possesse an identical structure to ircinistatin A from a *Psammocinia* sp. The name "psymberin" was derived from ***Ps****ammocinia* s***ymb***iont ped***erin***.[67]

In 2004, the configuration of ircinistatin A was first elucidated by the Pettit group.[70] The relative stereochemistry of the tetrahydropyran core in ircinistatin A was assigned as 8*R**, 9*S**, 11*R**, 13*R** by analysis of NOE data (**Figure 24**), however, only 4 chiral centres had been assigned.

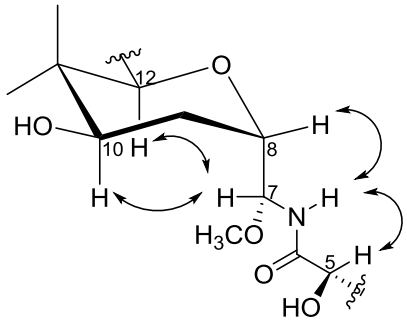

Figure 24 NOE contacts for C-5–C-12 Ircinistatin A.

Interestingly, attempts to interpret the stereochemistry of psymberin by the Crews group has assigned all the configurations except for the C-4 position to give 5*S**, 8*S**, 9*S**, 11*R**, 13*R**, 15*S**, 16*R**, 17*R** based on NOE data and comparison to the related structure of the natural product, pederin **130**.[67] The results were compared with findings presented by the Pettit group, however at that time, ircinistatin A and psymberin were believed to be diastereomers with different stereochemistry at the C-8 position. Because of the unsuccessful efforts to fully assign the stereochemistry for these two natural products by NMR spectroscopic data, the synthesis of its analogues was used.

In 2005, the Williams group initially confirmed the ambiguous configuration at C-4 position *via* synthesis of model compounds of both *anti* (4*S**,5*S**) **134** and *syn* (4*R**,5*S**) amide side chain **133** as shown in **Figure 25**.[72]

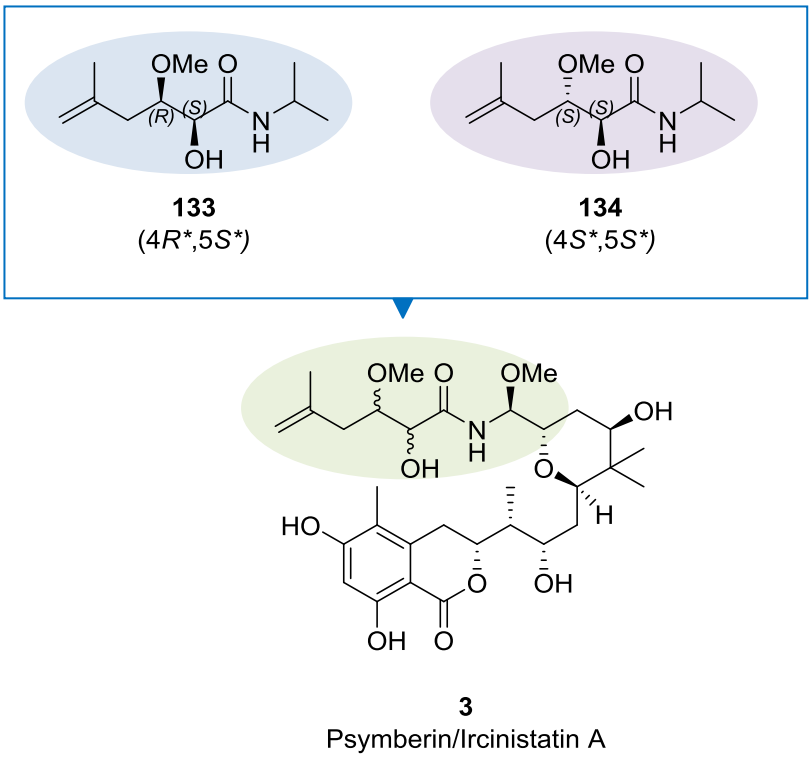

Figure 25 Synthesis of amide side chain **133** and **134** as reported by the Williams group.[72]

The structure of model compounds **133** and **134** were also confirmed by X-ray crystallographic analysis and concluded that the C-4 and C-5 stereocentres have an *anti* relationship. In the same year, the first total synthesis and completed stereochemical assignment of psymberin/irciniastatin A **3** was presented by De Brabander group, in which was confirmed that psymberin/irciniastatin A **3** had 9 chiral centres with 4*S**, 5*S**, 8*S**, 9*S**, 11*R**, 13*R**, 15*S**, 16*R**, 17*R** stereochemistry, and also clearly revealed that psymberin and irciniastatin A were identical.[73]

Table 8 Stereochemistry elucidated of psymberin/irciniastatin A **3** carried out by different groups.

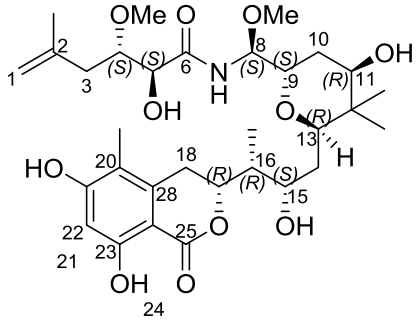

3
Psymberin/Ircinistatin A

	C-4	C-5	C-8	C-9	C-11	C-13	C-15	C-16	C-17
2004 Pettit group[70] (Ircinistatin A)	N/A	N/A	*R*	*S*	*R*	*R*	N/A	N/A	N/A
	Only elucidated 4 chiral centres								
2004 Crews group[67] (Psymberin)	N/A	*S*	*S*	*S*	*R*	*R*	*S*	*R*	*R*
	1. Elucidated all chiral centres except C-4 position 2. C-8 position is opposite to Ircinistatin A								
2005 Williams group[72]	*S*	*S*	N/A	N/A	N/A	N/A	N/A	N/A	N/A
	The first one to confirm the C-4 position								
2005 De Brabandergroup[73]	*S*	*S*	*S*	*S*	*R*	*R*	*S*	*R*	*R*
	1. The first total synthesis to confirm all stereochemistry 2. Ircinistatin A and psymberin are identical								

2.1.2. Biological activity

Natural products derived from marine organisms have attracted considerable interest in the search for therapeutic efficacy in the treatment of cancer.[74]

Psymberin/ircinistatin A **3**, natural products extracted from marine sponges, have shown to be potential anticancer drug candidates, because of their extremely potent cytotoxicity, and highly selectivity against numerous cancer cell lines.[67, 70]

Psymberin/ircinistatin A **3** was first isolated by using bioassay-guided techniques, in which it displayed strong growth inhibition (GI_{50}, 50% growth inhibition) at concentrations ranging from 4.1 to 2.4 nM to against the P388 leukemia and six other human cancer cell lines, including BXPC-3, MCF-7, SF268, NCI-H460, KM20L2 and DU-145.[70] In addition, psymberin/ircinistatin A **3** has also displayed antivascular activity and inhibited human umbilical vein endothelial cells (HUVEC) at GI_{50} <0.0005 μmg/mL, as shown in **Table 9**.

Table 9 Inhibition of cancer cell line growth (GI_{50}, μg/mL) by psymberin/ircinistatin A **3**.[70]

	Human cancer cell line	Psymberin/Ircinistatin A
pancreas	BXPC-3	0.0038
breast	MCF-7	0.0032
CNS	SF268	0.0034
lung	NCI-H460	<0.0001
colon	KM20L2	0.0027
prostate	DU-145	0.0024
leukemia[a]	P388	0.00413
normal endothelial	HUVEC[b]	<0.0005

[a] Murine. [b] BD-Biosciences Clontech.

Psymberin/ircinistatin A **3**, was further investigated by the national cancer institute (NCI), Developmental therapeutics program against 60 human cancer cell lines, as shown in **Table 10**.[67]

Table 10 Differential sensitivities (LC_{50}) of various cell lines to psymberin/ircinistatin A **3** as identified by the national cancer institute developmental therapeutics *in vitro* screening program.[67]

Cell line	LC_{50} (M)	Cell line	LC_{50} (M)
leukemia		**melanoma**	
CCRF-CEM	$>2.5 \times 10^{-5}$	LOX IMVI	$>2.5 \times 10^{-5}$
HL-60(TB)	$>2.5 \times 10^{-5}$	MALME-3M	$<2.5 \times 10^{-9}$
K-562	$>2.5 \times 10^{-5}$	SK-MEL-2	$>2.5 \times 10^{-5}$
MOLT-4	$>2.5 \times 10^{-5}$	SK-MEL-5	$<2.5 \times 10^{-9}$
RPMI-8226	$>2.5 \times 10^{-5}$	SK-MEL-28	1.41×10^{-5}
SR	$>2.5 \times 10^{-5}$	UACC-257	$>2.5 \times 10^{-5}$
		UACC-62	$<2.5 \times 10^{-9}$
breast cancer		**colon cancer**	
MCF7	$>2.5 \times 10^{-5}$	HCC-2998	3.76×10^{-7}
HS 578T	$>2.5 \times 10^{-5}$	HCT-116	$<2.5 \times 10^{-9}$
MDA-MB-435	$<2.5 \times 10^{-9}$	HT29	$>2.5 \times 10^{-5}$
NCI/ADR-RES	1.9×10^{-5}	SW-620	$>2.5 \times 10^{-5}$
T-47D	1.36×10^{-5}		

Psymberin/ircinistatin A **3** displayed excellent antitumor activity at the nanomolar level concentration with a LC_{50} value <2.5 x 10^{-9} M against colon cancer cell lines (HCT-116), melanoma cancer lines (MALME-3M, SK-MEL-5 and UACCC-62) and a breast cancer cell line (MDA-MB-435). Based on the results, psymberin/ircinistatin A **3** was found to have a high level of selectivity towards melanoma cancer cell lines, with 10^4-fold potency differences in cytotoxicity among some closely related cell lines.

2.1.3. Previous synthesis of the tetrahydropyran core of (±)-psymberin/ircinistatin A

Reviewing the literature, synthetic approaches to the total synthesis of psymberin/ircinistatin A **3** have been reported by 9 different research groups.[73, 75-82] Strategies to construct the tetrahydropyran core include oxidative cyclisation,[73, 83, 84] $PhI(OAc)_2$-mediated cyclisation,[76] oxidative cyclisation of allenic alcohols, intromolecular cyclisation of epoxy alcohols,[77, 80, 85, 86] lactone intermediate,[78, 79] and oxy-Michael addition.[81, 82, 87]

2.1.3.1. Synthesis of the tetrahydropyran core of (±)-psymberin/ircinistatin A *via* oxidative cyclisation

In 2005, the first total synthesis of psymberin/ircinistatin A **3** was carried out by De Brabande and co-workers (**Scheme 59**).[73] Retrosynthetically, psymberin/ircinistatin A **3** was disconnected to three main fragments, including psymberic acid **135**, aromatic aldehyde **136** and tetrahydropyran core **137**.

The key tetrahydropyran formation step was accessed by ozonolysis of **138** to provide lactol, which was then trapped as acetate and generated **139** in 81% yield, over two steps.

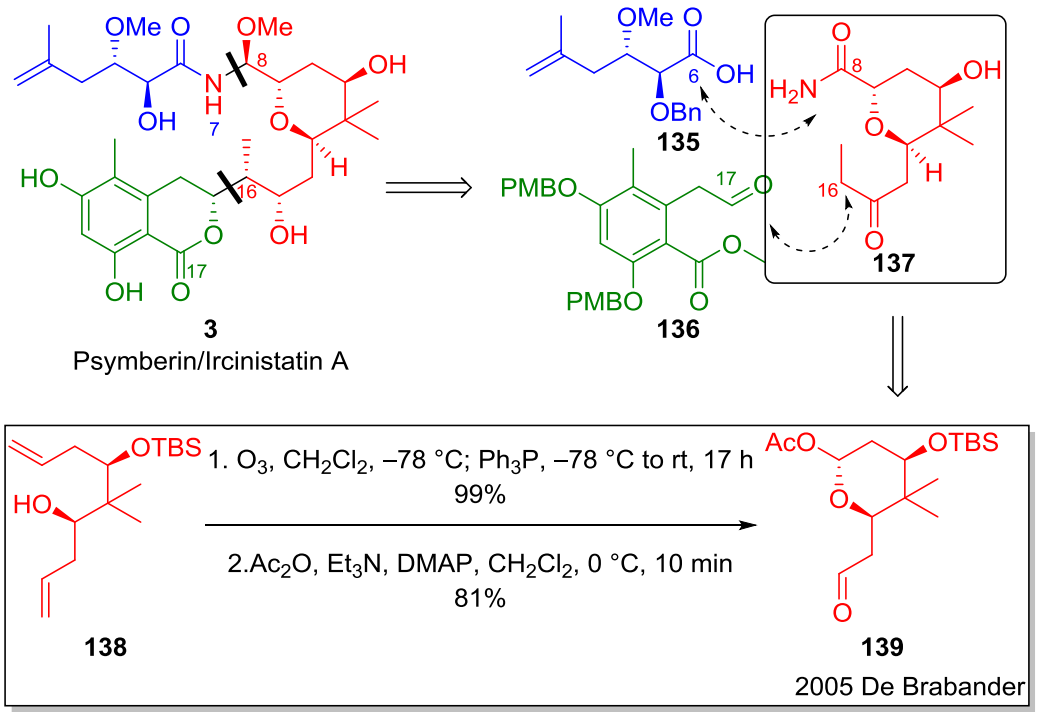

Scheme 59 Synthesis of the tetrahydropyran core of psymberin/ircinistatin A **139** as reported by De Brabander and co-workers.[73]

In the same year, Floreancig and co-workers presented partial synthesis of the N-7–C-25 fragment of psymberin/ircinistatin A **140**.[83] The key tetrahydropyran formation step used the same strategy as described by De Brabander group.[73]

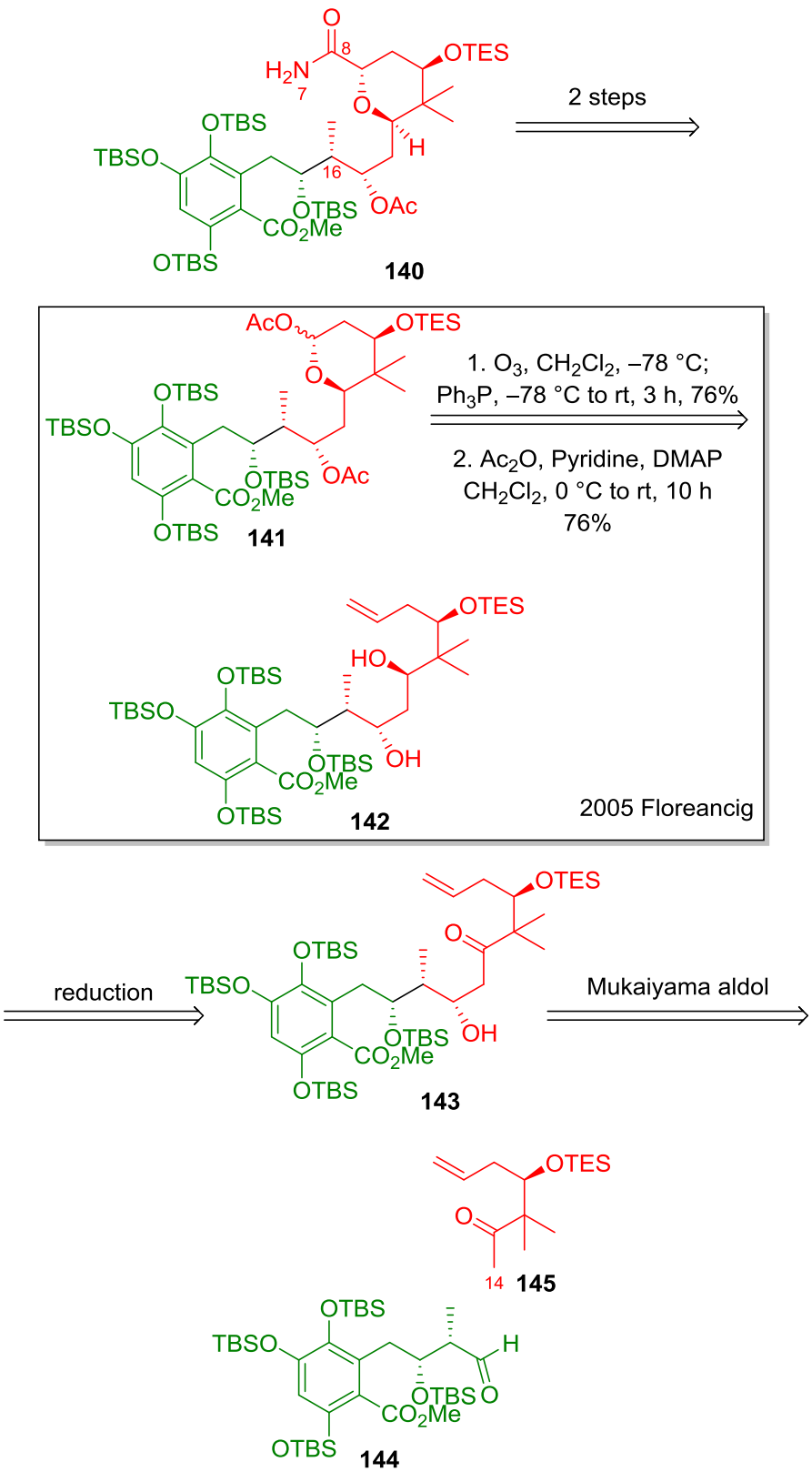

Scheme 60 Retrosynthetic analysis of N-7 to C-25 fragment of psymberin/ircinistatin A **140** as reported by Floreancig and co-workers.[83]

As presented in **Scheme 60**, the cyclisation precursor **143** was obtained *via* a Mukaiyama aldol reaction, which coupled the fragments **144** and **145**. Followed by the reduction of **143** to give **142**. Next, the key tetrahydropyran core **141** was synthesised by applying the ozonolysis and an acetylation reaction.

In 2013, Pietruszka and co-workers reported the synthesis of 8-desmethoxypsymberin **146**.[84] The retrosynthetic plan was to disconnect the 8-desmethoxypsymberin **146** into three fragments **147**, **150** and **151**, which were in a similar manner to the retrosynthetic plan proposed by De Brabander's group.[73] Ozonolysis, acetylation and allylation of diol **152** in the presence of allyltrimethylsilane and boron trifluoride diethyl etherate provided the tetrahydropyran core **153** in 60% yield (**Scheme 61**).

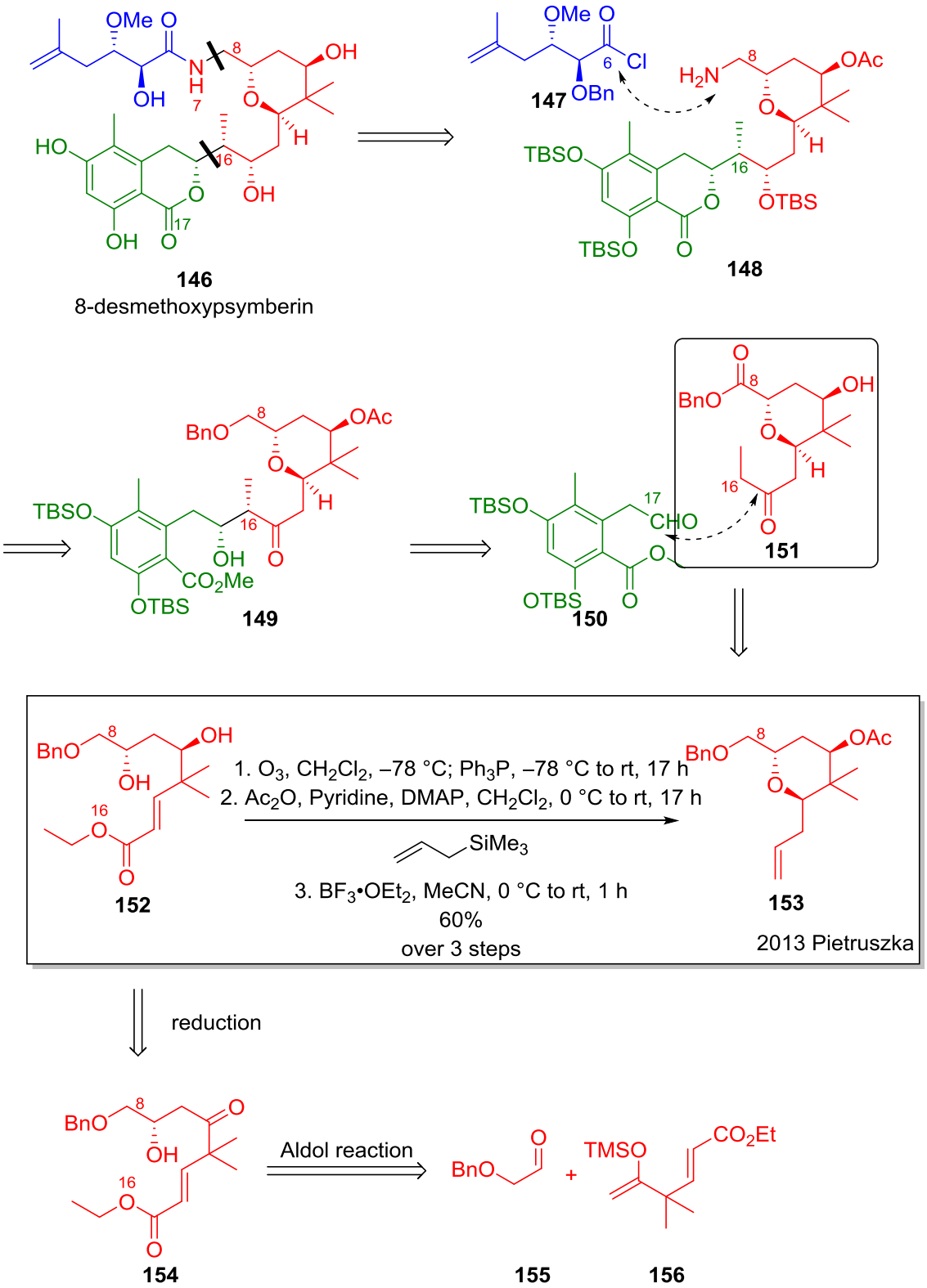

Scheme 61 Retrosynthetic analysis of desmethoxypsymberin **146** as reported by Pietruszka and co-workers.[84]

2.1.3.2. Synthesis of the tetrahydropyran core of (±)-psymberin/ircinistatin A *via* $PhI(OAc)_2$-mediated cyclisation

In 2007, the Huang group reported a new method for the synthesis of 2-(N-acylaminal)-substituted tetrahydropyrans **157** by the use of iodobenzene diacetate as an oxidant.[76]

Coupling the fragments **162** and **163** by a Mukaiyama aldol reaction provided **161**. The aldol product **161** was then carried through a multi-step sequence to prepare enamide **160**. The reactions included reduction of ketone to form diol, deprotection of the benzyl protecting group, and were followed by Dess–Martin oxidation and Takai vinyl iodide formation giving **160**. Next, the vinyl iodide **160** was coupled with amide **159**, which resulted in the cyclisation precursor **158**. The synthesis of 2-(N-acylaminal)-substituted tetrahydropyrans **157** was completed *via* a iodobenzene diacetate oxidative cyclisation (**Scheme 62**).

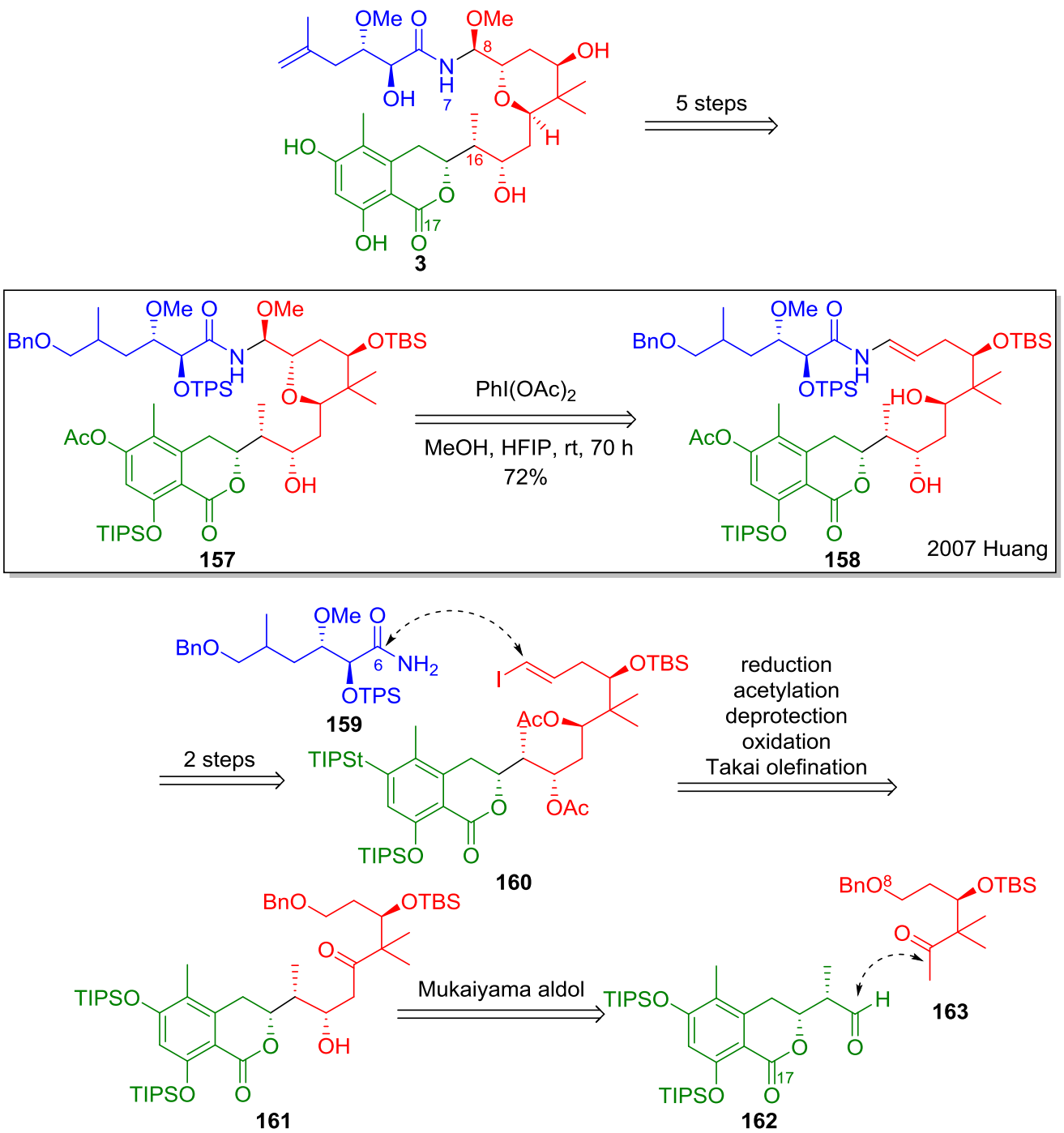

Scheme 62 Retrosynthetic analysis of psymberin/ircinistatin A **3** as reported by the Huang group.[76]

2.1.3.3. Synthesis of the tetrahydropyran core of (±)-psymberin/ircinistatin A *via* intromolecular cyclisation of epoxy alcohols

In 2008, Smith III and coworkers reported the total synthesis of psymberin/ircinistatin A **3** in a 21-step linear sequence.[85] The intermolecular cyclisation of **168** *via* a 6-*exo*-*tet* pathway was performed by using 20 mol% CSA and resulted in the desired *trans*-tetrahydropyran **167** in 74% yield (**Scheme 63**).

The other possible 7-*endo*-*tet* cyclised product was not observed by NMR. It was assumed that the cationic character in *α*-position was destablilised by the methyl ester electron-withdrawing group, thus the reaction favoured to occur in the *β*-position *via* a 6-*exo*-*tet* pathway.

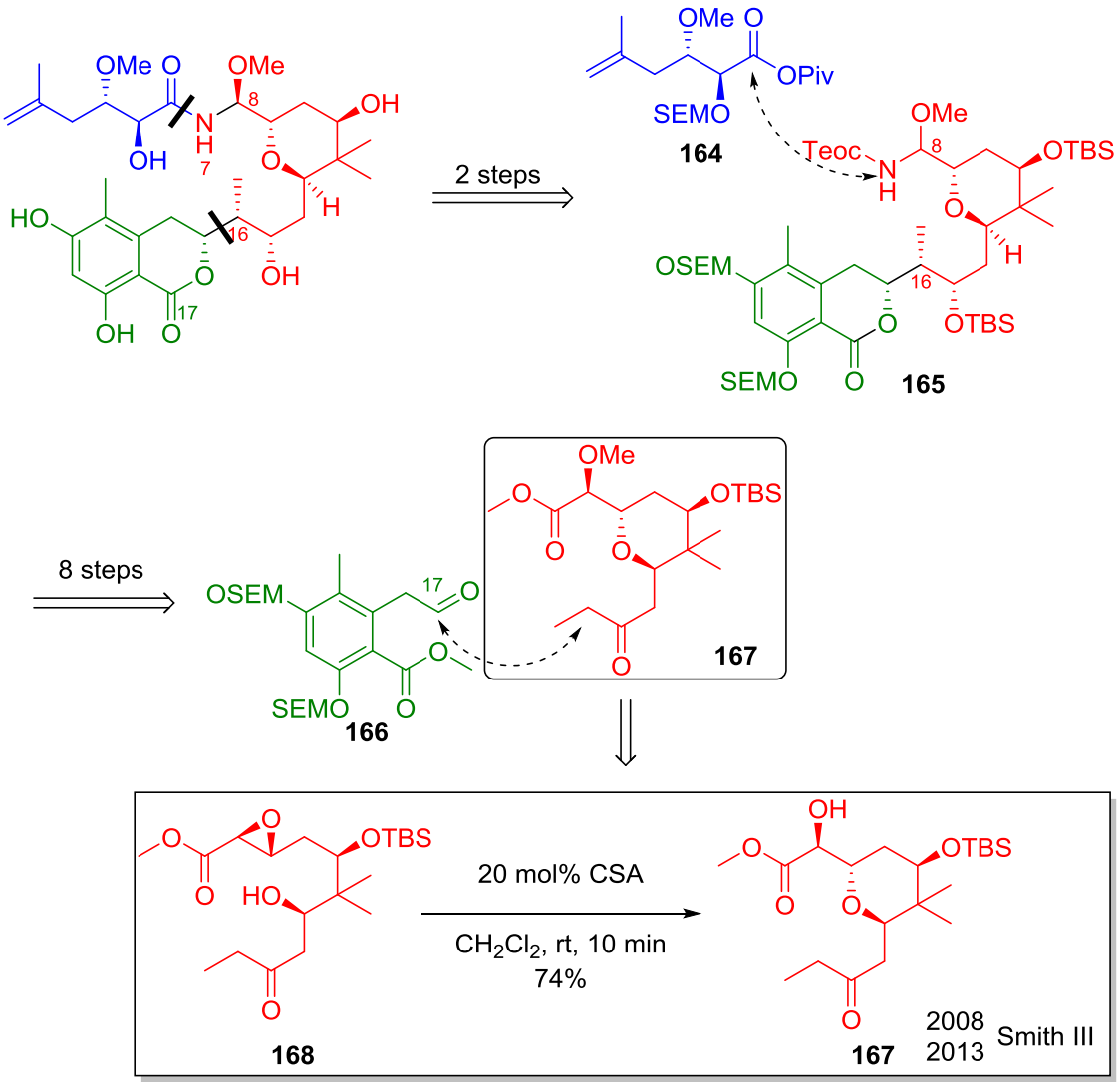

Scheme 63 Synthesis of the tetrahydropyran core **167** of psymberin/ircinistatin A as reported by Smith III and co-workers.[77, 85]

The same cyclisation method was also presented by Iwabuchi and co-workers.[80, 86] Treating **169** with catalytic amount of CSA led to the formation of the tetrahydropyran ring in 83% yield (**Scheme 64**).

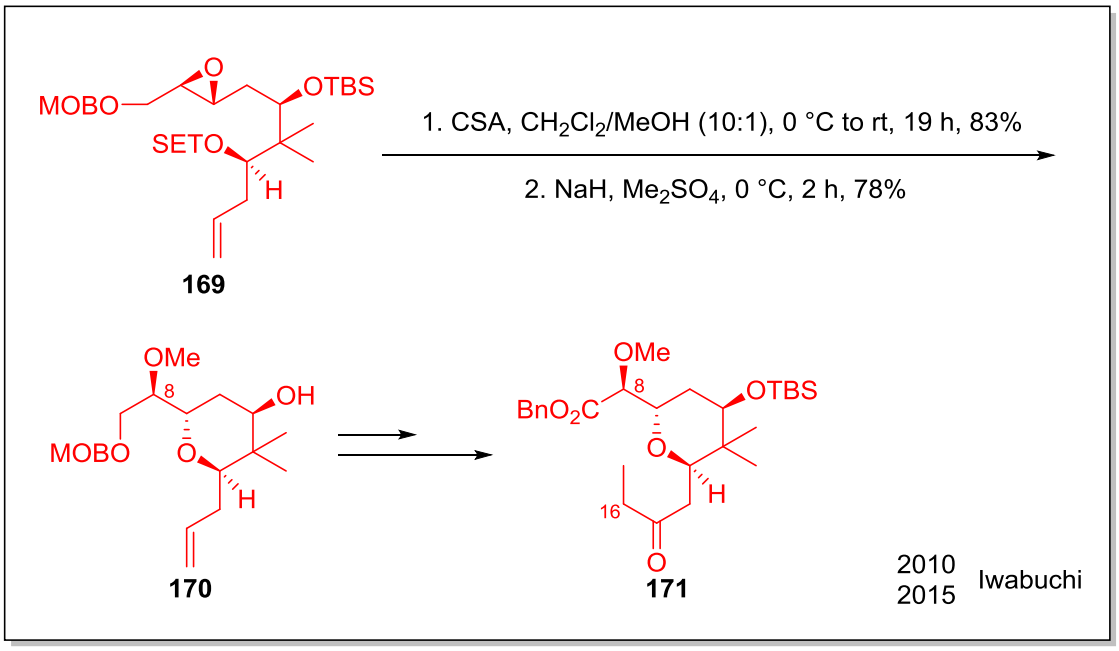

Scheme 64 Synthesis of the tetrahydropyran core of psymberin/ircinistatin A as reported by Iwabuchi and co-workers.[80, 86]

2.1.3.4. Synthesis of the tetrahydropyran core of (±)-psymberin/ircinistatin A *via* lactone intermediate

In 2000, Konopelski and co-workers demonstrated the total synthesis of psymberin/ircinistatin A **3**. Synthesis of the tetrahydropyran ring was achieved *via* the lactone intermediate **174** (**Scheme 65**).[78]

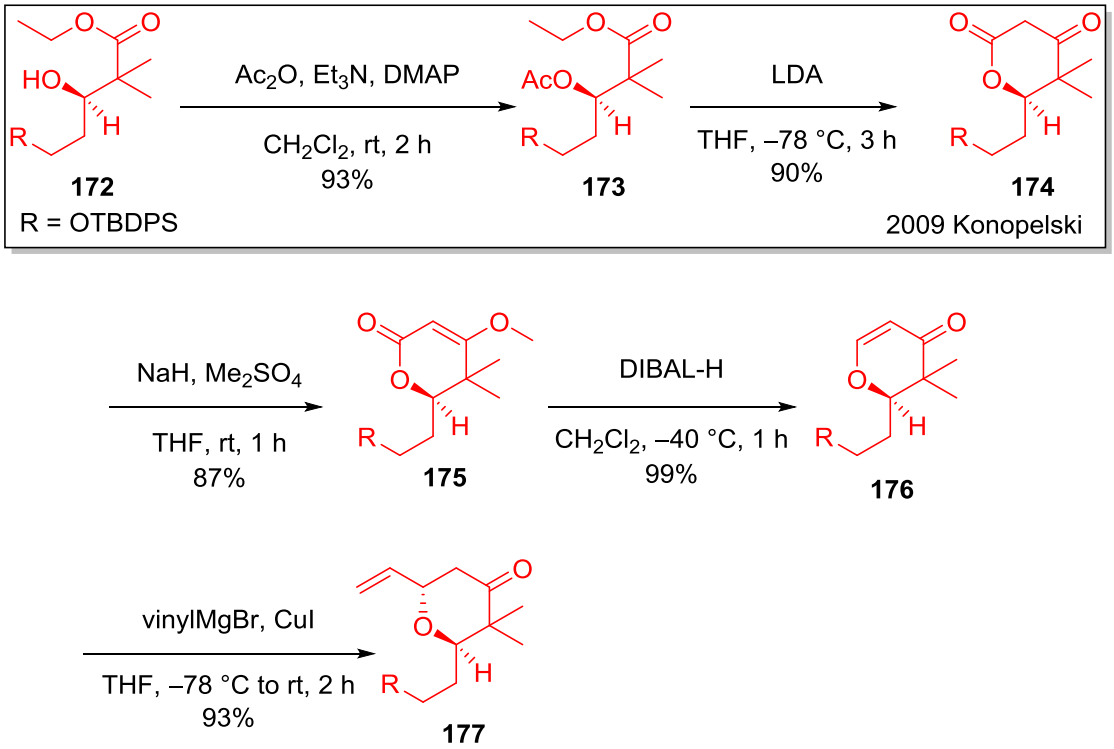

Scheme 65 Synthesis of the tetrahydropyran core of psymberin/ircinistatin A **177** as reported by Konopelski and co-workers.[78]

The reaction to form lactone involved acetylation of **172** followed by Dieckmann condensation to generate *β*-keto lactone **174**. The resulting intermediate **174** was then processed through the following 3-step sequence: methyl enol ether formation, DIBAL-H reduction and conjugate addition of vinylmagnesium bromide to the dihydropyranone **176**, which resulted in *β*-vinyl ketone **177**.

In the same year, Crimmins and co-workers reported the total synthesis of psymberin/ircinistatin A **3** in 19 steps with an overall yield of 6% (**Scheme 66** and **Scheme 67**).[79]

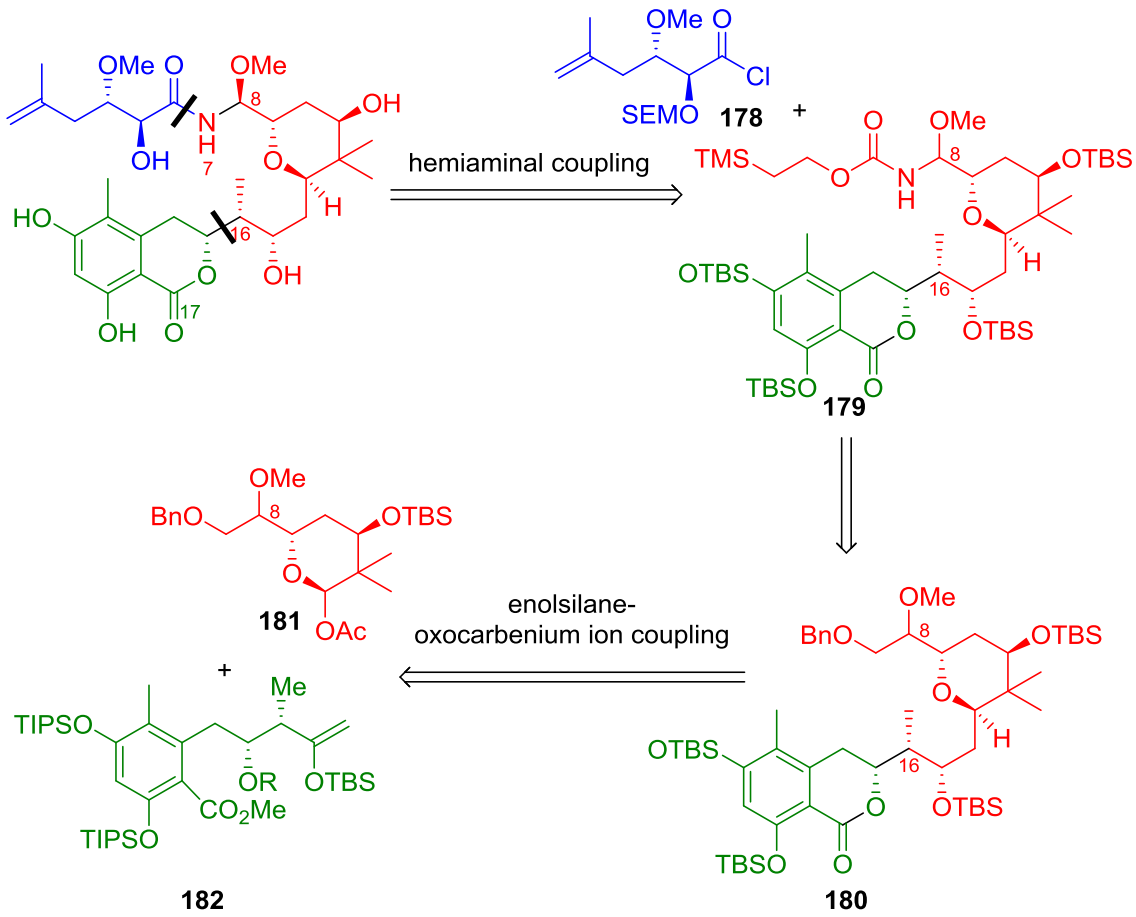

Scheme 66 Retrosynthetic analysis of psymberin/ircinistatin A **3** as reported by Crimmins and co-workers.[79]

The retrosynthetic disconnections for the psymberin/ircinistatin A **3** relied on the coupling of acid chloride **178** with hemiaminal **179**. The tetrahydropyran ring **180** was derived from the addition of enolsilane **182** to acetate **181**.

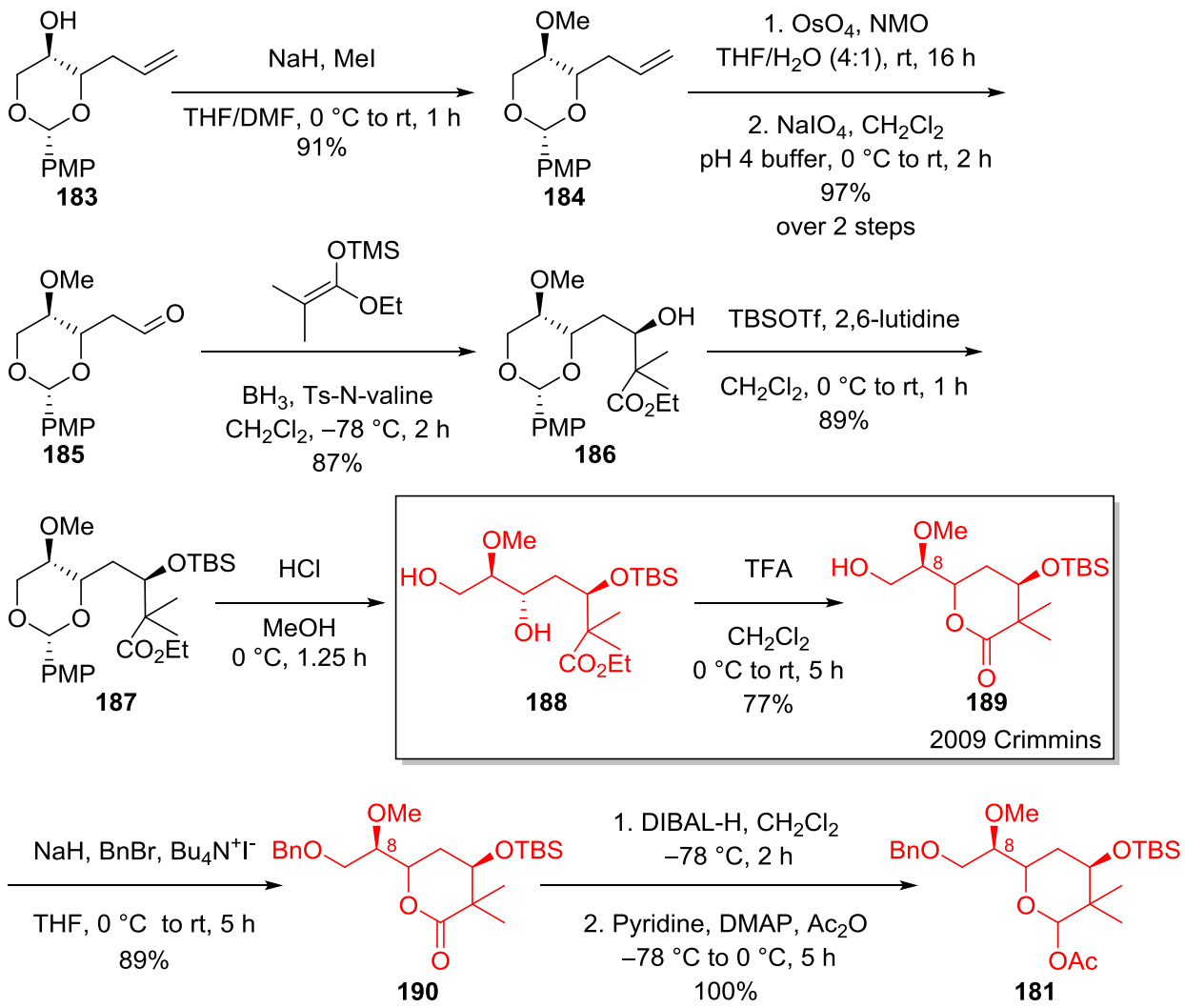

Scheme 67 Synthesis of tetrahydropyran core of psymberin/ircinistatin A **181** as reported by Crimmins and co-workers.[79]

Synthesis of the tetrahydropyran ring **181** began with *p*-methoxybenzylidine acetal **183**, which was obtained in 2 steps from 2-deoxy-D-ribose. The key lactone intermediate **189** was prepared in a multi-step sequence, including methylation of **183**, followed by dihydroxylation-oxidative cleavage, aldol reaction, TBS-protection and deprotection to yield the cyclisation precursor **188**. The cyclisation precursor

188 was then subjected to acid-catalysed cyclisation to provide lactone **189**. Subsequently, lactone **189** was protected as benzyl ether and then processed through reductive acetylation to generate acetate **181**.[88] Acetate **181** was obtained from 2-deoxy-D-ribose in 9 steps with an overall yield of 34% (**Scheme 67**).

2.1.3.5. Synthesis of the tetrahydropyran core of (±)-psymberin/ircinistatin A *via* oxy-Michael addition

In 2011, Hong and co-workers synthesised the psymberin/ircinistatin A **3** with 24 steps as the longest sequence.[81] The key tetrahydropyran was formed *via* organocatalytic oxa-conjugate addition of **191** in the presence of 9-anthracenecarboxylic acid, which catalysed the reaction to form the cyclised product **192** in 92% yield with a diastereomeric ratio of 10:1 (*trans*:*cis*) (**Scheme 68**).

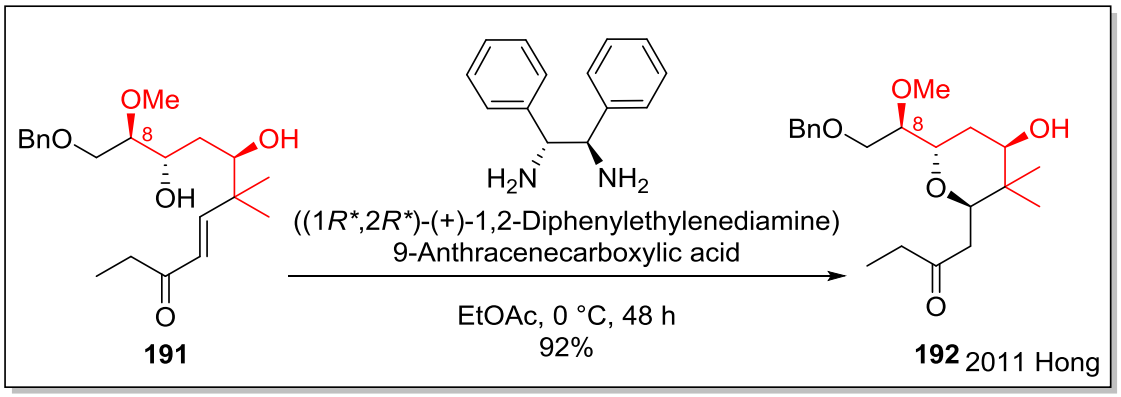

Scheme 68 Synthesis of the tetrahydropyran core of psymberin/ircinistatin A **192** as reported by Hong and co-workers.[81]

Both the Harrowven[82] and Pietruszka[87] groups also used the oxy-Michael addition to form the tetrahydropyran (**Scheme 69**).

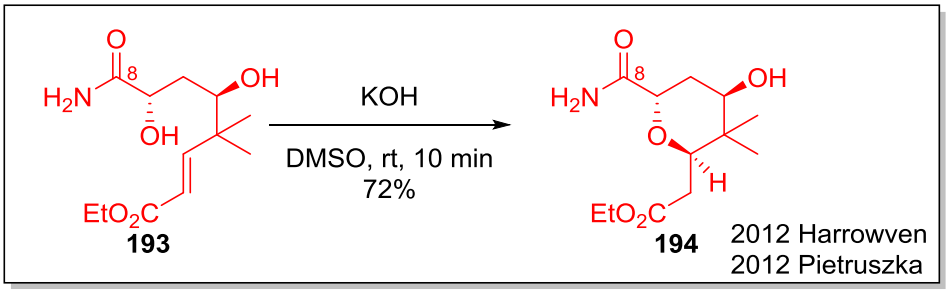

Scheme 69 Synthesis of the tetrahydropyran core of psymberin/ircinistatin A as reported by the Harrowven[82] and Pietruszka groups.[87]

The cyclisation precursor **193** was prepared from lactone **198** in the presence of liquid ammonia in THF. Both Harrowven[82] and Pietruszka[87] used the same lactone **198** to prepare the cyclisation precursor **193**. The synthesis of lactone **198** was shown in **Scheme 70**.

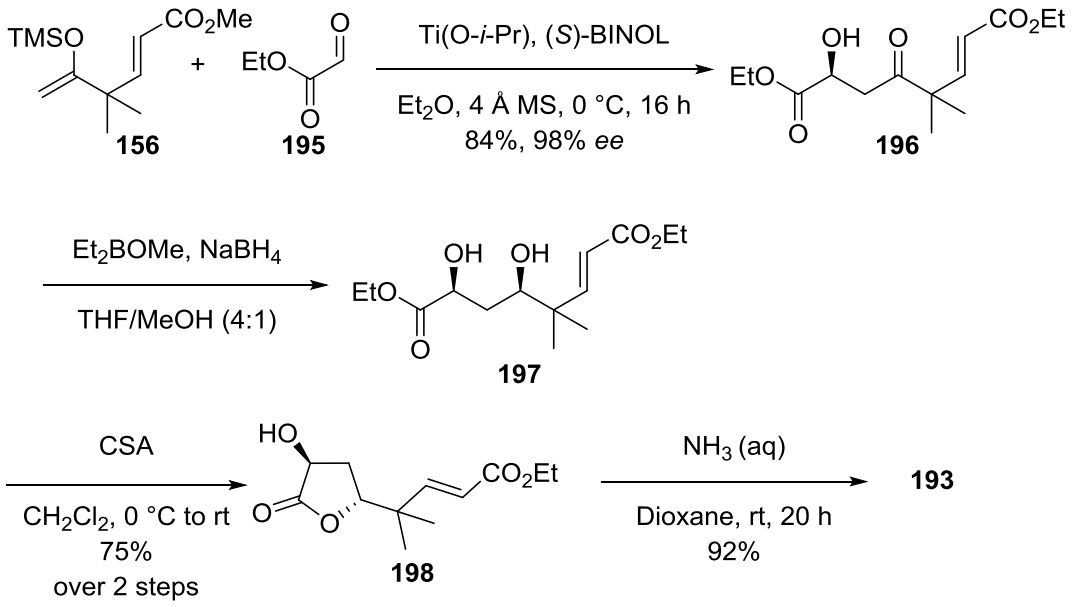

Scheme 70 Synthesis of lactone **198** as reported by the Pietruszka group.[87]

The synthesis began with aldol reaction between **156** and **195** to generate **196** in high yield (83%), followed by the reduction and acid-catalysed cyclisation to form

lactone **198** in 75% yield.

2.1.4. Structure–activity relationship (SAR)

Structure–activity relationships (SAR) provide a way to probe the relationship between chemical structures and their biological activities. Moreover, they help to determine the biological effects of certain structural features. Understanding the relationship between the structure of a drug and its biological activity enables the preparation of more effective drugs.[89, 90]

Many SAR studies of psymberin/ircinistatin A **3** have been reported.[71, 75, 80, 86, 91-96] In 2006, the first SAR study was carried out by De Brabander group, in which two psymberin/ircinistatin A analogues were synthesised: C-8 and C-4-epimers **199** and **200** (**Figure 26**).[71]

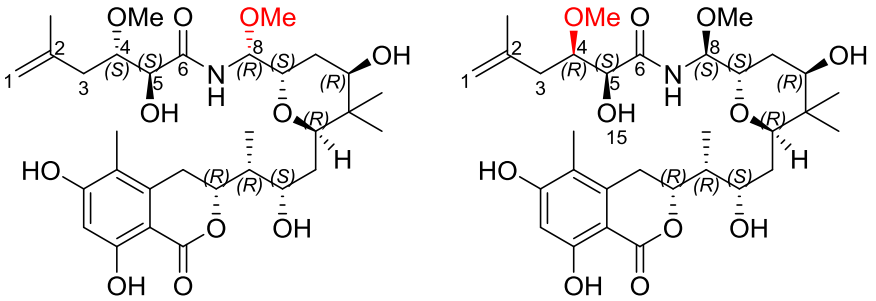

199
8-*epi*-psymberin/8-*epi*-ircinistatin A

200
4-*epi*-psymberin/4-*epi*-ircinistatin A

Figure 26 Structure of **199** and **200**.[71]

It was hypothesised that the dihydroisocoumarin fragment may be an important subunit, which showed distinct cytotoxicity in psymberin/ircinistatin A **3** among

other members of the pederin family. Based on this hypothesis, psympederin **201** and its epimer **202** were synthesised. The psymberin-pederin hybrid **201** and **202** were modified to contain a pederin-like side chain with a dimethoxy unit rather than containing the dihydroisocoumarin moiety present in the originally structure of psymberin/ircinistatin A **3** (**Figure 27**).[71]

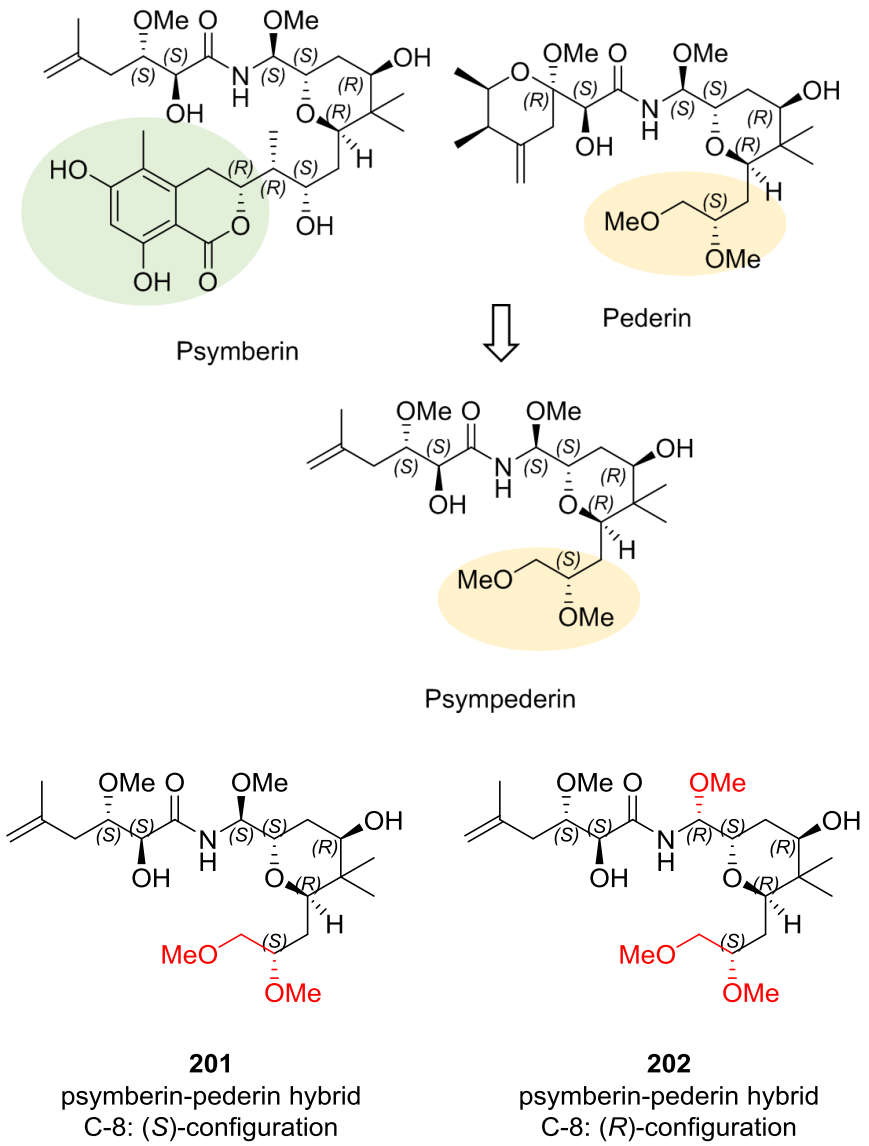

Figure 27 Structure of psympederin and its C-8 epimer **201** and **202**.[71]

The cytotoxicities of the four analogues (**199**, **200**, **201** and **202**) were tested for human cell lines, including colon tumour (KM12), prostate tumour (PC3), melanoma (SK-MEL-5) and glioblastoma (T98G), the results are summarised in **Table 11**.

Table 11 Cytotoxicities of psymberin/ircinistatin A **3** and its analogues **199**, **200**, **201** and **202** against various human tumour cell lines.[a71]

		IC_{50} [nM]			
Entry	**Compound**	**Colon tumour (KM12)**	**Prostate tumour (PC3)**	**Melanoma (SK-MEL-5)**	**Glioblastoma (T98G)**
1	**3**	0.45 ± 0.01	0.98 ± 0.12	2.29 ± 0.13	1.37 ± 0.06
2	**199**	37.1 ± 5.5	200.2 ± 27.6	352.0 ± 12.1	85.8 ± 48.4
3	**200**	126.08 ± 8.6	346.5 ± 102.8	762.8 ± 70.0	186.7 ± 51.3
4	**201**	710.9 ± 35.8	821.8 ± 89.1	>1000	>1000
5	**202**	>1000	255.5 ± 11.4	>1000	>1000

1. **[a] The Promega Cell Titer Glo assay was utilised to measure cell viability after cells were exposed to compounds for 48 hours.**
2. **IC_{50} values represent the mean of triplicate experiments ± standard error of the mean.**

As shown in **Table 11**, psymberin/ircinistatin analogues, C-8 epimer **199** and C-4 epimer **200** have displayed cytotoxicity activity against cancer lines (**Table 11**, **Entries 1**-**3**). However, analogues **199** and **200** were about 100-fold less active compared to psymberin/ircinistatin A **3**. Therefore, it was suggested that it is important to maintain the original stereochemistry of psymberin/ircinistatin A **3** at the C-4 and C-8 position. On the other hand, without the dihydroisocoumarin unit in psymberin-pederin hybrid **201** and its C-8 epimer **202**, a significant reduction in cytotoxicity was observed compared to psymberin/ircinistatin A **3** (**Table 11**, **Entries 4** and **5**). The dihydroisocoumarin moiety has been described as a significant fragment in psymberin/ircinistatin A **3**.

In 2008, psymberin/ircinistatin A **3** was synthesised *via* oxidised of *seco*-psymberin/ircinistatin A **203** by the Huang group (**Scheme 71**).[91]

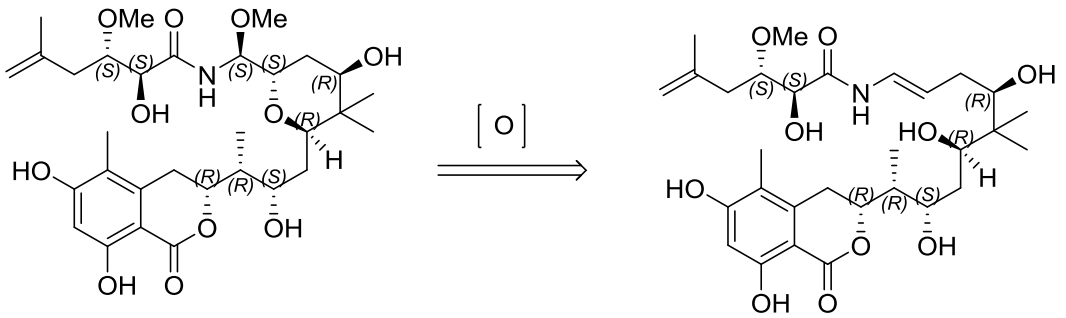

3
Psymberin/Ircinistatin A

203
seco-Psymberin/*seco*-Ircinistatin A

Scheme 71 Psymberin/ircinistatin A **3** was synthesised *via* an oxidisation of *seco*-psymberin/*seco*-ircinistatin A **203**.[91]

The antiproliferation activity of *seco*-psymberin/*seco*-ircinistatin **203** was evaluated in a human lung cancer cell line (HOP62). Interestingly, without the tetrahydropyran ring in the molecule, the antitumor activity of *seco*-psymberin/*seco*-ircinistatin A **203** was significantly reduced, with a IC_{50} value >1 x 10^4 nM. Convincingly, the 2-(N-acylaminal) substituted tetrahydropyran component in psymberin/ircinistatin A **3** was an essential structure for its potent cytotoxic activity.

In the same year, the Huang group published other SAR studies. The C-8 and C-9 epimer of psymberin/ircinistatin A **204** was initially chosen as an analogue for the treatment of different human cancer cell lines.[92, 93] The results are presented in **Table 12**.

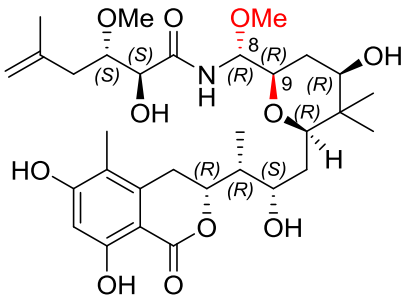

Figure 28 Structure of 8,9-*epi*-psymberin/8,9-*epi*-ircinistatin A **204**.[92, 93]

There is no doubt that psymberin/ircinistatin A **3** showed excellent cytotoxicity to all the cell lines investigated. However, the cytotoxic activity of the 8,9-*epi*-psymberin/8,9-*epi*-ircinistatin A **204** was markedly reduced. Therefore, it was determined that the stereochemistry at the C-8 and C-9 position affected psymberin/ircinistatin A **3** cytotoxicity.

Table 12 Cytotoxicities of psymberin/ircinistatin A **3** and 8,9-*epi*-psymberin/8,9-*epi*-ircinistatin A **204** against various human tumour cell lines.[92, 93]

Psymberin/ Ircinistatin A 3 (IC_{50} nM)	**8,9-*epi*-psymberin/ 8,9-*epi*-ircinistatin A 204 (IC_{50} nM)**	**Cell line**	**Human tissue type**
0.76 ± 0.07	6800 ± 244	ACHN	kidney
0.30 ± 0.03	3800 ± 301	DU145	prostate
0.18 ± 0.02	2400 ± 431	H226	lung
0.81 ± 0.14	4900 ± 187	HCT-116	colon
0.42 ± 0.02	4600 ± 68	HOP62	lung
0.27 ± 0.01	4200 ± 174	MB231	breast
0.28 ± 0.03	3600 ± 155	MB435	melanoma
0.28 ± 0.02	5200 ± 195	MKN45	gastric
0.19 ± 0.02	3100 ± 341	PC3	prostate
0.82 ± 0.04	4800 ± 177	SW620	colon
0.84 ± 0.08	n.d	NHDF	normal

1. **[a] The CellTiter-Glo Luminescent Cell Viability Assay (Promega, Technical bulletin 288) was employed in this study.**
2. **IC_{50} data are the mean value of six experiments with statistical significance calculated.**
3. **n.d., not detected**

In addition to the biological activities of the 8,9-*epi*-psymberin/8,9-*epi*-ircinistatin A **204**, modifications were made to the "psymberate" side chain of **205** and **206** and were tested against human lung cancer cell line HOP62. The results are displayed in **Table 13**.

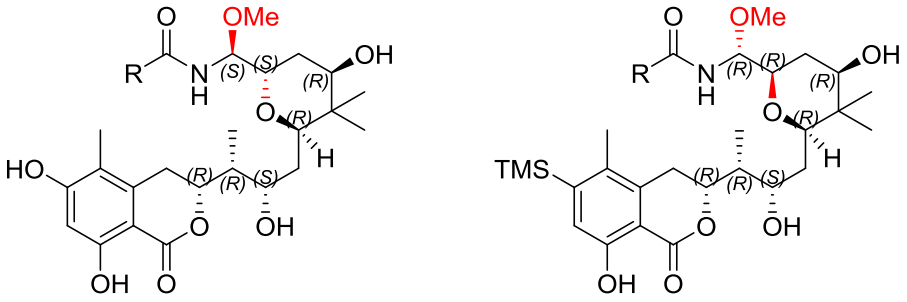

205 **206**

Figure 29 Structures of **205** and **206**.[92, 93]

When the side chain of psymberin/ircinistatin A **3** was modified to a methyl group (**Table 13**, **Entry 2**), the cytotoxic activities of both **205a** and **206a** were greatly decreased compared to that of psymberin/ircinistatin A **3**. By changing the terminal double bond to a hydroxy group in **205b** and **206b** (**Table 13**, **Entry 3**), it was found that **205b** was roughly 600-fold less effective when compared to psymberin/ircinistatin A **3**, although it still demonstrated good cytotoxic activity against cancer cell lines (HOP62). Therefore, the terminal olefin was assumed to be an important group for the biological activity of psymberin/ircinistatin A. By replacing the terminal double bond for an aryl group in **205c** and **206c** (**Table 13**, **Entry 4**), the cytotoxic activity was highly decreased (>10000 nM). However, substitution of the aryl side chain in **205d** and **206d** resulted in a moderate cytotoxicity (**Table 13**, **Entry 5**). Based on these studies, C-4 and C-5 substitution cannot be removed to maintain a high cytotoxicity. The cytotoxicity was not

significantly dependent on modifying the double bond of the psymberate side chain to an aryl group.

Table 13 Antitumor activities of "psymberate" side chain modified pysmberin/ircinistatin A **3** analogues against human lung cancer cell line (HOP62).[a 92, 93]

Entry	R	Compound	IC_{50} (nM)	Compound	IC_{50} (nM)
1	Psymberate	**3**	0.42 ± 0.02	**3**	4600 ± 68
2		**205a**	>10000	**206a**	>10000
3	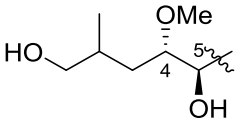	**205b**	260 ± 36	**206b**	>10000
4	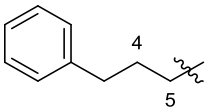	**205c**	>10000	**206c**	>10000
5	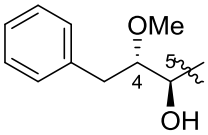	**205d**	32 ± 1	**206d**	615 ± 15

[a] The CellTiter-Glo Luminescent Cell Viability Assay (Promega, Technical bulletin 288) was employed in this study. IC_{50} data are the mean value of three experiments with statistical significance calculated. The value for psymberin/ircinistatin A in this assay is 0.42 nM.

The biological effect attributed to the tetrahydropyran core in psymberin/ircinistatin A **3** was then further studied.[92, 93] In a previous study, it was found that irciniastatin B **131** (C-11 substituted with O) was about 10 times more active in inhibiting cell growth compared to psymberin/ircinistatin A **3** (C-11 substituted with -OH).[70]

Therefore, 11-deoxy-psymberin/11-deoxy-ircinistatin A was chosen as a model for modification so as to confirm the importance of the C-11 position in the tetrahydropyran unit.

Four diastereomers of 11-deoxy-psymberin/11-deoxy-ircinistatin A were synthesised, including **207**, **208**, **209** and **210** (**Figure 30**), and the biological activities were tested in numerous human cancer cell lines.

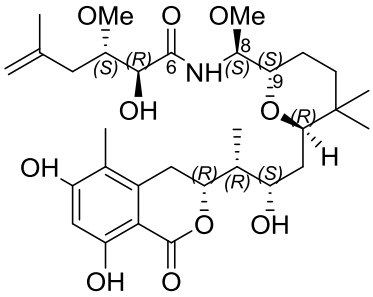

207
(8*S**,9*S**)
11-deoxy-psymberin/11-deoxy-ircinistatin A

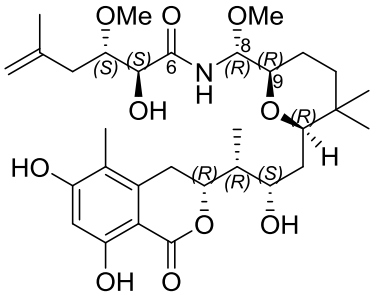

208
(8*R**,9*R**)
11-deoxy-psymberin/11-deoxy-ircinistatin A

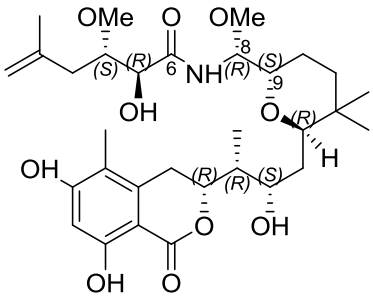

209
(8*R**,9*S**)
11-deoxy-psymberin/11-deoxy-ircinistatin A

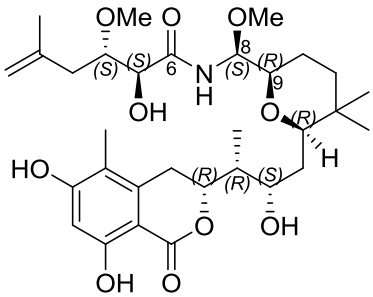

210
(8*S**,9*R**)
11-deoxy-psymberin/11-deoxy-ircinistatin A

Figure 30 Stracture of 11-deoxy-psymberin/11-deoxy-ircinistatin A **207** and its diastereomers **208**, **209** and **210**.[92, 93]

Table 14 Antitumour activity of psymberin/ircinistatin A **3**, 11-deoxy-psymberin/ 11-deoxy-ircinistatin A **207** and its diastereomers **208**, **209** and **210**.[92, 93]

Psymberin/Ircinistatin A 3	**(IC$_{50}$ nM)** **207**	**208**	**209**	**210**	**Cell line**
0.76	0.265 ± 0.008	n.d.	n.d.	8.7 ± 0.18	kidney (ACHN)
0.30	0.149 ± 0.005	n.d.	n.d.	5.9 ± 0.18	prostate (DU145)
0.18	0.034 ± 0.004	n.d.	n.d.	1.6 ± 0.27	lung (H226)
0.42	0.055 ± 0.002	177 ± 6	46 ± 7	3.0 ± 0.12	lung (HOP62)
0.27	0.142 ± 0.007	n.d.	n.d.	5.3 ± 0.15	breast (MB231)
0.28	0.076 ± 0.004	n.d.	n.d.	3.9 ± 0.48	gastric (MKN45)
0.19	0.073 ± 0.006	n.d.	n.d.	2.9 ± 0.21	prostate (PC3)
0.82	0.160 ± 0.015	n.d.	n.d.	6.1 ± 0.22	colon (SW620)
0.84	0.066 ± 0.004	n.d.	n.d.	3.8 ± 0.10	normal (NHDF)

IC$_{50}$ data are the mean value of three experiments with statistical significance calculated. n.d., not detected.

The data indicated that 11-deoxy-psymberin/11-deoxy-ircinistatin A **207** had a higher cytotoxic activity compared to psymberin/ircinistatin A **3**. However, the activities of the corresponding diastereomers **208**, **209** and **210** are weaker or not present at all. Therefore, the hydroxyl group at the C-11 position was not important for cytotoxicity.

In 2010, enantiomer of psymberin/ircinistatin A **211** and (+)-alkymberin **212** (**Figure 31**) were synthesised by the Iwabuchi group.[80] The cytotoxicity test of the enantiomer of psymberin towards HeLa cells indicated a GI_{50} value >1000 nM, which was not as efficient when compared to psymberin/ircinistatin A **3** (GI_{50} value of 1.2 nM). However, by modifying the terminal double bond to an alkyne group the cell growth inhibition value was similar to that of psymberin/ircinistatin A **3**. This was consistent with the results reported by the Huang group,[92] who showed that the terminal double bond was tolerated replacing it by various substituents which have π-character.

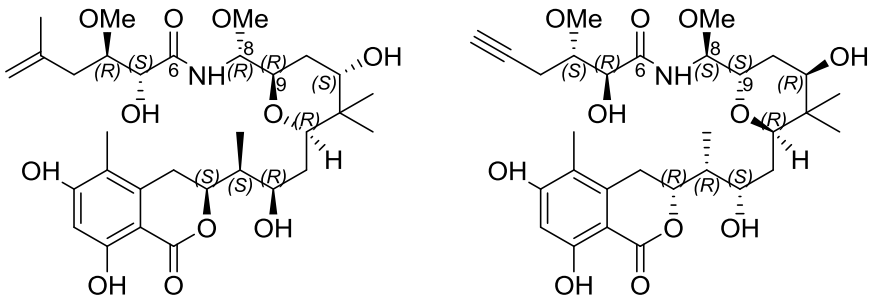

211
ent-psymberin/*ent*-ircinistatin A

212
(+)-alkymberin

Figure 31 Structure of *ent*-psymberin/*ent*-ircinistatin A **211** and (+)-alkymberin **212**.[80]

In 2011, Floreancig and co-workers synthesised various analogues **213**, **214**, and **215** of pederin **130** and psymberin/ircinistatin A **3**.[75] The HCT-116 cell line was chosen to test the cytotoxicity.

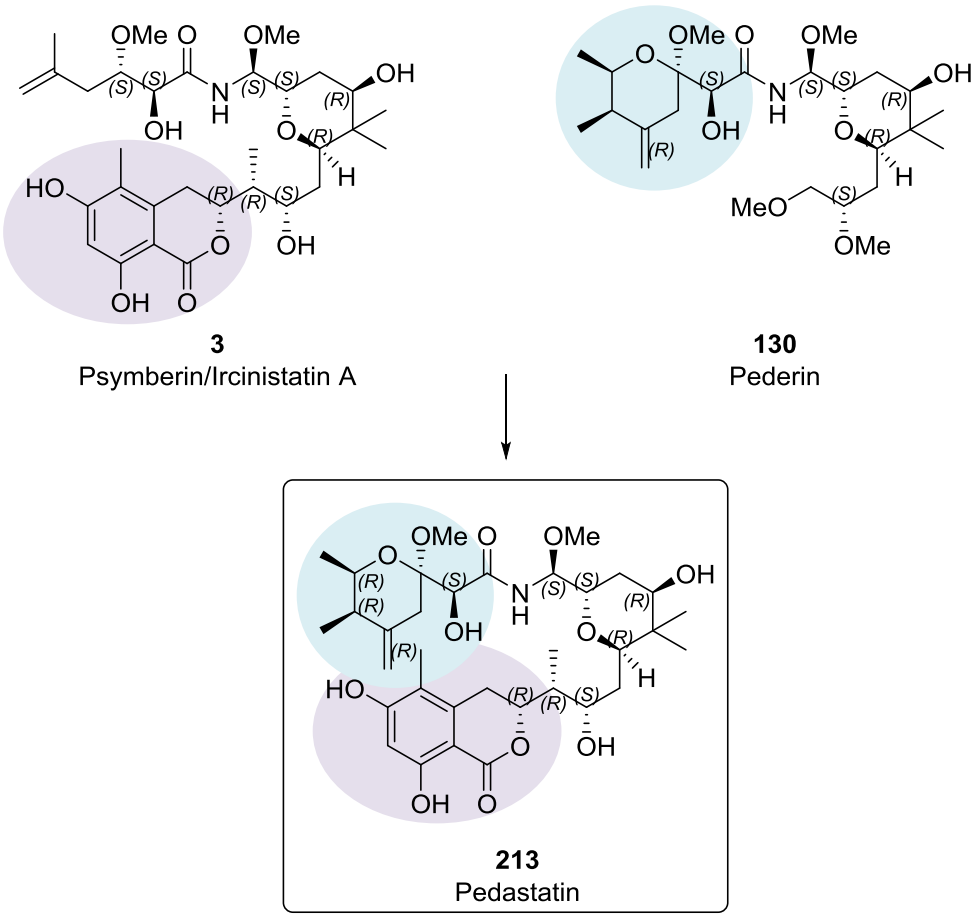

Figure 32 Structure of pedastatin **213**.[75]

Pedestatin **213** is a hybrid molecule of pederin **130** and psymberin/ircinistatin A **3** (**Figure 32**). Based on the findings of the De Brabander group,[71] the dihydroisocoumarin fragment in psymberin/ircinistatin A **3** was an important functional group for its cytotoxicity, for its cytotoxic activity, as was the cyclic pederate fragment in pederin **130**. Thus, pedestatin **213** was synthesised by combining these two subunits with the original tetrahydropyran core.

Table 15 GI_{50} values of the natural products and analogs against HCT-116 cells.[75]

Entry	Compound	GI_{50} (nM)
1	pederin **130**	0.6 ± 0.1
2	psymberin/ircinistatin A **3**	0.052 ± 0.02
3	pedestatin **213**	0.004 ± 0.003[a]
4	8-desmethoxy-psymberin/ 8-desmethoxy-ircinistatin A **214**	0.83 ± 0.1
5	10-desmethoxy-pedestatin **215**	0.068 ± 0.02

[a] Average of two independent experiments.

As shown in **Table 15**, the GI_{50} values of pedestatin **213** (0.004 ± 0.003 nM) indicated that it more efficient in inhibiting cell growth compared to both pederin **130** and psymberin/ircinistatin A **3**. These findings are consistent with the results reported by the De Brabander group (**Table 15**, **Entries 1-3**).[71]

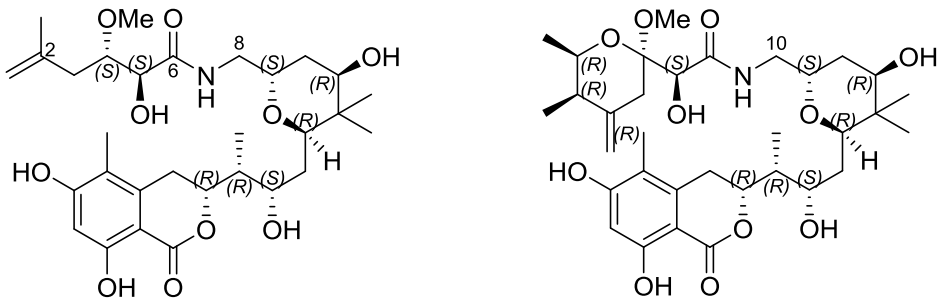

214
8-desmethoxy-psymberin/8-desmethoxy-ircinistatin A

215
10-desmethoxy-pedestatin

Figure 33 Structure of 8-desmethoxy psymberin/8-desmethoxy ircinistatin A **214** and 10-desmethoxy pedestatin **215**.[75]

The importance of the alkoxy group in the N-acyl aminal linkage was also studied. In comparison with the 8-desmethoxy-psymberin/8-desmethoxy-ircinistatin A **214** and 10-desmethoxy-pedestatin **215** (**Figure 33**) showed a weaker cytotoxicity compared to psymberin/ircinistatin A **3** and pedestatin **213**. However, compounds **214** and **215** retained excellent GI_{50} values (**Table 15**, **Entries 2**-**5**). Again, by comparing 8-desmethoxy-psymberin/8-desmethoxy-ircinistatin A **214** and 10-desmethoxy-pedestatin **215**, the pedestatin compound **215** proved to be more potent compared to the psymberin/ircinistatin A analogue **214** and showed a greater ability in inhibiting cell growth (**Table 15**, **Entries 4**-**5**). In summary, dihydroisocoumarin and cyclic pederate fragments play an important role in the activity of pedestatin. The alkoxy group in the N-acyl aminal linkage is not required for biological activity.

From previous reports, the hydroxyl group at C-11 position[92] as well as the C-8 position of methoxy group[75] in psymberin/ircinistatin A **3** has been shown to be inessential for retaining cytotoxicity. Therefore, (+)-8-desmethoxy-11-deoxy-12-didesmethyl-psymberin/(+)-8-desmethoxy-11-deoxy-12-didesmethyl-ircinistatin A **216** (**Figure 34**), which was synthesised by the Smith group in 2016,[96] was chosen as a psymberin/ircinistatin A **3** analogue. The gem-dimethyl group was assumed to be an important substituent for protein target binding.[75] However, by removal of the gem-dimethyl group, C-8 and C-11 substituents showed that **216** still possessed a good level of cytotoxicity to against HCT-116 cell line even though the biological activity was reduced 800-fold compared to psymberin/ircinistatin A **3** (**Table 16**).

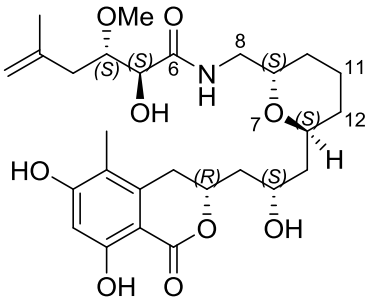

216

Figure 34 Stracture of **216**

(+)-8-desmethoxy-11-deoxy-12-didesmethyl-psymberin/

(+)-8-desmethoxy-11-deoxy-12-didesmethyl-ircinistatin A.[96]

Table 16 IC_{50} values of the psymberin/ircinistatin A **3** and **216** to against HCT-116 cell line.[96]

Entry	**Compound**	**IC_{50} (HCT-116) (nM)**
1	psymberin/ircinistatin A **3**	0.2
2	(+)-8-desmethoxy-11-deoxy-12-didesmethyl-psymberin/ (+)-8-desmethoxy-11-deoxy-12-didesmethyl-ircinistatin A **216**	160

The (+)-8-desmethoxy-11-deoxy-12-didesmethyl-psymberin/(+)-8-desmethoxy-11-deoxy-12-didesmethyl-ircinistatin A **216** was a good tumour cell growth inhibitor, however the presence of gem-dimethyl group was not essential for cytotoxic activity.

The tolerance of substituent at C-11 position was also investigated, and three analogues were synthesised (**Figure 35**). As shown in **Table 17**, 11-*epi*-psymberin/ 11-*epi*-ircinistatin A **217** proved to be very potent against cancer cell lines with a similar value compared to psymberin/ircinistatin A **3** (**Table 17**, **Entries 1** and **2**). The C-11 position was also modified to an acetyl functional group **218**, which gave similar cytotoxicity results when compared to psymberin/ircinistatin A **3** (**Table 17**, **Entries 1** and **3**). Previous studies reported that the benzoyl group in the C-11 position **219** possessed lower potency than psymberin/ircinistatin A **3**, **217** and **218**. However, compound **219** still maintained a good level of cytotoxicity (**Table 17**, **Entries 1**, **2**, **3** and **4**). Therefore, variations of C-11 did not significantly reduce the cytotoxic activity.

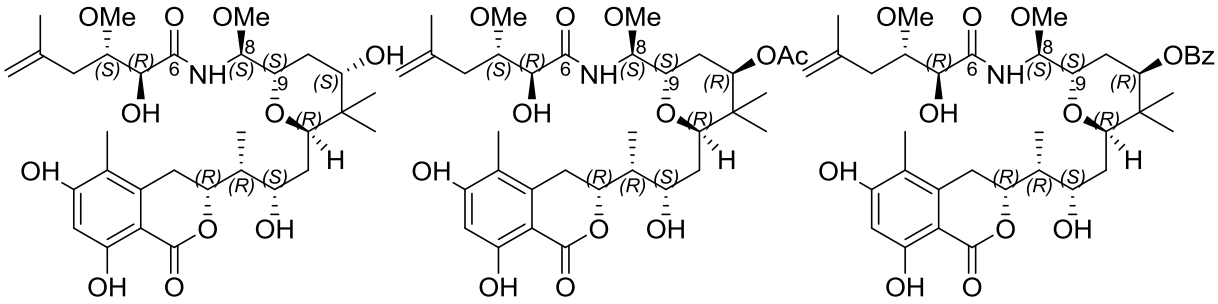

217
11-*epi*-psymberin/
11-*epi*-irciniastatin A

218
(+)-11-OAc-psymberin/
(+)-11-OAc-irciniastatin A

219
(-)-11-OBz-psymberin/
(-)11-OBz-irciniastatin A

Figure 35 Structure of C-11-psymberin/C-11-ircinistatin A analogues **217**, **218**, and **219**.[96]

Table 17 Proliferative cell growth inhibition assay and IMR-90 cytotoxicity assay IC_{50} values (nM) for psymberin/ircinistatin A **3** and C-11-psymberin/C-11-ircinistatin A analogues.[96]

		IC_{50} (cell line) (nM) (IC_{50} (IMR-90):IC_{50} (cell line))			
Entry	**Compound**	**A2058**	**H522-T1**	**HCT-116**	**IMR-90**
1	psymberin/ircinistatin A **3**	0.4 (68)	1 (27)	4 (7)	27
2	11-*epi*-psymberin/ 11-*epi*-irciniastatin A **217**	0.4 (85)	0.9 (38)	3 (11)	34
3	(+)-11-OAc-psymberin/ (+)-11-OAc irciniastatin A **218**	0.4 (68)	0.7 (39)	2 (14)	27
4	(−)-11-OBz-psymberin/ (−)-11-OBz-irciniastatin A **219**	2.7 (30)	5.4 (15)	NA	81

In summary, several important observations were obtained from the SAR studies carried out by different research groups (**Figure 36**). These include the following:

1. A terminal olefin in psymberate side chains may be changed to another group with π-character as long as the C-4 methoxyl group and C-5 hydroxy are present.
2. The dihydroisocoumarin unit and tetrahydropyran core are essential for the biological activity of psymberin/ircinistatin A **3**.
3. The C-8 methoxyl group, C-11 hydroxyl group and C-12 gem-dimethyl group are not essential for cytotoxic activity.
4. It is important to maintain the stereochemistry at the C-4, C-8 and C-9 positions.

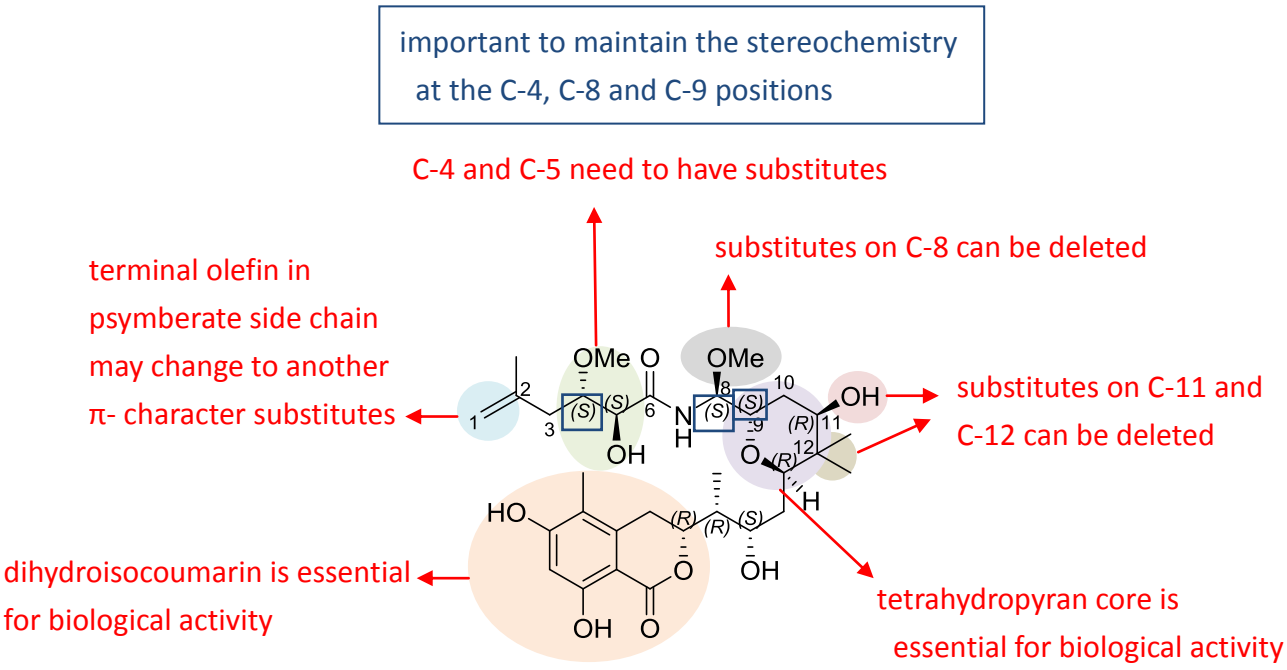

Figure 36 Structure–activity relationship studies of psymberin/ ircinistatin A **3**.

2.2. Results and discussion

2.2.1. Retrosynthetic approaches

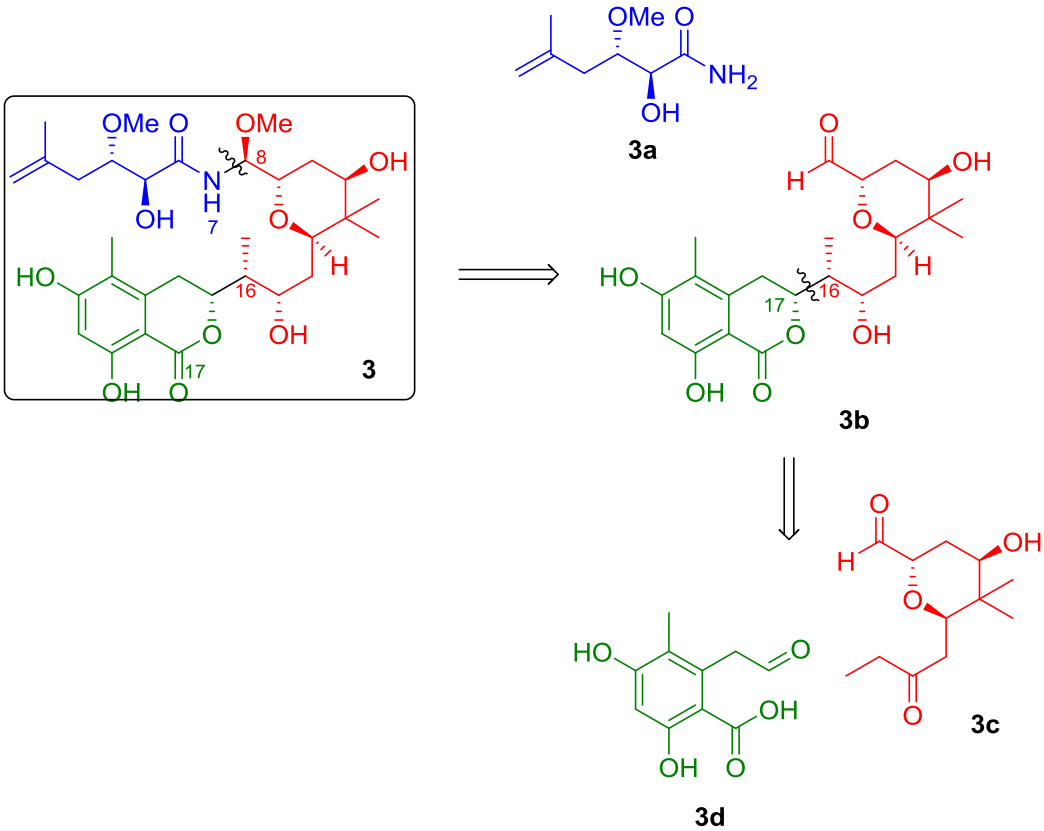

Scheme 72 Retrosynthetic analysis of psymberin/ircinistatin A **3**.

The retrosynthetic analysis of psymberin/ircinistatin A **3** is depicted in **Scheme 72**. From a synthetic perspective, we envisioned that psymberin/ircinistatin A **3** would be disconnected to three fragments, including the amide side chain **3a**, the tetrahydropyran core **3c** and the dihydroisocoumarin unit **3d**. The disconnection of the amide bond between N-7 and C-8, resulted in the amide side chain **3a** and aldehyde **3b**. Further disconnection at C-16 and C-17 of fragment **3b**, revealed the aromatic side chain **3d**, and the 2,6-*trans* tetrahydropyran core **3c** was obtained. Fragment **3b** could be prepared by coupling of **3c** and **3d** *via* an aldol reaction.

There are several known methods to construct the amide side chain **3a**[72, 97-99] and aromatic side chain **3d**.[83, 100] Therefore, we focused on the synthetic approach to synthesise the tetrahydropyran core **3c** *via* a stereodivergent oxy-Michael reaction.[41] According to the SAR studies reported by the Huang group, because of its potent cytotoxic activity, the tetrahydropyran core is an important feature in psymberin/ircinistatin A **3**.[91] Although many groups have proposed several synthetic approaches to construct psymberin/ircinistatin A **3**, the highly substituted of 2,6-*trans* tetrahydropyran unit, which contains the gem-dimethyl group, has been a challenge to synthesise.

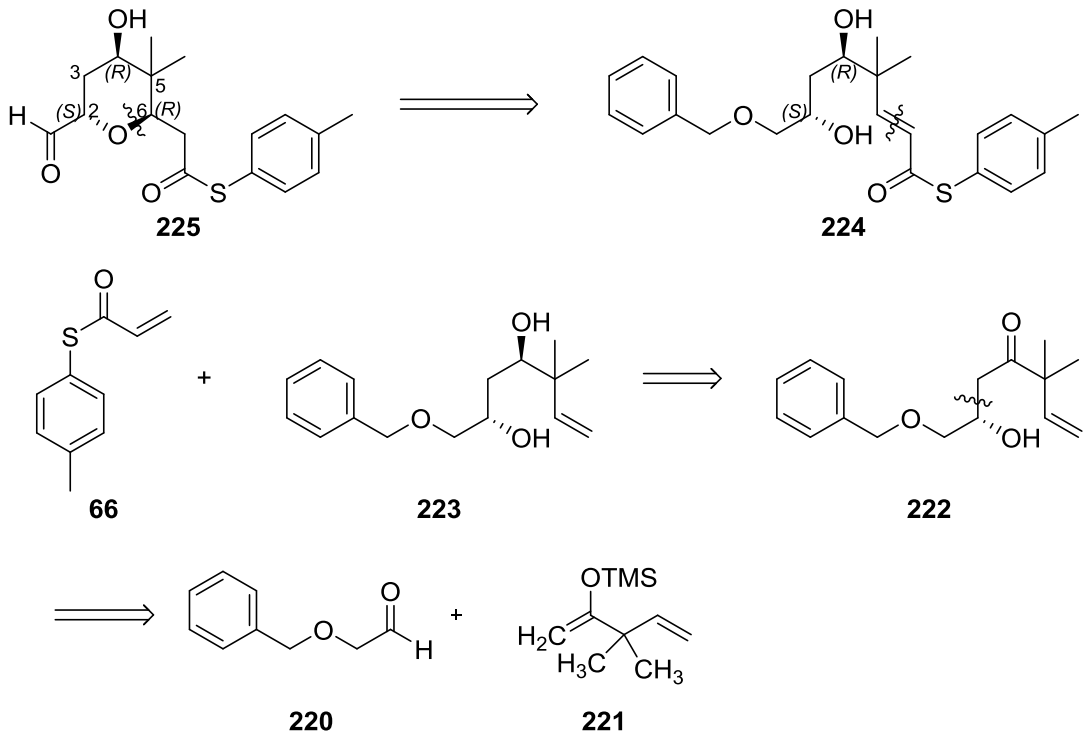

Scheme 73 Retrosynthetic analysis of the tetrahydropyran core of psymberin/ircinistatin A **225**.

Our retrosynthetic approach included, disconnection at the O-1 and C-6 bond of **225**, leading to the α,β-unsaturated thioester **224**. We envisioned that the tetrahydropyran core would be synthesised from the cyclisation precursor **224** by useing buffered TBAF oxy-Michael reaction conditions. These conditions had been successfully applied for the synthesis of diospongins **1** and **2** by the Clarke group.[41]

Cyclisation precursor **224** could be prepared through the cross metathesis of thioester **66** and diol **223**. Diol **223** could be prepared from diastereoselective reduction of the Mukaiyama aldol product **222.** The aldol product **222** would be generated from the Mukaiyama aldol reaction of 3,3-dimethyl-2-[(trimethylsilyl)oxy]-1,4-pentadiene **221** and benzyloxyacetoaldehyde **220** (**Scheme 73**).

2.2.2. Attempted synthesis of the tetrahydropyran core of psymberin/ircinistatin A *via* stereodivergent oxy-Michael cyclisation

The synthesis of 3,3-dimethyl-2-[(trimethylsilyl)oxy]-1,4-pentadiene **221** is presented in **Scheme 74**.

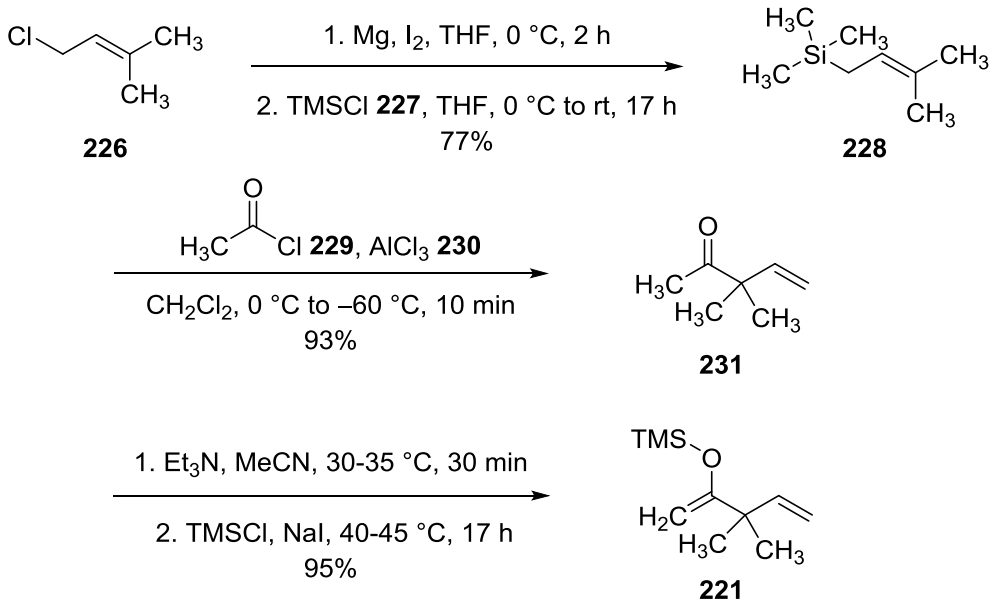

Scheme 74 Synthesis of 3,3-dimethyl-2-[(trimethylsilyl)oxy]-1,4-pentadiene **221**.

The synthesis began with Grignard formation and trapping with chlorotrimethylsilane. 1-Chloro-3-methyl-2-butene **226** and magnesium turnings were stirred at 0 °C in THF to form the Grignard reagent, then freshly distilled chlorotrimethylsilane **227** was added at room temperature. The mixture was stirred for 17 hours to give prenyltrimethylsilane **228** in a yield of 77%.[101] This reaction was carried out on a multi-gram scale (10 g) level, and further purification was not required.

It was envisioned that prenyltrimethylsilane **228** would be an important starting material for the synthesis of 3,3-dimethyl-2-[(trimethylsilyl)oxy]-1,4-pentadiene **221**. Allylic trimethylsilanes have been shown to be an useful intermediates in organic synthesis as they can react with electrophiles to give substitution reaction with allylic

rearrangement.[102-104] The general mechanism of electrophilic substitution of allyl silanes is shown in (**Scheme 75**).

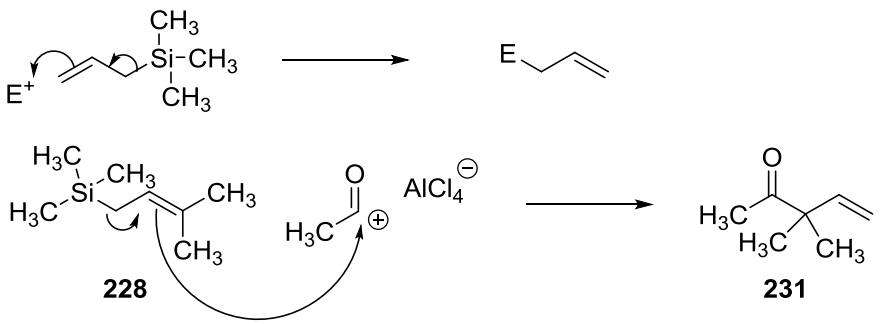

Scheme 75 General mechanism of electrophilic substitution of unsaturated silanes.

As shown in **Scheme 75**, prenyltrimethylsilane **228** would be transformed into 3,3-dimethyl-pent-4-en-2-one **231** by treatment with acetyl chloride **229** and aluminium chloride **230** to give product **231** in 93% yield.[103]

3,3-Dimethyl-pent-4-en-2-one **231** was reacted with trimethylchlorosilane in the presence of triethylamine and sodium iodide in acetonitrile to give 3,3-dimethyl-2-[(trimethylsilyl)oxy]-1,4-pentadiene **221** in 95% yield after distillation under reduced pressure.

Benzyloxyacetaldehyde **220** was synthesised in two steps according to the procedure reported by Oda.[105] For the initial reaction, commercially available *cis*-2-butene-1,4-diol **232** was used in the presence of sodium hydride in DMF to protect the hydroxyal groups as O-benzyl groups use of benzyl bromide, to give 1,4-bis(benzyloxy)but-2-ene **233** in 92% yield. The product was used directly without

any further purification. The subsequent oxidative cleavage of 1,4-bis(benzyloxy)but-2-ene **233** was achieved by ozonolysis, to form benzyloxyacetoaldehyde **220** in a yield of 93% (**Scheme 76**).

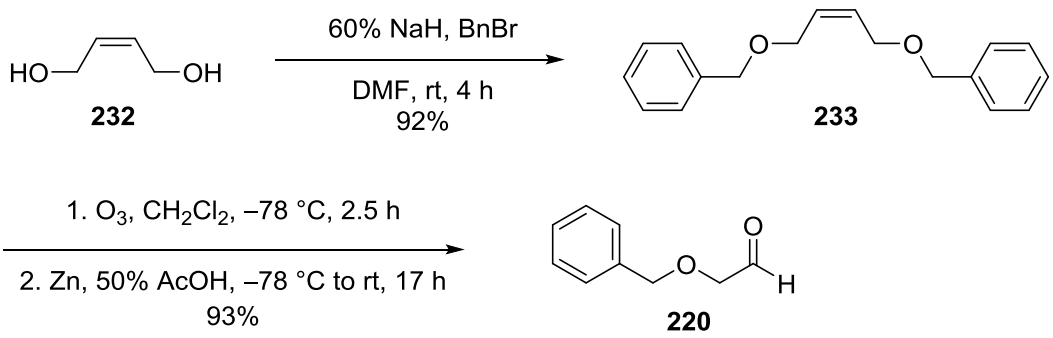

Scheme 76 Synthesis of benzyloxyacetoaldehyde **220**.

Following successful synthesis of 3,3-dimethyl-2-[(trimethylsilyl)oxy]-1,4-pentadiene **221** and benzyloxyacetoaldehyde **220**, attempts were made to investigate the conditions for the Mukaiyama aldol reaction in order to form the desired product **222**.

Initially, the aldol reaction was run at −78 °C in dichloromethane by treating 1.0 benzyloxyacetoaldehyde **220** with 1.0 equivalent of silyl enol ether **221** in the presence of 1.1 equivalents of titanium tetrachloride. After stirring for 7 hours at −78 °C, the reaction was not completed. Based on the ^{1}H NMR spectrum, the reaction had only given 7% conversion to the desired product (**Table 18**, **Entry 1**). As the reaction had not gone to completion, it was suggested that increasing the amount of silyl enol ether **221** would be required. The silyl enol ether **221** was increased to 1.1 equivalents (**Table 18**, **Entry 2**) and 2.0 equivalents (**Table 18**, **Entry 3**), respectively.

Analysis of the ^{1}H NMR spectra of the crude reaction showed that the conversion had increased, however, the reaction was still incomplete. Next, the temperature was changed to −40 °C, which again did not show any improvement. (**Table 18**, **Entry 4**) In order to optimise the conditions, changing the reaction time was evaluated next. Extending the reaction time to 17 hours resulted in completion of the reaction, resulting in 51% yield of the aldol product (**Table 18**, **Entry 5**). Due to the difficulty in maintaining the temperature under −78 °C for 17 hours, we next started the reaction at −78 °C, and gradually warmed up the temperature to room temperature. Interestingly, the aldol product **222** was obtained under these conditions.

Table 18 Investigating the reaction conditions in the Mukaiyama aldol reaction.

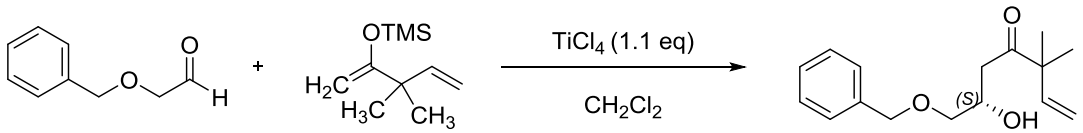

220 **221** **222**

Entry	220/eq.	221/eq.	Temperatur/°C	Time/h	Yield/%
1	1.0	1.0	−78	7	7 [1]
2	1.0	1.1	−78	7	23 [1]
3	1.0	2.0	−78	7	54 [1]
4	1.0	2.0	−40	7	26 [1]
5	1.0	2.0	−78 to rt.	17	51

1. **^{1}The conversion to form 222 was calculated by the ^{1}H NMR spectrum of the crude reaction mixture.**

The silyl enol ether **221** was difficult to purify. During the purification step, the use of Kugelrohr distillation resulted in decomposition, which meant the amount of the silyl enol ether **221** that could be utilised in the aldol reaction was small. Therefore, to scale up the aldol product in this step, alternative reaction conditions were investigated.

By avoiding the preparation step of silyl enol ether, the approach included direct deprotonation of 3,3-dimethyl-pent-4-en-2-one **231** using LDA at −78 °C, then benzyloxyacetoaldehyde **220** was added to generate the aldol product **222**. However, the yield of aldol product **222** under these reaction conditions was lower (30.4%) compared to the yield when using the Mukaiyama aldol reaction. The reasons of the lower yield may possibly be due to the retro-aldol reaction. Therefore, for further studies, the aldol product **222** was generated by using the Mukaiyama aldol reaction.

According to the literature, the relative stereochemical assignment of the C-2 and C-4 tetrahydropyran core is 2*S** and 4*R**.[67, 70, 73] Therefore, to generate the *syn*-1,3 diol **223**, a diastereoselective reduction of aldol product **222** was needed, as shown in **Scheme 77**.

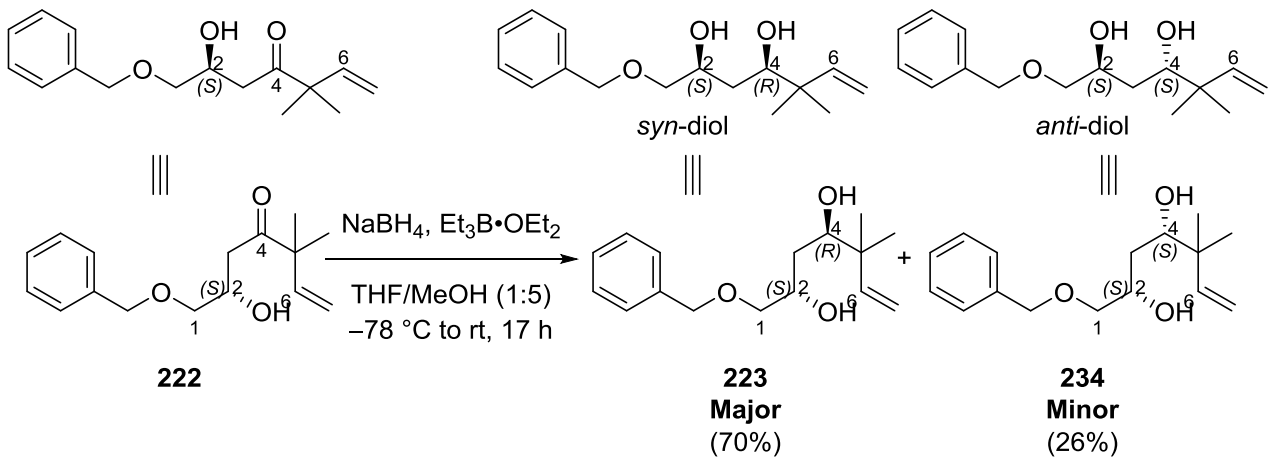

Scheme 77 Synthesis of *syn*-diol **223** under Narasaka–Prasad reduction.

In theory, *syn*-1,3 diol was expected to be a major product of Narasaka–Prasad reduction,[57, 58] while, Evans–Saksena reduction[54, 55] favours the formation of *anti*-1,3 diol over *syn*-1,3 diol (discussed in chapter **1.2.3**).

The Narasaka–Prasad reduction was successfully applied to the synthesis of *syn*-1,3 diol unit **79** in diospongin A **1** and diospongin B **2**, therefore, it was expected to reduce the aldol product **222** under the same reaction conditions to give *syn*-1,3 diol **223**. Synthesis of *syn*-1,3 diol **223** was achieved by using sodium borohydride and triethylborane as a chelating agent which led to the reduction of acylic *β*-hydroxyketone **222** in 96% crude yield. The product was analysed by the crude ^{1}H NMR spectrum. Interestingly, it was suggested that the product was a mixture of *syn* and *anti* diastereomers. However, it was difficult to determine the diastereomeric ratios by analysis of the crude ^{1}H NMR spectrum. Fortunately, these two diastereoisomers could be separated by using column chromatography, which gave a

major product in 70% yield and a minor product in 26%. Unfortunately, we were unable to determine the identity of the major diastereomer.

Meanwhile, the Evans–Saksena reduction was also carried out by reducing the acylic *β*-hydroxyketone **222** with sodium triacetoxyborohydride. As shown in **Scheme 78**, only one diastereomer **234** was generated for this reaction, however the yield was poor (32%). The ^{1}H NMR spectrum, matched the spectroscopic data of the minor product obtained from the Narasaka–Prasad reduction, therefore, the major product of the Narasaka–Prasad reduction was assumed to be the *syn*-1,3 diol.

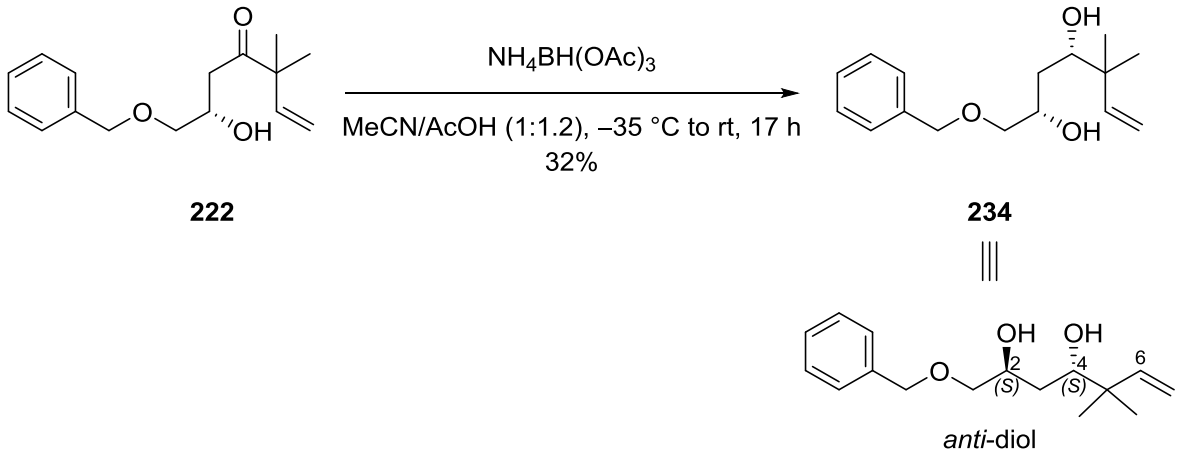

Scheme 78 Synthesis of *anti*-diol **234** under Evans–Saksena reduction.

Structural assignment of the *syn*-1,3 diol **223** and *anti*-1,3 diol **234** were further established by ^{13}C NMR studies of their 1,3-diol acetonides **235** and **236**, respectively. According to the literature, the stereochemistry of *syn*-1,3 diol and *anti*-1,3 diol were

able to be determined by converting them into acetonides.[106-108] The difference in structural configuration between *syn*-1,3 diol acetonides (chair configuration) **237** and *anti*-1,3 diol acetonides (twist-boat) **238**, resulted in different chemical shifts of the acetal methyl groups and acetal carbon in the ^{13}C NMR spectrum as shown in **Table 19**.

Table 19 ^{13}C NMR chemical shifts the gem-dimethyl groups in the *syn*- and *anti*-acetonides.

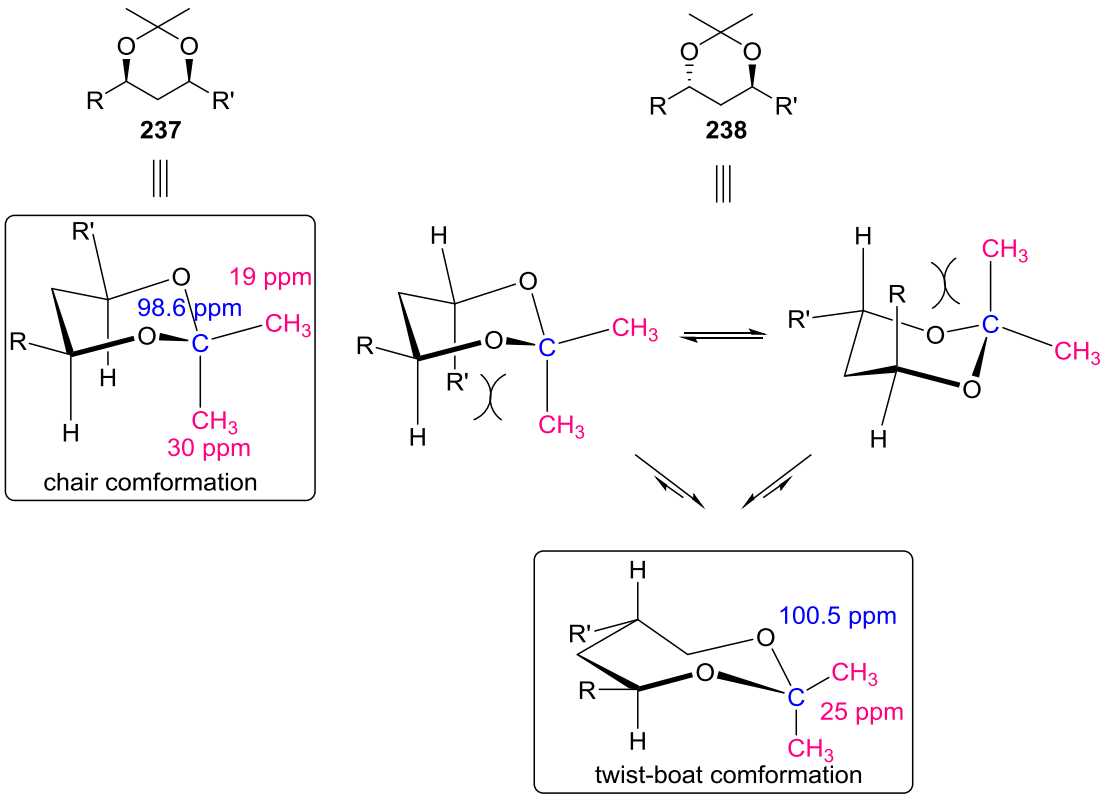

	***syn*-1,3-diol acetonide 237**	***anti*-1,3-diol acetonide 238**
acetal methyl	19 and 30 ppm	25 ppm
acetal carbon	98.6 ppm	100.5 ppm

In general, the ^{13}C NMRchemical shifts of the acetal methyl group in the *syn*-1,3 diol acetonide **237** were shown at 19 ppm for the axial carbon and 30 ppm for the equatorial carbon, and its acetal carbon was displayed at 98.6 ppm. In contrast, the acetal methyl group in the *anti*-acetonide **238** were shifted around 25 ppm and the acetal carbon was shifted at 100.5 ppm.

The synthesis of 1,3-diol acetonides **235** and **236** were accomplished by following the procedure reported by the Sabitha group (**Scheme 79**).[109]

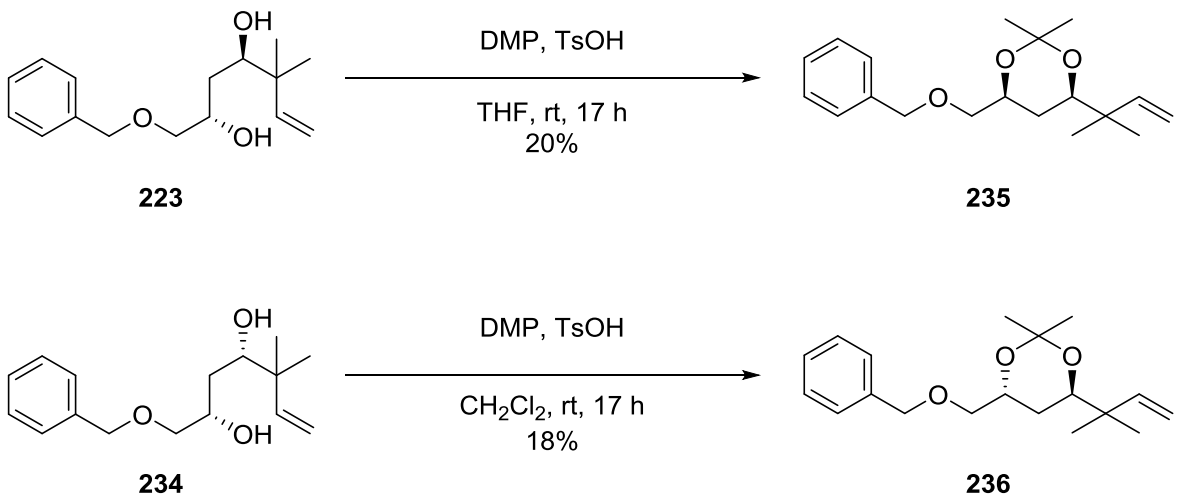

Scheme 79 Synthesis of 1,3-diol acetonides **235** and **236**.

Transformation of diols **223** and **234** to acetonides **235** and **236** were carried out by using 2,2-dimethoxypropane in the presence of a catalytic amount of 4-methylbenzenesulfonic acid. The reaction did not go to completion and resulted in a poor yield. However, enough product was formed to analyse the ^{13}C NMR spectrum after purification, and the results are presented in **Figure 37** and **Table 20**.

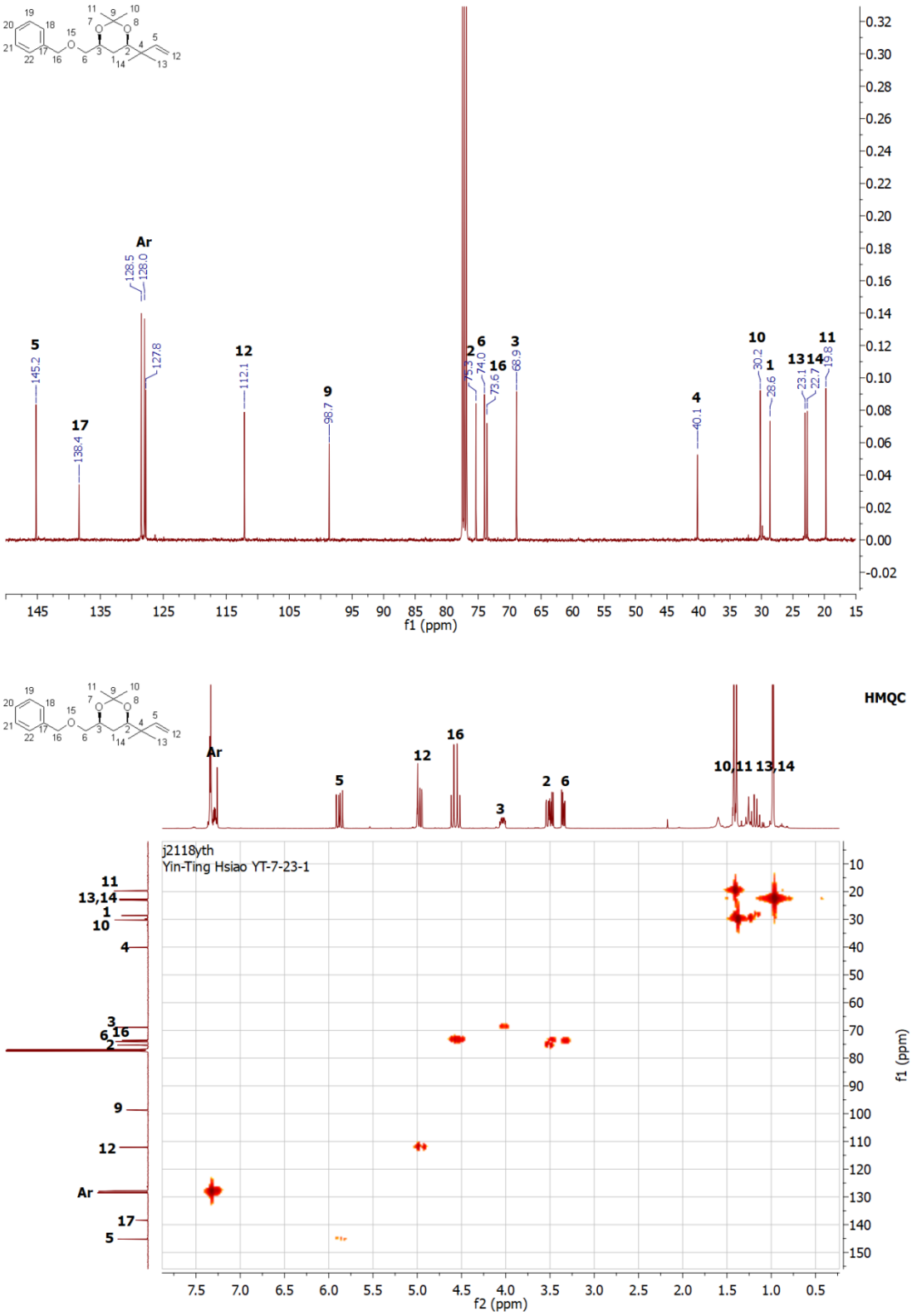

Figure 37 ^{13}C NMR and HMQC spectra of acetonide **235**.

Table 20 ^{13}C NMR data of compound **235** and **236**.

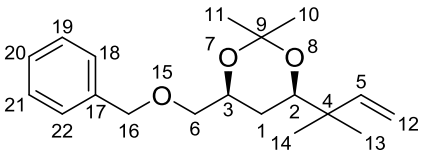 **235**	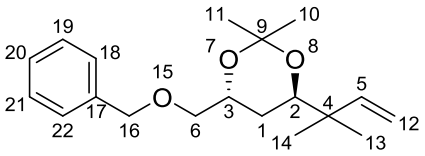 **236**
(400 MHz, $CDCl_3$)	**(400 MHz, $CDCl_3$)**
145.2 (C-5)	144.8 (C-5)
138.4 (C-17)	138.5 (C-17)
128.5, 128.0, 127.8 (C-Ar)	128.5, 127.9, 127.7 (C-Ar)
112.1 (C-12)	112.3 (C-12)
98.7 (C-9)	**100.6 (C-9)**
75.3 (C-2)	73.4 (C-16)
74.0 (C-6)	73.0 (C-2)
73.6 (C-16)	72.9 (C-6)
68.9 (C-3)	66.8 (C-3)
40.1 (C-4)	40.0 (C-4)
30.2 (C-10)	30.4 (C-1)
28.6 (C-1)	**24.9 (C-10)**
23.1 (C-13)	**24.3 (C-11)**
22.7 (C-14)	23.1 (C-13)
19.8 (C-11)	22.8 (C-14)

The chemical shift in the ^{13}C NMR spectrum of the resulting acetonide **235** is shown in **Table 20**. Its acetal methyl group (C-10 and C-11) and acetal carbon (C-9) were shown at 19.8, 30.2 and 98.7 ppm, respectively. All the spectroscopic data matched to those reported in the literature.[106-108] Therefore, the stereochemistry of **223** was

determined to be a *syn*-1,3 diol.

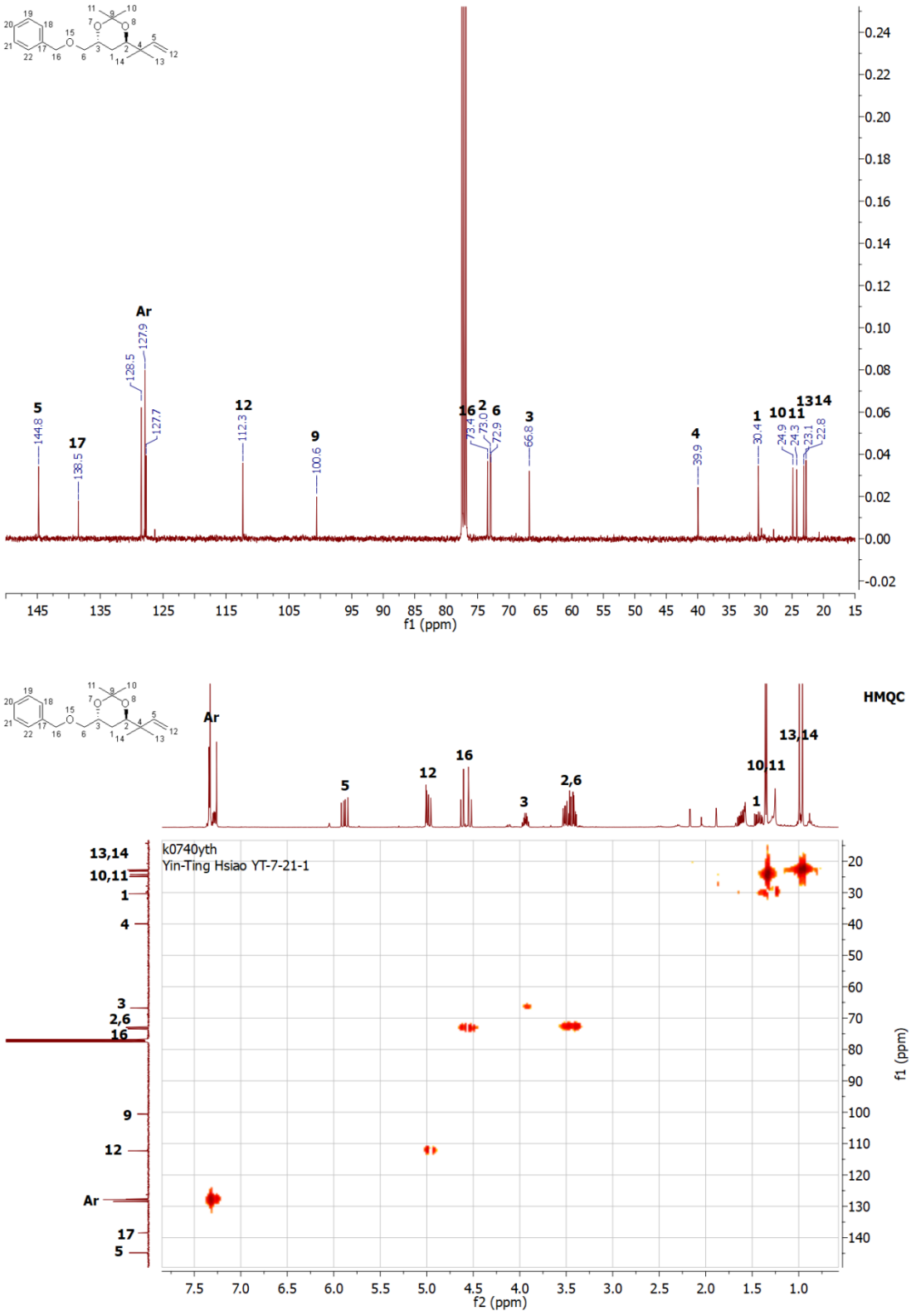

Figure 38 ^{13}C NMR and HMQC spectra of acetonide **236**.

The stereochemistry of *anti*-1,3 diol **234** was also established by the same method (**Table 20** and **Figure 38**). For acetonide **236**, which was obtained from **234**, the chemical shifts of the acetal methyl groups (C-10 and C-11) were 24.9 and 24.3 ppm and acetal carbon (C-9) shifted at 100.6 ppm. To our delight, all chemical shifts were identical to the results reported by Rychnovsky, suggesting that the stereochemistry of 1,3-diol **234** is *anti*.[106-108]

A related *syn*-1,3-diol acetonide **239** was synthesised by the Pietruszka group, which had a similar structure to our *syn*-1,3-diol acetonide **235**. By comparing the NMR spectroscopic data of our 1,3-diol acetonide product **235** with the reported NMR data of **239** by Pietruszka and co-workers (**Table 21**), it could be confirmed that 1,3-diol **223** had the *syn* stereochemistry.[84]

As shown in **Table 21**, in the Pietruszka group, the acetal methyl groups were assigned at 29.9 ppm and 19.6 ppm. The chemical shift of the acetal carbon (C-9) shifted at 98.7 ppm, which was in agreement with our findings. By comparing the ^{13}C NMR data of **235** and **239**, the stereochemistry of *syn*-1,3-diol **223** could also be confirmed.

Table 21 ^{13}C NMR data of compounds **235** and **239**.

Our results	**Pietruszka's results**[84]
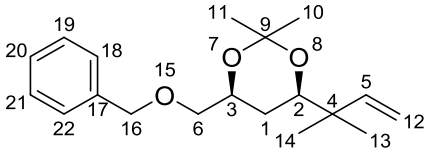	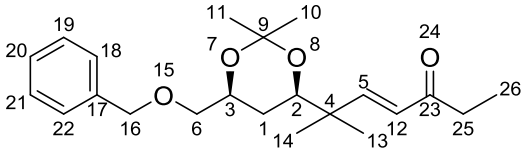
235 (400 MHz, $CDCl_3$)	**239** (600 MHz, $CDCl_3$)
-	167.0 (C-23)
145.2 (C-5)	155.0 (C-5)
138.4 (C-17)	138.2 (C-17)
128.5, 128.0, 127.8 (C-Ar)	127.6, 127.8, 128.4 (C-Ar)
112.1 (C-12)	119.3 (C-12)
98.7 (C-9)	**98.7 (C-9)**
75.3 (C-2)	74.8 (C-2)
74.0 (C-6)	73.7 (C-6)
73.6 (C-16)	73.5 (C-16)
68.9 (C-3)	68.6 (C-3)
-	60.7 (C-25)
40.1 (C-4)	40.3 (C-4)
30.2 (C-10)	**29.9 (C-10)**
28.6 (C-1)	28.7 (C-1)
23.1 (C-13)	22.6 (C-13)
22.7 (C-14)	22.6 (C-14)
19.8 (C-11)	**19.6 (C-11)**
-	14.3 (C-26)

To continue our synthesis of the tetrahydropyran core of **225** the next reaction to be performed was the cross-metathesis (**Table 22**).

Initially, it was envisaged that diol **223** and thioester **66** could be coupled using the metathesis procedure reported by Lipshutz.[59] Therefore, the synthesis of cyclisation precursor **224** was carried out using the 1.0 equivalent of diol **223** and 3.0 equivalents of thioester **66**. After treatment with 10 mol% of 2nd generation of Hoveyda-Grubbs catalyst and 10 mol% of copper(I) iodide in refluxing diethyl ether (**Table 22**, **Entry 1**), no reaction was observed. Next, the reaction was trialled using the optimised conditions reported previously to the synthesise the C-20–C-32 core of phorboxazole.[9] The amount of copper(I) iodide was increased to 15 mol%, however, the reaction failed to generate any product (**Table 22**, **Entry 2**). We next attempted to increase the amount of copper(I) iodide and catalyst loading to 50 mol% (**Table 22**, **Entry 3**), however again no product was formed. Next, we investigated changing the solvent from diethyl ether to dichloromethane and increasing the temperature to 40 °C (**Table 22**, **Entry 4**). Although many new spots were displayed on the TLC, ^{1}H NMR spectroscopic analysis of the crude reaction mixture showed no corresponding double bond signals of the desired product. Given that these reactions were unsuccessful, an alternative catalyst was tried. Disappointingly, the 2nd generation of Grubbs catalyst also failed to form the α,β-unsaturated thioester **224** (**Table 22**, **Entry 5**), even though the catalyst loading was increased to 50 mol% (**Table 22**, **Entry 6**). In addition, an excess in diol **223** was used (**Table 22**, **Entry 7**). It was assumed that stoichiometric excesses of olefin **223** may lead to some initiation. However, this too was unsuccessful.

Table 22 The reaction conditions attempted for the synthesis of compound **224**.

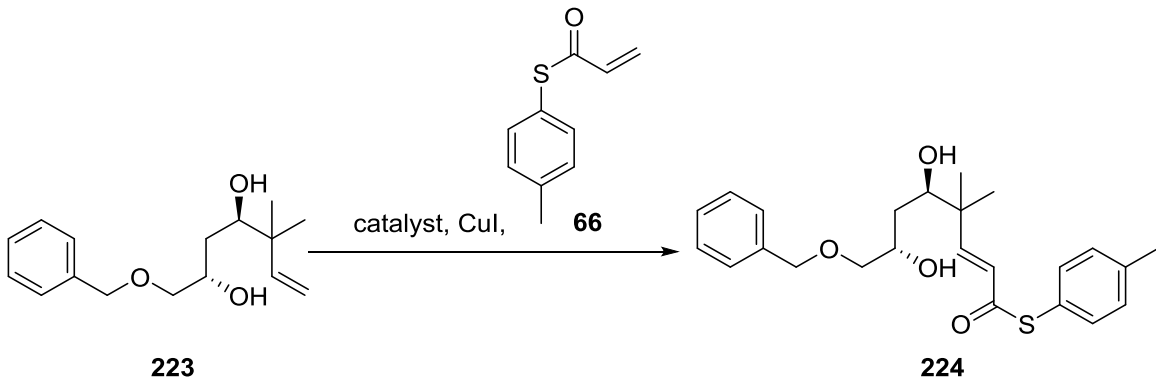

Entry	Diol 223/eq.	Thioester 66/eq.	Catalyst	CuI/mol%	Solvent	Temperature
1	1.0	3.0	Hoveyda-Grubbs 2nd 10 mol%	10	Et_2O	reflux
2	1.0	3.0	Hoveyda-Grubbs 2nd 10 mol%	15	Et_2O	reflux
3	1.0	3.0	Hoveyda-Grubbs 2nd 50 mol%	50	Et_2O	reflux
4	1.0	3.0	Hoveyda-Grubbs 2nd 10 mol%	10	CH_2Cl_2	reflux
5	1.0	3.0	Grubbs 2nd 10 mol%	-	CH_2Cl_2	reflux
6	1.0	3.0	Grubbs 2nd 50 mol%	-	CH_2Cl_2	reflux
7	3.0	1.0	Grubbs 2nd 10 mol%	15	CH_2Cl_2	reflux

It was envisaged that modifying acrolyl olefins **66** to crotyl olefin **240** may slow its homodimerization so cross metathesis can compete (**Scheme 80**). Unfortunately, under these reaction conditions, **224** was not observed by analysing the crude ^{1}H NMR spectrum, only recovered starting material.

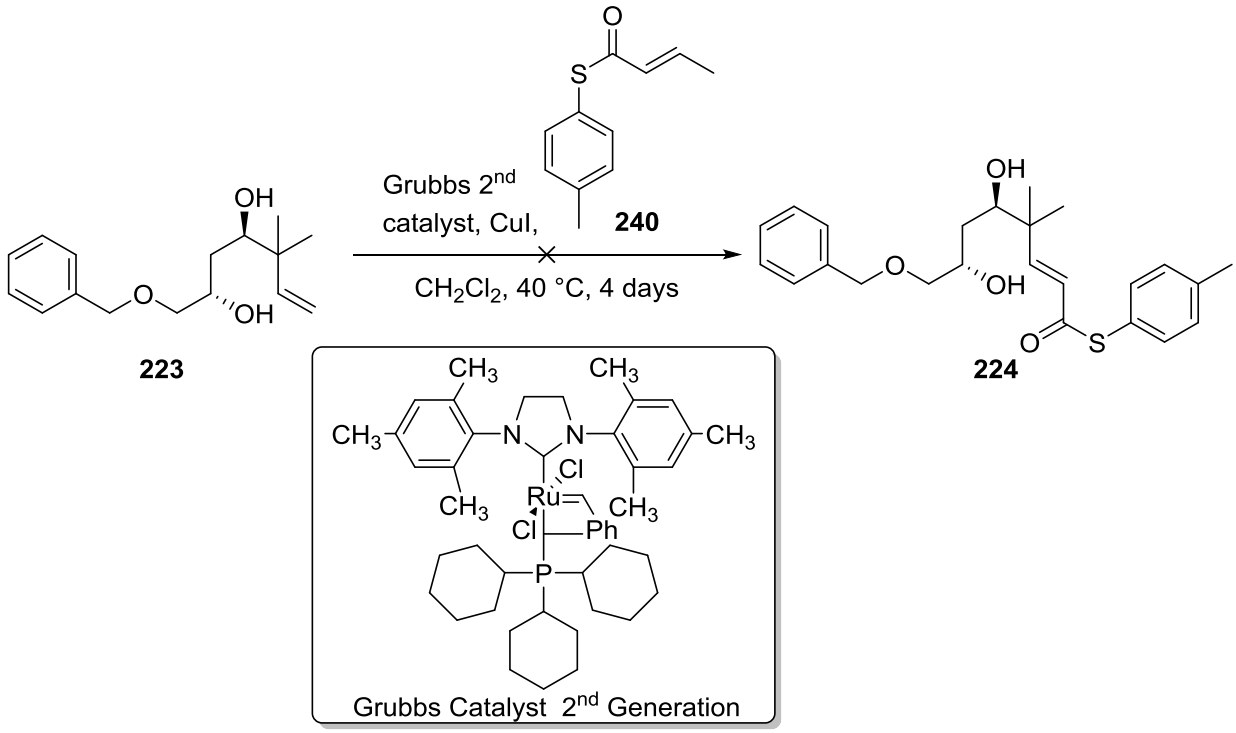

Scheme 80 Attempted synthesis of compound **224** by using cross-metathesis.

The sterically hindered substrate **223** could be classified as a type III olefins. Electron-deactivated olefins **66** was classified into types II olefin according to the classification method reported by Grubbs and co-workers.[110] To drive the cross metathesis between type III and type II olefins, the low reactivity of type III olefin required to use stoichiometric excesses and was carried out in neat reaction conditions. With the limited amount of type III olefin **223**, this synthentic route was

considered as an unsuitable one. An alternative route for synthesising *α*,*β*-unsaturated thioester **224** was sought. It was suggested that the *α*,*β*-unsaturated thioester **224** would be prepared in 3 different ways (**Scheme 81**).

1. Through a Reformatsky reaction of aldehyde **243** and thioester **244** (**Scheme 81**, **a**). It was assumed that the Reformastsky reaction may offer an attractive approach for the synthesis of *α*,*β*-unsaturated thioester **242** in the proposed system.[111] The resulting compound **241** obtained from Reformastsky reaction, would be eliminated in a subsequent step to afford the desired product **242**.
2. The *α*,*β*-unsaturated thioester **242** may be obtained from the aldol reaction between ketone **245** and aldehyde **243**, which was similar to the Reformastsky reaction (**Scheme 81**, **b**). Furthermore, the aldol product **241** would be eliminated to give *α*,*β*-unsaturated thioester **242**.
3. The *α*,*β*-unsaturated thioester **224** may be synthesised through a Wittig reaction between **246** and (2-oxo-2-(*p*-tolylthio)ethyl)triphenylphosphonium bromide **247** in the presence of base (potassium *tert*-butoxide) (**Scheme 81**, **c**).

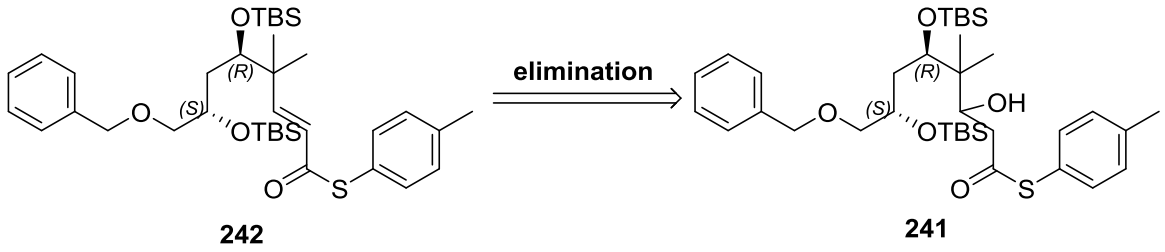

1. Reformatsky reaction

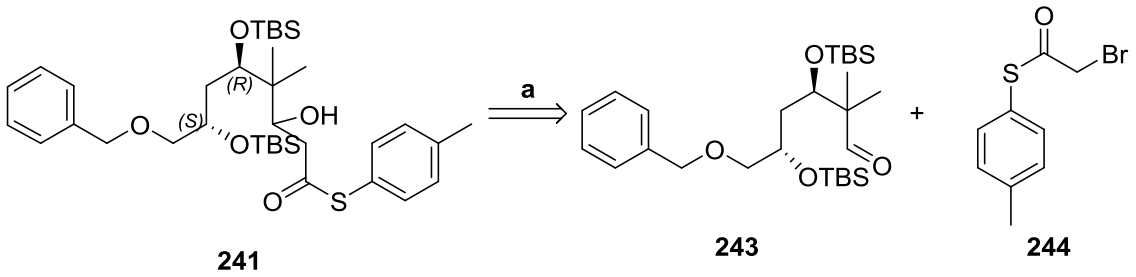

2. Aldol reaction

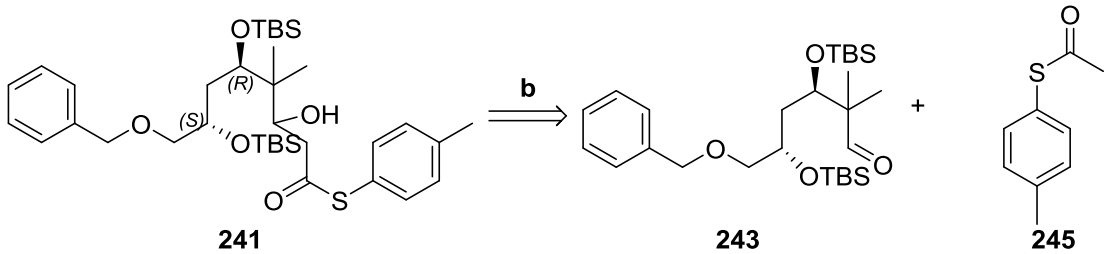

3. Wittig reaction

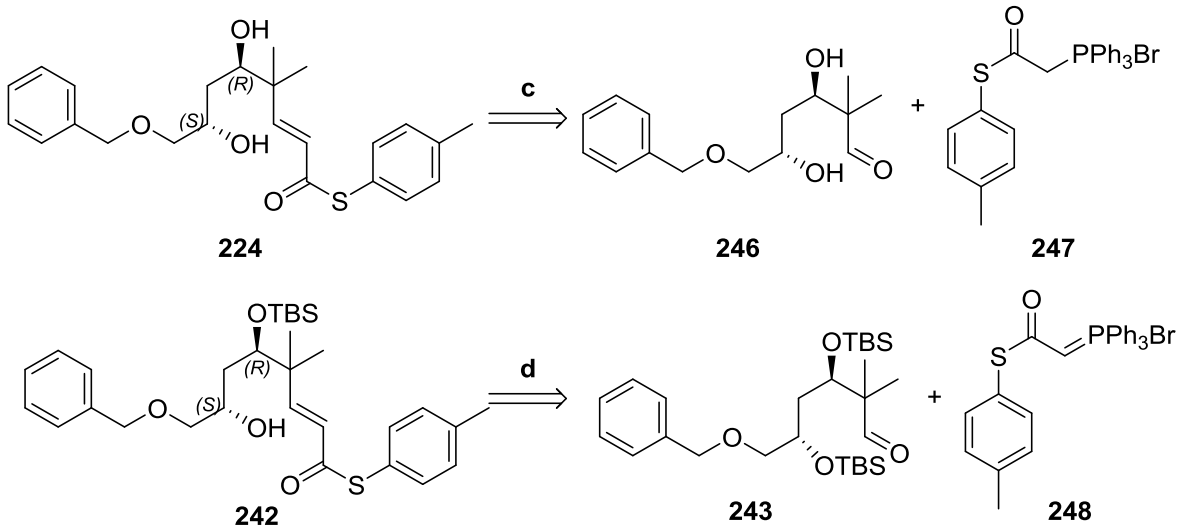

Scheme 81 Synthetic routes to prepare compounds **224** and **242**.

Initially, both the Reformastsky[111] and Aldol reactions were investigated (**Scheme 81**, **a** and **b**). The starting material **243** for both reactions was prepared in a 2-step sequence (**Scheme 82**).

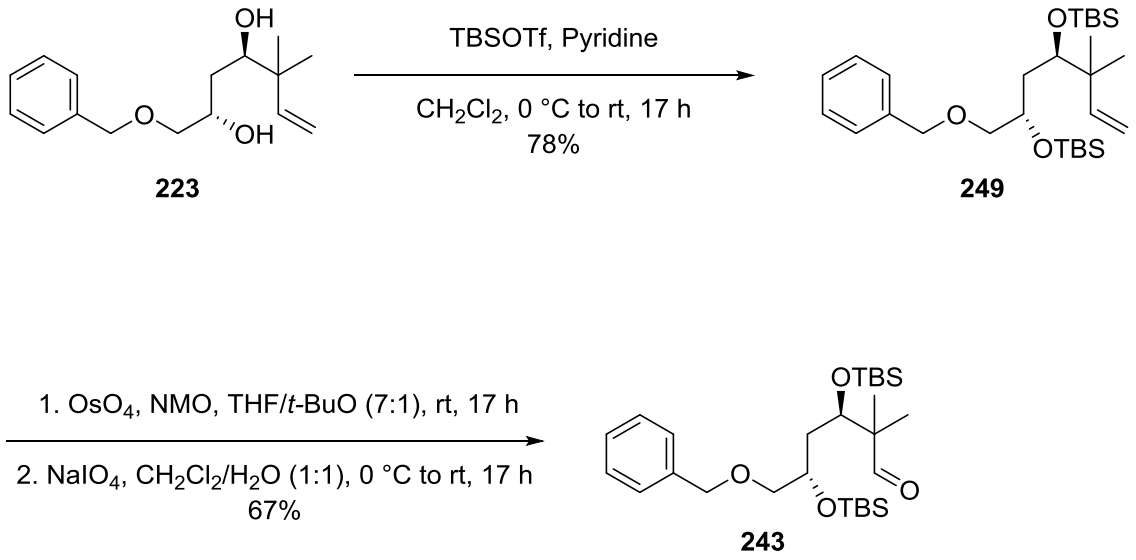

Scheme 82 Synthesis of TBS-protected aldehyde **243**.

Diol **223** was protected with TBSOTf to provide the TBS-ether **249** in a good yield (78%). The resulting TBS-ether **249** was converted to TBS-protected aldehyde **243** *via* ozonalysis of **249**. However, attempts to purify it by chromatography were challenging. Therefore, it was decided that another oxidative cleavage reaction should be introduced. The dihydroxylation of olefin **249** with catalytic amounts of osmium tetroxide and the co-oxidant NMO provided the diol compound, which was then treated with sodium (meta)periodate to give **243** in 67% yield. The **243** was pure enough to be utilised in the subsequent reaction.

Synthesis of S-*p*-tolyl 2-bromoethanethioate **244** was performed, following the procedure reported by Himber.[112] The reaction began with the use of commercially available bromoacetyl bromide **250** and 4-methylbenzenethiol **90** in the presence of pyridine to generate S-*p*-tolyl 2-bromoethanethioate **244** in 81% yield after purification (**Scheme 83**).

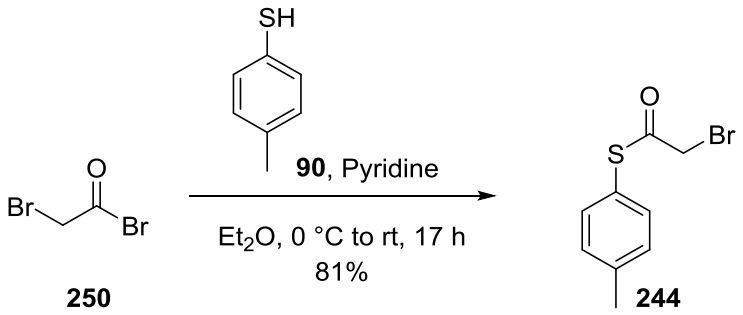

Scheme 83 Synthesis of S-*p*-tolyl 2-bromoethanethioate **244**.

The synthesis of S-(4-methylphenyl)ethanethioate **245** also began with commercially available acetyl chloride **229** and 4-methylbenzenethiol **90** in the presence of pyridine. After purification, S-(4-methylphenyl)ethanethioate **245** was obtained in 64% yield (**Scheme 84**).

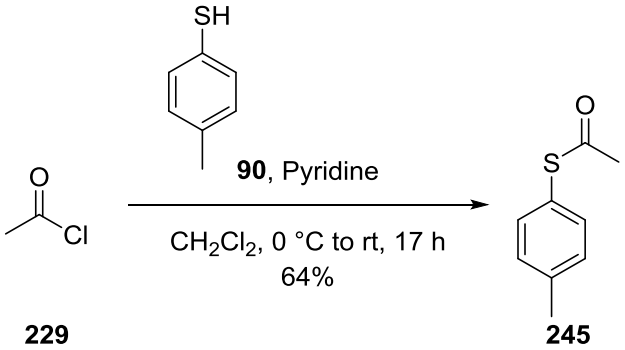

Scheme 84 Synthesis of S-(4-methylphenyl)ethanethioate **245**.

After completing the synthesis of all starting materials, attempted to synthesise **241** *via* Reformastsky[111] and aldol reactions (**Scheme 81**, **a** and **b**) were undertaken. Treating TBS-protected aldehyde **243** with **244** in refluxing THF and in the presence of Zn, the *β*-hydroxy thioesters **241** was obtained *via* a Reformastsky reaction (**Scheme 85**).

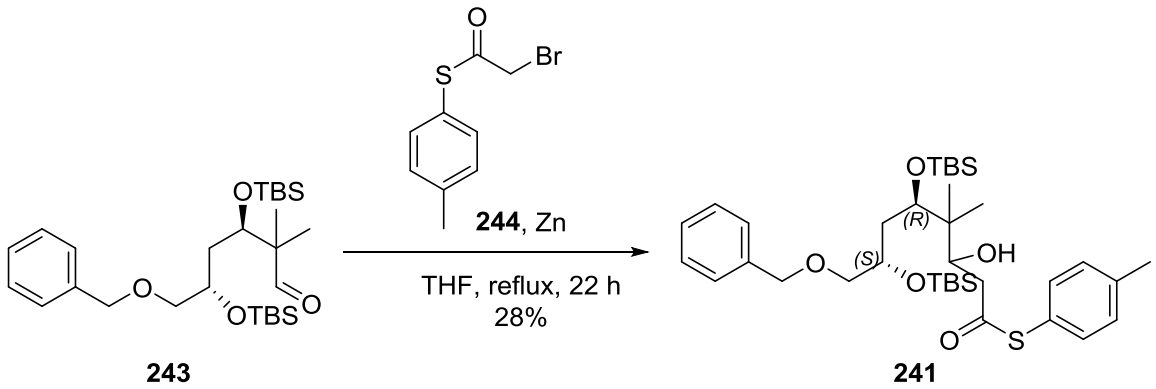

Scheme 85 Synthesis of **241** *via* a Reformastsky reaction.

Under aldol reaction conditions, deprotonation of **245** with LDA at −78 °C, followed by adding the aldehyde **243**, resulted in generation of the aldol product **241** (**Scheme 86**).

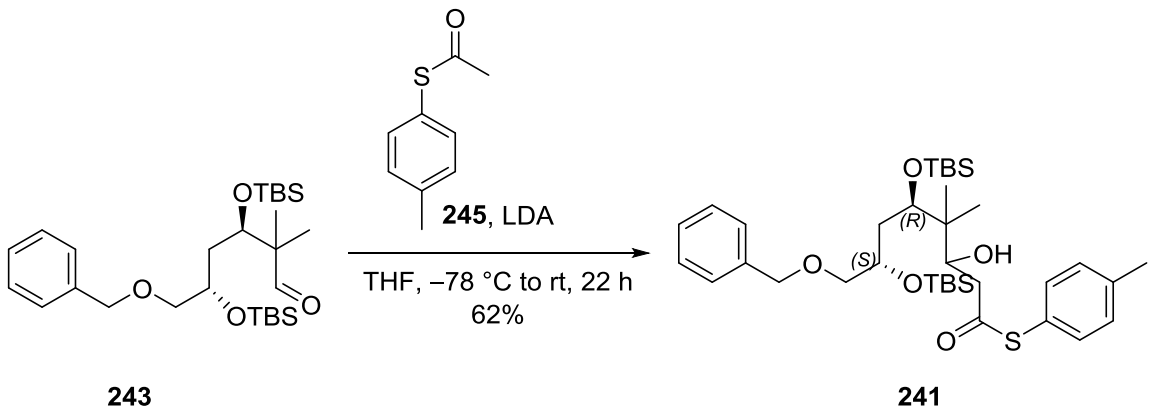

Scheme 86 Synthesis of **241** *via* the aldol reaction.

Interestingly, both reactions gave a spot with the same *Rf* value on the TLC, which was assumed to be the desired product **241**. The crude reaction mixture was purified by column chromatography, and many products were isolated. However, even after being purified multiple times with column chromatography, impurities were still present in the ^{1}H NMR spectrum of the most promising product. Because only a small amount of crude product was obtained, additional purification methods, such as recrystallization and distillation could not be performed. Therefore, this compound was used in the next step without any further purification.

In subsequent steps, the elimination reaction was investigated by following the reported mesylation procedure (**Scheme 87**).[113]

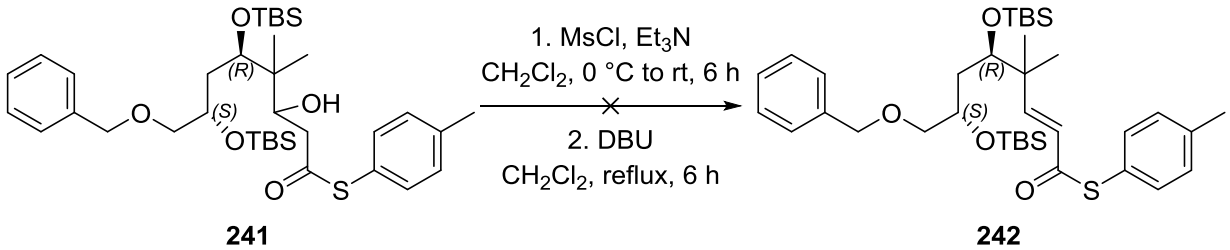

Scheme 87 Synthesis of compound **242** *via* the elimination reaction of **241**.

It was assumed that by treating **241** with methanesulfonyl chloride in the presence of triethylamine, followed by addition of DBU would result in formation of **242.** However, the reaction failed to generate any identifiable products.

Given that the elimination was unsuccessful, it was thought that by using alternative reaction conditions (with TFA in DCE and water) may result in the desired product **242** (**Scheme 88**).

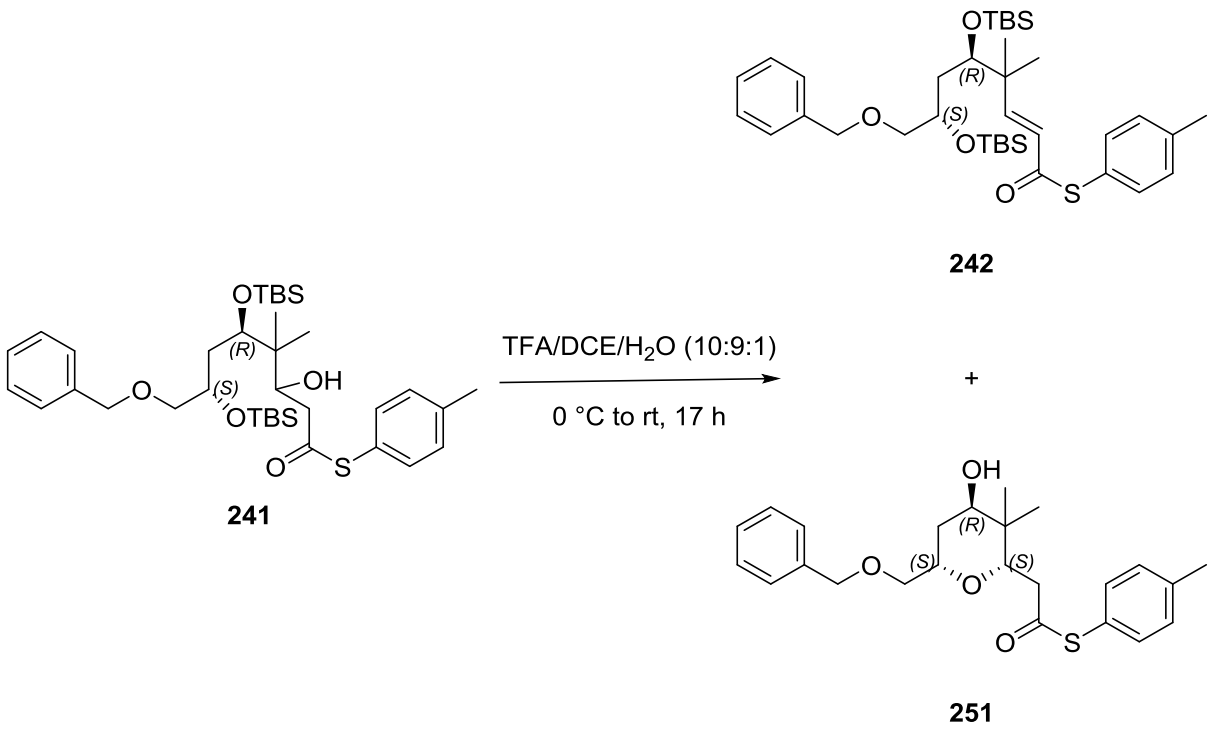

Scheme 88 Attempted synthesis of **242** under TFA acid condition.

According to the previous results regarding the synthesis of diospongin A **1** and B **2** in chapter **1.2.3**,[41] TFA could catalyse the oxy-Michael cyclisation to form the *cis*-tetrahydropyran ring. Therefore, it was envisaged that application of the TFA conditions in our elimination reaction, may result in both elimination of product **242** and undesired *cis*-tetrahydropyran **251** cyclised product.

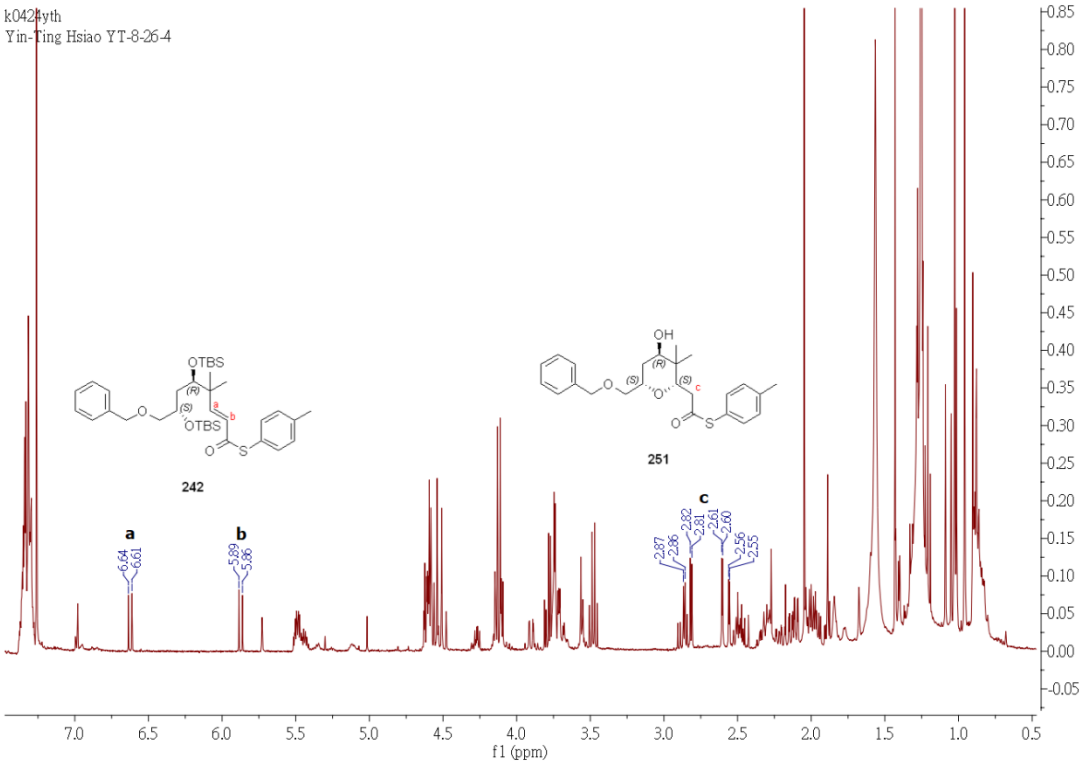

Figure 39 ^{1}H NMR spectrum of the elimination reaction crude product mixture from the **241**.

Whilst the results were not unexpected, treatment of **241** with TFA appeared to show the presence of the elimination product **242** and cyclised product **251**, as seen in the ^{1}H NMR spectrum of the unpurified reaction mixture (**Figure 39**). The characteristic (double bond) peaks **a** and **b** of elimination product **242** were observed at 6.64-6.61 ppm **242a** and 5.89-5.86 **242b** ppm, respectively. Additionally, as shown by our previous results, two protons next to the carbonyl group **c** of the *cis*-tetrahydropyran showed at 2.53-2.99 ppm (**Figure 40**). Therefore, the double-doublet peaks at 2.84 and 2.58 ppm with in the ^{1}H NMR spectrum were suggested to represent the two protons next to the carbonyl group of cyclised product **251c**.

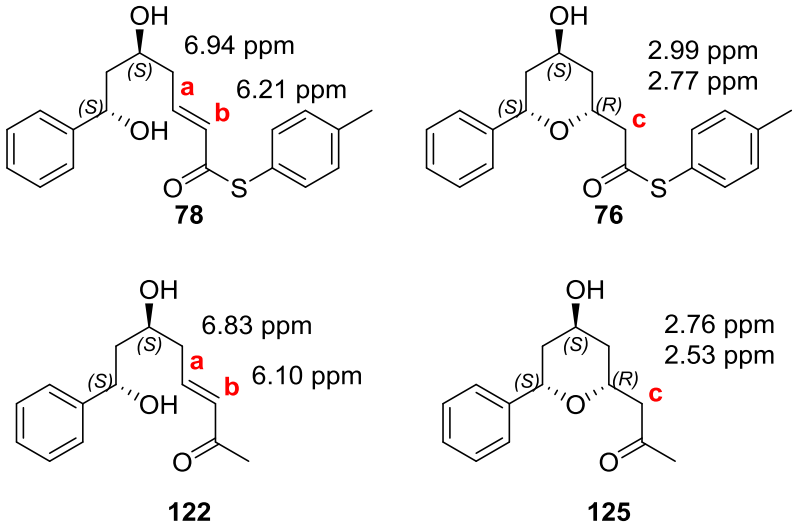

Figure 40 Chemical shifts of the cyclisation precursors **78** and **122** and the *cis*-tetrahydropyrans **76** and **125** at **a**, **b** and **c** positions.

The reaction mixture was purified by column chromatography on silica gel, unfortunately, due to time constraints, purification of the elimination product **242** and the cyclised product **251** could not be fully and conclusively characterised.

At the same time, the Wittig reaction was under investigated using **224** (**Scheme 81**, **c**).

Synthesis of the starting material **246** was achieved *via* oxidative cleavage of the double bond of diol **223** using ozone as an oxidant, followed by the addition of an excess amount of dimethyl sulfide to form aldehyde **246** in 92% yield (**Scheme 89**).

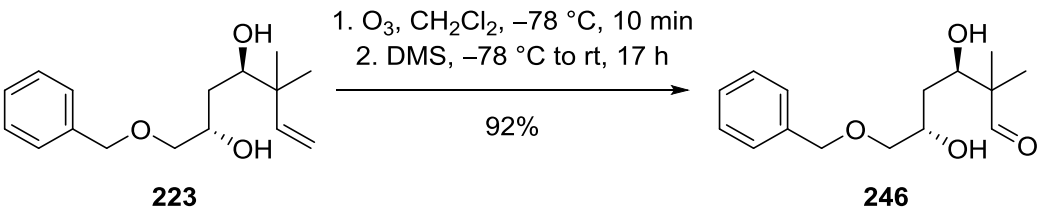

Scheme 89 Synthesis of compound **246** *via* ozonalysis.

Formation of the phosphonium salts **247** by treatment of S-*p*-tolyl 2-bromoethanethioate **244** with triphenylphosphine in benzene, proceeded smoothly and provided (2-oxo-2-(*p*-tolylthio)ethyl)triphenylphosphonium bromide **247** in 93% yield (**Scheme 90**).[114]

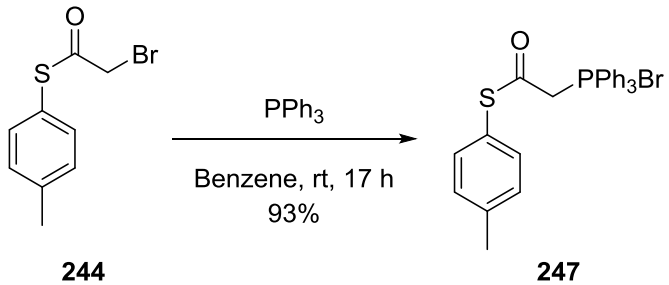

Scheme 90 Synthesis of phosphonium salt **247**.

Upon completion of the synthesis of both starting materials, **246** and **247**, we turned our attention to the Wittig reaction to construct the *α*,*β*-unsaturated thioester **224** (**Scheme 81**, **c**).

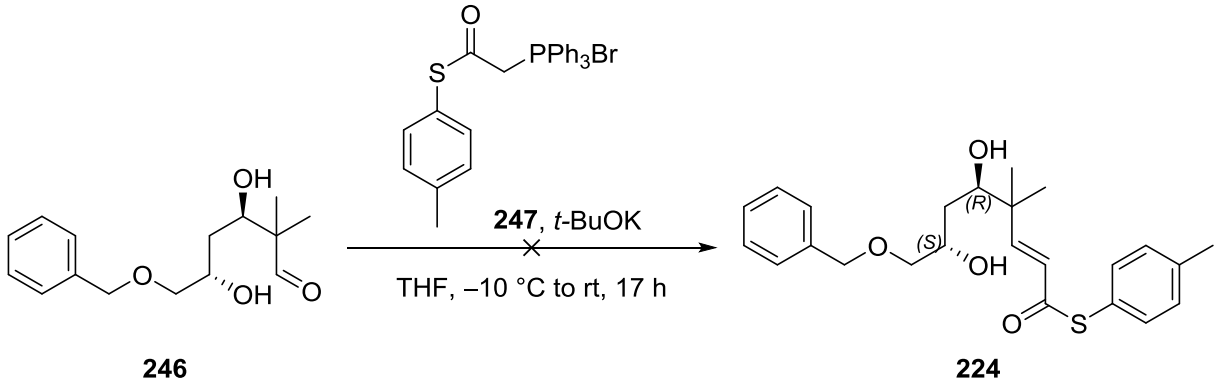

Scheme 91 Attempted synthesis of thioester **224**.

However, upon trying the Wittig reaction by treating **246** with **247** in the presence of potassium *tert*-butoxide in THF a complex crude reaction mixture was formed, which was apparent in many species on TLC and no obvious double bond peaks were present in the crude ^{1}H NMR spectrum. This may be due to the cyclisation that spontaneously occurred under these reaction conditions. Notably, **247** did not fully dissolve in THF, although a colour change was observed when it was deprotonated by potassium *tert*-butoxide. Without further separation and characterisation, the activity of the resulting ylide was unknown.

In order to examine the activity of ylide **248**, it was pre-made separately by the following procedure and characterised by ^{1}H NMR spectroscopy.[112] Ylide **248** was obtained by using triethylamine as a base to deprotonate **247** in a moderate yield (51%) (**Scheme 92**).

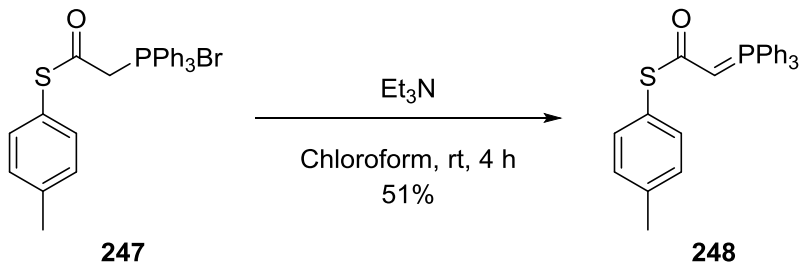

Scheme 92 Synthesis of ylide **248**.

Ylide **248** was then submitted to a model Wittig reaction with **220**. Given the successful transformation of aldehyde **220** to **252** by treating 2-benzyloxyacetoaldehyde **220** with ylide **248** in refluxing benzene, it was suggested that ylide **248** was successfully prepared and a promising compound for use in the real system. The isolated yield for this reaction, however, was low (20%) (**Scheme 93**).

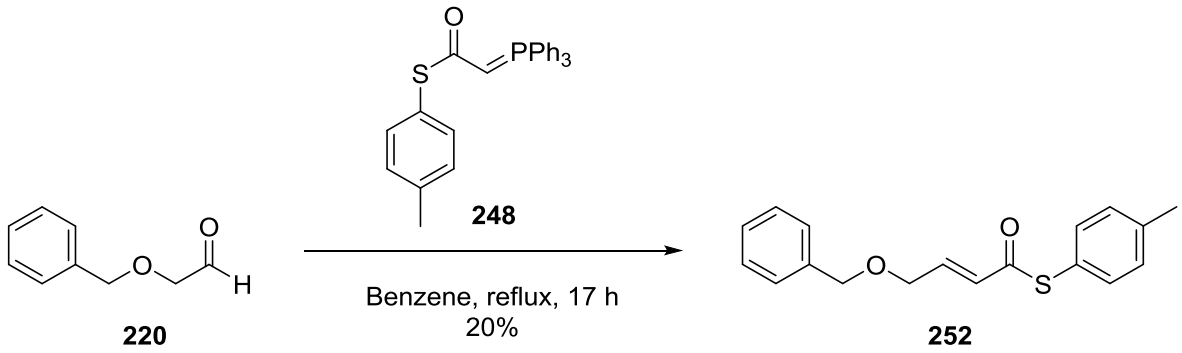

Scheme 93 Model study of the Wittig reaction.

Given the difficulties that were encountered during the purification of the reaction mixture by chromatography, and in order to prevent any cyclisastion in the Wittg reaction, TBS-protected aldehyde **243** was used.

Treatment of aldehyde **243** with ylide **248** in refluxing benzene for 17 hours, indicated that the reaction went to completion. Moreover, analysis of the crude reaction mixture by ^{1}H NMR spectroscopy, indicated that the desired product was present. Unfortunately, due to time constraints, did not lead to the isolation and assignment of the desired product **242** (**Scheme 94**).

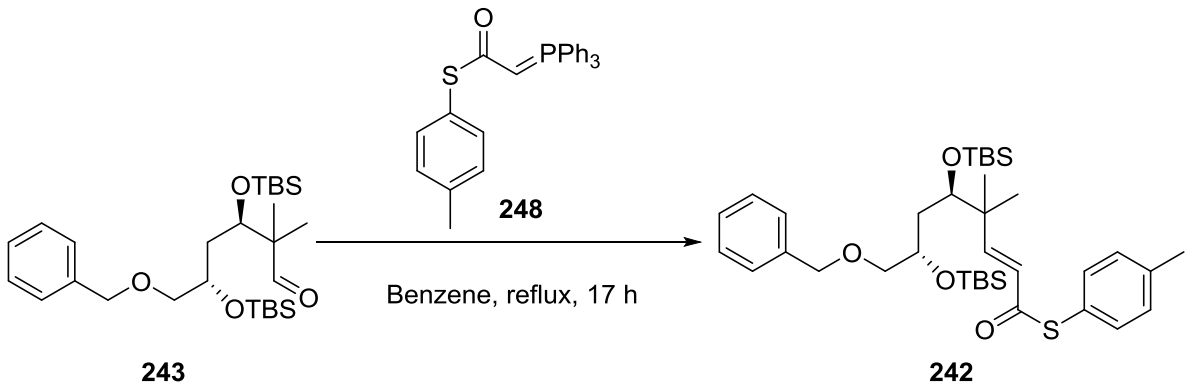

Scheme 94 Attempted synthesis of compound **242** *via* the Wittig reaction.

2.3. Conclusions and Future work

In this study, approaches toward the tetrahydropyran core of psymberin/ircinistatin A **225** were described. The synthetic plan to **225** focused on the ring closure step, which could be achieved *via* the stereodivergent oxy-Michael cyclisation.

To construct **225**, the aldol reaction between 3,3-dimethyl-2-[(trimethylsilyl)oxy]-1,4-pentadiene **221** and benzyloxyacetoaldehyde **220** was applied in 51% yield. The C-2 and C-4 stereocentres of **225** were installed followed by a reduction of **222** under Narasaka–Prasad conditions to afford 1,3-*syn* diol **223** in 70% yield. Next, the synthesis of cyclisation precursor **224** was attempted *via* cross metathesis of thioester **66** and diol **223**. However, the synthesis of cyclisation precursor **224** failed even after many attempts. The other reactions were revised to form the cyclisation precursor **224**. To achieve this, the Aldol reaction and the Reformatsky reaction followed by elimination were tried. To our delight, the cyclisation precursor **242** and spontaneous cyclised product **251** were formed in the elimination step.

Further studies were aimed to optimise the cyclisation precursor forming step and to characterise both the cyclisation precursor **242** and the spontaneously cyclised product **251** formed in the elimination step. Also, synthesis of the tetrahydropyran core of psymberin/ircinistatin A **225**.

3. Studies Towards the (*L*)-Proline Benzyl Ester-catalysed Asymmetric Aldol Reaction in Aqeous Conditions

3.1. Introduction

3.1.1. Asymmetric aldol reactions

The aldol reaction has been recognised as one of the most commonly used carbon–carbon bond-forming reactions in organic synthesis.[115]

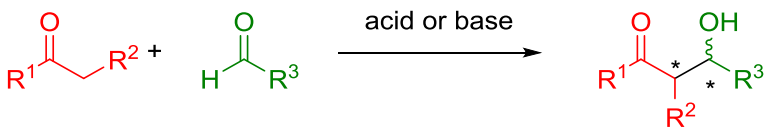

Scheme 95 General reaction scheme of the aldol reaction.

In general, the aldol reaction joins with two carbonyl group-containing molecules under either acid or base catalysis to form a *β*-hydroxyketone (**Scheme 95**), and has the potential to install one or two stereogenic centres. Several methods have been developed to control both the relative and absolute stereochemistry of these centres.

Recently, List, Barbas, Lerner and their co-workers have presented a new strategy that (*L*)-proline can act as an efficient and remarkably selective organocatalyst, which was enabled for use in the intermolecular direct aldol reaction.[116, 117] Therefore, proline and its derivatives have received increased attention and have been applied as an enamine catalyst in many research areas.

3.1.2. Proline as an organocatalyst

In the early 1970s, proline was first applied to Robinson annulation reactions by two research groups independently Hajos and Parrish,[118] and Eder, Sauer and Wiechert.[119]

Hajos and Parrish showed that proline catalysed the formation of **255** from triketone **253** by using 3 mole percent of *(L)*-proline **254** in DMF in a high yield (100%) and enantioselectivities (93% *ee*) (**Scheme 96**).[118]

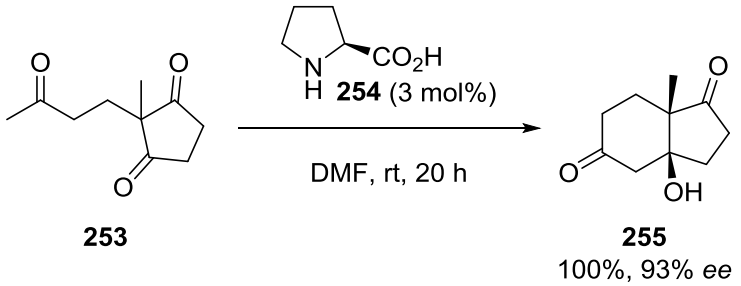

Scheme 96 *(L)*-Proline-catalysed asymmetric Robinson annulations.[118]

However, over 30 years later, proline was not fully and widely studied until it was reinvestigated by List and co-workers in 2000.[116] List, Lerner and Barbas have demonstrated the use of proline as a catalyst for the direct asymmetric aldol reaction between acetone **256** and a variety of aldehydes to form aldol products **261**-**266** in moderate to good yields and enantioselectivities (**Scheme 97**).

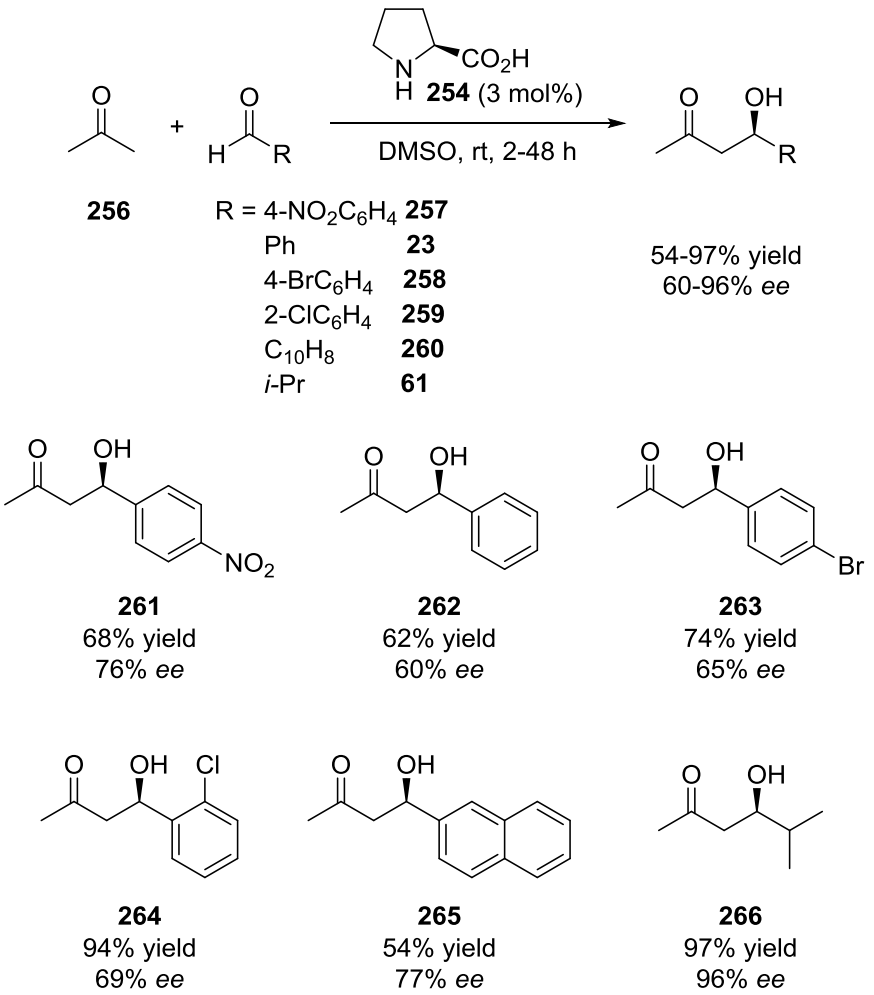

Scheme 97 *(L)*-Proline-catalysed direct aldol reactions between acetone and aldehydes.[116]

The work by List on the intermolecular application of the proline-catalysed direct asymmetric aldol reaction opened a new field of enamine-catalysed aldol reactions. The concept of the application of small organic molecules (organocatalysts) as catalysts has received significant attention from the organic chemistry community. Since then, many researchers have carried out the mechanistic studies and investigated the new types of chiral amines as catalysts.

3.1.3. Mechanism of the proline-catalysed aldol reaction

To date, several mechanisms have been proposed to account for proline-catalysed asymmetric aldol reaction.[118, 120-125] However, the generally accepted mechanism was most recently proposed by List and co-workers (**Figure 41**).[116, 126]

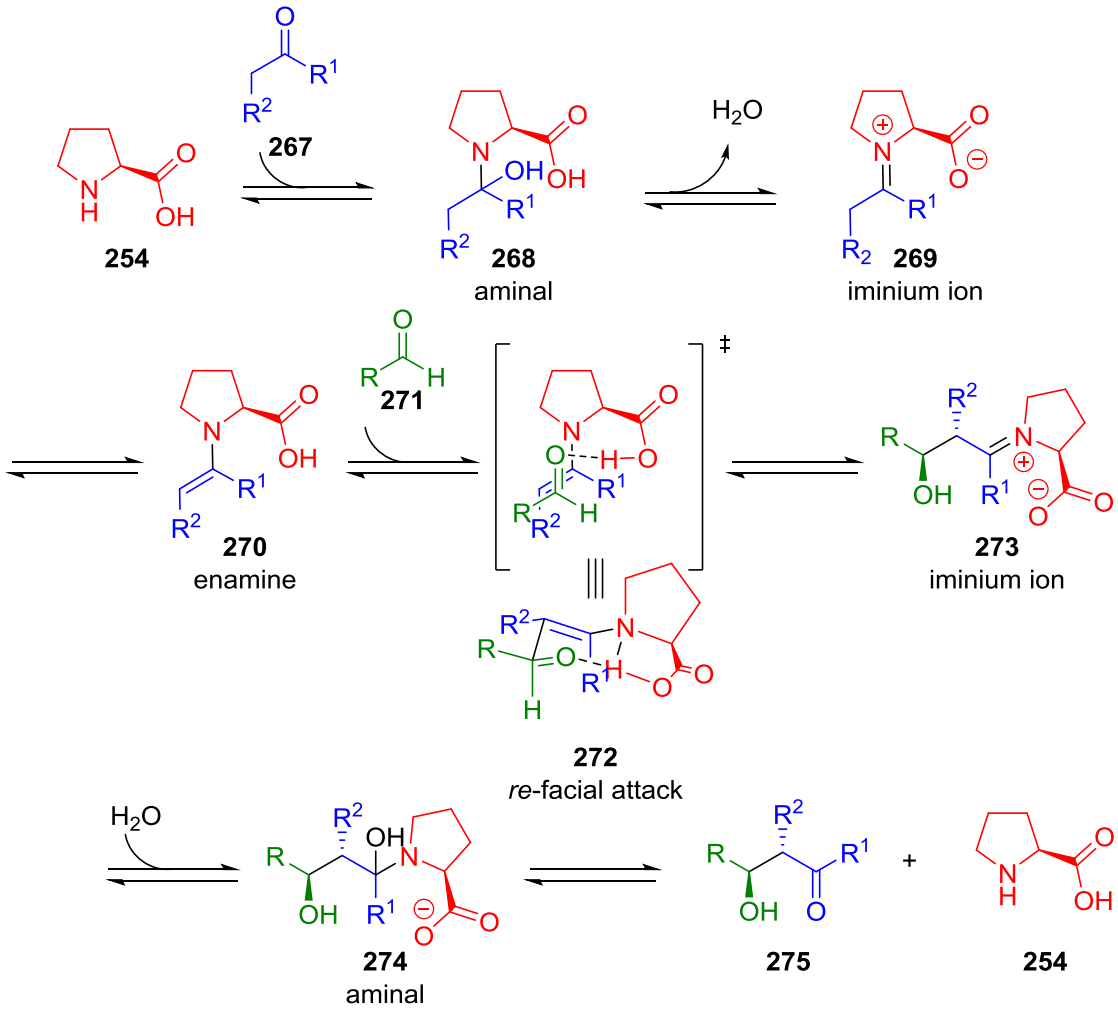

Figure 41 Proposed mechanistic cycle for proline-catalysed intermolecular aldol reaction.[116, 126]

The mechanism involved the formation of aminal **268** and **274**, iminium ions **269** and **273** and proceeded *via* an enamine intermediate **270**. The carbonyl compound **267** first reacted with the amino group to form the aminal intermediate **268**, and then generated an iminium intermediate **269**. Next, tautomerisation resulted in the formation of key enamine intermediate **270**. The carbon-carbon bond forming step was proceeded through a Zimmerman-Traxler-type transition state **272**, then both hydrolysis of the iminium **273** and aminal **274** intermediate to afforded the aldol product **275** and recovered the catalyst **254**. This mechanism was analogous to the accepted aldolase type I reaction mechanism in nature (**Figure 42**).

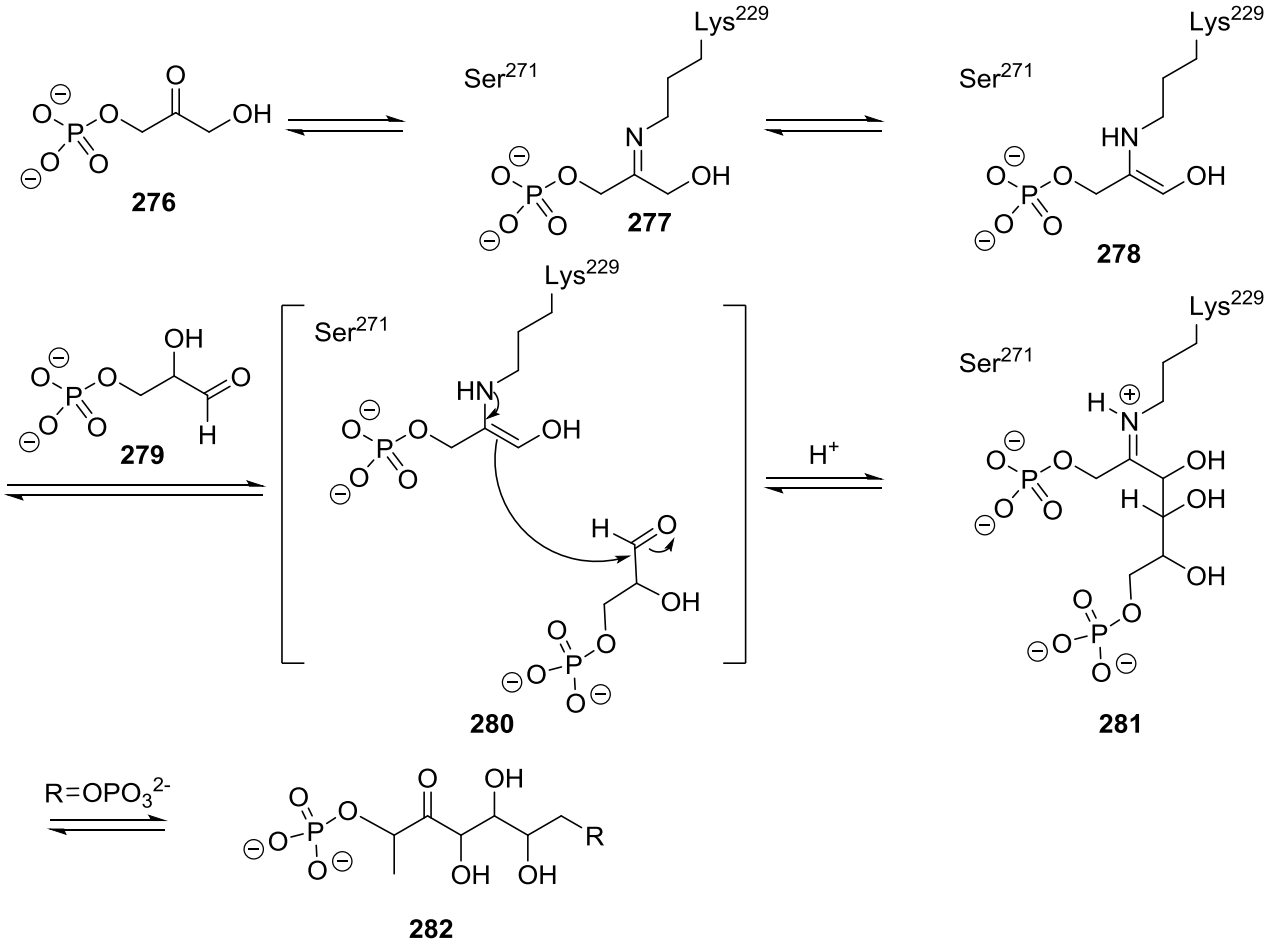

Figure 42 Mechanism of type I aldolases.[127]

Type I aldolases was accessed *via* an enamine mechanism. The enzyme first reacts with the compound **276** to generate a nucleophilic enamine **278**. Then this intermediate undergoes addition to **279** leading to the formation of iminium adduct **281**. Finally give the aldol adduct **282** is obtained from the hydrolysis of the substrate from the enzyme (**Figure 42**).

The proline catalyst can hence be regarded as a mimic of the type I aldolase metal-free enzyme. From this mechanism, it is assumed that the proline can be regarded as a bifunctional catalyst since amine can be treated as an enamine catalyst, and carboxylic acid is acting as Brønsted acid co-catalyst. The carboxylic acid was proposed to protonate of the carbonyl group acceptor in C-C bond formation step. Later the Houk group[128] conducted computational studies, which were able to support the mechanism proposed by List in which the hydrogen bonding of the carboxylic acid to carbonyl group, provided an intramolecular acid catalysis.

There were several reasons why proline has become an important molecule in asymmetric catalysis. Proline is an amino acid, which is an abundant chiral molecule readily available in both enantiomeric forms, less toxic and inexpensive than metal catalysts and gives high stereoselectivity. Additionally, proline contained two functional groups, a carboxylic acid and an amine group, which may act as both acid and base. The carboxylic group was significantly important to activate the carbonyl acceptor *via* hydrogen-bonding. For these reasons, proline was an effective catalyst in the aldol reaction.

3.1.4. Highly diastereo- and enantioselective direct aldol reactions in water

From the green chemistry perspective, water is the solvent of interest. In 1980, Breslow and co-workers presented an example by using water as a reaction medium that lead to increased reactivity of Diels–Alder reactions.[129, 130] Since then, reactions carried out in water have received much attention by organic chemists.

Organocatalysts are less sensitive to the presence of water compared to metal catalysts. The study of aldol reaction in the use of organocatalysts in aqueous solutions has recently gained considerable attention. In 2001, a study conducted by Barbas group, demonstrated that the aldol reaction was tolerant of the addition of small amounts of water (up to 4 vol% corresponding to ca. 20 eq. in a 0.1 M reaction), without affecting the enantiomeric excess of the aldol product.[117]

Later studies on the effect of water as an additive in proline catalysed aldol reactions were conducted by Pihko[131, 132] and co-workers in 2004 (**Scheme 98**).

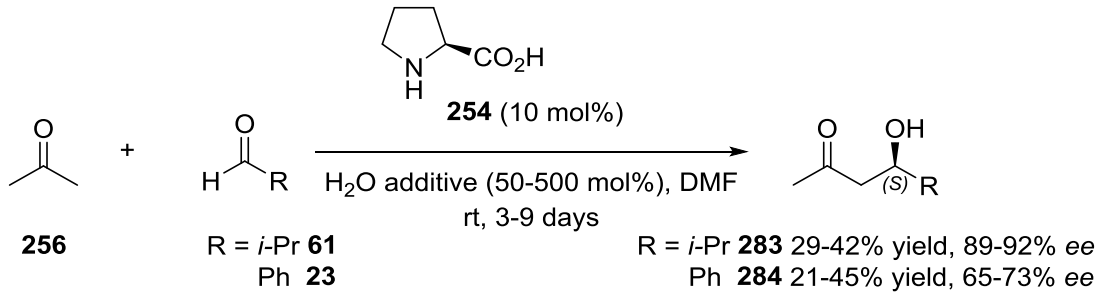

Scheme 98 Aldol reaction between acetone and *iso*-butyraldehyde and benzaldehyde in DMF with water as additive as reported by the Pihko group.[131]

Their results showed an increase in stereoselectivity and yield compared to the findings presented by Barbas.[117] The aldol reactions between acetone **256** with *iso*-butyraldehyde **61** and benzaldehyde **23** showed significantly higher yields. In addition, better stereoselectivity was achieved after the addition of water (50-500 mol%). Pihko had stated that there were two main reasons why water additives may accelerate the reaction and increase the stereoselectivity: (a) because water increased the solubility of the reaction mixture and (b) to hydrolyse the oxazolidinone intermediate. In 2007, the formation of the oxazolidinone in proline catalysed aldol reaction in water was further proven by Blackmond and co-workers (**Figure 43**).[133]

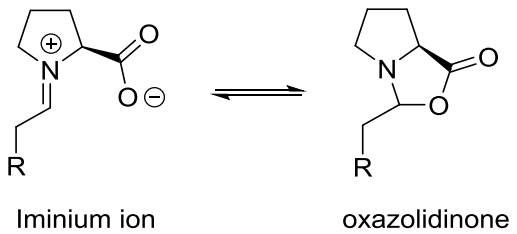

Figure 43 Equilibrium of iminium ion and oxazolidinone.[133]

In 2002, the Janda group reported the first organocatalytic aqueous aldol reaction between acetone **256** and 4-chlorobenzaldehyde **285** in water by using nornicotine **286** as catalyst (**Scheme 99**).[134]

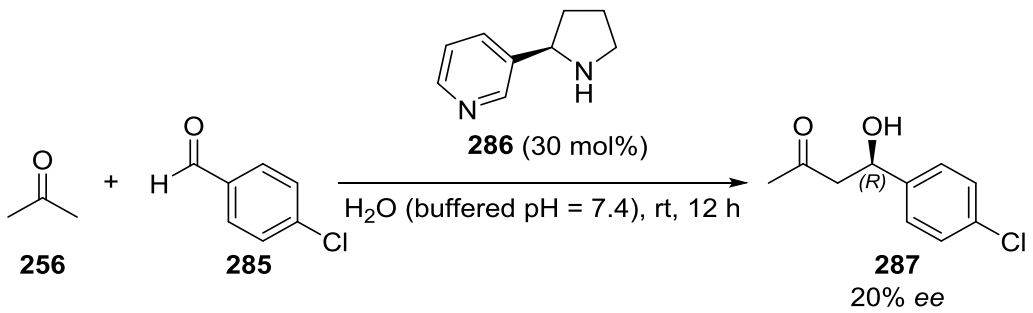

Scheme 99 Organocatalytic aqueous aldol reaction as reported by the Janda group.[134]

Although the enantioselectivity was low, it provided promising results that organocatalytic aldol reactions could be carried out in an aqueous environment. Further studies, have been undertaken to develop catalysts that would allow for the aldol reactions to be conducted in water as a sole solvent. Inspired by natural aldolase antibodies that the hydrophobic active site in their structure allowed the reaction occurring in water.[135] Therefore, modifying the proline catalyst with the hydrophobic groups was sought.

In 2006, the Barbas group[136] developed a diamine-based catalyst **289** (with a hydrophobic long chains) with TFA additive (0.05 mol),[137, 138] which catalysed the direct asymmetric aldol reaction of cyclohexanone **288** with 4-nitrobenzaldehyde **257** in water to provide **290** in a high yield (99%) and excellent enantioselectivity (up to 94% *ee*) (**Scheme 100**).

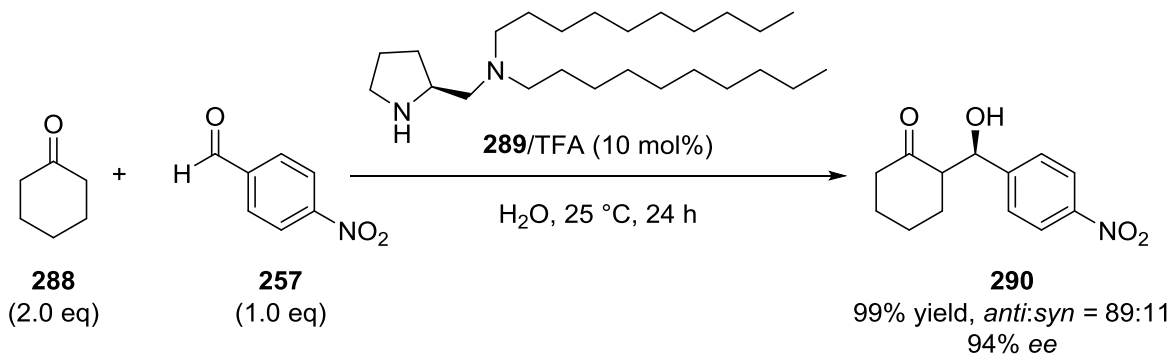

Scheme 100 Diamine **289**/TFA-catalysed aldol reactions in water.[136]

In the same year, the Hayashi group reported the use of a silyloxyproline **291** as a catalyst for the direct aldol reactions in the presence of water (**Scheme 101**).[139]

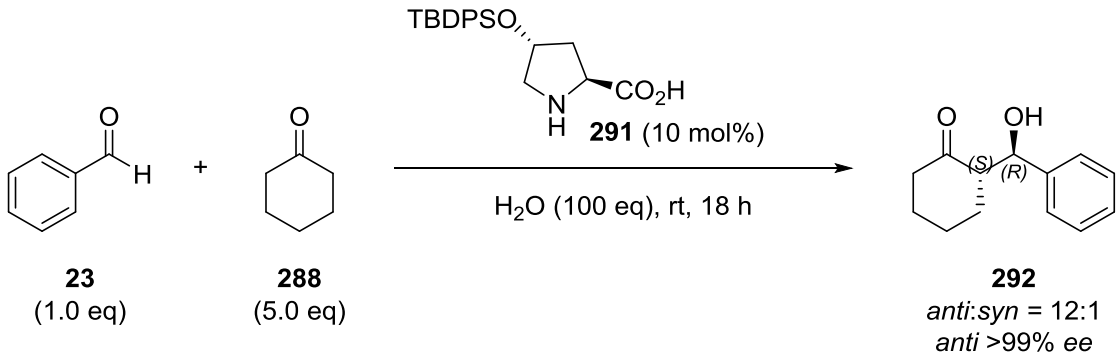

Scheme 101 Silyloxyproline-catalysed direct aldol reactions in water.[139]

By using 10 mol% of the catalyst **291**, excellent enantioselectivities of *anti*-aldol products were obtained. However, both reactions conducted by Barbas and Hayashi group have the same problem, the volume of ketone present in the reaction is greater than that of water. Therefore, these reactions cannot be classified as truly run "in water", it can simply be defined as run ''in the presence of water''. The

reaction proceeded in a biphasic system with water being present as a second phase.[140]

Previous studies by our group, successfully demonstrated the aldol dimerisation of TIPS-protected glycolaldehyde **293** in water. The use of (*L*)-proline benzyl ester **294** as a catalyst for a reaction time of 5 hours resulted in **295** in 80% yield and 15% *ee*. (**Scheme 102**).[141, 142]

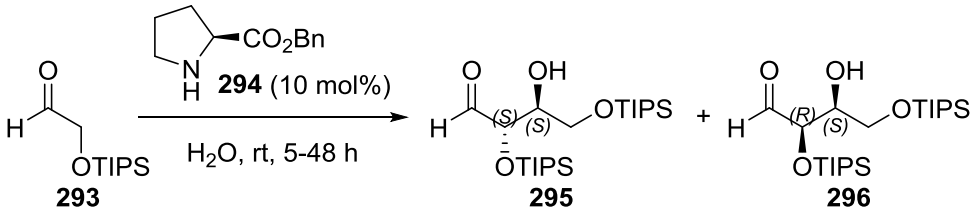

Scheme 102 Aldol dimerisation of protected glycolaldehyde in water.[141, 142]

The enantioselectivity of this reaction is lower than those of the organocatalysed aldol reactions run in organic solvents reported by List,[116] MacMillan and Córdova.[143-145] However, the enantioselectivity higher than the previous reactions that were run in purely aqueous solution.[146-148]

Janda stated that competing mechanisms between enamine catalyst and general base catalysis will be present in water. In order to confirm this hypothesis, further reactions were conducted at pH 7 (buffered) and pH 6 (buffered) and compared to those run in water.[149] The results are presented in **Table 23**.

Table 23 The dimerisation of TIPS-protected glycolaldehyde run at different pH levels.[141, 142]

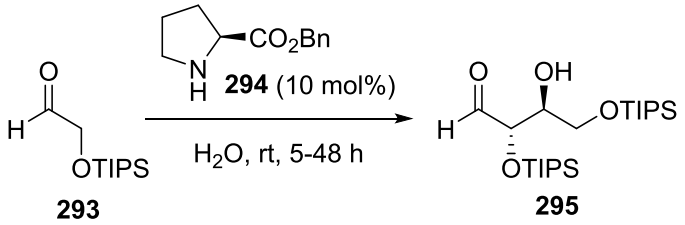

Entry	Medium	Yield/%	*ee*/%
1	water	80	15
2	pH 7 phosphate buffer	70	47
3	pH 6 citric acid phosphate buffer	33	22

The reaction run in pH 7 phosphate buffer solution provided the highest *ee* (47% *ee*), however, in pH 6 buffer solution and water media, lower enantioselectivities were obtained. These results confirmed that general base and acid catalyst competed with the enamine catalyst resulting in the formation of a non-enantioselective product, which resulted in a reduction of the enantioselectivities.

The reaction run in water and pH 7 phosphate buffer solution gave a similar yield. This may explain that the enamine-catalysed reaction was as active as the base-catalysed reaction. However, the yield dropped to 33% under pH 6 phosphate buffer. It was suggested presumably that the (*L*)-proline benzyl ester was hydrolysed to the corresponding acid and alcohol in acid media, thus the concentration of the catalyst was decreased, leading to a lower yield.[150]

Given the successful results of aldol dimerisation in water by using the (*L*)-proline benzyl ester as a catalyst. In order to assess the ability of (*L*)-proline benzyl ester to catalyse aqueous aldol reactions. The reaction of cyclohexanone with a variety of aldehyde acceptors was chosen at pH 6 and pH 7 phosphate buffer and water, over periods of 5 hours and 24 hours.

3.2. Results and discussion

3.2.1. Background and previous results

In previous studies, (*L*)-proline benzyl ester **294** was used as an organocatalyst in the aqueous aldol dimerisation of **293** to give **295** in 70% yield and 47% *ee* (**Scheme 103**).[141, 142, 150]

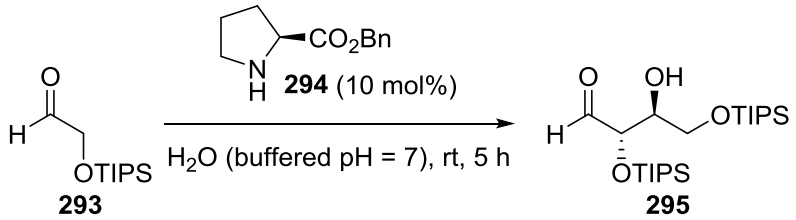

Scheme 103 The aldol dimerisation of protected glycolaldehyde in water.[141, 142, 150]

Further studies to determine whether catalyst **294** was able to promote other aqueous aldol reactions were undertaken.[150] The reaction between cyclohexanone **288** and 4-nitrobenzaldehyde **257** in aqueous solution was chosen, as this reaction had been widely studied before.[117, 139] Moreover, the conditions for the analysis of both the % d.r. and *ee* are well documented (**Scheme 104**).[151]

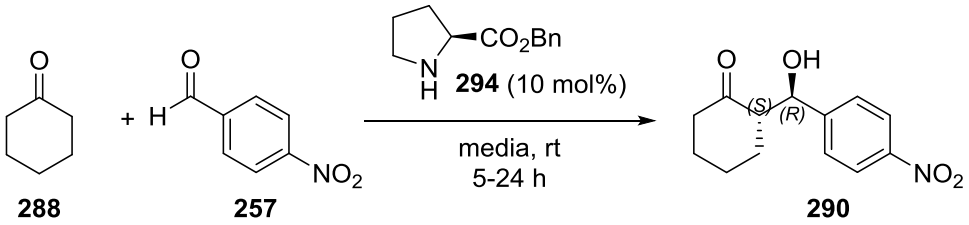

Scheme 104 *(L)*-proline-catalysed aldol reaction between cyclohexanone **288** and 4-nitrobenzaldehyde **257**.[150]

The pH value in water was found to be around pH 8-9. To determine the effect of pH on enantioselectivities and yield the studies were run in both water and pH 7 buffer solution for comparison. It was assumed that the enantioselectivities would be higher in pH 7 buffer solution compared to the reactions run in water. As the slightly basic condition in water will make general base catalysed reaction compete with the enamine formation mechanism, which can lead to a decrease in enantioselectivities.

Table 24 The aldol reaction of cyclohexanone **288** and 4-nitrobenzaldehyde **257** in water and pH 7 media catalysed by (*L*)-proline benzyl ester.[141, 142, 150]

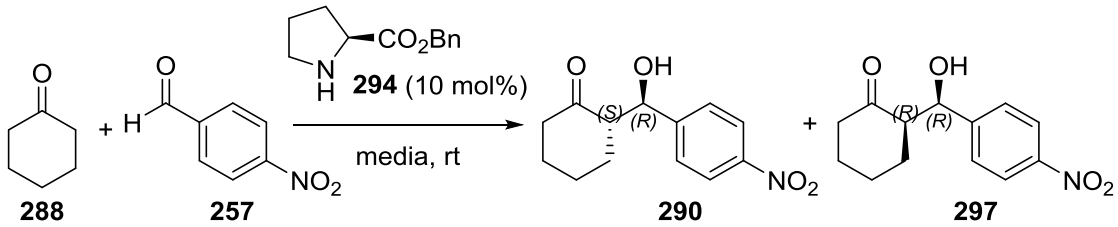

Entry	Media	Time/h	Conversion /%	d.r. (*anti*:*syn*)	Major Product	% *ee* (*anti*)	% *ee* (*syn*)
1	water	5	74	3:1	**290**	31	13
2	water	48	77	8:1	**290**	21	6
3	pH 7	5	74	4:1	**290**	43	19
4	pH7	48	57	5:1	**290**	46	11

As shown in **Table 24**, in general, the *anti*-aldol adduct **290** was the major product and the *ee* for the *anti* product **290**, which were much higher than the *ee* of the *syn* product **297**. To our delight, compared to the reaction run in water, the higher enantioselectivity was obtained in pH 7 buffer solution over the entire reaction

period, which confirmed the hypothesis that the reaction run in neutral condition had the highest enantioselectivity. These results were explained by maximising the enamine-mediated reaction pathway and minimizing the racemic general base-catalysed pathway in pH 7 media. The lower enantioselectivity in water clearly explained that the general base catalyst existed in the reaction.

In previous studies, Burroughs demonstrated that the catalyst would be degraded from the ester substituent to the corresponding acid and alcohol with a longer reaction period.[150] Therefore, 5 hours was chosen as the optimal reaction time. When increasing the reaction period, the enantiomeric excess decreased from 31% *ee* to 21% *ee* (**Table 24**, **Entries 1** and **2**). In contrast, in pH 7 buffer solution, enantioselectivities were of a similar value.

To evaluate if the retro-Aldol reactions occurred with longer reaction times in water, the *syn* enantiomer **297** was treated with 10 mol% of (*L)*-proline benzyl ester **294** in water for 48 hours.[150] It was found that the enantioselectivities decreased from 19% to 8%, which can be explained by the presence of the retro-aldol reaction (**Scheme 105**).

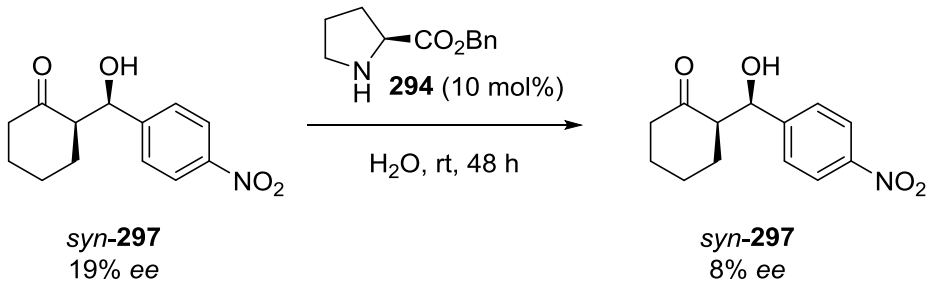

Scheme 105 Retro-aldol investigation conducted by Burroughs.[150]

Further investigation into the reactions run in pH 6 buffer solution were carried out by a fellow member of the Clarke's group, Sharp.[152] The results are presented in **Table 25**.

Table 25 The aldol reaction of cyclohexanone **288** and 4-nitrobenzaldehyde **257** in pH 6 media catalysed by (*L*)-proline benzyl ester.[152]

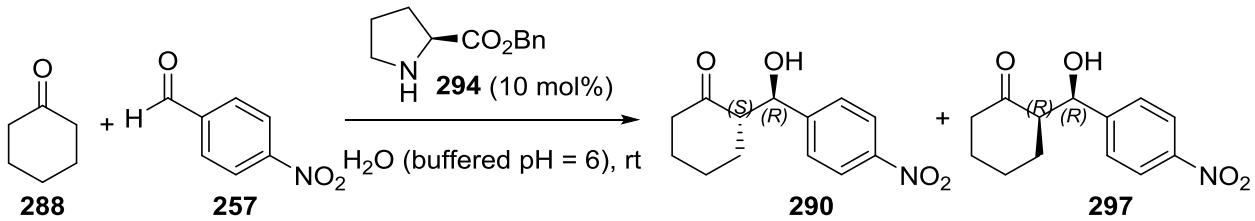

Entry	Time/h	Conversion/%	d.r. (*anti*:*syn*)	Major Product	% *ee* (*anti*)	% *ee* (*syn*)
1	5	27	3:1	**290**	30	21
2	24	21	2:1	**290**	76	18

When comparing the enantioselectivities between pH 7 (**Table 24**, **Entries 3** and **4**), water (**Table 24**, **Entries 1** and **2**) and pH 6 buffer solution (**Table 25**, **Entries 1** and **2**), the reaction run in pH 6 buffer solution presented the lowest enantiomeric excess during a 5-hour reaction time. Most surprisingly was the *anti*- product increase in enantioselectivity from 30% to 76% *ee* over 24 hours (**Table 25**, **Entries 1** and **2**), which was not consistent with the expected trend. It was envisioned that the acid-mediated mechanism will competed with the enamine formation, thereby leading to a decrease in the resulting enantioselectivity. The reason behind this may

be that the optimal conditions for enamine formation are under acid conditions. Previous studies by Singh and co-workers in 2009 indicated that the highest enantiomeric excess was obtained for the aldol reaction of cyclohexanone **288** and 4-nitrobenzaldehyde **257** at pH 4-5 for 24-hour reaction times (**Scheme 106**).[153] The pH 6 buffer solution was closer to the optimal pH for enamine formation.

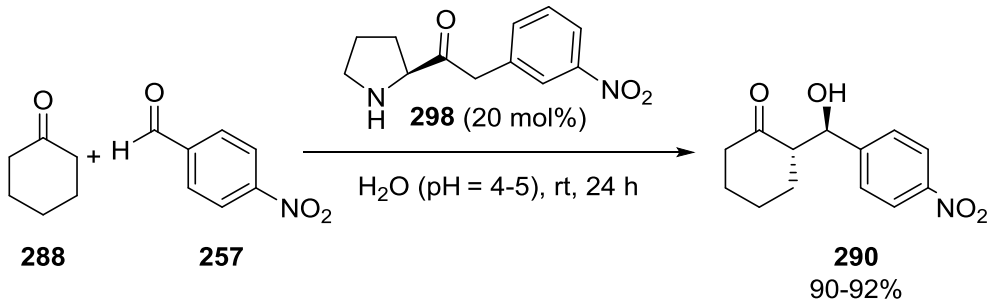

Scheme 106 The aldol reaction of cyclohexanone **288** and 4-nitrobenzaldehyde **257** in pH 4-5 media as reported by Singh and co-workers.[153]

Hayashi and co-workers investigated the same reaction in the presence of water using catalyst **291** and obtained aldol product **290** in 86% yield, with an enantioselectivity over 99% *ee*, and diastereoselectivity of 20:1 *anti*:*syn* (**Scheme 107**).[139]

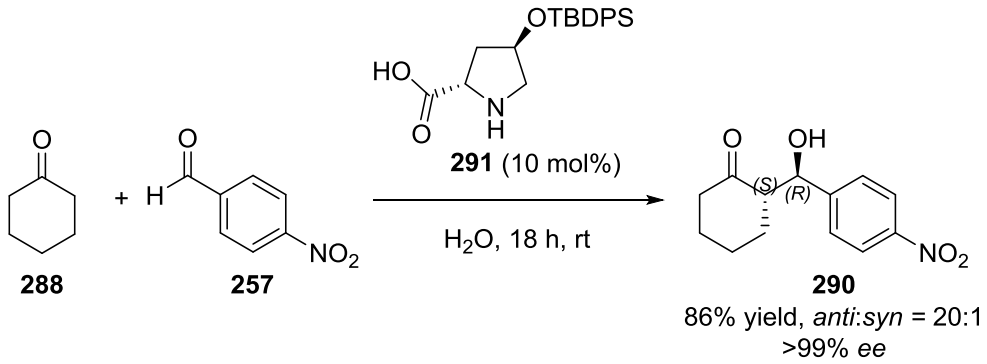

Scheme 107 Silyloxyproline-catalysed direct aldol reactions in water.[139]

In another study by Barbas and co-workers,[136] TFA was used as a co-catalyst to generate an *ee* of 94%, with a yield of 99% and diastereoselectivity of 89:11 *anti*:*syn* (**Scheme 100**). Unfortunately, the enantioselectivities decreased to 1% *ee* when no acid co-catalyst was being used. The reason for this was that TFA may act as a buffer to maximum the enamine catalysis in the reaction. The general base catalysis caused by the addition of the diamine to water may be reduced.

However, studies by both the Hayashi group and Barbas group have the same problem; an excess of cyclohexanone **288** being present in the reaction, means that cyclohexanone **288** can be regarded as an organic solvent and that water can only act as a co-solvent.

Clarke's group built on earlier work of Janda,[154] showing that the pyrrolidine catalyst required electron-withdrawing substituents on the arylpyrrolidines substrate for it to become an effective catalyst. In comparison to the catalyst conducted by Janda, the (*L*)-proline benzyl ester **294** was chosen by Burroughs (Clarke group), as this proline derivative also possessed an electron withdrawing group, which could be a potent catalyst in the aldol reaction between cyclohexanone **287** and 4-nitrobenzaldehyde **257**.[150] In addition, (*L*)-proline benzyl ester did not have a carboxylic acid group that provides essential hydrogen-bonding interactions in organic solvents. Therefore, unlike proline, the lack of hydrogen bonding interaction in water (*L*)-proline benzyl ester can still serve as an efficient catalyst.

3.2.2. Cross-Aldol reaction between cyclohexanone and different aryl aldehydes

Further studies focused on the scope of the aqueous aldol reaction and examined the crossed-aldol reaction between cyclohexanone and different substituted of benzaldehydes by using (*L*)-proline benzyl ester as a catalyst under pH 7 buffer solution for 5 hours and 24 hours, respectively the results can be found in **Table 26**.

In general, it was observed that *anti*-aldol adduct was the major product for all reactions. The value of conversion was calculated by crude NMR as the reaction did not go to completion in 24 hours. The conversion increased with longer reaction times (**Table 26**, **Entries 1**-**16**) which were contrary to previously published results. In previous studies, the yield of the aldol reaction between cyclohexanone **288** and 4-nitrobenzaldehyde **257** decreased in the longer reaction period (**Table 24**, **Table 25**). However, the lower yield may be due to the reactivity of these aldehyde substrates, which was less than 4-nitrobenzaldehyde **257**. All aldehydes matched up this trend, except for anisaldehyde **299** (**Table 26**, **Entries 7** and **8**), which failed to form the product, and only starting material was recovered. The heteroaromatic aldehyde, 4-pyridinecarboxaldehyde **302** was seemed to be more reactive than other aldehydes that reacted with cyclohexanone. The reaction was nearly complete in 5 hours with good *ee* (60%). Treating 4-pyridinecarboxaldehyde **302** at a longer reaction times also resulted in a similar *ee* (**Table 26**, **Entries 15** and **16**).

Table 26 The aldol reaction between cyclohexanone and different aldehydes.

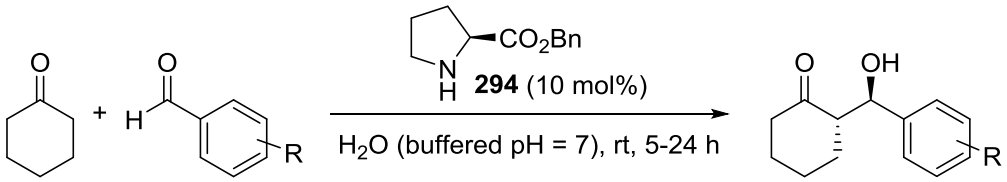

Entry	R	T/h	Conversion /%	% *ee* (*anti*)	d.r. (*anti*:*syn*)	Major Product
1	4-Br **258**	5	72	38	3:1	***anti*-303**
2	4-Br **258**	24	84	28	4:1	***anti*-303**
3	4-Cl **285**	5	44	27	6:1	***anti*-304**
4	4-Cl **285**	24	66	13	5:1	***anti*-304**
5	H **23**	5	13	89	4:1	***anti*-305**
6	H **23**	24	70	74	6:1	***anti*-305**
7	OMe **299**	5	0	-	-	***anti*-306**
8	OMe **299**	24	0	-	-	***anti*-306**
9	2-Cl **259**	5	41	23	2:1	***anti*-307**
10	2-Cl **259**	24	76	7	2:1	***anti*-307**
11	2-NO_2 **300**	5	38	35	1:1	***anti*-308**
12	2-NO_2 **300**	24	88	26	1:1	***anti*-308**
13	2-furaldehyde **301**	5	19	41	2:1	***anti*-309**
14	2-furaldehyde **301**	24	45	32	1:1	***anti*-309**
15	4-pyridinecarboxaldehyde **302**	5	99	60	3:1	***anti*-310**
16	4-pyridinecarboxaldehyde **302**	24	100	64	2:1	***anti*-310**

In contrast to the conversion, the *ee* value of the reaction decreased with increasing reaction time. This implies retro-aldol domination over a longer reaction times. (**Table 26**, **Entries 1**-**14**).

The aldehyde acceptor with the electron-withdrawing group at *para*-position may accelerate rates. However, it was disappointing that the *ee* of these aldehyde acceptors like 4-bromobenzaldehyde **258** and 4-chlorobenzaldehyde **285** (**Table 26**, **Entries 1**-**4**) were substantially lower compared to previous findings in 4-nitrobenzaldehyde **257**. The highest *ee* obtained was 89% *ee* for benzaldehyde **23** (**Table 26**, **Entry 5**). The *ee* for 2-Cl **259** and 2-NO_2 benzaldehyde **300** (**Table 26**, **Entries 5**-**6** and **9**-**12**) was also lower than the 4-nitrobenzaldehyde **257**. Interestingly, the aldehyde with an electron donating group at *para*-position **299** (**Table 26**, **Entries 7** and **8**) did not form any aldol products. This may be due to the reduced electrophilicity of the aldehyde acceptor.

3.2.3. Cross-Aldol reaction between various ketone donors and 4-nitrobenzaldehyde

The cross-aldol reaction was further carried out between different ketone donors and 4-nitrobenzaldehyde **257**. Actone **256** (**Table 27**, **Entries 1** and **2**) and 3-pentanone **311** (**Table 27**, **Entries 3** and **4**) were chosen for further studies.

Table 27 The aldol reaction between various ketones with 4-nitrobenzaldehyde by using (*L*)-proline benzyl ester as a catalyst.

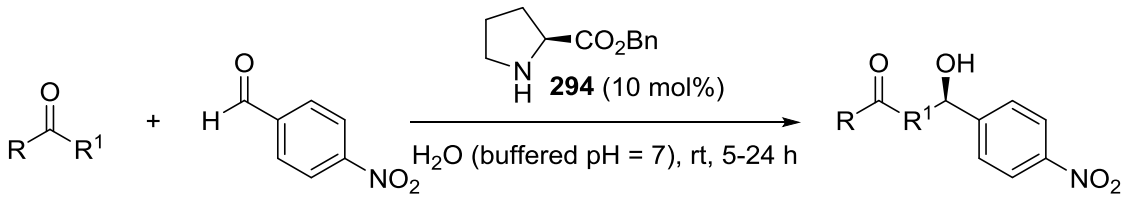

Entry	Ketone	Time/h	Conversion/%	% ee (*anti*)	dr (*anti*:*syn*)	Major product
1	Acetone **256**	5	62	13	2:1	***anti*-261**
2	Acetone **256**	24	98	61	10:1	***anti*-261**
3	3-Pentanone **311**	5	0	-	-	-
4	3-Pentanone **311**	24	0	-	-	-

Results can be found in **Table 27**. The reactions were not completed during a 5 or 24 hours reaction time. As shown in the crude ^{1}H NMR spectra, the aldehyde peak was presented and the reaction with only 62% of conversion in 5 hours. The conversion increased with longer reaction times, however, after 24 hours, starting material could still be observed in the crude ^{1}H NMR spectrum. The use of acetone **256** (**Table 27**, **Entries 1** and **2**) as a ketone donor gave products with a low *ee* compared to cyclohexanone **288**. Unfortunately, the reaction with 3-pentanone **311** (**Table 27**, **Entries 3** and **4**) failed to give any product. The *ee* increased from 13% to 61% over 24 hours. It seems that these two ketone donors were less active to react with

4-nitrobenzaldehyde **257** under buffered conditions for 24 hours compared to the use of cyclohexanone **288** as a ketone source.

3.3. Conclusions and Future work

In summary, the wide scope of aqueous aldol reactions between cyclohexanone and different substituted of benzaldehydes has been demonstrated.The (*L*)-proline benzyl ester was used as a catalyst, which was successfully proven to be an accessible organocatalyst to promote the asymmetric aldol reaction with diverse aldehyde acceptors in water. This organocatalyst system provided a moderate yield and *ee*, and no excess ketone or acid additive was required.

In general, investigating of the aldol reactions between cyclohexanone and a variety of benzaldehydes presented some trends. The major diastereomer was the *anti* product and all the reactions had not gone to completion within 24 hours, except for the 4-pyridinecarboxaldehyde. It was found that the conversion increased with longer reaction times. In contrast, the *ee* dropped with longer reaction times. This trend was consisted with previous results reported by Burroughs who found the *ee* decreased because of degradation of the catalyst at longer periods.[150] The highest *ee* was observed when using benzaldehyde as an acceptor with a 5-hour reaction time under pH 7 buffer media to give 89% *ee*. Aldehydes with an electron donating group at the *para*- position did not provide any aldol products. This may be due to the reduced electrophilicity of the aldehyde acceptor.

Moreover, the (*L*)-proline benzyl ester was capable to catalyse the acetone and cyclic ketone donor with 4-nitrobenzaldehyde to form an aldol product in a moderate yield and *ee*. However, 3-pentanone failed to give any aldol products.

Further studies may be focoused on the mechanistic studies, which may help to account for the diastereoselectivity. Investigating the reaction under pH 6 (buffered solution) is worthwhile, as the pH 6 media was proposed to be closer to the optimal pH for the formation of enamine.[153]

4. Experimental

4.1. General experimental

All reagents were commercially available and used as received except for the TMSCl. The TMSCl was distilled over calcium hydride before use. All the reactions were carried out under an inert atmosphere conditions in a closed system. ^{1}H NMR spectra were recorded on a Jeol ECX-400 (400 MHz), Jeol ECS-400 (400 MHz) or a Bruker DRX 500 (500 MHz) spectrometer at ambient temperature. ^{13}C NMR spectra were recorded on a Jeol ECX-400 (101 MHz) or Jeol ECS-400 (101 MHz) spectrometer. Spectra were processed using MestreNova. Data are reported as follows: chemical shift are reported in parts per million (ppm) and δ 7.26 ppm was referenced to $CDCl_3$; coupling constants (*J*) are quoted in Hertz; multiplicity (s = singlet, d = doublet, t = triplets, br = broad, m = multiplet). Enantiomer ratios were determined by HPLC on an Agilent 1100 Series system with the use of Chiralpak OD, OJ-H, AS-H column or Chiralcel AD-H column in comparison with literature. TLC was utilised the glass-backed plates coated with Merck Silica gel 60 F_{254}, and the compounds were visualised by irradiation with UV light or by treatment with a anisaldehyde stain or a cerium ammonium molybdate stain. Purification of the product was carried out by flash column chromatography using high-purity grade silica gel, pore size 60 Å, 200-425 mesh particle size supplied by Sigma-Aldrich.

4.2. Experimental Procedures for Chapter one

Octa-1,7-diene-4,5-diol 84

Lab book: YT-4-58, NMR: a2326yth (YT-2-63-5-2)

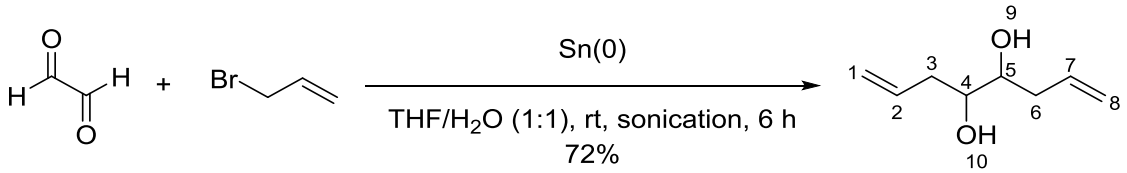

Allyl bromide (14.29 mL, 20.00 g, 165.32 mmol, 2.40 eq.) and 40% aqueous glyoxal (7.91 mL, 10.05 g, 68.88 mmol, 1.00 eq.) were dissolved in a THF/water (1:1 v/v, 140 mL, 0.50 M) solvent mixture. Tin powder (19.63 g, 165.32 mmol, 2.40 eq.) was added. After sonicating for 6 hours, the reaction mixture was quenched with 25% potassium hydroxide solution (56 mL, w/w in water) and diluted with diethyl ether (60 mL). Solid sodium chloride was added until the aqueous phase was saturated and the solution was filtered through celite. The aqueous phase was extracted with diethyl ether (3 x 20 mL). The combined organic extracts were dried (magnesium sulfate), filtered and concentrated *in vacuo* to give a crude product, which was then purified by flash column chromatography on silica (1:1, ethyl acetate-hexane) to give octa-1,7-diene-4,5-diol **84** as a yellow oil (7.12 g, 72%). **^{1}H NMR** (400 MHz, $CDCl_3$): δ 5.87-5.76 (2H, m, H-2, H-7), 5.14-5.06 (4H, m, H-1, H-8), 3.66-3.46 (2H, m, H-4, H-5), 2.92 (1H, br, OH), 2.33-2.18 (4H, m, H-3, H-6); **^{13}C NMR** (101 MHz, $CDCl_3$): δ 134.9 (C-2), 134.6 (C-7), 118.0 (C-1), 117.9 (C-8), 73.1 (C-4), 72.9 (C-5), 38.2 (C-3), 36.3 (C-6); **IR** (film): ν_{max} 3368.7, 3077.0, 2983.9, 2909.3, 1640.9, 1432.4, 1418.0, 1046.3, 991.1,

912.1, 868.0 cm^{-1}; **ESI-MS**: *m/z* calcd for $C_8H_{14}NaO_2$ [M+Na^+] 165.0886, found 165.0888 (−1.2 ppm error). The ^{1}H NMR data was in agreement with the literature.[155]

But-3-enal 70

Lab book: YT-2-92, NMR: c8727yth (YT-2-72)

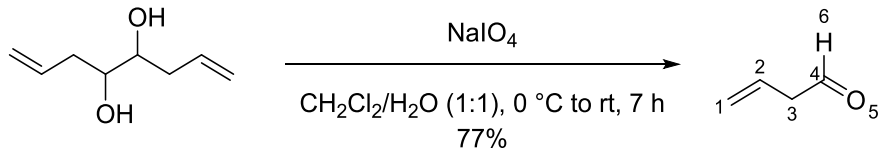

Octa-1,7-diene-4,5-diol **84** (1.69 g, 12.00 mmol, 1.00 eq.) was dissolved in a dichloromethane/water (1:1 v/v, 20 mL, 0.60 M) solvent mixture. Sodium (meta)periodate (3.05 g, 14.26 mmol, 1.20 eq.) was added at 0 °C. After stirring for 30 minutes, the reaction was allowed to warm to room temperature and stirred for another 7 hours. The organic phase was separated and washed with water (2 x 20 mL), brine (2 x 20 mL), dried (magnesium sulfate) and filtered to give but-3-enal **70** as a colourless solution in dichloromethane. The crude product was used directly without further purification. **^{1}H NMR** (400 MHz, $CDCl_3$): δ 9.69 (1H, t, *J* = 1.9 Hz, H-6), 5.91 (1H, ddt, *J* = 17.2, 10.3, 6.9 Hz, H-2), 5.36-5.26 (2H, m, H-1), 3.19 (2H, ddd, *J* = 6.9, 3.1, 1.9 Hz, H-3). The ^{1}H NMR data was in agreement with the literature.[156]

Trimethyl((1-phenylvinyl)oxy)silane 81

Lab book: YT-3-40, NMR: d2663yth (YT-3-30)

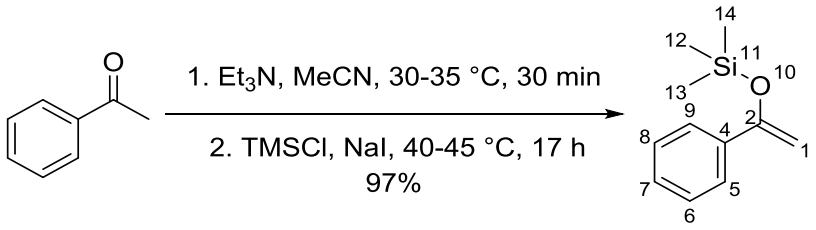

Acetophenone (4.00 g, 3.89 mL, 33.29 mmol, 1.00 eq.) was dissolved in dry acetonitrile (200 mL, 0.16 M) under N_2 at room temperature. Triethylamine (26.83 g, 36.96 mL, 166.45 mmol, 5.00 eq.) was added dropwise over 30 minutes to the solution which was then heated to 30-35 °C. After stirring for 30 minutes, chlorotrimethylsilane (14.47 g, 17.02 mL, 133.16 mmol, 4.00 eq.) and sodium iodide (9.98 g, 66.58 mmol, 2.00 eq.) were added. The reaction temperature was then raised to 40-45 °C and stirred for 17 hours. After cooling the reaction mixture to room temperature, the solution was filtered through celite and washed with hexane (100 mL). The filtrate was then extracted with hexane and concentrated *in vacuo* to give trimethyl((1-phenylvinyl)oxy)silane **81** as a colourless oil (6.20 g, 97%). **^{1}H NMR** (400 MHz, $CDCl_3$): δ 7.60-7.57 (2H, m, H-Ar), 7.35-7.28 (3H, m, H-Ar), 4.92 (1H, d, *J* = 1.7 Hz, H-1a), 4.43 (1H, d, *J* = 1.7 Hz, H-1b), 0.27 (9H, s, H-12, H-13, H-14). The ^{1}H NMR data was in agreement with the literature.[50, 157]

3-Hydroxy-1-phenylhex-5-en-1-one 80

Lab book: YT-6-8, NMR: a2298yth (YT-4-16-2)

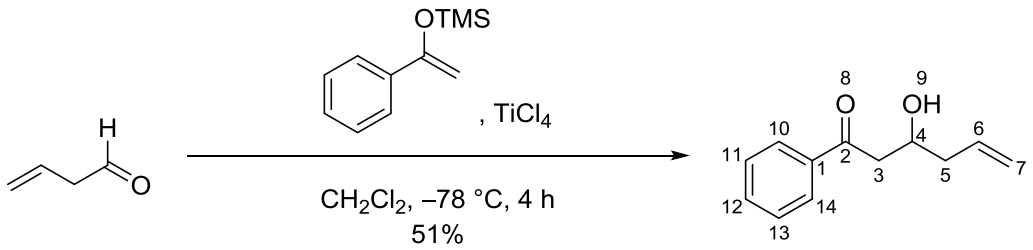

Trimethyl((1-phenylvinyl)oxy)silane **81** (3.18 g, 16.55 mmol, 1.00 eq.) was dissolved in dry dichloromethane (40 mL, 0.40 M). But-3-enal **70** (1.16 g, 16.55 mmol, 1.00 eq.) was added dropwise at −78 °C under N_2. After stirring for 15 minutes, titanium tetrachloride (1.99 mL, 18.21 mmol, 1.10 eq.) was added and stirred for 4 hours. The reaction mixture was quenched with cold water (20 mL) and saturated sodium bicarbonate solution (20 mL). The organic phase was separated and the aqueous phase was extracted with dichloromethane (3 x 20 mL). The combined organic extracts were dried (magnesium sulfate), filtered and concentrated *in vacuo* to give a crude product, which was then purified by flash column chromatography on silica (1:3, ethyl acetate-hexane) to give 3-hydroxy-1-phenylhex-5-en-1-one **80** as a yellow oil (1.60 g, 51%). **^{1}H NMR** (400 MHz, $CDCl_3$): δ 7.95-7.92 (2H, m, Ar-H), 7.59-7.54 (1H, m, Ar-H), 7.47-7.43 (2H, m, Ar-H), 5.87 (1H, ddt, *J* = 17.2, 10.2, 7.1 Hz, H-6), 5.18-5.11 (2H, m, H-7), 4.30 (1H, ddt, *J* = 8.7, 6.2, 3.1 Hz, H-4), 3.33 (1H, br, OH), 3.17 (1H, dd, *J* = 17.6, 3.1 Hz, H-3a), 3.06 (1H, dd, *J* = 17.6, 8.7 Hz, H-3b), 2.42-2.29 (2H, m, H-5); **^{13}C NMR** (101 MHz, $CDCl_3$): δ 200.7 (C-2), 136.8 (C-Ar), 133.6 (C-Ar), 128.2 (C-Ar), 118.0 (C-7), 67.2 (C-4), 44.3 (C-3), 41.02 (C-5); **IR** (film): ν_{max} 3438.1, 3076.4, 2980.2, 2904.2, 1675.8, 1597.0, 1580.1, 1448.5, 1209.5, 1044.9, 1000.7, 916.3, 753.0, 688.7, 584.2

cm^{-1}; **ESI-MS**: *m/z* $C_{12}H_{14}NaO_2$ [M+Na$^+$] 213.0886, found 213.0883 (1.3 ppm error).

(1*S,3*S**)-1-phenylhex-5-ene-1,3-diol 79**

Lab book: YT-5-24, NMR: p3591yth (YT-4-63)

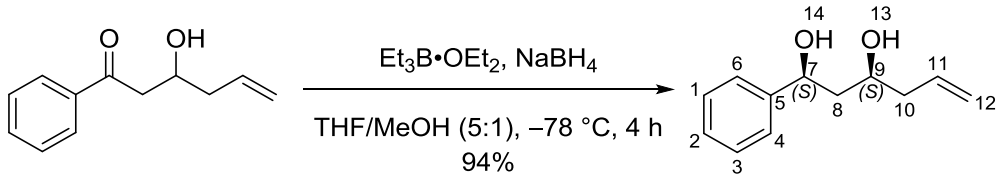

A 1.00 M solution of triethyl borane in hexanes (5.79 mL, 5.79 mmol, 1.10 eq.) was dissolved in a THF/methanol (5:1, v/v, 12 mL) solvent mixture under N_2 at room temperature. After stirring the reaction mixture for 2 hours, the solution was cooled down to −78 °C and 3-hydroxy-1-phenylhex-5-en-1-one **80** (1.00 g, 5.25 mmol, 1.00 eq.) was added slowly. After stirring for 30 minutes sodium borohydride (219.04 mg, 5.79 mmol, 1.10 eq.) was added in one portion and stirred for another 4 hours. The reaction mixture was quenched with saturated ammonium chloride solution (10 mL) and then diluted with ethyl acetate (10 mL). The organic phase was separated and the aqueous phase was extracted with ethyl acetate (3 x 10 mL) and the combined organics extracts were dried (magnesium sulfate), filtered and concentrated *in vacuo* to give a crude product, which was then purified by flash column chromatography on silica (1:3, ethyl acetate-hexane) to yield (1*S**,3*S**)-1-phenylhex-5-ene-1,3-diol **79** as a yellow oil (954.70 mg, 94%). **^{1}H NMR** (400 MHz, $CDCl_3$): δ 7.29-7.18 (5H, m, Ar-H), 5.76-5.5.65 (1H, m, H-11), 5.04-4.99 (2H, m, H-12), 4.77 (1H, dd, *J* = 8.4, 4.7 Hz, H-7), 4.35 (1H, br, OH), 3.90 (1H, br, OH), 3.86-3.80 (1H, m, H-9), 2.15-2.12 (2H, m, H-10), 1.76-1.65 (2H, m, H-8); **^{13}C NMR** (101 MHz, $CDCl_3$): δ 144.4 (C-Ar), 134.2 (C-11), 128.4

(C-Ar), 127.5 (C-Ar), 125.7 (C-Ar), 118.0 (C-12), 74.8 (C-7), 71.5 (C-9), 44.5 (C-8), 42.3 (C-10); **IR** (film): ν_{max} 3364.1, 2910.5, 1398.6, 1323.6, 1063.5, 914.8, 756.9, 699.5, 662.0, 556.8 cm^{-1}; **ESI-MS**: *m/z* $C_{12}H_{16}NaO_2$ [M+Na^+] 215.1043, found 215.1040 (1.0 ppm error).

S-*p*-tolyl prop-2-enethioate 66

Lab book: YT-2-82-1, NMR: d0260yth (YT-2-82-1)

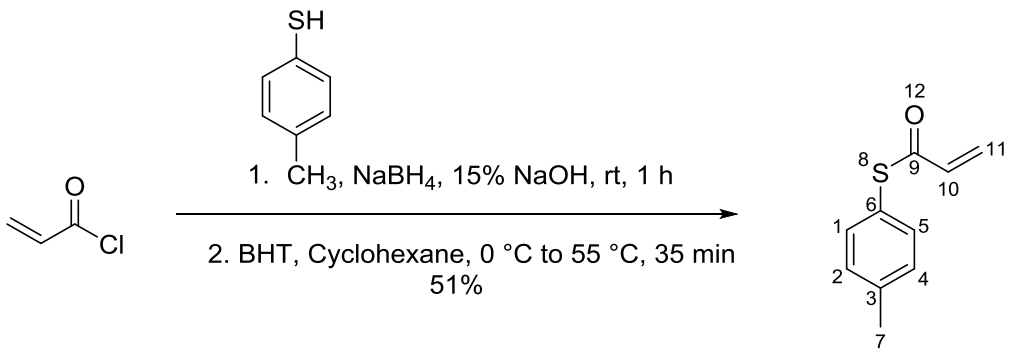

Sodium borohydride (62.50 mg, 1.65 mmol, 0.03 eq.) and 4-methylbenzenethiol (6.85 g, 55.15 mmol, 1.00 eq.) were stirred in 15% sodium hydroxide aqueous solution (25 mL) at room temperature under N_2 for 1 hour to give a solution of *p*-$CH_3C_6H_4S^-Na^+$. This solution was cooled to 0 °C before use.

In a separate flask, BHT (170.00 mg, 0.77 mmol, 1.40 mol%) and acryloyl chloride (6.72 mL, 7.49 g, 82.73 mmol, 1.50 eq.) were dissolved in cyclohexane (35 mL) and cooled to 0 °C. The cold solution of *p*-$CH_3C_6H_4S^-Na^+$ was then added to this solution at 0 °C. After addition was completed, the resultant biphasic mixture was stirred at 55 °C for 35 minutes. The reaction was extracted with diethyl ether and washed with saturated sodium bicarbonate solution and brine, the combined organic extracts

were dried (magnesium sulfate), filtered and concentrated *in vacuo*. BHT (91.00 mg) was added to the solution before concentrated *in vacuo* to prevent polymerization. The crude product was then purified by flash column chromatography on silica (1:30, ethyl acetate-hexane) to yield S-(4-methylphenyl) 2-propenthioate **66** as a colourless oil (5.04 g, 51%). **^{1}H NMR** (400 MHz, $CDCl_3$): δ 7.35-7.22 (4H, m, H-Ar), 6.46 (1H, dd, *J* = 17.2, 9.6 Hz, H-10), 6.38 (1H, dd, *J* = 17.2, 1.6 Hz, H-11a), 5.76 (1H, dd, *J* = 9.6, 1.6 Hz, H-11b), 2.39 (3H, s, H-7); **^{13}C NMR** (101 MHz, $CDCl_3$): δ 189.1 (C-9), 140.0 (C-Ar), 134.7 (C-Ar), 134.5 (C-11), 130.2 (C-Ar), 127.4 (C-10), 123.7 (C-Ar), 21.5 (C-7); **IR** (film): ν_{max} 3022.7, 2920.8, 2862.3, 1902.7, 1681.3, 1611,4, 1597.6, 1493.4, 1447.8, 1393.4, 1303.9, 1276.1, 1201.0, 1181.4, 1159.9, 1116.4, 1095.1, 1041.0, 1018.6, 986.2, 940.0, 834.7, 806.2, 721.8, 627.6, 592.5, 528.1, 407.7 cm^{-1}; **ESI-MS**: *m/z* $C_{10}H_{11}OS$ $[M+H^+]$ 179.0525, found 179.0524 (0 ppm error).

(5*S,7*S**,*E*)-S-p-tolyl 5,7-dihydroxy-7-phenylhept-2-enethioate 78**

Lab book: YT-3-67, NMR: p2148yth (YT-3-79-4)

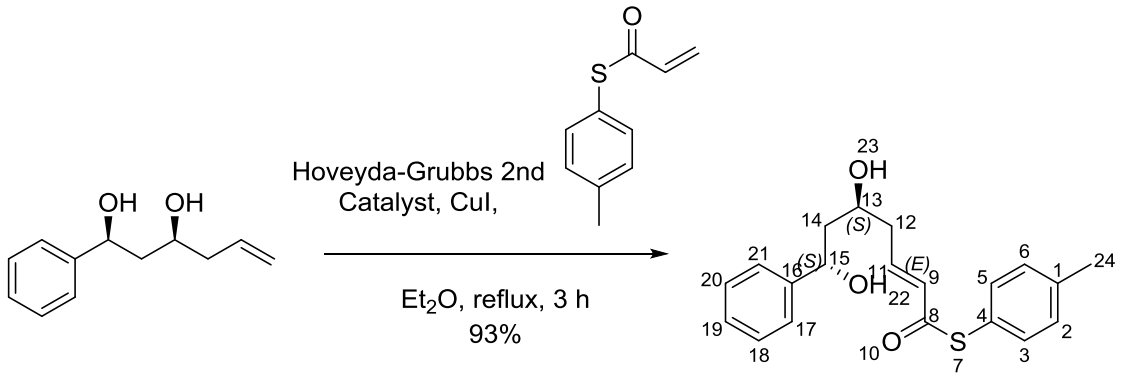

(1*S**,3*S**)-1-Phenylhex-5-ene-1,3-diol **79** (463.77 mg, 2.40 mmol, 1.00 eq.) and S-(4-methylphenyl) 2-propenthioate **66** (1.28 g, 7.23 mmol, 3.00 eq.) were dissolved in dry diethyl ether (24 mL, 0.10 M) under N_2 at room temperature. Copper (I) iodide

(45.71 mg, 0.24 mmol, 10.00 mol%) and Hoveyda-Grubbs 2nd generation catalyst (150.39 mg, 0.24 mmol, 10.00 mol%) were added and the reaction mixture was heated to reflux. After stirring for 3 hours the reaction mixture was concentrated *in vacuo* to give a crude product, which was then purified by flash column chromatography on silica (1:1, ethyl acetate-hexane) to yield (5*S**,7*S**,*E*)-S-*p*-tolyl 5,7-dihydroxy-7-phenylhept-2-enethioate **78** as a colourless oil (766.20 mg, 93%). **^{1}H NMR** (400 MHz, $CDCl_3$): δ 7.42-7.22 (9H, m, Ar-H), 6.94 (1H, dt, *J* = 15.0, 7.3 Hz, H-11), 6.21 (1H, d, *J* = 15.0 Hz, H-9), 4.86 (1H, dd, *J* = 9.9, 3.0 Hz, H-15), 4.11 (1H, br, OH), 4.05-4.00 (1H, m, H-13), 2.39 (3H, s, H-24), 2.37-2.31 (2H, m, H-12a, H-14a), 1.88-1.70 (2H, m, H-12b, H-14b); **^{13}C NMR** (101 MHz, $CDCl_3$): δ 188.7 (C-8), 144.1 (C-Ar), 142.1 (C-11), 139.7 (C-Ar), 134.6 (C-Ar), 130.1 (C-9), 128.6 (C-Ar), 128.5 (C-Ar), 127.7 (C-Ar), 125.7 (C-Ar), 123.8 (C-Ar), 74.9 (C-15), 70.9 (C-13), 44.7 (C-12), 40.6 (C-14), 21.4 (C-24); **IR** (film): ν_{max} 3356.4, 3032.0, 2917.2, 2251.0, 1672.9, 1631.4, 1493.4, 1463.0, 1303.8, 1016.7, 907.7, 807.6, 758.3, 728.7, 706.2, 547.1, 475.6 cm^{-1}; **ESI-MS**: *m/z* $C_{20}H_{22}NaO_3S$ [M+Na$^+$] 365.1182, found 365.1184 (−0.7 ppm error).

S-*p*-tolyl 2-((2*R,4*S**,6*S**)-4-hydroxy-6-phenyltetrahydro-2H-pyran-2-yl) ethanethioate 76**

Lab book: YT-3-29, NMR: a2299yth (YT-3-29-2)

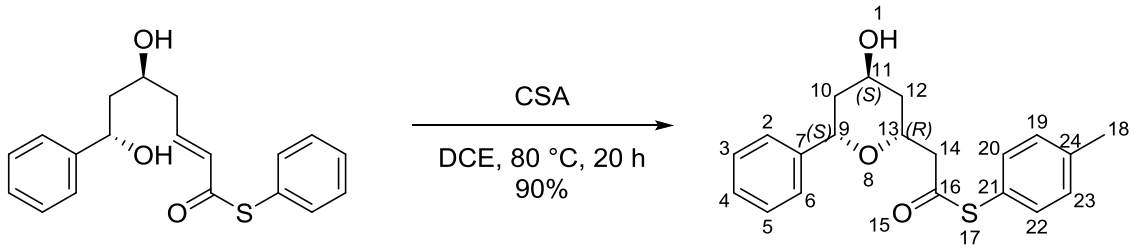

(5*S**,7*S**,*E*)-S-p-Tolyl 5,7-dihydroxy-7-phenylhept-2-enethioate **78** (171.20 mg, 0.50 mmol, 1.00 eq.) and CSA (58.08 mg, 0.25 mmol, 0.50 eq.) were dissolved in DCE (5 mL, 0.10 M) under N_2 and heated to 80 °C. After stirring at this temperature for 20 hours, the reaction was quenched with triethylamine (0.2 mL) and washed with saturated sodium bicarbonate solution (3 x 5 mL) and brine (3 x 5 mL). The combined organic extracts were dried (magnesium sulfate), filtered and concentrated *in vacuo* to give a crude product which was then purified by flash column chromatography on silica (1:3, ethyl acetate-hexane) to give S-*p*-tolyl 2-((2*R**,4*S**,6*S**)-4-hydroxy-6-phenyltetrahydro-2H-pyran-2-yl) ethanethioate **76** as a colourless oil (154.60 g, 90%). **^{1}H NMR** (400 MHz, $CDCl_3$): δ 7.37-7.17 (9H, m, Ar-H), 4.89 (1H, dd, *J* = 11.8, 2.2 Hz, H-9), 4.49 (1H, dddd, *J* = 11.7, 6.9, 6.0, 2.1 Hz, H-13), 4.31 (1H, p, *J* = 2.8 Hz, H-11), 2.98 (1H, dd, *J* = 14.8, 6.9 Hz, H-14a), 2.77 (1H, dd, *J* = 14.8, 6.0 Hz, H-14b), 2.34 (3H, s, H-18), 1.95-1.90 (1H, m, H-10a), 1.87 (1H, br, OH), 1.83-1.79 (1H, m, H-12a), 1.72 (1H, ddd, *J* = 14.5, 11.8, 2.8 Hz, H-10b), 1.65 (1H, ddd, *J* = 14.3, 11.7, 2.8 Hz, H-12b); **^{13}C NMR** (101 MHz, $CDCl_3$): δ 196.0 (C-16), 142.7 (C-Ar), 139.8 (C-Ar), 134.5 (C-Ar), 130.1 (C-Ar), 128.4 (C-Ar), 127.4 (C-Ar), 125.9 (C-Ar), 124.3 (C-Ar), 73.6 (C-9), 69.2 (C-13), 64.6 (C-11), 49.8 (C-14), 40.0 (C-10), 38.0 (C-12), 21.4 (C-18); **IR** (film): ν_{max} 3417.0, 3057.9, 3032.0, 2914.5, 2254.6, 1698.3, 1599.4, 1494.0, 1451.0, 1377.1, 1306.5, 1211.8, 1058.6, 972.8, 909.2, 807.1, 730.6, 697.7 cm^{-1}; **ESI-MS**: *m/z* $C_{20}H_{22}NaO_3S$ [M+Na^+] 365.1182, found 365.1177 (1.2 ppm error).

S-*p*-tolyl 2-((2*S,4*S**,6*S**)-4-hydroxy-6-phenyltetrahydro-2H-pyran-2-yl) ethanethioate 77**

Lab book: YT-4-70, NMR: p2148yth (YT-4-37-3)

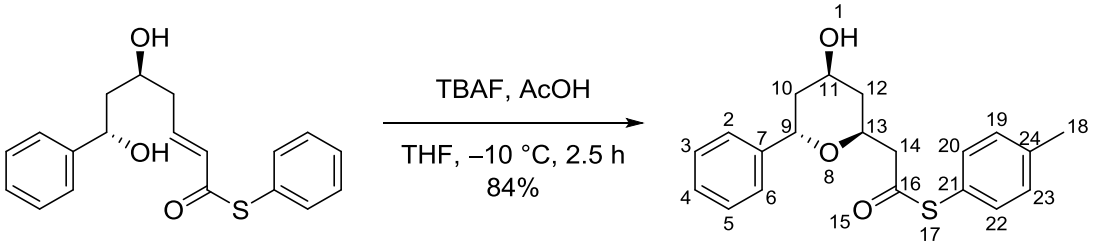

(5*S**,7*S**,*E*)-S-*p*-Tolyl 5,7-dihydroxy-7-phenylhept-2-enethioate **78** (366.00 mg, 1.07 mmol, 1.00 eq.) was dissolved in dry THF (2 mL, 0.54 M) under N_2 at room temperature. Then 1.00 M TBAF in THF (0.32 mL, 0.32 mol, 0.30 eq.) and acetic acid (2.56 μL, 3.60 mg, 0.06 mmol, 0.06 eq.) were added to the reaction mixture at −10 °C. After stirring for 2.5 hours, the reaction was quenched saturated sodium bicarbonate solution (2 mL). The aqueous phase was extracted with diethyl ether (3 x 2 mL) and the combined organic extracts were dried (magnesium sulfate), filtered and concentrated *in vacuo* to give a crude product, which was then purified by flash column chromatography on silica (1:1, ethyl acetate-hexane) to give S-*p*-tolyl 2-((2*S**,4*S**,6*S**)-4-hydroxy-6-phenyltetrahydro-2H-pyran-2-yl) ethanethioate **77** as a colourless oil (306.30 mg, 84%). **^{1}H NMR** (400 MHz, $CDCl_3$): δ 7.33-7.11 (7H, m, Ar-H), 4.89 (1H, dd, *J* = 7.0 Hz, H-9), 4.15-4.08 (1H, m, H-11), 3.26-3.19 (1H, m, H-13), 2.80 (1H, dd, *J* = 17.8, 5.8 Hz, H-14a), 2.36 (1H, dd, *J* = 17.8, 10.9 Hz, H-14b), 2.33 (3H, s, H-18), 2.23-2.21 (2H, m, H-10a, H-12a), 1.84 (1H, ddd, *J* = 14.1, 7.0, 4.5 Hz, H-10b), 1.56 (1H, dt, *J* = 13.7, 11.7 Hz, H-12b); **^{13}C NMR** (101 MHz, $CDCl_3$): δ 169.5 (C-16), 143.5 (C-Ar), 138.9 (C-Ar), 134.4 (C-Ar), 130.1 (C-Ar), 128.7 (C-Ar), 127.9 (C-Ar), 127.7

(C-Ar), 126.1 (C-Ar), 77.7 (C-11), 70.9 (C-9), 44.6 (C-10), 39.2 (C-13), 36.6 (C-14), 35.4 (C-12), 21.2 (C-18); **IR** (film): ν_{max} 3419.7, 3029.0, 2921.3, 2248.1, 1721.6, 1492.3, 1240.3, 1056.7, 909.0, 810.5, 729.2, 700.9 cm^{-1}; **ESI-MS**: *m/z* $C_{20}H_{22}NaO_3S$ [M+Na^+] 365.1182, found 365.1171 (2.4 ppm error).

Diospongin A 1

Lab book: YT-3-33, NMR: d3154yth, b9994yth (YT-3-33)

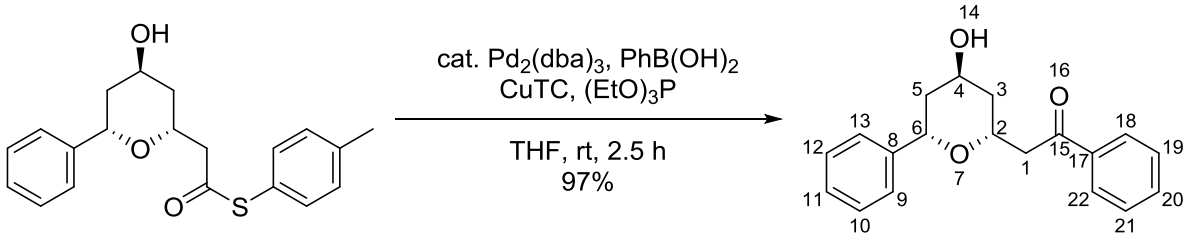

S-*p*-Tolyl 2-((2*R**,4*S**,6*S**)-4-hydroxy-6-phenyltetrahydro-2H-pyran-2-yl) ethanethioate **76** (54.00 mg, 0.16 mmol, 1.00 eq.), tris(dibenzylideneacetone) dipalladium(0) (14.65 mg, 16.00 μmol, 10.00 mol%), phenylboronic acid (58.53 mg, 0.48 mmol, 3.00 eq.), and copper(I)-thiophene-2-carboxylate (91.53 mg, 0.48 mmol, 3.00 eq.) were dissolved in dry THF (1.6 mL, 0.10 M) under N_2 at room temperature. Then triethylphosphite (2.19 μL, 12.8 *μmol,* 8.00 mol%) was added at the same temperature. After stirring for 2.5 hours, the reaction mixture was diluted with diethyl ether, washed with saturated sodium bicarbonate solution (3 x 5 mL) and brine (3 x 5 mL). The combined organic extracts were dried (magnesium sulfate), filtered and concentrated *in vacuo* to give a crude product, which was then purified by flash column chromatography on silica (1:1, ethyl acetate-hexane) to give diospongin A **1** as a colourless oil (46.00 mg, 97%). **^{1}H NMR** (500 MHz, $CDCl_3$): δ 7.98

(2H, dd, *J* = 5.2, 3.3 Hz, H-Ar), 7.56 (1H, t, *J* = 7.4 Hz, H-Ar) 7.46 (2H, t, *J* = 7.6 Hz, H-Ar), 7.31-7.21 (5H, m, H-Ar), 4.93 (1H, dd, *J* = 11.8, 2.0 Hz, H-6), 4.68-4.62 (1H, m, H-2), 4.38 (1H, p, *J* = 2.8 Hz, H-4), 3.42 (1H, dd, *J* = 16.0, 5.8 Hz, H-1a), 3.07 (1H, dd, *J* = 16.0, 6.8 Hz, H-1b), 1.99-1.93 (2H, m, H-3a, H-5a), 1.76 (1H, ddd, *J* = 14.4, 11.8, 2.8 Hz, H-5b), 1.69 (1H, ddd, *J* = 14.2, 11.4, 2.8 Hz, H-3b); **^{13}C NMR** (101 MHz, $CDCl_3$): δ 198.4 (C-15), 142.8 (C-Ar), 137.4 (C-Ar), 133.3 (C-Ar), 128.7 (C-Ar), 128.5 (C-Ar), 128.4 (C-Ar), 127.4 (C-Ar), 126.0 (C-Ar), 73.9 (C-6), 69.2 (C-2), 64.8 (C-4), 45.3 (C-1), 40.2 (C-5), 38.6 (C-3); **IR** (film): ν_{max} 3439.2, 3065.3, 3028.3, 2917.5, 2850.6, 1736.4, 1681.7, 1599.4, 1449.1, 1288.5, 1210.7, 1058.1, 981.2, 751.6, 697.9 cm^{-1}; **ESI-MS**: *m/z* $C_{19}H_{20}NaO_3$ [M+Na^+] 319.1305, found 319.1289 (4.3 ppm error). The ^{1}H NMR data was in agreement with the literature.[22]

Diospongin B 2

Lab book: YT-5-32, NMR: p6233yth (YT-5-32-7)

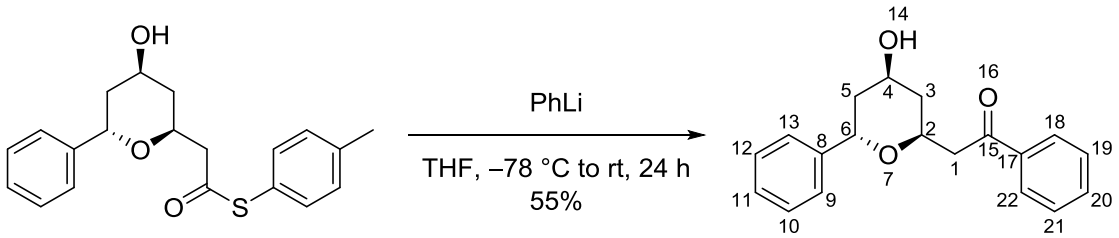

S-*p*-Tolyl 2-((2*S**,4*S**,6*S**)-4-hydroxy-6-phenyltetrahydro-2H-pyran-2-yl) ethanethioate **77** (25.00 mg, 73.00 μmol, 1.00 eq.) was dissolved in dry THF (0.2 mL). Phenyllithium (0.25 mL, 160.60 μmol, 2.20 eq., 1.54 M) was added under N_2 at −78 °C then was allowed to warm to room temperature. After stirring for 24 hours, the reaction mixture was quenched with chlorotrimethylsilane (92.65 μL, 0.73 mmol,

10.00 eq.), diluted with diethyl ether and saturated sodium bicarbonate solution was added. The aqueous phase was extracted with diethyl ether (3 x 2 mL) and the combined organic extracts were dried (magnesium sulfate), filtered and concentrated *in vacuo* to give a crude product, which was then purified by flash column chromatography on silica (1:1, ethyl acetate-hexane) to give diospongin B **2** as a yellow oil (12.00 mg, 55%). **^{1}H NMR** (500 MHz, $CDCl_3$): δ 8.00-7.98 (2H, m, H-Ar), 7.60-7.53 (1H, m, H-Ar), 7.49-7.46 (2H, m, H-Ar), 7.37-7.22 (4H, m, H-Ar), 7.24-7.22 (1H, m, H-Ar), 5.20 (1H, t, *J* = 4.3 Hz, H-6), 4.24 (1H, dddd, *J* = 9.5, 6.6, 7.0, 3.0 Hz, H-2), 4.06-4.00 (1H, m, H-4), 3.46 (1H, dd, *J* = 15.8, 7.0 Hz, H-1a), 3.18 (1H, dd, *J* = 15.8, 6.6 Hz, H-1b), 2.53 (1H, ddt, *J* = 13.8, 4.3, 1.7 Hz, H-5a), 2.09-2.04 (1H, m, H-3a), 1.92 (1H, ddd, *J* = 13.8, 9.9, 4.3 Hz, H-5b), 1.51 (1H, dt, *J* = 12.5, 9.5 Hz, H-3b); **^{13}C NMR** (101 MHz, $CDCl_3$): δ 198.5 (C-15), 140.4 (C-Ar), 137.4 (C-Ar), 133.3 (C-Ar), 128.8 (C-Ar), 128.7 (C-Ar), 128.4 (C-Ar), 127.3 (C-Ar), 126.5 (C-Ar), 72.5 (C-6), 67.1 (C-2), 64.4 (C-4), 44.8 (C-1), 40.3 (C-3) and 36.9 (C-5); **IR** (film): ν_{max} 3411.0, 2924.3, 2855.2, 1943.2, 1939.3, 1664.1, 1448.4, 1053.7, 692.5 cm^{-1}; **ESI-MS**: *m/z* $C_{20}H_{22}NaO_3S$ [M+Na^+] 319.1305, found 319.1317 (−4.2 ppm error). The ^{1}H NMR data was in agreement with the literature.[33]

S-*p*-tolyl 2-((2*S,4*S**,6*S**)-6-phenyl-4-((triisopropylsilyl)oxy)**

tetrahydro-2H-pyran-2-yl)ethanethioate 113

Lab book: YT-3-89, NMR: p2461yth (YT-3-89-3)

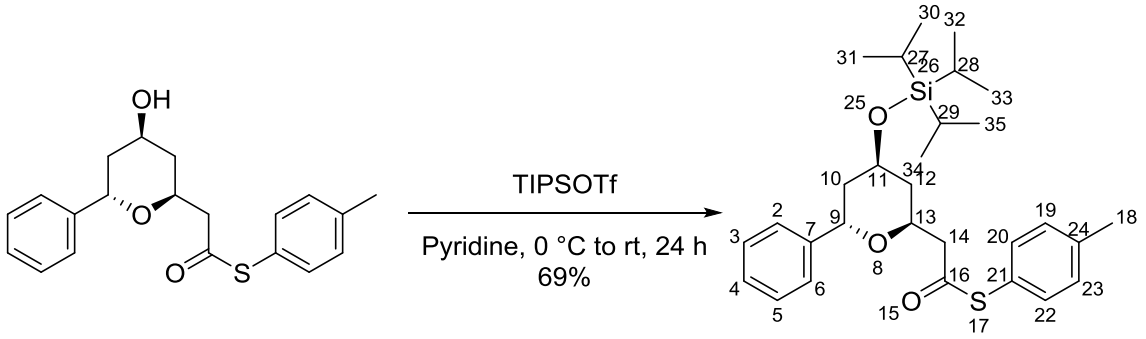

S-*p*-Tolyl 2-((2*S**,4*S**,6*S**)-4-hydroxy-6-phenyltetrahydro-2H-pyran-2-yl) ethanethioate **77** (227.40 mg, 0.66 mmol, 1.00 eq.) was dissolved in pyridine (522.06 mg, 0.53 mL, 6.60 mmol, 10.00 eq.). TIPSOTf (0.71 mL, 808.95 mg, 2.64 mmol, 4.00 eq.) was added to the reaction mixture under N_2 at 0 °C. After 30 minutes the reaction was allowed to warm to room temperature and stirred for 24 hours. The reaction mixture was then diluted with diethyl ether and washed with saturated copper(II) sulfate solution (5 mL). The aqueous phase was extracted with diethyl ether (3 x 5 mL) and the combined organic extracts were dried (magnesium sulfate), filtered and concentrated *in vacuo* to give a crude product, which was then purified by flash column chromatography on silica (1:8, ethyl acetate-hexane) to give S-*p*-tolyl 2-((2*S**,4*S**,6*S**)-6-phenyl-4-((triisopropylsilyl)oxy)tetrahydro-2H-pyran-2-yl) ethanethioate **113** as a yellow solid (225.80 mg, 69%). **^{1}H NMR** (400 MHz, $CDCl_3$): δ 7.34-7.22 (7H, m, Ar-H), 7.12 (2H, d, *J* = 7.9 Hz, Ar-H), 5.02 (1H, dd, *J* = 9.1, 4.7 Hz, H-9), 3.78 (1H, ddt, *J* = 11.5, 9.5, 3.3 Hz, H-11), 3.23-3.15 (1H, m, H-13), 2.85 (1H, ddd, *J* = 17.9, 6.0, 2.1 Hz, H-14a), 2.38 (1H, dd, *J* = 17.9, 10.9 Hz, H-14b), 2.34 (3H, s, H-18),

2.26 (1H, ddd, *J* = 14.0, 9.5, 4.7 Hz, H-10a), 2.10-2.05 (1H, m, H-12a), 1.86 (1H, ddd, *J* = 14.0, 9.1, 3.3 Hz, H-10b), 1.54 (1H, dt, *J* = 13.9, 11.5 Hz, H-12b), 1.04-0.91 (21H, m, H-1); **^{13}C NMR** (101 MHz, $CDCl_3$): δ 169.5 (C-16), 143.9 (C-Ar), 139.0 (C-Ar), 134.6 (C-Ar), 130.1 (C-Ar), 128.4 (C-Ar), 127.8 (C-Ar), 127.6 (C-Ar), 126.5 (C-Ar), 76.88 (C-11), 71.4 (C-9), 46.9 (C-10), 39.5 (C-13), 36.8 (C-14), 36.2 (C-12), 21.3 (C-18), 18.11, 18.01, 12.26; **IR** (film): ν_{max} 2943.0, 2865.4, 1738.6, 1492.5, 1462.8, 1388.4, 1369.9, 1228.5, 1090.3, 882.6, 811.3, 701.7, 681.9 cm^{-1}; **ESI-MS**: *m/z* $C_{29}H_{42}NaO_3SSi$ [M+Na$^+$] 521.2516, found 521.2491 (4.8 ppm error).

S-*p*-tolyl

2-((2*S,4*S**,6*S**)-4-((tert-butyldimethylsilyl)oxy)-6-phenyltetrahydro-2H-pyran-2-yl) ethanethioate 114**

Lab book: YT-3-74, NMR: k0602yth (YT-3-74-2-2)

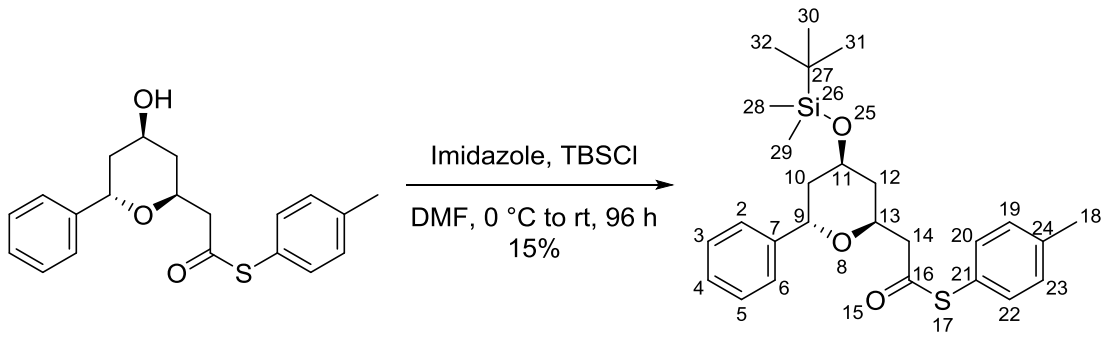

S-*p*-Tolyl 2-((2*S**,4*S**,6*S**)-4-hydroxy-6-phenyltetrahydro-2H-pyran-2-yl) ethanethioate **77** (98.40 mg, 0.29 mmol, 1.00 eq.) and imidazole (59.23 mg, 0.87 mmol, 3.00 eq.) were dissolved in dry DMF (2 mL, 0.15 M). TBSCl (66.32 mg, 0.44 mmol, 1.50 eq.) was added to the reaction mixture under N_2 at 0 °C. After 30 minutes the reaction was allowed to warm to room temperature and stirred for 96

hours. The reaction was then quenched with 2 M hydrochloric acid (2 mL). The organic phase was separated and the aqueous phase was extracted with dichloromethane (3 x 2 mL). The combined organic extracts were dried (magnesium sulfate), filtered and concentrated *in vacuo* to give a crude product, which was then purified by flash column chromatography on silica (1:1, ethyl acetate-hexane) to give S-*p*-tolyl 2-((2*S**,4*S**,6*S**)-4-((tert-butyldimethylsilyl)oxy)-6-phenyltetrahydro-2H-pyran-2-yl) ethanethioate **114** as a yellow oil (19.80 mg, 15%). **^{1}H NMR** (400 MHz, $CDCl_3$): δ 7.30-7.09 (9H, m, H-Ar), 4.84 (1H, dd, *J* = 7.3, 6.3 Hz, H-9), 3.96-3.88 (1H, m, H-11), 3.25-3.14 (1H, m, H-13), 2.81 (1H, dd, *J* = 17.7, 5.9 Hz, H-14a), 2.38 (1H, dt, *J* = 17.7, 11.0 Hz, H-14b), 2.31 (3H, s, H-18), 2.20 (1H, ddd, *J* = 14.0, 7.9, 6.2 Hz, H-10a), 2.15-2.10 (1H, m, H-12a), 1.79 (1H, ddd, *J* = 14.0, 7.3, 5.3 Hz, H-10b), 1.60-1.48 (1H, m, H-12b), 0.82-0.78 (9H, s, H-30, H-31, H-32), −0.06 (3H, s, H-28), −0.25 (3H, s, H-29); **^{13}C NMR** (101 MHz, $CDCl_3$): δ 169.6 (C-16), 143.7 (C-Ar), 139.0 (C-Ar), 134.6 (C-Ar), 130.1 (C-Ar), 128.5 (C-Ar), 127.9 (C-Ar), 127.7 (C-Ar), 126.3 (C-Ar), 77.1 (C-11), 71.4 (C-9), 46.3 (C-10), 39.7 (C-13), 36.7 (C-14), 35.8 (C-12), 25.9 (C-30, C-31, C-32), 21.3 (C-18), 18.2 (C-27), −4.6 (C-28), −5.0 (C-29); **IR** (film): ν_{max} 3337.5, 2970.0, 2932.2, 2883.5, 2658.3, 1407.5, 1466.5, 1378.7, 1340.6, 1306.5, 1160.1, 1128.1, 1107.5, 816.6, 789.7, 751.5 cm^{-1}; **ESI-MS**: *m/z* $C_{26}H_{36}NaO_3SSi$ [M+Na^+] 479.2047, found 479.2025 (4.0 ppm error).

(6*S,8*S**,*E*)-6,8-dihydroxy-8-phenyloct-3-en-2-one 122**

Lab book: YT-6-13, NMR: r3291yth (YT-6-13-6)

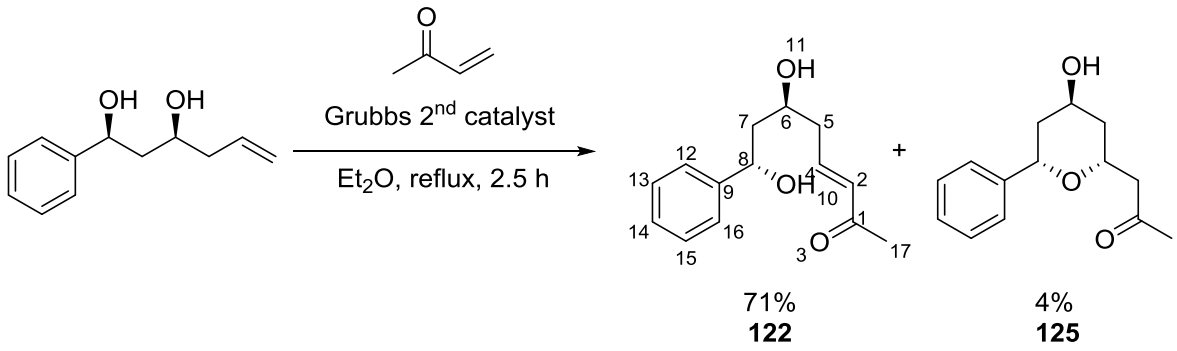

(1*S**,3*S**)-1-Phenylhex-5-ene-1,3-diol **79** (200.00 mg, 1.04 mmol, 1.00 eq.) and 3-buten-2-one (145.79 mg, 0.17 mL, 2.08 mmol, 2.00 eq.) were dissolved in dry diethyl ether (10 mL, 0.10 M) under N_2 at room temperature. Grubbs 2nd generation catalyst (88.29 mg, 104.00 μmol, 10.00 mol%) was added and the reaction was heated to reflux. After stirring for 2.5 hours the reaction mixture was concentrated *in vacuo* to give a crude product, which was then purified by flash column chromatography on silica (2:1, ethyl acetate-hexane) to yield (6*S**,8*S**,*E*)-6,8-dihydroxy-8-phenyloct-3-en-2-one **122** as a yellow oil (171.80 mg, 71%) and 1-((2*R**,4*S**,6*S**)-4-hydroxy-6-phenyltetrahydro-2H-pyran-2-yl)propan-2-one **125** as a colourless oil (9.50 mg, 4%). The data for compound **122**: **^{1}H NMR** (400 MHz, $CDCl_3$): δ 7.39-7.27 (5H, m, H-Ar), 6.83 (1H, dt, *J* = 16.0, 7.2 Hz, H-4), 6.10 (1H, d, *J* = 16.0 Hz, H-2), 4.93 (1H, dd, *J* = 10.1, 2.7 Hz, H-8), 4.13-4.08 (1H, m, 1H, H-6), 3.81 (1H, br, OH), 3.24 (1H, br, OH), 2.42-2.39 (2H, m, H-5), 2.24 (3H, s, H-17), 1.88 (1H, dt, *J* = 14.6, 10.1 Hz, H-7a), 1.76 (1H, dt, *J* = 14.6, 2.7 Hz, H-7b); **^{13}C NMR** (101 MHz, $CDCl_3$): δ 198.9 (C-1), 144.2 (C-4), 144.1 (C-2), 133.6 (C-Ar), 128.8 (C-Ar), 128.0 (C-Ar), 125.7 (C-Ar), 75.4 (C-8), 71.2 (C-6), 45.0 (C-7), 40.9 (C-5), 27.1 (C-17); **IR**

(film): ν_{max} 3386.1, 2914.8, 1667.8, 1424.6, 1362.6, 1259.8, 1064.1, 980.0, 758.6, 701.6, 545.2 cm^{-1}; **ESI-MS**: *m/z* $C_{14}H_{18}NaO_3$ [M+Na$^+$] 257.1148, found 257.1148 (−0.7 ppm error).

1-((2*R,4*S**,6*S**)-4-hydroxy-6-phenyltetrahydro-2H-pyran-2-yl) propan-2-one 125**

Lab book: YT-6-16 and 6-17, NMR: r3506yth (YT-6-16-3)

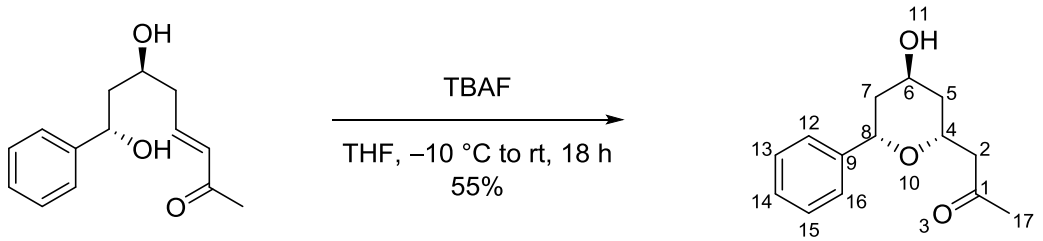

(6*S**,8*S**,*E*)-6,8-dihydroxy-8-phenyloct-3-en-2-one **122** (36.00 mg, 0.15 mol. 1.00 eq.) was dissolved in dry THF (1.50 mL, 0.10 M) under N_2 at room temperature. Then 1 M TBAF in THF (0.60 mL, 0.60 mol, 4.00 eq.) was added at −10 °C and the reaction was allowed to warm to room temperature. After stirring for 18 hours, the reaction was quenched with saturated sodium bicarbonate solution (2 mL). The aqueous phase was extracted with diethyl ether (3 x 2 mL) and the combined organic extracts were dried (magnesium sulfate), filtered and concentrated *in vacuo* to give a crude product, which was then purified by flash column chromatography on silica (3:1, ethyl acetate-hexane) to give 1-((2*R**,4*S**,6*S**)-4-hydroxy-6-phenyltetrahydro-2H-pyran-2-yl) propan-2-one **125** as a yellow oil (19.90 mg, 55%).

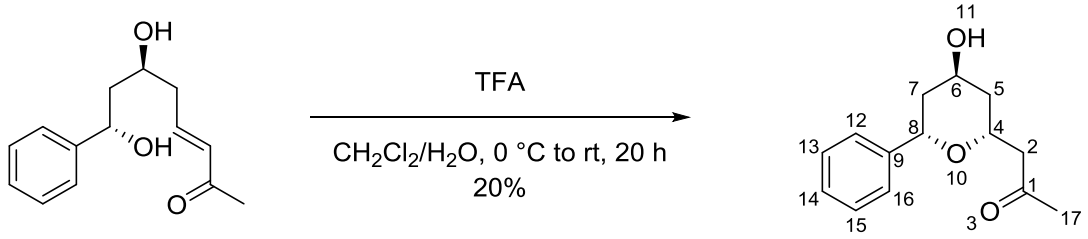

(6*S**,8*S**,*E*)-6,8-dihydroxy-8-phenyloct-3-en-2-one **122** (34.50 mg, 0.15 mmol, 1.00 eq.) was dissolved in dichloromethane (3.00 mL, 0.05 M) and water (0.30 mL, 0.50 M) under N_2 at room temperature. Then TFA (2.50 mL, 0.06M) was added at 0 °C and the reaction was allowed to warm to room temperature. After stirring for 20 hours, the reaction was quenched with saturated sodium bicarbonate solution (3 x 10 mL). The aqueous phase was extracted with dichloromethane (3 x 10 mL) and the combined organic extracts were dried (magnesium sulfate), filtered and concentrated *in vacuo* to give a crude product which was then purified by flash column chromatography on silica (2:1, ethyl acetate-hexane) to give 1-((2*R**,4*S**,6*S**)-4-hydroxy-6-phenyltetrahydro-2H-pyran-2-yl)propan-2-one **125** as a yellow oil (6.90 mg, 20%). **^{1}H NMR** (400 MHz, $CDCl_3$): δ 7.36-7.20 (5H, m, H-Ar), 4.90 (1H, dd, *J* = 11.8, 2.3 Hz, H-8), 4.50-4.43 (1H, m, H-4), 4.36 (1H, p, *J* = 2.9 Hz, H-6), 2.76 (1H, dd, *J* = 15.5, 7.4 Hz, H-2a), 2.53 (1H, dd, *J* = 15.5, 5.3 Hz, H-2b). 2.20 (3H, s, H-17), 1.96-1.91 (1H, m, H-7a), 1.83-1.77 (1H, m, H-5a), 1.75-1.71 (1H, m, H-7b), 1.67-1.58 (1H, m, H-5b); **^{13}C NMR** (101 MHz, $CDCl_3$): δ 207.6 (C-1), 142.7 (C-Ar), 128.5 (C-Ar), 127.5 (C-Ar), 125.9 (C-Ar), 73.8 (C-8), 69.0 (C-4), 64.8 (C-6), 50.1 (C-2), 40.3 (C-5), 38.3 (C-7), 31.2 (C-17); **IR** (film): ν_{max} 3351.2, 2969.9, 1706.7, 1465.8, 1378.7, 1305.4, 1160.6, 1128.1, 950.7, 816.2, 597.2 cm^{-1}; **ESI-MS**: *m/z* $C_{14}H_{18}NaO_3$ [M+Na^+] 257.1148, found 257.1158 (−3.4 ppm error).

1-Phenylprop-2-en-1-one 128

Lab book: YT-6-24, NMR: r3763yth (YT-6-19-1-r)

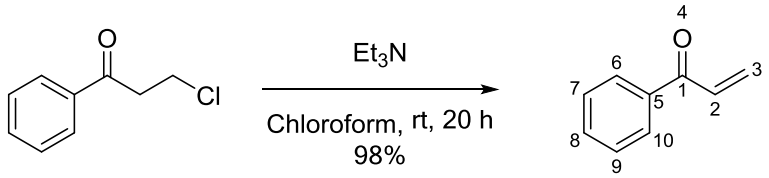

3-Chloropropiophenone (1.50 g, 8.90 mol, 1.00 eq.) was dissolved in chloroform (20 mL, 0.45 M) under N_2 at room temperature. Triethylamine (4.74 mL, 21.36 mol, 2.40 eq.) was added and stirred for 20 hours. The reaction was quenched with 0.1 M hydrochloric acid (20 mL) and washed with saturated sodium bicarbonate solution and brine, the combined organic extracts were dried (magnesium sulfate), filtered and concentrated *in vacuo* to give a crude product which was then purified by flash column chromatography on silica (1:10, ethyl acetate-hexane) to give 1-phenylprop-2-en-1-one **128** as a colourless oil (1.16 g, 98%). **^{1}H NMR** (400 MHz, $CDCl_3$): δ 7.95-7.92 (2H, m, H-Ar), 7.58-7.54 (1H, m, H-Ar) 7.48-7.44 (2H, m, H-Ar), 7.15 (1H, dd, *J* = 17.0, 10.6 Hz, H-2,), 6.43 (1H, dd, *J* = 17.0, 1.7 Hz, H-3a), 5.91 (1H, dd, *J* = 10.6, 1.7 Hz, H-3b); **^{13}C NMR** (101 MHz, $CDCl_3$): δ 191.1 (C-1), 137.3 (C-Ar), 133.1 (C-Ar), 132.4 (C-2), 130.3 (C-3), 128.8 (C-Ar), 128.7 (C-Ar); **IR** (film): ν_{max} 3060.9, 1670.5, 1656.0, 1595.9, 1578.8, 1447.8, 1402.8, 1304.9, 1285.6, 1179.6, 1159.5, 1101.1, 1077.5, 1030.1, 1002.8, 992.6, 978.9, 963.7, 815.3, 747.8, 724.7, 687.9, 652.8, 552.6 cm^{-1}; **ESI-MS**: *m/z* $C_{18}H_{17}O_2$ $[M+H^+]$ 265.1223, found 265.1224 (0.9 ppm error). The ^{1}H NMR data was in agreement with the literature.[66]

(5*S,7*S**,*E*)-5,7-dihydroxy-1,7-diphenylhept-2-en-1-one 123**

Lab book: YT-6-23, NMR: r4068yth (YT-6-28-3)

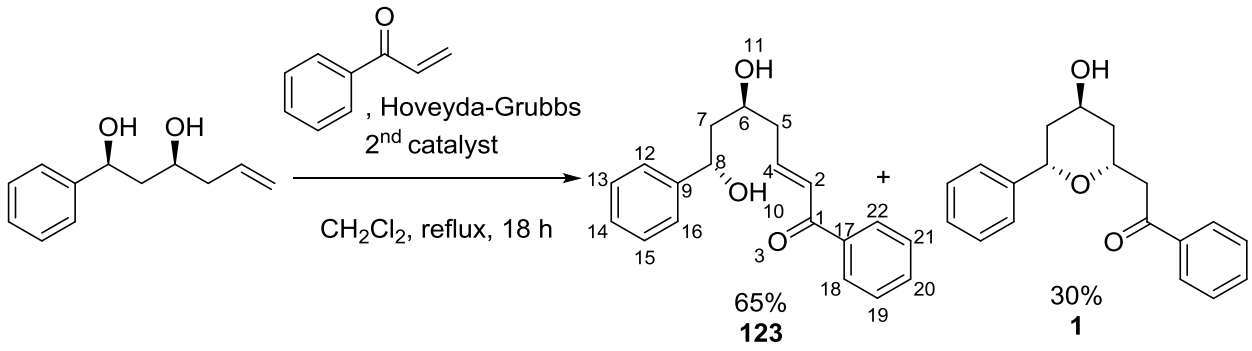

(1*S**,3*S**)-1-Phenylhex-5-ene-1,3-diol **79** (23.27 mg, 0.12 mmol, 1.00 eq.) and 1-phenylprop-2-en-1-one **128** (31.72 mg, 0.24 mmol, 2.00 eq.) were dissolved in dry dichloromethane (1 mL, 0.12 M) under N_2 at room temperature. Hoveyda-Grubbs 2nd generation catalyst (7.52 mg, 12.00 μmol, 10.00 mol%) was added and the reaction was stirred at refluxing dichloromethane. After stirring for 18 hours the reaction mixture was concentrated *in vacuo* to give a crude product, which was then purified by flash column chromatography on silica (1:1, ethyl acetate-hexane) to yield (5*S**,7*S**,*E*)-5,7-dihydroxy-1,7-diphenylhept-2-en-1-one **123** as a yellow oil (23.20 mg, 65%) and diospongin A **1** as a colourless oil (10.50 mg, 30%). The data for compound **123**: **^{1}H NMR** (400 MHz, $CDCl_3$): δ 7.95-7.89 (2H, m, 1H, H-Ar), 7.58-7.54 (1H, m, 1H, H-Ar), 7.48-7.15 (2H, m, H-Ar), 7.35 (4H, m, H-Ar), 7.32-7.27 (1H, m, H-Ar), 7.10-7.03 (1H, m, H-4), 6.97 (1H, d, *J* = 15.6 Hz, H-2), 4.98 (1H, dd, *J* = 9.9, 2.5 Hz, H-8), 4.21-4.16 (1H, m, H-6), 3.44 (1H, br, OH), 2.86 (1H, br, OH), 2.60-2.49 (2H, m, H-5), 1.99-1.90 (2H, m, H-7); **^{13}C NMR** (101 MHz, $CDCl_3$): 190.7 (C-1), 145.2 (C-2), 144.2 (C-4), 137.8 (C-Ar), 133.0 (C-Ar), 128.0 (C-Ar), 125.8 (C-Ar), 75.4 (C-8), 71.3 (C-6), 45.1 (C-7), 41.4 (C-5); **IR** (film): ν_{max} 3333.4, 29.69.7, 2930.3, 2883.2, 2659.0, 1718.8,

1466.6, 1407.9, 1378.4, 1340.4, 1306.1, 1160.1, 1107.5, 1128.0, 951.0, 816.6, 724.6, 686.3, 673.7, 647.1, 597.6, 487.0 cm^{-1}; **ESI-MS**: *m/z* $C_{19}H_{20}NaO_3$ [M+Na^+] 319.1305, found 319.1305 (−0.5 ppm error).

Dodecanethioic acid S-*p*-tolyl ester 107

Lab book: YT-5-17, NMR: p5551yth (YT-5-17-2-1)

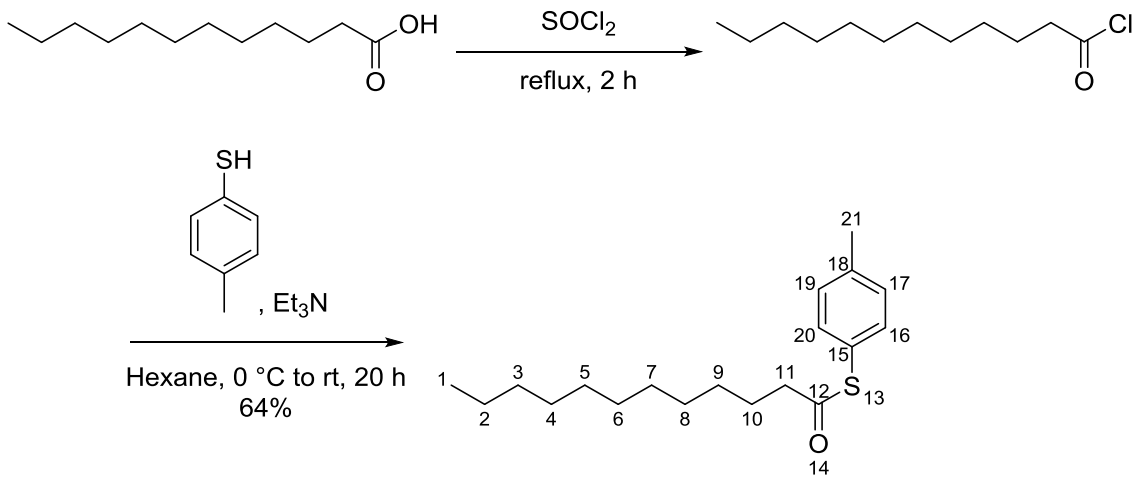

Dodecanoic acid (711.50 mg, 3.55 mmol, 1.00 eq.) was dissolved in refluxing thionyl chloride (16.14 mL, 0.22 M) at 80 °C, under N_2 for 2 hours. The reaction mixture was concentrated *in vacuo* and used for the next step without any purification. The resulting acid chloride and 4-methylbenzenethiol (529.13 mg, 4.26 mmol, 1.20 eq.) were dissolved in hexane (35.5 mL, 0.10 M). Triethylamine (0.99 mL, 718.45 mg, 7.10 mmol, 2.00 eq.) was added at 0 °C and the reaction was allowed to warm to room temperature. After stirring for 20 hours, the reaction was filter through celite and washed with 1:1 mixture of hexanes and diethyl ether and the combined organic filtrates were concentrated *in vacuo* to give a crude product, which was then purified by flash column chromatography on silica (50:1, dichloromethane-methanol) to give

dodecanethioic acid S-*p*-tolyl ester **107** as a colourless oil (694.00 mg, 64%). **^{1}H NMR** (400 MHz, $CDCl_3$): δ 7.27 (2H, d, *J* = 8.1 Hz, H-Ar), 7.18 (2H, d, *J* = 8.1 Hz, H-Ar), 2.61 (2H, t, *J* = 7.5 Hz, H-11), 2.34 (3H, s, H-21), 1.69 (2H, p, *J* = 7.5 Hz, H-10), 1.36-1.22 (16H, m, H-2, H-3, H-4, H-5, H-6, H-7, H-8, H-9), 0.88 (3H, t, *J* = 5.4 Hz, H-1); **^{13}C NMR** (101 MHz, $CDCl_3$): δ 197.7 (C-12), 139.4 (C-Ar), 134.4 (C-Ar), 129.9 (C-Ar), 124.5 (C-Ar), 43.6 (C-11), 31.9 (C-2), 29.6 (C-3), 29.5 (C-4), 29.4 (C-5), 29.3 (C-6), 29.0 (C-7), 25.6 (C-10), 22.7 (C-8), 21.3 (C-21), 14.1 (C-1). The ^{1}H and ^{13}C NMR data were in agreement with the literature.[60]

1-Furan-2-yl-dodecan-1-one 110

Lab book: YT-5-26-2, NMR: p5971yth (YT-5-26-2)

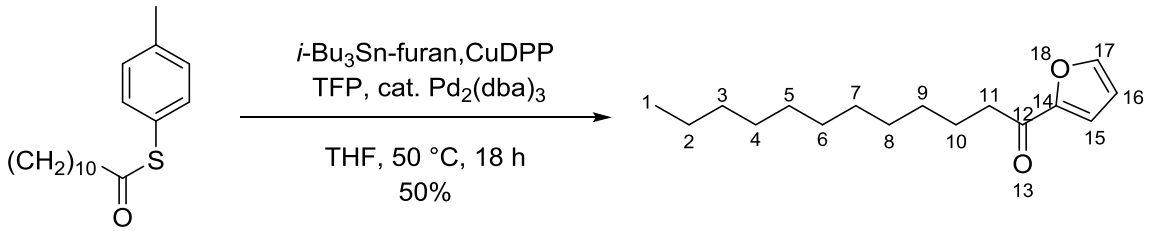

2-(Tri-*n*-butylstannyl)furan (125.34 mg, 0.35 mmol, 1.10 eq.), dodecanethioic acid S-*p*-tolyl ester (98.00 mg, 0.32 mmol, 1.00 eq.), CuDPP (106.68 mg, 0.38 mmol, 1.20 eq.), TFP (5.94 mg, 8.00 mol%, 25.60 µmol) and tris(dibenzylideneacetone) dipalladium(0) (2.93 mg, 1.00 mol%, 3.20 µmol) were in a Schlenk tube under N_2. Dry THF (5.1 mL) was added and the mixture was heated to 50 °C. After stirring for 18 hours, a hexane/dichloromethane (10:1, v/v, 10 mL) solvent mixture was added and then the reaction was filtered through a celite. The combined organic filtrates were concentrated *in vacuo* to give a crude product, which was then purified by flash column chromatography on silica (5:1, hexane-dichloromethane) to give

1-furan-2-yl-dodecan-1-one **110** as a colourless oil (39.90 mg, 50%). **^{1}H NMR** (400 MHz, $CDCl_3$): δ 7.57 (1H, d, *J* = 1.2 Hz, H-17), 7.17 (1H, d, *J* = 3.6 Hz, H-15), 6.52 (1H, dd, *J* = 3.6, 1.7 Hz, H-16), 2.80 (2H, t, *J* = 7.5 Hz, H-11), 1.71 (2H, p, *J* = 7.5 Hz, H-10), 1.38-1.22 (16H, m, H-2, H-3, H-4, H-5, H-6, H-7, H-8, H-9), 0.87 (3H, t, *J* = 6.8 Hz, H-1). The ^{1}H NMR data was in agreement with the literature.[63]

4.3. Experimental Procedures for Chapter two

Prenyltrimethylsilane 228

Lab book: YT-7-26, NMR: r8502yth (YT-6-62)

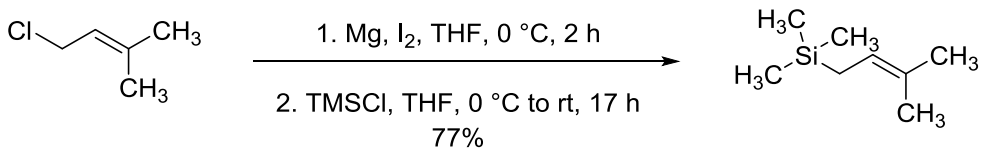

Magnesium turnings (10.00 g, 411.35 mmol, 2.00 eq.) and catalytic amount of iodine (129.44 mg, 0.51 mmol, 0.25 mol%) were dissolved in dry THF (500 mL, 0.40 M) under N_2 at room temperature. When the solution changed colour from dark brown to colourless, the solution was cooled to 0 °C and 1-chloro-3-methyl-2-butene (21.51 g, 23.18 mL, 205.68 mol, 1.00 eq.) was added dropwise over 1 hour. After stirring for 1 hour, the reaction mixture was allowed to warm to room temperature and freshly distilled chlorotrimethylsilane (22.35 g, 26.11 mL, 205.68 mmol, 1.00 eq.) was added slowly *via* syringe pump over 1 hour (the white solid magnesium chloride was precipitated). After stirring for 17 hours, the reaction mixture was filtered through celite and washed with hexane (250 mL). The pale yellow solution was collected, then water was added and then extracted with hexane (3 x 100 mL). The combined organic extracts were dried (magnesium sulfate), filtered and concentrated *in vacuo* to give prenyltrimethylsilane **228** as a colourless oil and was used without any further purification (22.50 g, 77%). ^{1}**H NMR** (400 MHz, $CDCl_3$): δ 5.16-5.12 (1H, t, *J* =

8.5 Hz, H-2), 1.69 (3H, s, H-4), 1.55 (3H, s, H-5), 1.37 (2H, d, *J* = 8.5 Hz, H-1), −0.02 (9H, s, H-7, H-8, H-9); **^{13}C NMR** (101 MHz, $CDCl_3$): 128.8 (C-3), 120.1 (C-2), 25.9 (C-4), 18.7 (C-1), 17.7 (C-5), -1.6 (C-7, C-8, C-9). The ^{1}H and ^{13}C NMR data were in agreement with the literature.[158]

3,3-dimethyl-pent-4-en-2-one 231

Lab book: YT-7-51, NMR: r8965yth (YT-6-75-d-2-3)

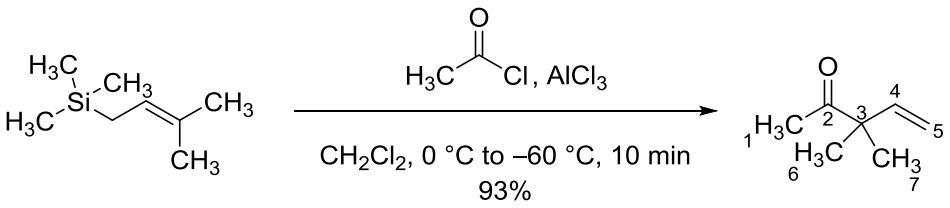

Aluminum chloride (4.31 g, 32.32 mmol, 1.00 eq.) was dissolved in dry dichloromethane (65 mL, 0.50 M) then acetyl chloride (2.77 g, 2.66 mL, 35.55 mmol, 1.10 eq.) was added slowly at 0 °C under N_2. After stirring for 30 minutes, the reaction mixture was cooled to −60 °C and prenyltrimethylsilane **228** (4.60 g, 32.32 mmol, 1.00 eq.) was added and stirred for another 10 minutes. After this, ice and saturated ammonium chloride solution (50 mL) was added. The aqueous phase was extracted with dichloromethane (50 mL x 3). The combined organic extracts were dried (magnesium sulfate), filtered, concentrated *in vacuo* and purified by Kugelrohr distillation (70 °C at 200 mbar) to give 3,3-dimethylpent-4-en-2-one **231** as a colourless oil (3.35 g, 93%). **^{1}H NMR** (400 MHz, $CDCl_3$): δ 5.92 (1H, dd, *J* = 17.7, 10.5 Hz, H-4), 5.17-5.13 (2H, m, H-5), 2.11 (3H, s, H-1), 1.23 (6H, s, H-6, H-7); **^{13}C NMR** (101 MHz, $CDCl_3$): 192.3 (C-2), 142.6 (C-4), 114.4 (C-5), 51.1 (C-3), 25.6 (C-1), 23.6

(C-6, C-7); **IR** (film): ν_{max} 3410.0, 3088.9, 2973.1, 2928.4, 2868.6, 1949.3, 1709.9, 1634.8, 1414.4, 1353.5, 1259.9, 1123.9, 1001.8, 917.7, 804.3, 651.4, 598.0, 475.6 cm^{-1}; **ESI-MS**: *m/z* calcd for $C_7H_{12}O_1$ [M+H$^+$] 113.1312, found 113.0961. The ^{1}H and ^{13}C NMR data were in agreement with the literature.[159]

3,3-dimethyl-2-[(trimethylsilyl)oxy]-1,4-pentadiene 221

Lab book: YT-7-46, NMR: b3244yth (6-78-d-3-2)

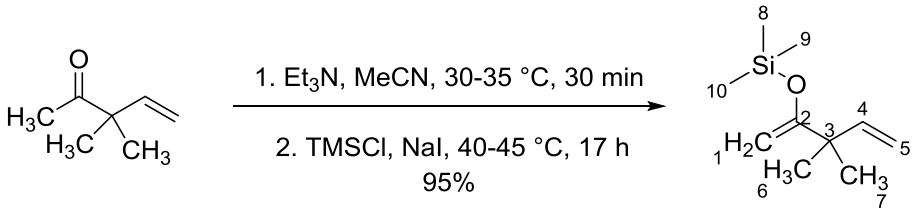

3,3-Dimethyl-pent-4-en-2-one **231** (3.00 g, 26.75 mmol, 1.00 eq.) was dissolved in dry acetonitrile (40 mL, 0.67 M) under N_2 at room temperature. Then triethylamine (13.53 g, 18.63 mL, 133.75 mmol, 5.00 eq.) was added dropwise over 30 minutes to the solution and then heated to 30-35 °C. After stirring for 30 minutes, chlorotrimethylsilane (5.81 g, 6.79 mL, 53.50 mmol, 2.00 eq.) and sodium iodide (8.02 g, 53.50 mmol, 2.00 eq.) were added. The reaction temperature was then raised to 40-45 °C and stirred for 17 hours. After cooling the reaction mixture to room temperature, the solution was filtered through celite and washed with hexane (100 mL). The filtrate was then extracted with hexane and concentrated *in vacuo*, to give 3,3-dimethyl-2-[(trimethylsilyl)oxy]-1,4-pentadiene **221** as a colourless oil (4.67 g, 95%). **^{1}H NMR** (400 MHz, $CDCl_3$): δ 5.93 (1H, dd, *J* = 17.5, 10.6 Hz, H-4), 5.01 (1H, dd, *J* = 10.6, 1.3 Hz, H-5a), 4.97 (1H, dd, *J* = 17.5, 1.3 Hz, H-5b), 4,12 (1H, d, *J* = 1.3 Hz, H-1a), 3.98 (1H, d, *J* = 1.3 Hz, H-1b), 1.14 (6H, s, H-6, H-7), 0.20 (9H, s, H-8, H-9, H-10);

^{13}C NMR (101 MHz, $CDCl_3$): 165.0 (C-2), 145.9 (C-4), 111.3 (C-5), 87.5 (C-1), 42.8 (C-3), 25.4 (C-6, C-7), −1.8 (C-8, C-9, C-10); **IR** (film): ν_{max} 3123.5, 3088.9, 2963.3, 1619.8, 1468.1, 1417.8, 1373.7, 1354.8, 1252.8, 1156.1, 1015.4, 912.9, 873.9, 844.09, 597.2 cm^{-1}. The ^{1}H and ^{13}C NMR data were in agreement with the literature.[160]

(*Z*)-1,4-Bis(benzyloxy)but-2-ene 233

Lab book: YT-7-70, NMR: j3066yth (YT-7-30-13)

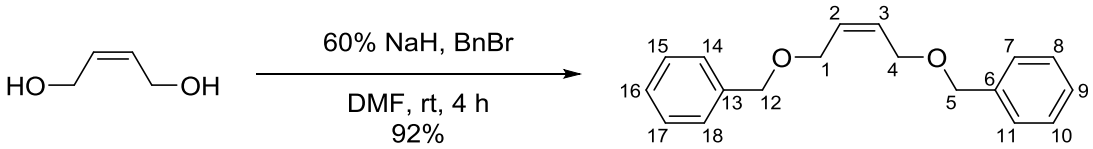

60% Sodium hydride suspension in mineral oil (11.80 g, 295.07 mol, 2.60 eq.) was suspended in DMF (300 mL, 0.4 M), at 0 °C *cis*-2-butene-1,4-diol (10.00 g, 113.49 mmol, 1.00 eq.) was added to the reaction mixture and was allowed to warm to room temperature. After stirring for 1 hour, benzyl bromide (67.94 g, 47.25 mL, 397.22 mmol, 3.50 eq.) was added dropwise to the reaction mixture and stirred for 4 hours at room temperature. The reaction was then quenched with saturated ammonium chloride solution, diluted with diethyl ether, and washed with water and brine. The combined organic extracts were dried (magnesium sulfate), filtered and concentrated *in vacuo* to give a crude product which was then purified by flash column chromatography on silica (1:8, ethyl acetate-hexane) to give (*Z*)-1,4-bis(benzyloxy)but-2-ene **233** as a colourless oil (28.02 g, 92%). **^{1}H NMR** (400 MHz, $CDCl_3$): δ 7.40-7.28 (10 H, m, H-Ar), 5.83-5.81 (2H, m, H-2, H-3), 4.51 (4H, s, H-5, H-12), 4.09 (4H, d, *J* = 4.9 Hz, H-1, H-4); **^{13}C NMR** (101 MHz, $CDCl_3$): 138.2 (C-Ar),

129.6 (C-2, C-3), 128.5 (C-Ar), 127.9 (C-Ar), 127.8 (C-Ar), 72.4 (C-5, C-12), 65.9 (C-1, C-4); **IR** (film): ν_{max} 3327.4, 3030.8, 2862.3, 1719.8, 1698.0, 1495.9, 1453.4, 1364.1, 1313.4, 1270.8, 1204.5, 1071.0, 1026.5, 827.4, 737.9, 697.2, 649.6, 604.8 cm^{-1}; **ESI-MS**: *m/z* $C_{18}H_{20}NaO_2$ [M+Na$^+$] 291.1350, found 291.1356 (2.1 ppm error). The ^{1}H and ^{13}C NMR data were in agreement with the literature.[105]

2-Benzyloxyacetoaldehyde 220

Lab book: YT-7-43, NMR: j9360yth (YT-7-43)

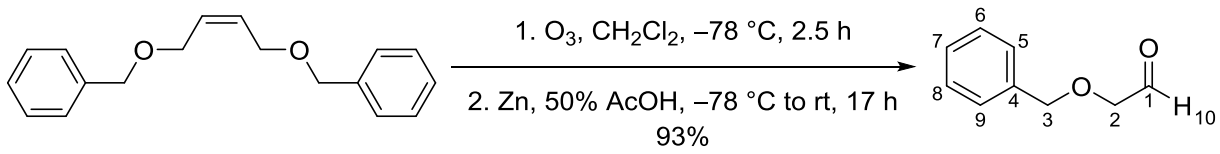

*Ozone is a toxic gas. The ozonolysis experiment must be carried out in the fume hood. Avoid inhalation and skin or eye contact.

(*Z*)-1,4-bis(benzyloxy)but-2-ene **233** (31.90 g, 118.87 mmol, 1.00 eq.) was dissolved in dry dichloromethane (400 mL, 0.3 M) under N_2 at −78 °C. Ozone was then bubbled through the solution until the solution changed to a blue colour. **Keep the fume hood fully down while passing ozone through the solution.** After stirring for 2.5 hours, zinc powder (11.34 g, 178.31 mmol, 1.50 eq.) and 50% acetic acid solution (71.46 g, 1.19 mol, 10.00 eq.) were added and the reaction was allowed to warm to room temperature. After stirring for 17 hours, the reaction mixture was washed with water (200 mL) and extracted with dichloromethane (200 mL x 3). The combined organic extracts were washed with saturated sodium bicarbonate solution, dried

(magnesium sulfate), filtered and concentrated *in vacuo* to give 2-benzyloxyacetoaldehyde **220** as a colourless oil (33.25 g, 93%). **^{1}H NMR** (400 MHz, $CDCl_3$): δ 9.73 (1H, s, H-10), 7.39-7.32 (5H, m, H-Ar), 4.64 (2H, s, H-3), 4.11 (2H, s, H-2); **^{13}C NMR** (101 MHz, $CDCl_3$): 200.6 (C-1), 136.9 (C-Ar), 128.8 (C-Ar), 128.4 (C-Ar), 128.2 (C-Ar), 75.4 (C-2), 73.8 (C-3); **IR** (film): ν_{max} 3449.2, 3063.9, 3031.2, 2861.8, 2719.9, 1734.4, 1605.2, 1496.4, 1454.2, 1373.6, 1317.0, 1258.9, 1206.3, 1107.6, 1027.9, 983.0, 911.3, 853.2, 738.0, 697.3, 597.7, 524.0, 470.0, 484.7, 464.0, 477.5 cm^{-1}; **ESI-MS**: *m/z* $C_9H_{10}NaO_2$ [M+Na$^+$] 173.0573, found 173.0572 (−0.2 ppm error). The ^{1}H and ^{13}C NMR data were in agreement with the literature.[105]

7-(benzyloxy)-6-hydroxy-3,3-dimethylhept-1-en-4-one 222

Lab book: YT-7-17, NMR: j1191yth (YT-7-17-2)

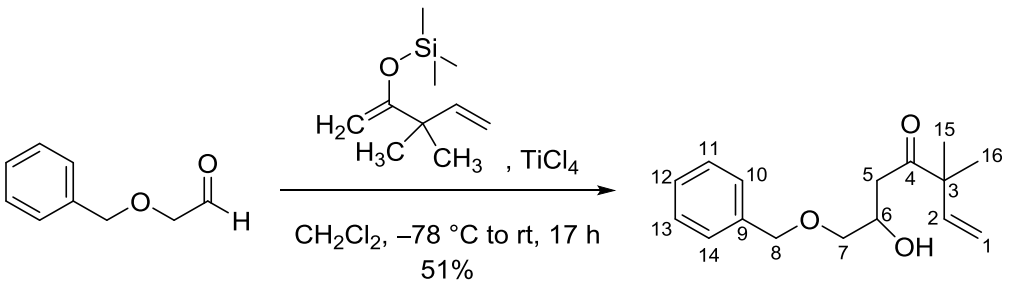

3,3-Dimethyl-2-[(trimethylsilyl)oxy]-I,4-pentadiene **221** (3.19 g, 17.30 mmol, 2.00 eq.) was dissolved in dry dichloromethane (20 mL, 0.43 M) and 2-benzyloxyacetalaldehyde **220** (1.30 g, 8.65 mmol, 1.00 eq.) was added dropwise at −78 °C under N_2. After stirring for 15 minutes, titanium tetrachloride (1.05 mL, 9.52 mmol, 1.10 eq) was added and the reaction was allowed to warm to room temperature. After stirring for 17 hours, the reaction mixture was quenched with

cold water (10 mL) and saturated sodium bicarbonate solution (10 mL). The aqueous phase was extracted with dichloromethane (20 x 3 mL) and the combined organic extracts were dried (magnesium sulfate), filtered and concentrated *in vacuo* to give a crude product, which was then purified by flash column chromatography on silica (1:2, ethyl acetate-hexane) to give **222** as a yellow oil (1.13 g, 51%). **^{1}H NMR** (400 MHz, $CDCl_3$): δ 7.37-7.27 (5H, m, H-Ar), 5.89 (1H, dd, *J* = 10.6, 17.4 Hz, H-2), 5.18-5.14 (2H, m, H-1), 4.55 (2H, s, H-8), 4.25-4.19 (1H, m, H-6), 3.49-3.42 (2H, m, H-7), 3.07 (1H, br, OH), 2.71-2.68 (2H, m, H-5), 1.23 (3H, s, H-15), 1.22 (3H, s, H-16); **^{13}C NMR** (101 MHz, $CDCl_3$): 213.5 (C-4), 142.1 (C-2), 138.1 (C-9), 128.7 (C-Ar), 128.6 (C-Ar), 127.9 (C-Ar), 115.0 (C-1), 73.5 (C-8), 73.3 (C-7), 67.1 (C-6), 51.1 (C-3), 40.9 (C-5), 23.5 (C-15), 23.4 (C-16); **IR** (film): ν_{max} 3449.4, 2972.8, 2927.5, 2868.7, 1706.3, 1635.4, 1453.7, 1363.5, 1098.6, 1027.6, 919.3, 736.5, 698.1, 597.8 cm^{-1}; **ESI-MS**: *m/z* $C_{16}H_{22}NaO_3$ [M+Na$^+$] 285.1461, found 285.1450 (3.8 ppm error).

(2*S,4*R**)-1-(benzyloxy)-5,5-dimethylhept-6-ene-2,4-diol 223**

Lab book: YT-8-25, NMR: b3025yth (YT-6-74-2-2)

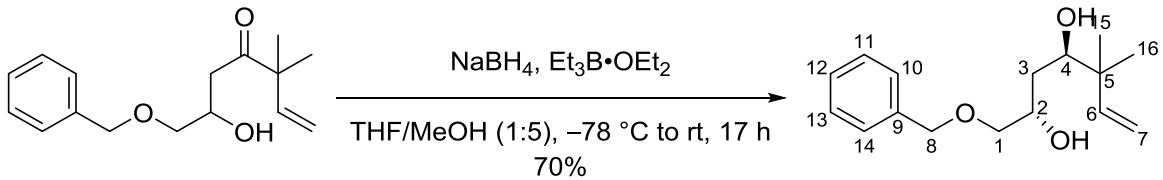

1.00 M Solution of triethyl borane in hexanes (1.74 mL, 1.74 mmol, 1.10 eq.) was added to a THF/methanol (1:5, v/v, 12 mL) solvent mixture under N_2 at room temperature. After stirring the reaction mixture for 2 hours, the solution was cooled down to −78 °C and 7-(benzyloxy)-6-hydroxy-3,3-dimethylhept-1-en-4-one **222**

(415.60 mg, 1.58 mmol, 1.00 eq.) was added slowly. After stirring for 30 minutes, sodium borohydride (65.82 mg, 1.74 mmol, 1.10 eq.) was added in one portion and then reaction was allowed to warm to room temperature. After stirring the reaction for 17 hours, the reaction mixture was quenched with saturated ammonium chloride solution (10 mL) and then diluted with ethyl acetate (10 mL). The aqueous phase was extracted with ethyl acetate (3 x 10 mL) and the combined organic extracts were dried (magnesium sulfate), filtered and concentrated *in vacuo* to give a crude product, which was then purified by flash column chromatography on silica (1:2, ethyl acetate-hexane) to yield **223** as a yellow oil (292.40 mg, 70%). **^{1}H NMR** (400 MHz, $CDCl_3$): δ 7.38-7.28 (5H, m, H-Ar), 5.83 (1H, dd, *J* = 17.5, 10.8 Hz, H-6), 5.07 (1H, dd, *J* = 17.5, 1.3 Hz, H-7a), 5.04 (1H, dd, *J* = 10.8, 1.3 Hz, H-7b), 4.56 (2H, s, H-8), 4.06-4.00 (1H, m, H-2), 3.56 (1H, dd, *J* = 10.5, 1.6 Hz, H-4), 3.45 (1H, dd, *J* = 9.4, 4.0 Hz, H-1a), 3.40 (1H, dd, *J* = 9.4, 7.0 Hz, H-1b), 3.27 (1H, br, OH), 3.07 (1H, br, OH), 1.68-1.64 (1H, m, H-3a), 1.46-1.40 (1H, m, H-3b), 1.01 (6H, s, H-15, H-16); **^{13}C NMR** (101 MHz, $CDCl_3$): 145.4 (C-6), 138.0 (C-9), 128.6 (C-Ar), 128.0 (C-Ar), 127.9 (C-Ar), 113.3 (C-7), 78.8 (C-4), 74.4 (C-1), 73.5 (C-8), 71.9 (C-2), 41.6 (C-5), 33.9 (C-3), 22.6 (C-15), 22.5 (C-16); **IR** (film): ν_{max} 3391.8, 3085.7, 3063.7, 3032.2, 2959.9, 2925.2, 2864.9, 1637.8, 1496.1, 1453.6, 1414.8, 1362.7, 1309.7, 1204.2, 1093.4, 1028.0, 1005.4, 911.9, 846.1, 734.8, 697.5, 608.9, 586.0, 551.9, 518.0, 507.0, 495.6, 484.6, 473.6, 462.7 cm^{-1}; **ESI-MS**: *m/z* $C_{16}H_{24}NaO_3$ [M+Na^+] 287.1618, found 287.1614 (1.2 ppm error).

(2*R,4*R**)-1-(benzyloxy)-5,5-dimethylhept-6-ene-2,4-diol 234**

Lab book: YT-7-19, NMR: j1534yth (YT-7-19-4)

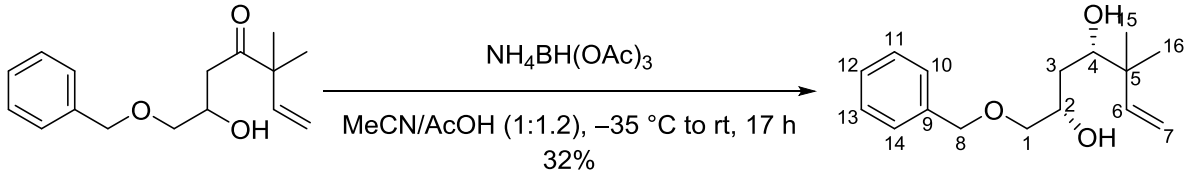

Sodium triacetoxyborohydride (146.40 mg, 0.56 mmol, 1.00 eq.) was dissolved in a acetonitrile/acetic acid (1:1.2, v/v, 11 mL) solvent mixture under N_2 at room temperature. 7-(benzyloxy)-6-hydroxy-3,3-dimethylhept-1-en-4-one **222** (1.03 g, 3.29 mmol, 7.00 eq.) was added to the solution at −35 °C and then reaction was allowed to warm to room temperature. After stirring the reaction for 17 hours, the reaction mixture was quenched with 10% Rochelle salt (10 mL) and extracted with ethyl acetate (40 mL). The combined organic extracts were dried (magnesium sulfate), filtered and concentrated *in vacuo* to give a crude product, which was then purified by flash column chromatography on silica (1:2, ethyl acetate-hexane) to yield **234** as a yellow oil (47.50 mg, 32%). **^{1}H NMR** (400 MHz, $CDCl_3$): δ 7.38-7.28 (5H, m, H-Ar), 5.82 (1H, dd, *J* = 17.4, 11.0 Hz, H-6), 5.08 (1H, dd, *J* = 11.0, 1.3 Hz, H-7a), 5.04 (1H, dd, *J* = 17.4, 1.3 Hz, H-7b), 4.57 (1H, s, H-8a), 4.56 (1H, s, H-8b), 4.14-4.08 (1H, m, H-2), 3.63 (1H, dd, *J* = 13.2, 1.6 Hz, H-4), 3.53 (1H, dd, *J* = 9.4, 3.5 Hz, H-1a), 3.36 (1H, dd, *J* = 9.4, 7.8 Hz, H-1b), 2.65 (1H, br, OH), 2.10 (1H, br, OH), 1.65-1.59 (1H, m, H-3a), 1.45-1.38 (1H, m, H-3b), 1.01 (3H, s, H-15), 1.00 (3H, s, H-16); **^{13}C NMR** (101 MHz, $CDCl_3$): 145.3 (C-6), 138.0 (C-9), 128.6 (C-Ar), 127.9 (C-Ar), 127.9 (C-Ar), 113.4 (C-7), 74.6 (C-1), 74.3 (C-4), 73.4 (C-8), 68.1 (C-2), 41.4 (C-5), 34.2 (C-3), 23.0 (C-15), 22.3 (C-16); **IR** (film): ν_{max} 2965.6, 2252.1, 1454.0, 1365.3, 1091.7, 904.3, 726.9, 649.9,

597.8, 476.9 cm^{-1}; **ESI-MS**: *m/z* $C_{16}H_{24}NaO_3$ [M+Na^+] 287.1618, found 287.1619 (0.0 ppm error).

(4*S,6*R**)-4-((benzyloxy)methyl)-2,2-dimethyl-6-(2-methylbut-3-en-2-yl)-1,3-dioxane 235**

Lab book: YT-7-23-1, NMR: j2118yth (YT-7-23-1)

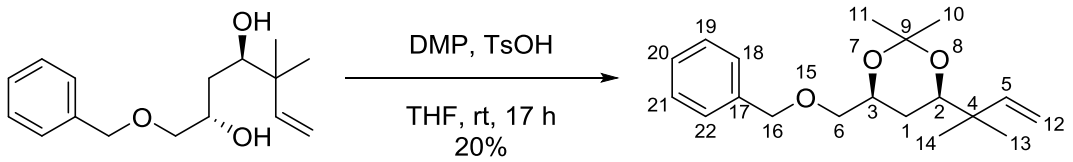

Diol **223** (48.50 mg, 0.18 mmol, 1.00 eq.) and 4-methylbenzenesulfonic acid (3.42 mg, 18.00 μmol, 0.10 eq.) were dissolved in dry THF (1.8 mL, 0.10 M), then 2,2-dimethoxypropane (44.27 μL, 37.49 mg, 0.36 mmol, 2.00 eq.) was added at room temperature and stirred for 17 hours. The reaction was quenched with saturated sodium bicarbonate solution (5 mL) and extracted with dichloromethane (5 mL). The combined organic extracts were dried (magnesium sulfate), filtered and concentrated *in vacuo* to give a crude product, which was then purified by flash column chromatography on silica (1:5, ethyl acetate-hexane) to yield **235** as a yellow oil (11.10 mg, 20%).^{1}**H NMR** (400 MHz, $CDCl_3$): δ 7.37-7.27 (5H, m, H-Ar), 5.88 (1H, dd, *J* = 17.4, 11.1 Hz, H-5), 4.99 (1H, dd, *J* = 11.1, 1.5 Hz, H-12a), 4.97 (1H, dd, *J* = 17.4, 1.5 Hz, H-12b), 4.60 (1H, d, *J* = 12.3 Hz, H-16a), 4.53 (1H, d, *J* = 12.3 Hz, H-16b), 4.07-4.00 (1H, m, H-3), 3.53 (1H, dd, *J* = 11.8, 2.4 Hz, H-2), 3.48 (1H, dd, *J* = 10.0, 6.0 Hz, H-6a), 3.35 (1H, dd, *J* = 10.0, 4.9 Hz, H-6b), 1.42 (3H, s, H-10), 1.39 (3H, s, H-11), 1.21-1.01 (2H, m, H-1), 0.99 (3H, s, H-13), 0.98 (3H, s, H-14); ^{13}**C NMR** (101 MHz, $CDCl_3$): 145.2

(C-5), 138.4 (C-17), 128.5 (C-Ar), 128.0 (C-Ar), 127.8 (C-Ar), 112.1 (C-12), 98.7 (C-9), 75.3 (C-2), 74.0 (C-6), 73.6 (C-16), 68.9 (C-3), 40.1 (C-4), 30.2 (C-10), 28.6 (C-1), 23.1 (C-13), 22.7 (C-14), 19.8 (C-11); **IR** (film): ν_{max} 3439.2, 2924.6, 2861.7, 1637.8, 1496.4, 1453.7, 1415.1, 1378.9, 1261.5, 1199.8, 1169.3, 1100.5, 1028.3, 1000.2, 911.5, 866.8, 850.3, 802.6, 735.1, 697.1, 608.2, 524.5, 475.7 cm^{-1}; **ESI-MS**: *m/z* $C_{19}H_{28}NaO_3$ [M+Na^+] 327.1931, found 327.1927 (1.3 ppm error).

(4*R,6*R**)-4-((benzyloxy)methyl)-2,2-dimethyl-6-(2-methylbut-3-en-2-yl)-1,3-dioxane 236**

Lab book: YT-7-21-1, NMR: k0740yth (YT-7-21-1)

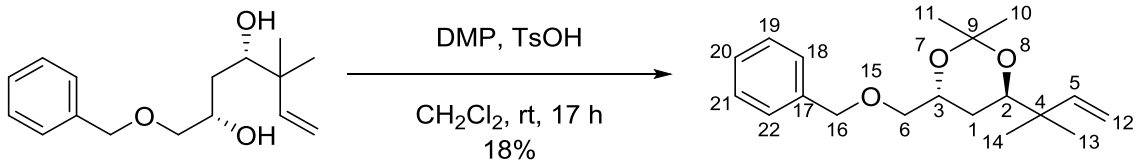

Diol **234** (72.90 mg, 0.28 mmol, 1.00 eq.) and 4-methylbenzenesulfonic acid (5.33 mg, 28.00 μmol, 0.10 eq.) were dissolved in dry dichloromethane (1.75 mL), then 2,2-dimethoxypropane (58.32 mg, 68.85 μL, 0.56 mmol, 2.00 eq.) was added at room temperature and stirred for 17 hours. The reaction was quenched with saturated sodium bicarbonate solution and extracted with dichloromethane (5 mL). The combined organic extracts were dried (magnesium sulfate), filtered and concentrated *in vacuo* to give a crude product, which was then purified by flash column chromatography on silica (1:4, ethyl acetate-hexane) to yield **236** as a yellow oil (15.50 mg, 18%). **^{1}H NMR** (400 MHz, $CDCl_3$): δ 7.36-7.26 (5H, m, H-Ar), 5.88 (1H, dd, *J* = 17.4, 11.0 Hz, H-5), 5.00 (1H, dd, *J* = 11.0, 1.4 Hz, H-12a), 4.58 (1H, dd, *J* = 17.4, 1.4

Hz, H-12b), 4.62 (1H, d, *J* = 12.3 Hz, H-16a), 4.54 (1H, d, *J* = 12.3 Hz, H-16b), 3.97-3.91 (1H, m, H-3), 3.51 (1H, dd, *J* = 10.0, 6.3 Hz, H-2), 3.47 (1H, dd, *J* = 10.4, 6.5 Hz, H-6a), 3.41(1H, dd, *J* = 10.4, 4.0 Hz, H-6b), 1.67-1.38 (2H, m, H-1), 1.36 (3H, s, H-10), 1.34 (3H, s, H-11), 0.99 (3H, s, H-13), 0.96 (3H, s, H-14); **^{13}C NMR** (101 MHz, $CDCl_3$): 144.8 (C-5), 138.5 (C-17), 128.5 (C-Ar), 127.9 (C-Ar), 127.7 (C-Ar), 112.3 (C-12), 100.6 (C-9), 73.4 (C-16), 73.0 (C-2), 72.9 (C-6), 66.8 (C-3), 40.0 (C-4), 30.4 (C-1), 24.9 (C-10), 24.3 (C-11), 23.1 (C-13), 22.8 (C-14); **IR** (film): ν_{max} 3332.4, 2969.7, 2931.7, 2882.5, 2658.8, 1466.6, 1378.5, 1367.9, 1340.5, 1306.4, 1160.1, 1128.1, 1108.0, 951.0, 816.7 cm^{-1}; **ESI-MS**: *m/z* $C_{19}H_{28}NaO_3$ [M+Na^+] 327.1931, found 327.1918 (4.0 ppm error).

(*E*)-2-ButenoicAcid S-(4-Methylphenyl)Ester 240

Lab book: YT-7-37-3, NMR:j2256yth (YT-7-37-3)

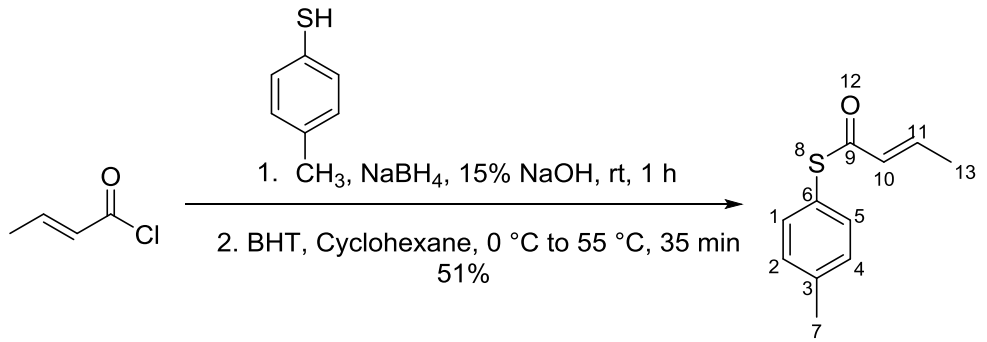

Sodium borohydride (12.48 mg, 0.33 mmol, 0.03 eq.) and 4-methylbenzenethiol (1.37 g, 11.03 mmol, 1.00 eq.) were stirred in 15% sodium hydroxide aqueous solution (5 mL) at room temperature under N_2 for 1 hour to give a solution of *p*-$CH_3C_6H_4S^-Na^+$. This solution was cooled to 0 °C before use.

In a separate flask, BHT (33.05 mg, 0.15 mmol, 1.40 mol%) and crotonoyl chloride (1.73 g, 1.59 mL, 16.55 mmol, 1.50 eq.) were dissolved in cyclohexane (7 mL) and cooled to 0 °C. The cold solution of *p*-$CH_3C_6H_4S^-Na^+$ was then added to this solution at 0 °C. After addition was completed, the reaction was left to warm to 55 °C for 35 minutes. The reaction was extracted with diethyl ether and washed with saturated sodium bicarbonate solution and brine, the combined organic extracts were dried (magnesium sulfate), filtered and concentrated *in vacuo*. BHT (18.20 mg) was added to the solution before concentrated *in vacuo* to prevent polymerization. The crude product was then purified by flash column chromatography on silica (1:30, ethyl acetate-hexane) to yield (*E*)-2-butenoicacid S-(4-Methylphenyl)ester **240** as a colourless oil (1.09 g, 51%). **^{1}H NMR** (400 MHz, $CDCl_3$): δ 7.33-7.21 (4H, m, H-Ar), 6.99 (1H, dq, *J* = 15.3, 1.5 Hz, H-10), 6.21 (1H, dq, *J* = 15.3, 6.9 Hz, H-11), 2.38 (3H, s, H-7), 1.92 (3H, dd, *J* =6.9, 1.5 Hz, H-13); **^{13}C NMR** (101 MHz, $CDCl_3$): 188.6 (C-9), 142.0 (C-10), 139.7 (C-Ar), 134.8 (C-Ar), 130.1 (C-Ar), 129.5 (C-11), 124.2 (C-Ar), 21.5 (C-7), 18.2 (C-13); **IR** (film): ν_{max} 3026.0, 2979.2, 2916.0, 2866.0, 2252.4, 1905.4, 1678.2, 1636.0, 1597.8, 1493.2, 1440.2, 1398.8, 1375.7, 1303.3, 1210.0, 1181.7, 1153.4, 1116.7, 1084.5, 1037.7, 1017.9, 959.2, 933.0, 907.1, 805.3, 729.9, 705.2, 646.9, 619.7, 572.9, 534.0, 509.2, 474.5 cm^{-1}; **ESI-MS**: *m/z* $C_{11}H_{12}NaO_2$ [M+Na^+] 215.0501, found 215.0497 (1.7 ppm error). The ^{1}H and ^{13}C NMR data were in agreement with the literature.[161]

S-*p*-tolyl 2-bromoethanethioate 244

Lab book: YT-7-53-2, NMR: j4392yth (YT-7-53-2)

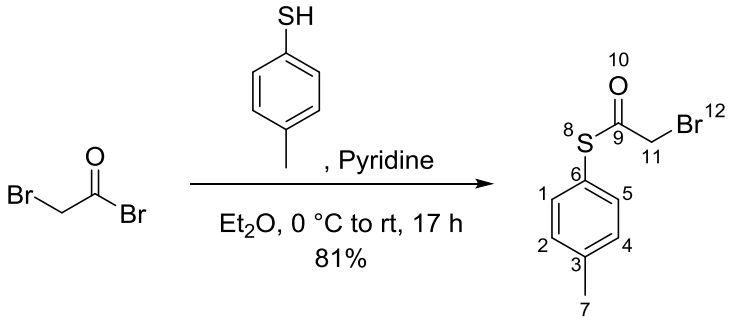

4-Methylbenzenethiol (2.00 g, 16.10 mmol, 1.00 eq.) was dissolved in diethyl ether (30 mL, 0.54 M), then pyridine (1.30 mL, 1.27 g, 16.10 mmol, 1.00 eq.) was added at room temperature under N_2. After stirring for 20 minutes, bromoacetyl bromide (1.40 mL, 3.25 g, 16.10 mmol, 1.00 eq.) was added to the solution at 0 °C and then reaction was allowed to warm to room temperature. After stirring the reaction for 17 hours, the reaction mixture was quenched with water (15 mL) and saturated sodium bicarbonate solution (15 mL). The aqueous phase was extracted with diethyl ether (3 x 30 mL). The combined organic extracts were washed with copper(II) sulfate (3 x 30 mL), dried (magnesium sulfate), filtered and concentrated *in vacuo* to give a crude product which was then purified by flash column chromatography on silica (1:8, ethyl acetate-hexane) to give S-*p*-tolyl 2-bromoethanethioate **244** as a yellow oil (3.20 g, 81%). **^{1}H NMR** (400 MHz, $CDCl_3$): δ 7.47-7.19 (4H, m, H-Ar), 4.10 (2H, s, H-11), 2.34 (3H, s, H-7); **^{13}C NMR** (101 MHz, $CDCl_3$): 191.7 (C-9), 140.5 (C-Ar), 134.6 (C-Ar), 130.4 (C-Ar), 123.3 (C-Ar), 33.3 (C-11), 21.5 (C-7); **IR** (film): ν_{max} 2923.8, 2252.9, 1697.3, 1598.1, 1493.8, 1398.1, 1213.2, 1151.6, 1063.2, 904.6, 808.4, 726.8, 649.5, 625.8, 597.6, 545.9, 506.8, 471.0 cm^{-1}; **ESI-MS**: *m/z* $C_9H_9BrNaO_2$ [M+Na$^+$]

266.9450, found 266.9442 (2.9 ppm error), $C_9H_{10}BrO_2$ [M+Na$^+$] 244.9630, found 266.9625 (−1.5 ppm error). The ^{1}H and ^{13}C NMR data were in agreement with the literature.[112]

(2-oxo-2-(*p*-tolylthio)ethyl)triphenylphosphonium bromide 247

Lab book: YT-7-71, NMR: j8469yth (YT-7-71-crude)

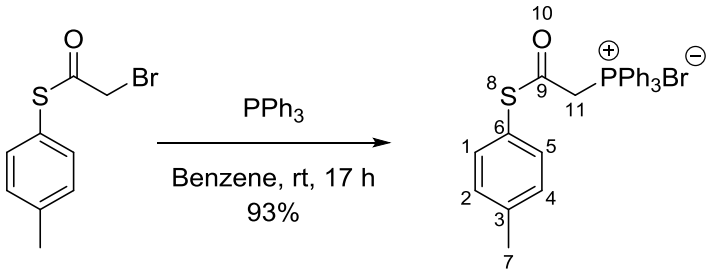

S-*p*-tolyl 2-bromoethanethioate **244** (6.18 g, 25.21 mmol, 1.00 eq.) was dissolved in benzene (10 mL, 2.50 M), then triphenylphosphine (6.61 g, 25.21 mmol, 1.00 eq.) was added under N_2 at room temperature. After stirring for 17 hours, the white solid was collected and washed with benzene. The solvent was removed under *vacuo* to give (2-oxo-2-(*p*-tolylthio)ethyl)triphenylphosphonium bromide **247** as a white solid (11.91 g, 93%). **^{1}H NMR** (400 MHz, $CDCl_3$): δ 7.82-6.93 (19H, m, H-Ar), 5.94 (2H, d, *J* = 13.32 Hz, H-11), 2.22 (3H, s, H-7); **^{13}C NMR** (101 MHz, $CDCl_3$): 190.4 (C-9), 140.8 (C-Ar), 135.2 (C-Ar), 135.2 (C-Ar), 134.4 (C-Ar), 134.4 (C-Ar), 134.3 (C-Ar), 134.1 (C-Ar), 134.0 (C-Ar), 130.6 (C-Ar), 130.5 (C-Ar), 130.4 (C-Ar), 130.3 (C-Ar), 129.9 (C-Ar), 128.5 (C-Ar), 118.6 (C-Ar), 117.7 (C-Ar), 40.7 (C-11), 21.5 (C-7); **IR** (film): ν_{max} 3055.9, 3019.4, 2825.3, 1727.3, 1586.9, 1485.2, 1438.1, 1342.1, 1110.7, 996.5, 864.4, 808.3, 749.7,

720.8, 688.3, 523.7 cm^{-1}; **ESI-MS**: *m/z* $C_{27}H_{24}OPS$ 427.1280, found 427.1271 (3.6 ppm error). The ^{1}H and ^{13}C NMR data were in agreement with the literature.[112]

S-*p*-tolyl 2-(triphenylphosphoranylidene) ethanethioate 248

Lab book: YT-8-16, NMR: c0071yth (YT-8-16)

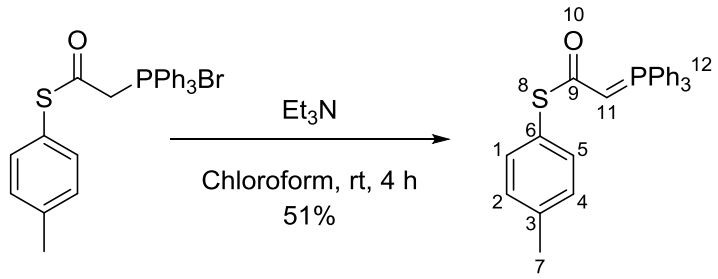

(2-oxo-2-(*p*-tolylthio)ethyl)triphenylphosphonium bromide **247** (133.80 mg, 0.26 mmol, 1.00 eq.) was dissolved in chloroform (1.3 mL, 0.20 M) under N_2 at room temperature, then triethylamine (0.12 mL, 87.02 mg, 0.86 mmol, 3.30 eq.) was added. After stirring for 4 hours, water (1.3 mL) was added and the aqueous phase was extracted with dichloromethane (3 x 5 mL) and the combined organic extracts were dried (magnesium sulfate), filtered and concentrated *in vacuo* to give S-*p*-tolyl 2-(triphenylphosphoranylidene) ethanethioate **248** as a colourless oil (57.14 mg, 51%). **^{1}H NMR** (400 MHz, $CDCl_3$): δ 7.79-7.09 (19H, m, H-Ar), 3.62 (1H, d, *J* = 22.2 Hz, H-11), 2.29 (3H, s, H-7). The ^{1}H NMR data was in agreement with the literature.[112]

(5*S,7*R**)-5-((benzyloxy)methyl)-2,2,3,3,9,9,10,10-octamethyl-7-(2-methylbut-3-en-2-yl)-4,8-dioxa-3,9-disilaundecane 249**

Lab book: YT-7-75-1, NMR: j6596yth (YT-7-75-1)

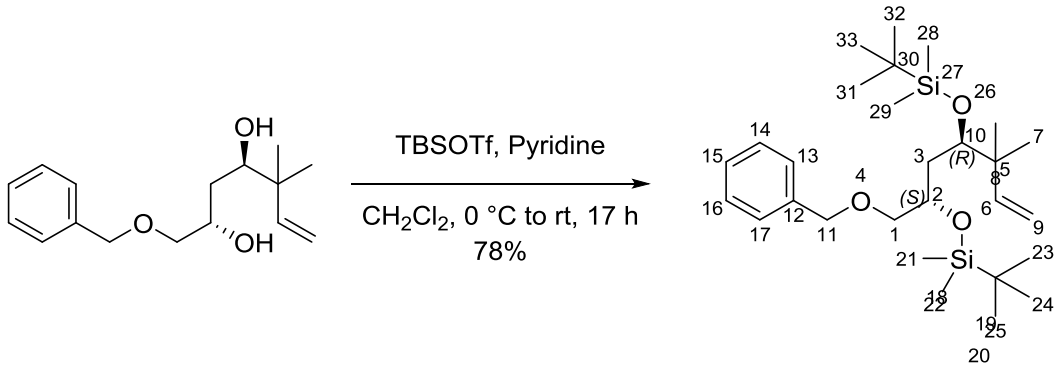

Diol **223** (327.90 mg, 1.24 mmol, 1.00 eq.) was dissolved in dry dichloromethane (12.0 mL, 0.10 M), then pyridine (0.50 mL, 490.42 mg, 6.20 mmol, 5.00 eq.) was added to the solution at 0 °C under N_2. After stirring for 20 minutes, TBSOTf (1.14 mL, 1.31 g, 4.96 mmol, 4.00 eq.) was added to the solution at 0 °C and then reaction was allowed to warm to room temperature. After stirring the reaction for 17 hours, the reaction mixture was quenched with saturated sodium bicarbonate solution (10 mL) and extracted with dichloromethane (3 x 10 mL). The organic phase was washed with copper(II) sulfate (3 x 10 mL) and brine (3 x 10 mL). The combined organic extracts were dried (magnesium sulfate), filtered and concentrated *in vacuo* to give a crude product, which was then purified by flash column chromatography on silica (1:5, ethyl acetate-hexane) to yield **249** as a yellow oil (456.5 mg, 78%). **^{1}H NMR** (400 MHz, $CDCl_3$): δ 7.36-7.25 (5H, m, H-Ar), 5.85 (1H, dd, *J* = 17.9, 10.5 Hz, H-6), 4.98 (1H, dd, *J* = 17.5, 1.5 Hz, H-9a), 4.94 (1H, dd, *J* = 10.5, 1.5 Hz, H-9b), 4.51 (2H, s, H-11), 4.00-3.94 (1H, m, H-2), 3.46 (1H, dd, *J* = 6.7, 4.4 Hz, H-10), 3.39 (1H, dd, *J* = 9.8, 4.0 Hz, H-1a), 3.35 (1H, dd, *J* = 9.8, 5.6 Hz, H-1b), 1.88-1.44 (2H, m, H-3), 0.96 (6H, s, H-7,

H-8), 0.89 (6H, s, H-23, H-24, H-25), 0.88 (6H, s, H-31, H-32, H-33), 0.08-0.05 (12H, m, H-21, H-22, H-28, H-29); **^{13}C NMR** (101 MHz, $CDCl_3$): 146.2 (C-6), 138.7 (C-12), 128.4 (C-Ar), 127.7 (C-Ar), 127.6 (C-Ar), 111.8 (C-9), 75.7 (C-10), 75.1 (C-1), 73.4 (C-11), 70.0 (C-2), 42.6 (C-5), 39.9 (C-3), 26.3 (C-20), 26.1 (C-30), 24.7 (C-7), 22.4 (C-8), 18.4 (C-23, C-24, C-25), 18.4 (C-31, C-32, C-33), −3.1 (C-21), −4.0 (C-22), −4.2 (C-28), −4.3 (C-29); **IR** (film): ν_{max} 2954.8, 2928.6, 2885.7, 2856.0, 1637.5, 1496.4, 1471.9, 1462.7, 1414.0, 1377.7, 1360.3, 1251.5, 1212.9, 1089.1, 1058.7, 1028.7, 1004.4, 973.2, 938.7, 911.6, 834.2, 807.5, 773.3, 7333.2, 696.4, 666.3, 611.5, 565.4, 462.2 cm^{-1}; **ESI-MS**: *m/z* $C_{28}H_{52}NaO_3Si_2$ [M+Na$^+$] 515.334719, found 515.333206 (3.3 ppm error).

(3*R,5*S**)-6-(benzyloxy)-3,5-bis((tert-butyldimethylsilyl)oxy)-2,2-dimethylhexanal**

243

Lab book: YT-8-12, NMR: j8794yth (YT-8-12)

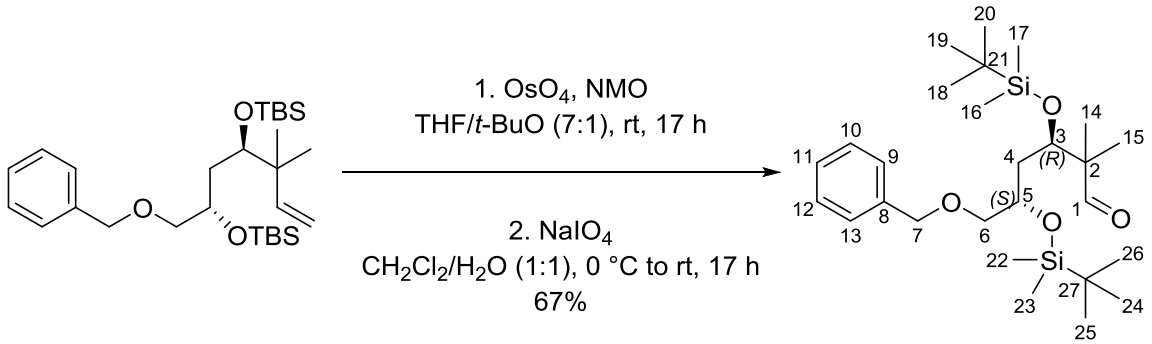

(5*S**,7*R**)-5-((benzyloxy)methyl)-2,2,3,3,9,9,10,10-octamethyl-7-(2-methylbut-3-en-2-yl)-4,8-dioxa-3,9-disilaundecane **249** (48.00 mg, 97.38 μmol, 1.00 eq.) and NMO (22.82 mg, 194.76 μmol, 2.00 eq.) were dissolved in a *tert*-butanol/THF (1:7, v/v, 2 mL) solvent mixture. Then osmium tetroxide (0.50 mg, 1.95 μmol, 0.02 eq.) was added to the reaction mixture under N_2 at room temperature and stirred for 17

hours. The reaction was diluted with dichloromethane and washed with sodium thiosulfate. The aqueous phase was extracted with dichloromethane (3 x 10 mL) and the combined organic extracts were dried (magnesium sulfate), filtered and concentrated *in vacuo* to give a crude product, which was then dissolved in water (1 mL) and dichloromethane (1 mL). Then sodium (meta)periodate (41.66 mg, 194.76 μmol, 2.00 eq.) was added to the solution at 0 °C and then reaction was allowed to warm to room temperature. After stirring the reaction for 17 hours, the reaction mixture was washed with brine (3 x 5 mL) and water (3 x 5 mL). The combined organic extracts were dried (magnesium sulfate), filtered and concentrated *in vacuo* to give (3*R**,5*S**)-6-(benzyloxy)-3,5-bis((tert-butyldimethylsilyl)oxy)-2,2-dimethylhexanal **243** as a yellow oil (32.40 mg, 67%). **^{1}H NMR** (400 MHz, $CDCl_3$): δ 9.54 (1H, s, H-1), 7.37-7.26 (5H, m, H-Ar), 4.52 (2H, s, H-7), 3.97-3.91 (2H, m, H-3, H-5), 3.43-3.37 (2H, m, H-6), 1.91-1.55 (2H, m, H-4), 1.05 (3H, s, H-14), 0.99 (3H, s, H-15), 0.89 (9H, s, H-18, H-19, H-20), 0.86 (9H, s, H-24, H-25, H-26), 0.08-0.06 (12H, m, H-16, H-17, H-22, H-23); **^{13}C NMR** (101 MHz, $CDCl_3$): 206.5 (C-1), 138.4 (C-8), 128.5 (C-Ar), 127.8 (C-Ar), 127.7 (C-Ar), 74.7 (C-6), 73.5 (C-7), 72.6 (C-3), 69.3 (C-5), 51.7 (C-2), 39.5 (C-4), 26.1 (C-18, 19, 20, 24, 25, 26), 19.1 (C-14), 18.3 (C-21), 18.3 (C-27), 17.5 (C-15), −3.3 (C-16), −4.2 (C-17), −4.3 (C-22), −4.4 (C-23); **IR** (film): ν_{max} 2954.1, 2928.2, 2855.8, 1727.2, 1471.6, 1361.1, 1253.1, 1092.3, 1005.0, 835.7, 808.9, 775.1, 733.8, 697.2 cm^{-1}; **ESI-MS**: *m/z* $C_{27}H_{50}NaO_4Si_2$ $[M+Na^+]$ 517.313984, found 517.313295 (2.1 ppm error).

S-(4-methylphenyl) ethanethioate 245

Lab book: YT-8-18-2, NMR: j9533yth (YT-8-18-2)

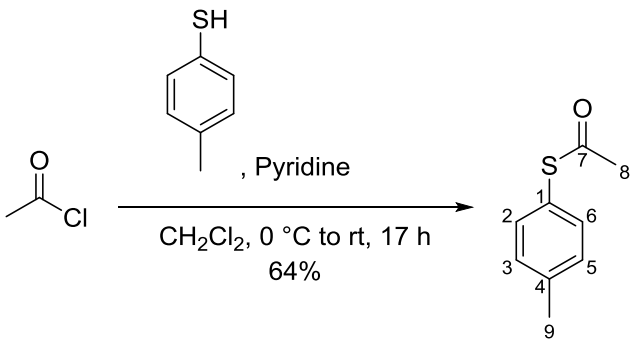

4-Methylbenzenethiol (1.30 g, 10.47 mmol, 1.00 eq.) was dissolved in dry dichloromethane (4 mL, 2.62 M) under N_2 at room temperature, then pyridine (0.85 mL, 818.18 mg, 10.47 mmol, 1.00 eq.) was added slowly at the same temperature and stirred for 30 minutes. The solution was then cooled down to 0 °C and acetyl chloride (0.74 mL, 817.18 mg, 10.47 mmol, 1.00 eq.) was added. After stirring for 30 minutes, the reaction was allowed to warm to room temperature. After stirring the reaction for 17 hours, the reaction mixture was quenched with water (4 mL) and washed with saturated sodium bicarbonate solution (4 mL). The aqueous phase was extracted with dichloromethane (3 x 10 mL) and the combined organic extracts were dried (magnesium sulfate), filtered and concentrated *in vacuo* to give a crude product which was then purified by flash column chromatography on silica (1:8, ethyl acetate-hexane) to give S-(4-methylphenyl) ethanethioate **245** (1.11 g, 64%). **^{1}H NMR** (400 MHz, $CDCl_3$): δ 7.31-7.21 (4H, m, H-Ar), 2.41 (3H, s, H-8), 2.38 (3H, s, H-9); **^{13}C NMR** (101 MHz, $CDCl_3$): 194.8 (C-7), 139.9 (C-Ar), 134.6 (C-Ar), 130.2 (C-Ar), 124.5 (C-Ar), 30.3 (C-8), 21.5 (C-9); **IR** (film): ν_{max} 3396.3, 3024.8, 2968.7, 2922.3, 2870.5,

1902.9, 1703.5, 1597.9, 1493.7, 1399.2, 1378.0, 1352.1, 1303.9, 1209.7, 1181.7, 1114.4, 1093.7, 1040.5, 1018.1, 949.4, 806.5, 704.3, 642.8, 609.5, 527.0, 507.2, 469.2 cm^{-1}; **ESI-MS**: *m/z* $C_{27}H_{50}NaO_4Si_2$ $[M+Na^+]$ 517.313984, found 517.313295 (2.1 ppm error). The ^1H and ^{13}C NMR data were in agreement with the literature.[162]

4.4. Experimental Procedures for Chapter three

4.4.1 The preparation of (*L*)-Proline benzyl ester

(*L*)-Proline benzyl ester 294

NMR: k5895yth

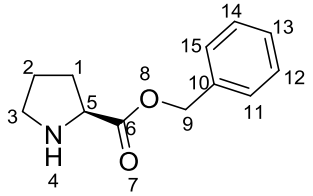

(*L*)-Proline benzyl ester hydrochloride (24.20 mg, 0.10 mmol) was washed with saturated sodium bicarbonate solution (2 mL) then extracted with chloroform (3 × 1 mL). The combined organic extracts were dried (magnesium sulfate), filtered and concentrated *in vacuo* to provide the free ester. (22.19 mg, 92%). **^{1}H NMR** (400 MHz, $CDCl_3$): δ 7.39-7.31 (5H, m, Ar), 5.16 (2H, s, H-9), 3.87 (1H, dd, *J* = 8.6, 5.7 Hz, CHNH), 3.14-2.93 (2H, m, NHCH), 2.21-2.12 (1H, m, NHCH).

4.4.2 General Procedure for the Preparation of Aldol Products

To a mixture of the pH 7 buffer solution (1 mL) and aldehyde (1.00 mmol) was added the corresponding ketone donor (1.00 mmol) followed by (*L*)-proline benzyl ester (0.10 mmol). After stirring for 5-24 hours, the reaction mixture was diluted with water (10 mL) and the aqueous phase was extracted with ethyl acetate (3 x 10 mL). The organic extracts were combined, dried (magnesium sulfate), filtered and concentrated *in vacuo* to give a crude product which was then purified by flash column chromatography to provide the aldol product.

2-[Hydroxy-(4-bromo-phenyl)-methyl]-cyclohexan-1-one 303

NMR: m7069yth

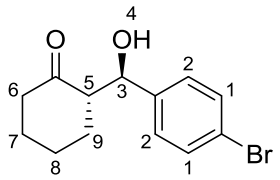

^{1}H NMR (400 MHz, $CDCl_3$): δ 7.49-7.45 (2H, m, H-1), 7.21-7.18 (2H, m, H-2), 4.75 (1H, dd, *J* = 8.7, 2.7 Hz, H-3), 3.98 (1H, d, *J* = 2.8 Hz, OH), 2.59-2.45 (1H, m, H-5), 2.39-2.31 (1H, m, H-6), 2.13-2.04 (1H, m, H-6), 1.83-1.78 (1H, m, H-9), 1.71-1.48 (5H, m, H-7, H-8, H-9). The enantiomeric excess was determined by HPLC with a Chiralcel AD-H column, *i*-PrOH:Hexane = 10:90, flow rate 0.8 mL/min, t_R = 18.36 min (minor), t_R = 21.91 min (major). The ^{1}H NMR data was in agreement with the literature.[163]

2-[Hydroxy-(4-chloro-phenyl)-methyl]-cyclohexan-1-one 304

NMR: m6244yth

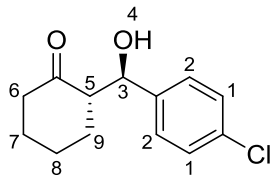

^{1}H NMR (400 MHz, $CDCl_3$): δ 7.33-7.30 (2H, m, H-1), 7.27-7.24 (2H, m, H-2), 4.76 (1H, dd, *J* = 8.7, 2.5 Hz, H-3), 3.99 (1H, d, *J* = 2.8 Hz, OH), 2.59-2.52 (1H, m, H-5), 2.51-2.45 (1H, m, H-6), 2.39-2.31 (1H, m, H-6), 2.13-2.06 (1H, m, H-7), 1.83-1.48 (5H, m, H-7, H-8, H-9). The enantiomeric excess was determined by HPLC with a Daicel Chiralpak AD column, *i*-PrOH:Hexane = 10:90, flow rate 0.5 mL/min, t_R = 27.37 min (minor), t_R =

31.94 min (major). The ^{1}H NMR data was in agreement with the literature.[164]

2-[Hydroxy-(2-chloro-phenyl)-methyl]-cyclohexan-1-one 307

NMR: m7712yth

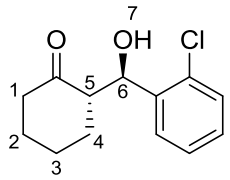

^{1}H NMR (400 MHz, $CDCl_3$): δ 7.54 (1H, dd, *J* = 7.7, 1.7 Hz, H-Ar), 7.37-7.28 (2H, m, H-Ar), 7.23-7.19 (1H, m, H-Ar), 5.35 (1H, dd, *J* = 8.1, 3.9 Hz, H-6), 4.03 (1H, d, *J* = 4.0 Hz, OH), 2.71-2.64 (1H, m, H-5), 2.49-2.44 (1H, m, H-1), 2.38-2.30 (1H, m, H-1), 2.12-2.05 (1H, m, H-2), 1.84-1.49 (5H, m, H-2, H-3, H-4). The enantiomeric excess was determined by HPLC with a Daicel Chiralpak OD column, *i*-PrOH:Hexane = 5:95, flow rate 0.8 mL/min, t_R = 12.08 min (major), t_R = 15.04 min (minor). The ^{1}H NMR data was in agreement with the literature.[164]

2-[Hydroxy-(2-nitro-phenyl)-methyl]-cyclohexan-1-one 308

NMR: m7107yth

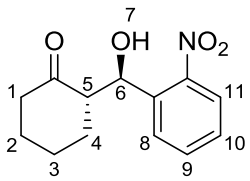

^{1}H NMR (400 MHz, $CDCl_3$): δ 7.85 (1H, dd, *J* = 8.2, 1.3 Hz, H-Ar), 7.77 (1H, dd, *J* = 7.9, 1.2 Hz, H-Ar), 7.64 (1H, td, *J* = 7.8, 1.3 Hz, H-Ar), 7.45-7.41 (1H, m, H-Ar), 5.45 (1H,

dd, *J* = 6.7, 3.4 Hz, H-6), 4.18 (1H, d, *J* = 4.3 Hz, OH), 2.79-2.72 (1H, m, H-5), 2.48-2.43 (1H, m, H-1), 2.38-2.29 (1H, m, H-1), 2.14-2.07 (1H, m, H-2), 1.88-1.83 (1H, m, H-2), 1.88-1.63 (4H, m, H-3, H-4). The enantiomeric excess was determined by HPLC with a Daicel Chiralpak OJ column, *i*-PrOH:Hexane = 5:95, flow rate 1.0 mL/min, t_R = 21.40 min (minor), t_R = 23.39 min (major). The ^{1}H NMR data was in agreement with the literature.[164]

2-[Hydroxy-phenyl-methyl]-cyclohexan-1-one 305

NMR: m6674yth

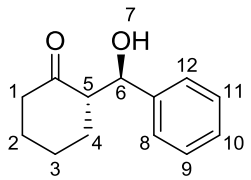

^{1}H NMR (400 MHz, $CDCl_3$): δ 7.38-7.27 (5H, m, H-Ar), 4.79 (1H, dd, *J* = 8.8, 2.3 Hz, H-6), 3.96 (1H, d, *J* = 2.7 Hz, OH), 2.65-2.58 (1H, m, H-5), 2.53-2.46 (2H, m, H-1), 2.40-2.28 (3H, m, H-2, H-3), 2.12-2.01 (3H, m, H-3, H-4). The enantiomeric excess was determined by HPLC with a Daicel Chiralpak OJ column, *i*-PrOH:Hexane = 10:90, flow rate 1.0 mL/min, t_R = 8.65 min (major), t_R = 10.44 min (minor). The ^{1}H NMR data was in agreement with the literature.[164]

2-[Hydroxy-(pyridin-4-yl)-methyl]-cyclohexan-1-one 310

NMR: m8227yth

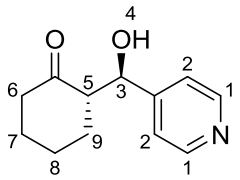

^{1}H NMR (400 MHz, $CDCl_3$): δ 8.64-8.55 (2H, m, H-1), 7.25-7.23 (2H, m, H-2), 4.77 (1H, d, *J* = 8.2 Hz, H-3), 4.03 (1H, br, OH), 2.62-2.55 (1H, m, H-5), 2.51-2.45 (1H, m, H-6), 2.42-2.31 (1H, m, H-6), 1.85-1.64 (6H, m, H-7, H-8, H-9). The enantiomeric excess was determined by HPLC with a Daicel Chiralpak AD column, *i*-PrOH:Hexane = 10:90, flow rate 1.0 mL/min, t_R = 22.76 min (minor), t_R = 24.80 min (major). ^{1}H NMR data was in agreement with the literature.[164]

2-[Hydroxy-(furan-2-yl)-methyl]-cyclohexan-1-one 309

NMR: m7330yth

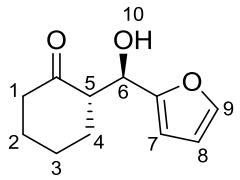

^{1}H NMR (400 MHz, $CDCl_3$): δ 7.38-7.37 (1H, m, H-9), 6.33-6.27 (2H, m, H-7, H-8), 4.82 (1H, d, *J* = 8.5 Hz, H-6), 3.90 (1H, br, OH), 2.94-2.87 (1H, m, H-5), 2.49-2.31 (2H, m, H-1), 1.84-1.58 (6H, m, H-2, H-3, H-4). The enantiomeric excess was determined by HPLC with a Daicel Chiralpak AD column, *i*-PrOH:Hexane = 10:90, flow rate 0.5 mL/min, t_R = 28.20 min (minor), t_R = 29.91min (major). The ^{1}H NMR data was in

agreement with the literature.[163]

4-[hydroxy-4-(4-nitrophenyl)]-butan-2-one 261

NMR: m9017yth

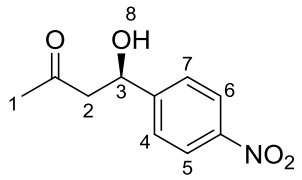

^{1}H NMR (400 MHz, $CDCl_3$): δ 8.12-8.09 (2H, m, H-5, H-6), 7.48 (2H, d, *J* = 8.7 Hz, H-4, H-7), 5.21 (1H, t, *J* = 6.1 Hz, H-3), 3.86 (1H, br, OH), 2.82 (2H, d, *J* = 6.6 Hz, H-2), 2.17 (3H, s, H-1). The enantiomeric excess was determined by HPLC with an AS-H column column, *i*-PrOH:Hexane = 30:70, flow rate 0.5 mL/min, t_R = 27.96 min (major), t_R = 34.65 min (minor). The ^{1}H NMR data was in agreement with the literature.[165]

5. Appendices

Chemical Science

EDGE ARTICLE

View Article Online
View Journal | View Issue

Cite this: *Chem. Sci.*, 2017, **8**, 482

The stereodivergent formation of 2,6-*cis* and 2,6-*trans*-tetrahydropyrans: experimental and computational investigation of the mechanism of a thioester oxy-Michael cyclization†

Kristaps Ermanis, Yin-Ting Hsiao, Uğur Kaya, Alan Jeuken and Paul A. Clarke*

The origins of the stereodivergence in the thioester oxy-Michael cyclization for the formation of 4-hydroxy-2,6-*cis*- or 2,6-*trans*-substituted tetrahydropyran rings under different conditions was investigated both computationally and experimentally. Synthetic studies showed that the 4-hydroxyl group was essential for stereodivergence. When the 4-hydroxyl group was present, TBAF-mediated conditions gave the 2,6-*trans*-tetrahydropyran and trifluoroacetic acid-mediated conditions gave the 2,6-*cis*-tetrahydropyran. This stereodivergence vanished when the hydroxyl group was removed or protected. Computational studies revealed that: (i) the trifluoroacetic acid catalysed formation of 2,6-*cis*-tetrahydropyrans was mediated by a trifluoroacetate-hydroxonium bridge and proceeded *via* a chair-like transition state; (ii) the TBAF-mediated formation of 2,6-*trans*-tetrahydropyrans proceeded *via* a boat-like transition state, where the 4-hydroxyl group formed a crucial hydrogen bond to the cyclizing alkoxide; (iii) both reactions are under kinetic control. The utility of this stereodivergent approach for the formation of 4-hydroxy-2,6-substituted tetrahydropyran rings has been demonstrated by the total syntheses of the anti-osteoporotic natural products diospongin A and B.

Received 4th August 2016
Accepted 26th August 2016

DOI: 10.1039/c6sc03478k

www.rsc.org/chemicalscience

Introduction

2,6-Disubstituted tetrahydropyran (THP) rings form key structural motifs in many potent biologically active natural products,[1] including the phorboxazoles,[2] lasonolide A,[3] the diospongins[4] and psymberin.[5] These biological activities and complex molecular frameworks have prompted a large amount of work aimed at increasing the efficiency of the syntheses of THP rings,[6] which, problematically, are often formed as mixtures of 2,6-*cis*- and 2,6-*trans*-diastereomers. One fundamental strategy regularly used for their formation is the oxy-Michael cyclization onto an α,β-unsaturated carbonyl group, which often leads to the formation of both possible diastereomeric THPs. Here, we report a stereodivergent oxy-Michael reaction which can lead to the diastereoselective formation of either the 2,6-*cis*- or the 2,6-*trans*-THP in up to 20 : 1 diastereoselectivity (Scheme 1). We have also conducted computational and experimental studies which elucidate the origin of this stereodivergence and show the importance of a H-bond between the 4-hydroxyl group and the cyclizing alkoxide in the oxy-Michael cyclization. These studies allow us to propose a general set of guidelines for future syntheses of 2,6-disubstituted THPs.

Previous studies have investigated oxy-Michael cyclizations in order to gain an understanding of the factors governing the stereoselectivity of the cyclization. This has led to the general opinion that the formation of the 2,6-*cis*-THP may be favored by performing an oxy-Michael reaction onto an α,β-unsaturated ester under thermodynamic conditions, while the 2,6-*trans*-THP may be favored by performing the same reaction under kinetically controlled conditions. In practice, the situation is not so straightforward. While 2,6-*trans*-THPs tend to be formed in good yields with moderate to good diastereoselectivities,[11] the higher temperatures and longer reaction times required for the

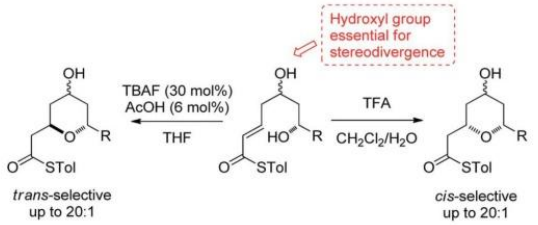

Scheme 1 The stereodivergent thioester oxy-Michael cyclization.

Department of Chemistry, University of York, Heslington, York, North Yorkshire, YO10 5DD, UK. E-mail: paul.clarke@york.ac.uk

† Electronic supplementary information (ESI) available: Experimental procedures, compound characterization data and details of the computational studies. See DOI: 10.1039/c6sc03478k

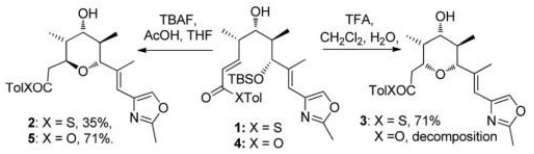

Scheme 2 Stereodivergence in the thioester oxy-Michael cyclization to form the C20–C32 fragment of the phorboxazoles.

formation of the 2,6-*cis*-THP ring often result in lower diastereoselectivities and yields.[12] The origin of this moderate 2,6-*trans*-selectivity is generally accepted as arising from better orbital overlap in the transition state of the kinetic cyclization leading to the 2,6-*trans*-THP compared to the 2,6-*cis*-THP.[8] Although there is no generally accepted mechanism for the acid-mediated cyclization, it has been proposed that the formation of the 2,6-*cis*-THP is favored due to greater stereoelectronic stabilization of the transition state from both the FMO coefficients of the allylic cation and orbital overlap with the oxygen lone pair, compared to the transition state leading to the 2,6-*trans*-THP.[9]

In our studies on the synthesis of the C20–C32 pentasubstituted tetrahydropyran core of the phorboxazoles we encountered an occurrence of stereodivergence[13] while utilizing thioesters as electophiles in an oxy-Michael cyclization.[14] In this case, stereodivergence occurred when the conditions for the deprotection of a TBS-ether were changed. Deprotection of **1** with AcOH buffered TBAF led to the formation of the 2,6-*trans*-THP **2** with no trace of **3** being detected. However, deprotection with TFA resulted in the formation of the 2,6-*cis*-THP product **3** in >13 : 1 selectivity (Scheme 2). It is worth noting that when the conventional oxoester **4** was submitted to these conditions the 2,6-*trans*-THP **5** resulted from treatment with TBAF buffered with AcOH in THF; no trace of the *cis*-diastereomer was seen. However, only decomposition occurred when **4** was treated with TFA.[13] Intrigued by these results, especially by the dramatic change in diastereoselectivity seen in the thioester substrate, we resolved to carry out synthetic and computational studies to elucidate the mechanistic origins of this stereodivergence and to establish more general synthetic guidelines for the diastereoselective synthesis of 2,6-disubstituted THPs. The results of these studies are reported in this paper.

Results and discussion

Synthetic investigation into the generality of stereodivergence

We initially decided to probe whether the stereodivergence was specific to **1** or whether it was a more general phenomenon. To this end we synthesized cyclization substrates **6a–c**, which had the same relative configuration as **1** and **9a–c**, which had the opposite relative configuration.[15] Each substrate was submitted to both the buffered TBAF and the TFA mediated conditions (Tables 1 and 2).

Substrates **6a**, **b**, **c**, which contain the 4-hydroxyl group were submitted to both the TBAF-mediated and the Brønsted acid promoted cyclization conditions (Table 1). In this case, TBAF mediated reactions smoothly generated 2,6-*trans*-THP products **7a–c** in good yields and with excellent selectivity (with the exception of **6c**), while Brønsted acid promoted conditions gave the 2,6-*cis*-THP products **8a–c** with excellent selectivity and in good yields. In the case of the phenyl substituted compound **6b**, the TFA conditions led to decomposition although the CSA conditions led to 2,6-*cis*-THP product being isolated in 74% yield.

Diastereomeric diol substrates **9a**, **b**, **c** were studied next (Table 2). Once again, TBAF-mediated cyclizations generated the 2,6-*trans*-THP predominantly. As before, Brønsted acid promoted conditions gave the 2,6-*cis*-THP products **11a–c** with excellent selectivity and in good yields. In the case of **9b** (R = Ph), CSA promoted conditions had to be used to avoid

Table 1 Stereodivergent oxy-Michael cyclizations of 4-hydroxyl-containing substrates **6a**, **b** and **c**

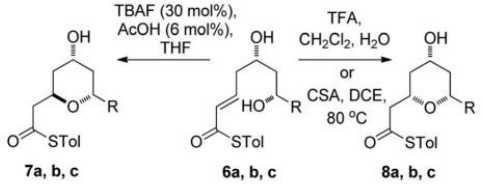

Entry	Ratio *cis* : *trans*[a]	TBAF yield[b] (%)	R	TFA/CSA[b] yield (%)	Ratio *cis* : *trans*[a]
a	1 : 7	69	iPr	66[c]	20 : 1
b	1 : 6	40	Ph	74[d]	10 : 1
c	2 : 3	41	C_7H_{14}	47[c]	20 : 1

[a] Ratios obtained from integration of ^{1}H NMR signals. [b] Isolated yields after chromatography. [c] TFA, CH_2Cl_2, H_2O. [d] CSA, DCE, 80 °C.

Table 2 Stereodivergent oxy-Michael cyclizations of 4-hydroxyl-containing substrates **9a**, **b** and **c**

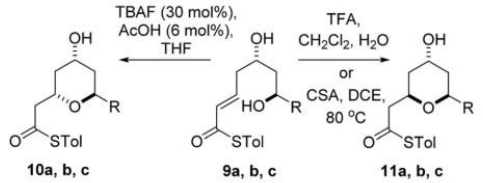

Entry	Ratio *cis* : *trans*[a]	TBAF yield[b] (%)	R	TFA/CSA yield[b] (%)	Ratio *cis* : *trans*[a]
a	1 : 8	69	iPr	66[c]	20 : 1
b	1 : 20	40	Ph	74[d]	7 : 1
c	1 : 20	48	C_7H_{15}	65[c]	20 : 1

[a] Ratios obtained from integration of ^{1}H NMR signals. [b] Isolated yields after chromatography. [c] TFA, CH_2Cl_2, H_2O. [d] CSA, DCE, 80 °C.

decomposition under TFA conditions. Thus it would appear that the stereodivergence seen in the cyclization of **1** is not limited to that particular system.

In order to ascertain if the reactions were under thermodynamic control 2,6-*cis*-substrate **11b** was submitted to the TBAF conditions and found to be unchanged after several hours and 2,6-*trans*-substrate **10b** was submitted to the Brønsted acid conditions and was also re-isolated unchanged. These results imply that both the TBAF and TFA-mediated reactions are *not* under thermodynamic control.

Computational studies on the stereodivergence

With stereodivergent behavior being exhibited by all the substrates investigated, we decided to conduct DFT studies in order to elucidate the origin of this behaviour. DFT investigations were conducted on both the buffered TBAF-mediated reaction which produced the 2,6-*trans*-THPs **2**, **7a–c** and **10a–c** and the TFA-mediated reactions which produced 2,6-*cis*-THPs **3**, **8a–c** and **11a–c**. Conformation searches were conducted at the molecular mechanics level and using MacroModel and MMFF force field.[16] DFT geometries were optimized and energies calculated using the B3LYP density functional,[17] and split-valence polarized 6-31G*+ basis set with diffuse functions.[18] Geometries were first optimized in gas-phase and afterwards in the solvent indicated using PBF solvent model.[19]

Fluoride-mediated cyclization

As all of the TBAF-mediated reactions were *trans*-selective we initially chose to model the cyclization of **6a** to **7a** (Scheme 3). We rationalized that the active molecule is the alkoxide **12**, which then attacks the conjugate double bond to form either the enolate of the 2,6-*trans*-THP **13** or of 2,6-*cis*-THP **14**. The enolates can be formed as either E or Z-isomers. Since the interconversion would likely be slow, the enolate geometry should be determined by the thioester conformation (*s-cis* or *s-trans*) in the transition state.

With this in mind, a thorough search for the transition states leading to the four possible enolates **E-13**, **Z-13**, **E-14**, **Z-14** was conducted. Several transition states leading to each of the enolates were found, lowest energy of which are shown in Fig. 1. Notably, the conformations of the lowest energy TSs were boat-like instead of the more common chair-like conformation. A strong intramolecular hydrogen bond between the 4-hydroxyl and the alkoxide stabilizes this conformation and makes it more favourable.[20,21]

Alternative chair-like transition states leading to both products were also found and are shown in Fig. 1. These, however, are significantly higher in energy, and therefore not significant.

E-transition states are lower than the corresponding Z-transition states, but the differences are not large. Similarly, the Z-thioenolates **Z-13** and **Z-14** are higher in energy than E-thioenolates because of the increased steric interactions. Once the product is formed, the boat conformation is no longer favourable and the THP thioenolates relax to the chair conformations, all of which were calculated to be lower in energy by 2–4 kcal mol^{-1}.

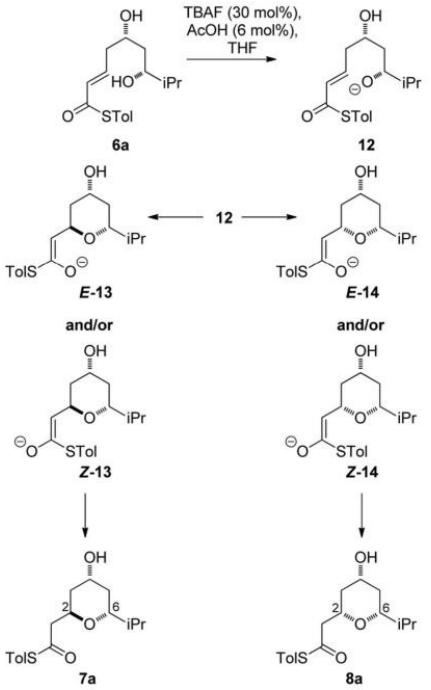

Scheme 3 Mechanistic considerations for the TBAF cyclization.

While normal ester enolates are much more basic than alkoxides, thioester enolate pK_a is much lower and comparable to alkoxides.[22] It is therefore not surprising that the E-thioenolates and the 4-alkoxides were found to be quite similar in energy. For the 2,6-*trans*-substrate the reaction end point before reprotonation would be the E-enolate, with the alkoxide being 1.5 kcal mol^{-1} higher in energy. For the 2,6-*cis*-substrate the 4-alkoxide is favoured over the E-thioenolate by 1.6 kcal mol^{-1}. The overall thermodynamic product of the reaction should be the 2,6-*cis*-4-alkoxide, which is 0.5 kcal mol^{-1} lower in energy than the 2,6-*trans*-E-thioenolate. This adds further support to kinetic control in this reaction, because the major observed product is the 2,6-*trans*-THP.

Using all of this information a reaction energy profile was constructed (Fig. 2). The barrier for the forward reaction is 9.1 kcal mol^{-1} for the 2,6-*trans*-product and 10.4 kcal mol^{-1} for the 2,6-*cis*-product. Both are very low and are consistent with the observed speed of the reaction, which is usually complete in less than 10 minutes at or below room temperature. For the reverse reaction, the total energy barrier is 14.4 kcal mol^{-1}, making it several orders of magnitude slower. This clearly shows that the reaction is under kinetic control, which matches experimental observations. Therefore the activation energies for the diastereomeric pathways are also determining the diastereoselectivity of the reaction. The 2,6-*trans*-boat transition state is 1.3 kcal mol^{-1} lower than the 2,6-*cis*-boat transition state, matching the observed diastereoselectivity well. One possible

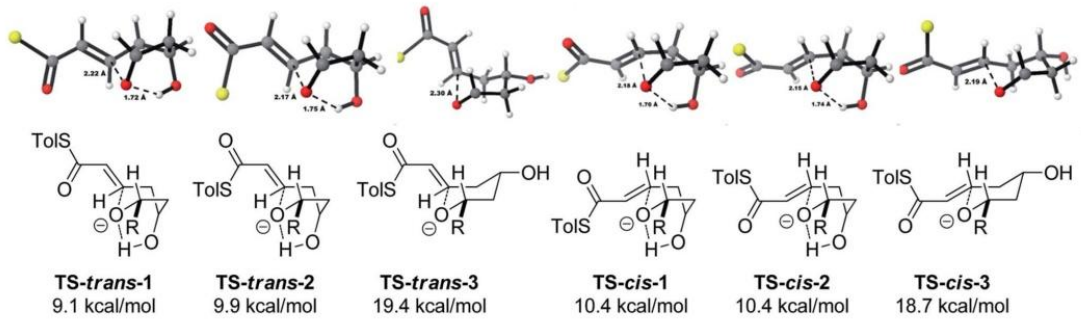

Fig. 1 Transition states for the TBAF mediated cyclization. Activation enthalpies calculated in THF implicit solvent model and shown relative to the ground state conformation of alkoxide **12**. Tolyl and iPr groups omitted for clarity.

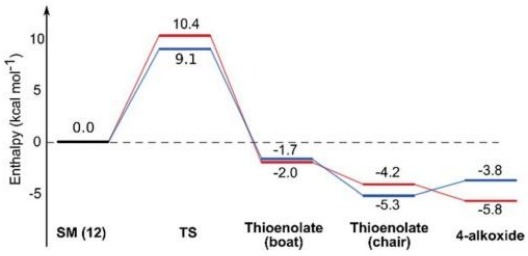

Fig. 2 Energy diagram for the TBAF mediated lowest energy pathways to the 2,6-*trans* **7a** (blue) and 2,6-*cis* **8a** (red). Enthalpies calculated in THF implicit solvent model and are relative to the ground state conformation of alkoxide **12**.

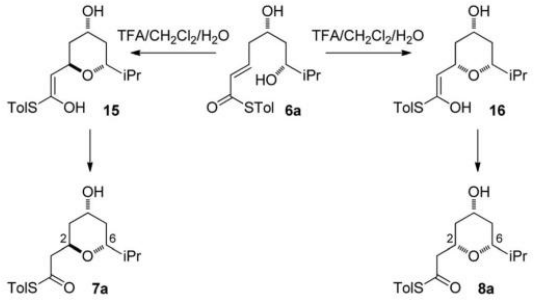

Scheme 4 Mechanistic considerations for the acid-mediated cyclization.

reason for this energy difference is the semi-eclipsed interaction of the β and γ-hydrogen atoms of the α,β-unsaturated thioester. This is present in the **TS-*cis*-1** (dihedral angle 37°), but not in the **TS-*trans*-1** (dihedral angle 161°). Another contributing factor would be the increased steric clash in the **TS-*cis*-1** from a pseudo-1,3-diaxial interaction between the protons at the 2- and 6- positions in the forming ring. This interaction is absent in the *trans*-transition states, but could be particularly pronounced in the *cis*-transition states because the protons are pointing slightly towards each other to allow the alkoxide attack from a favourable trajectory.

Acid-mediated cyclization

With an explanation in hand for the *trans*-selectivity of the buffered TBAF-mediated reaction we turned our attention to the TFA-mediated *cis*-selective cyclization reaction (Scheme 4). As shown by Fuwa and ourselves in interconversion experiments, the process is likely to be under kinetic control.[13,14] Therefore a simple thermodynamic preference for the 2,6-*cis*-diastereomers is not an adequate explanation for the observed stereoselectivity.

Currently there is no generally accepted mechanism for the acid mediated oxy-Michael cyclization. Based on studies by Houk,[8a] Fuwa proposed an allylic cation type mechanism[23] (Scheme 5), although no further experimental evidence to support this proposal has been reported.

Firstly, the viability of the allylic carbocation mechanism was tested by DFT calculations. When the lowest energy conformations of the cyclized intermediates **18** and **19** were submitted to geometry optimization at the DFT level, the THP rings opened back up during the process. This implies that there is no energy barrier for the opening of the ring and that the protonated cyclized intermediates **18** and **19** are unstable. Therefore it is highly unlikely that a simple protonation is the mechanism for the acid catalysis in this reaction. This mechanism would also provide little room to explain the different levels of diastereoselectivity achieved by the use of different acids as reported by Fuwa.[14]

Other potential modes of activation were then explored (Fig. 3). Among the mechanisms identified were two where TFA acts as

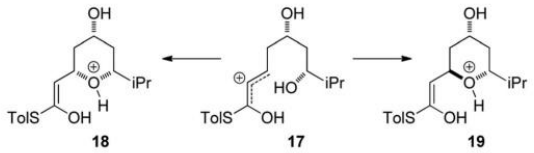

Scheme 5 Allylic cation mechanism.

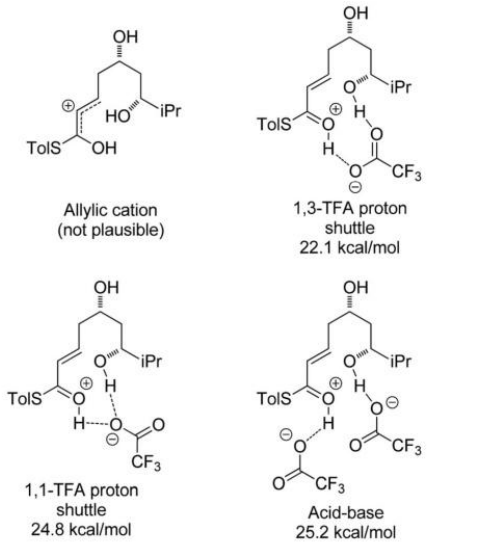

Fig. 3 Possible activation modes in TFA mediated cyclization. Enthalpies shown are the activation enthalpies calculated in gas phase relative to the corresponding starting material-TFA complex ground state conformation.

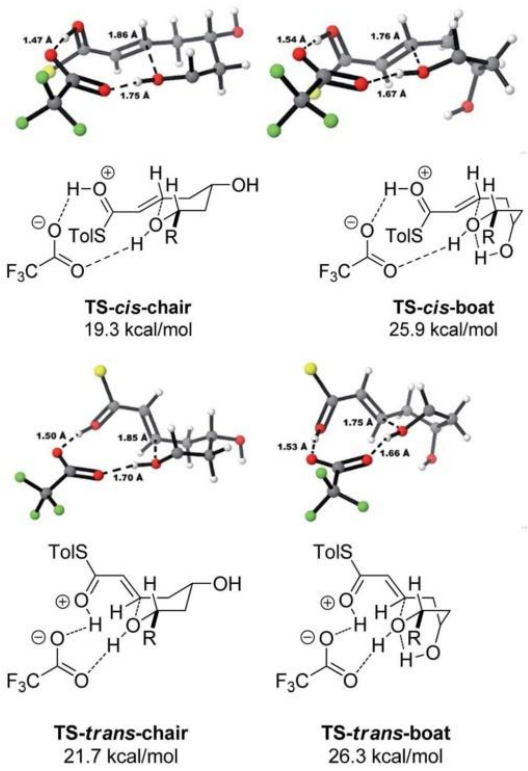

Fig. 4 Transition states for the TFA mediated cyclization. Activation enthalpies calculated in DCM implicit solvent model and shown relative to the ground state conformation of diol **7a** complex with TFA. Tolyl and iPr groups omitted for clarity.

proton shuttle, protonating the thioester and deprotonating the alcohol almost simultaneously. Another potential mechanism requires two different molecules of TFA, one of which acts as an acid and protonates the thioester and the other one acts as a base and deprotonates the alcohol nucleophile during the attack. Of these three mechanisms the 1,3-TFA proton shuttle mechanism was calculated to have the smallest activation energy, and the rest of the computational study focused on investigating it.

A thorough search for transition states leading to the two diastereomeric enols **15** and **16** revealed several chair- and boat-like transition states, of which the lowest energy ones are shown in Fig. 4. Because the TFA proton shuttle imposes a distance constraint between the alcohol and the thioester carbonyl group, only the transition states leading to the E-enols **15** and **16** are possible. The activation enthalpies were calculated to be 19.3 kcal mol^{-1} for the 2,6-*cis*-chair-like transition state and 21.7 kcal mol^{-1} for the 2,6-*trans*-chair-like transition state. **TS-*cis*-chair** is 1.9 kcal mol^{-1} lower in energy, consistent with the observed diastereoselectivity. The higher energy of the *trans*-transition state appears to be caused by an increased pseudo-1,3-diaxial steric clash between the 6-proton and the 2-thioester substituent. This interaction is not present in the *cis*-transition state. In all of the transition states, there are two hydrogen bonds between the TFA anion and the alcohol, and between the TFA anion and the protonated thioester. This allows the TFA to act as a proton shuttle and to simultaneously improve the electrophilicity of the thioester and the nucleophilicity of the alcohol.

In contrast with the TBAF case, the 4-hydroxyl group is not directly involved in the stabilization of the transition state, and the boat-like transition states are both some 5 kcal mol^{-1} higher in energy than the corresponding chair-like transition states. Calculations also *confirmed kinetic control* in this reaction, as the activation energy of the reverse reaction is 8.4 kcal mol^{-1} higher than the forward reaction (Fig. 5).

Synthetic investigation of the role of the 4–OH group

As the computational studies had implicated the 4-hydroxyl as the source of the stereodivergence, it was decided to test this hypothesis on a number of substrates. Substrates chosen for study were **20a**, **20b** and **20c**, which did not have the 4-hydroxyl group present and a substrate where the hydroxyl group was protected as a methyl ether **22**.

When TFA was used the cyclization of **20a**, **b**, **c** proceeded smoothly to form the 2,6-*cis*-THP products **21a**, **b**, **c** in moderate to good yields and with reasonable diastereoselectivities, however, the products of the TBAF mediated cyclization reactions were also the 2,6-*cis*-THP **21a**, **b**, **c** and were formed with even higher diastereoselectivity than under the TFA-mediated reaction conditions (Table 3).

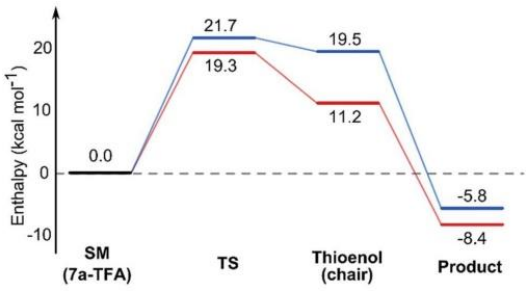

Fig. 5 Energy diagram for the TBAF mediated lowest energy pathways to the 2,6-*cis* **9a** (red) and 2,6-*trans* **8a** (blue). Enthalpies calculated in DCM implicit solvent model and are relative to the ground state conformation of **7a** complex with TFA.

The final substrate studied was where the 4-hydroxyl group was capped as a methyl ether **22** (Scheme 6). Cyclization precursor **22** was subjected to both sets of cyclization conditions. While the TFA-mediated conditions yielded the *cis*-diastereomer **23** cleanly, the TBAF-mediated conditions proceeded very slowly, with substantial hydrolysis of the thioester. However, despite this ^{1}H NMR analysis of the crude reaction mixture showed that only the *cis*-product **23** had been formed, confirming our hypothesis and previous results that a hydrogen-bond donor in the 4-position is required for the formation of the 2,6-*trans*-diastereomer under buffered TBAF-mediated conditions. The results of these synthetic studies are in complete agreement with the predictions of the computational studies. The computational studies showed that chair-like transition states in the TBAF-mediated reaction would provide the reverse diastereoselectivity with the 2,6-*cis*-chair TS being 1.5 kcal mol^{-1} lower in energy than the 2,6-*trans*-chair TS. This explains why the 2,6-*trans* selectivity is not observed in the 4-dehydroxy substrates **20a–c** and the methyl ether **22**, because

Table 3 Cyclization of substrates without the 4-hydroxyl

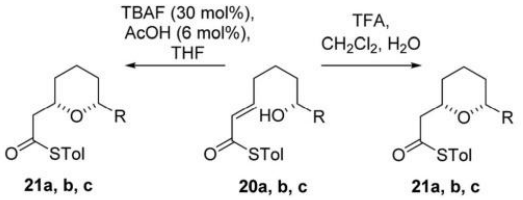

Entry	Ratio *cis* : *trans*[a]	TBAF yield[b] (%)	R	TFA yield[b] (%)	Ratio *cis* : *trans*[a]
a	>20 : 1	27	iPr	47	4 : 1
b	>20 : 1	53	Ph	56	8 : 1
c	>20 : 1	25	C_7H_{15}	36	5 : 1

[a] Ratios obtained from integration of ^{1}H NMR signals. [b] Isolated yields after chromatography.

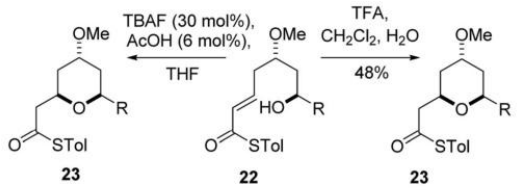

Scheme 6 Cyclization of methyl ether **23**.

in those cases there is no way of stabilizing the boat-like TS and the chair-like transition state would be more favoured, giving the 2,6-*cis* products.

Differences in the reactivity of thioester 1 and oxoester 4

With explanations for the origins of the stereodivergence in the cyclization reactions, the last remaining question for the computational study was the dramatic difference in the reactivity of thioester **1** and oxoester **4** in this oxy-Michael cyclization. Only the 2,6-*cis*-pathways were investigated as we were primarily interested in the reactivity of the substrate: thioester **1** cyclised to the 2,6-*cis*-THP whereas oxoester **4** decomposed. We identified a similar transition state for the oxoester as in the case of thioester, however, the energy profile of the reaction showed a much higher transition state energy for oxoester. This difference of 7.6 kcal mol^{-1} compared to the thioester would make the oxoester cyclization much slower. The slower cyclization would allow for competing decomposition reactions to dominate. One possible decomposition pathway is that the potentially acid sensitive styrenyl alcohol's ionization competes with conjugate addition under the Brønsted acid conditions. The transition state geometries of the thioester and oxoester cyclizations are very similar and therefore it appears very unlikely that steric effects would be the cause for the dramatic difference. An alternative cause would be the differences in the electronic structure; that the oxoester **4** is a less efficient electrophile than the thioester **1**, which would manifest itself in the LUMOs of the substrates.

Two very similar low lying conformations of the thioester-TFA and the oxoester-TFA complex were compared (Fig. 6). The electron density distribution is very similar for both substrates but the energy for the thioester-TFA complex LUMO is −1.43 eV and −1.06 eV for the oxoester-TFA complex. While this difference is relatively small, it is significant and shows that the sulfur atom makes the LUMO more accessible for nucleophiles.

A possible explanation for the difference in the LUMO energies between thioesters and oxoesters might be that sulfur lone pair (in sp3 orbital made up from a contribution of the 3p orbitals) has a smaller overlap with the C=O π* orbital of the ester than the oxygen lone pair (in sp3 orbital made up from a contribution of the 2p orbitals). This would have the effect of making the thioester electrophile more enone-like and more electrophilic in comparison with the α,β-unsaturated oxoester,[24] this reactivity profile has recently been reported in an

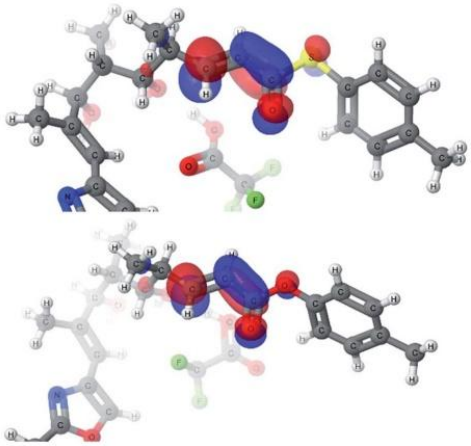

Fig. 6 LUMOs of the thioester-TFA complex (top) and oxoester-TFA complex (bottom).

intramolecular oxy-Michael cyclization onto an enone *versus* an α,β-unsaturated oxoester.[10a]

Stereodivergent synthesis of diospongins A and B

We realized that compounds **10b** and **11b**, the products of the stereodivergent oxy-Michael reactions of **9b**, were possible precursors to the natural products diospongins B and A respectively. Diospongins A and B are members of the biaryl heptanoid class of natural products and have been reported to exhibit anti-osteoporotic activity.[4] There have been several syntheses of these molecules,[25] but none to date have exploited the potential for a stereodivergent synthesis from a common precursor, and so we sought to showcase the stereodivergent oxy-Michael reaction with a synthesis of both these natural products. In theory both diospongin A and B could be accessed in one step from these precursors by a Liebeskind–Srogl type coupling reaction of the thioester with phenyl boronic acid under Pd-catalysis.[26,14a] Indeed this reaction was successfully employed in the synthesis of diospongin A **25**, from **11b** in 75% yield (Scheme 7). However, application of the same conditions to **10b** resulted only in re-isolation of starting material. Despite the investigation of several different solvents, temperatures and catalyst loadings and ligands we were unable to get **10b** to react. Application of the alternative Liebeskind organostannane conditions[27] also resulted in no reaction taking place. We are unable to explain this lack of reactivity for the 2,6-*trans*-diastereomer **10b** at this time. We therefore had to adopt an alternative strategy for the conversion of the thioester to the desired phenyl ketone. Tetrahydropyran-4-ol **10b** was instead treated with PhLi at −78 °C and warmed to RT overnight, which did give diospongin B **24** in 52% yield (Scheme 7). Spectroscopic data of both diospongins were identical to those reported previously in the literature.[25] This marks the first syntheses of these diastereomeric natural products using a stereodivergent process from the same common precursor.

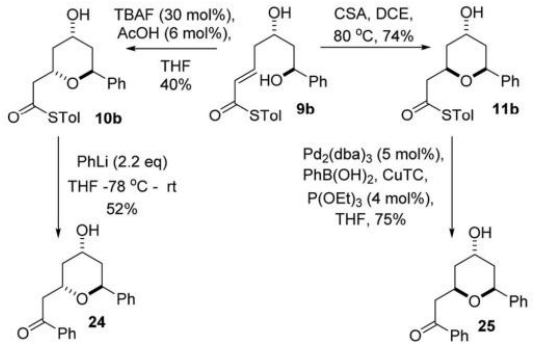

Scheme 7 Stereodivergent synthesis of diospongins A and B.

Conclusions

A stereodivergence was observed in the oxy-Michael reaction of α,β-unsaturated thioesters to form THP rings. These THP rings are present in a large number of structurally complex and biologically active natural products. Computational investigations of this stereodivergence indicated that it resulted from the participation of the 4-hydroxyl group in a hydrogen bond with the cyclising alkoxide which enforced a boat-like transition state in the buffered TBAF mediated reaction which led to the 2,6-*trans*-THP product. The Brønsted acid mediated reaction had no such interaction and proceeded through a chair-like transition state to generate the 2,6-*cis*-THPs. These computational studies suggested that *both reactions were under kinetic control*. Synthetic studies confirmed these computational predictions. When the 4-hydroxyl group was present the substrates exhibited stereodivergent reaction pathways under the reaction conditions. However, when the 4-hydroxyl group was removed or protected no stereodivergence was seen. These results allow us to suggest guidelines for the future diastereoselective synthesis of 2,6-disubstituted THPs.

- Use α,β-unsaturated thioesters: they are more reactive in cyclizations than α,β-unsaturated oxoesters.
- For the formation of 2,6-*cis*-THPs use a Brønsted acid promoted cyclization.
- For the formation of 2,6-*trans*-THPs, a 4-hydroxyl group is essential in a buffered TBAF promoted cyclization.

The utility of these guidelines and the stereodivergent oxy-Michael reaction was further demonstrated by the stereodivergent synthesis of the anti-osteoporotic natural products diospongin A and B from a common precursor.

In summary, we have used a combined computational and experimental approach to develop a robust and simple procedure for the synthesis of 4-hydroxy-2,6-*cis*- and 4-hydroxy-2,6-*trans*-THP rings and elucidated the mechanism of this stereodivergence. We believe this knowledge will be extremely useful for those seeking to synthesize functionalized THP rings in high yields and with high selectivities in the context of natural product synthesis.

Acknowledgements

We acknowledge the University of York, Department of Chemistry's Wild Fund (K. E. and Y.-T. H) and the EU's ERASMUS + program (U. K.) for financial support.

Notes and references

1 (*a*) N. M. Nasir, K. Ermanis and P. A. Clarke, *Org. Biomol. Chem.*, 2014, **12**, 3323; (*b*) K. W. Armbrust, M. G. Beaver and T. F. Jamison, *J. Am. Chem. Soc.*, 2015, **137**, 6941; (*c*) B. A. Loy, A. B. Lesser, D. Staveness, K. L. Billingsley, L. Cegelski and P. A. Wender, *J. Am. Chem. Soc.*, 2015, **137**, 3678; (*d*) B. M. Trost, C. E. Stivala, K. L. Hull, A. Huang and D. R. Fandrick, *J. Am. Chem. Soc.*, 2014, **136**, 88; (*e*) H. Kraus, A. Français, M. O'Brien, J. Frost, A. Diéguez-Vázquez, A. Polara, icordi, R. Horan, D.-S. Hau, T. Tsunoda and S. V. Ley, *Chem. Sci.*, 2013, **4**, 1989.

2 P. A. Searle and T. F. Molinski, *J. Am. Chem. Soc.*, 1995, **117**, 8126.

3 P. A. Horton, F. E. Koehn, R. E. Longley and O. J. McConnell, *J. Am. Chem. Soc.*, 1994, **116**, 6015.

4 J. Yin, K. Kouda, Y. Tezuka, Q. Le Tran, T. Miyahara, Y. Chen and S. Kadota, *Planta Med.*, 2004, **70**, 54.

5 F. A. Cichewicz and P. Crews, *Org. Lett.*, 2004, **6**, 1951.

6 (*a*) M. A. Perry, S. D. Rychnovsy and N. Sizemore, *Synthesis of Saturated Oxygen Heterocycles I, Topics in Heterocyclic Chemistry 35*, ed. J. Cossy, Springer-Verlag, Berlin, Heidelberg, 2014, pp. 43–95; (*b*) R. J. Beattie, T. W. Hornsby, G. Craig, M. C. Galan and C. L. Willis, *Chem. Sci.*, 2016, **7**, 2743; (*c*) H. Faustino, I. Varela, J. Mascareñas and F. López, *Chem. Sci.*, 2015, **6**, 2903; (*d*) Y. Xie and P. E. Floreancig, *Chem. Sci.*, 2011, **2**, 2423.

7 (*a*) For a review see: C. F. Nising and S. Bräse, *Chem. Soc. Rev.*, 2012, **41**, 988; (*b*) For an example in the synthesis of aspergillide A and B see: M. Kanematsu, M. Yoshida and K. Shishido, *Angew. Chem., Int. Ed.*, 2011, **50**, 2618.

8 (*a*) M. G. Banwell, C. T. Bui, H. T. T. Pham and G. W. Simpson, *J. Chem. Soc., Perkin Trans. 1*, 1996, 967; (*b*) J. M. Betancourt, V. S. Martín, J. M. Padrón, J. M. Palazón, M. A. Ramírez and M. A. Soler, *J. Org. Chem.*, 1997, **62**, 4570; (*c*) M. A. Ramírez, J. M. Padrón, J. M. Palazón and V. S. Martín, *J. Org. Chem.*, 1997, **62**, 4584; (*d*) M. G. Banwell, B. D. Bissett, C. T. Bui, H. T. T. Pham and G. W. Simpson, *Aust. J. Chem.*, 1998, **51**, 9; (*e*) C. Schneider and A. Schuffenhauer, *Eur. J. Org. Chem.*, 2000, 73; (*f*) K. N. Houk, M. N. Paddon-Row, N. G. Rondan, Y.-D. Wu, F. K. Brown, D. C. Spellmeyer, J. T. Metz, Y. Li and R. J. Loncharich, *Science*, 1986, **231**, 1108.

9 (*a*) K. N. Houk and R. W. Strozier, *J. Am. Chem. Soc.*, 1973, **95**, 4094; (*b*) J. L. Jensen and D. J. Carré, *J. Org. Chem.*, 1974, **39**, 2103; (*c*) J. L. Jensen and A. T. Thibeault, *J. Org. Chem.*, 1977, **42**, 2168.

10 (*a*) For computational and synthetic studies on an intramolecular system see: T. P. A. Hari, B. I. Wilke, J. A. Davey and C. N. Boddy, *J. Org. Chem.*, 2016, **81**, 415; (*b*) In a spiroketal system see: Y. Y. Khomutnyk, A. J. Arguelles, G. A. Winschel, Z. Sun, P. M. Zimmerman and P. Nagorny, *J. Am. Chem. Soc.*, 2016, **138**, 444.

11 (*a*) K. Lee, H. Kim and J. Hong, *Org. Lett.*, 2011, **13**, 2722; (*b*) S. R. Byeon, H. Park, H. Kim and J. Hong, *Org. Lett.*, 2011, **13**, 5816; (*c*) W. J. Buffham, N. A. Swain, S. L. Kostiuk, T. P. Goncalves and D. C. Harrowven, *Eur. J. Org. Chem.*, 2012, 1217; (*d*) S. Athe, B. Chandrasekhar, S. Roy, T. K. Pradhan and S. Ghosh, *J. Org. Chem.*, 2012, **77**, 9840.

12 (*a*) M. Ball, B. J. Bradshaw, R. Dumeunier, T. J. Gregson, S. MacCormick, H. Omori and E. J. Thomas, *Tetrahedron Lett.*, 2006, **47**, 2223; (*b*) I. Paterson and L. E. Keown, *Tetrahedron Lett.*, 1997, **38**, 5727; (*c*) C. S. Lee and C. J. Forsyth, *Tetrahedron Lett.*, 1996, **37**, 6449.

13 P. A. Clarke and K. Ermanis, *Org. Lett.*, 2012, **14**, 5550.

14 (*a*) H. Fuwa, K. Noto and M. Sasaki, *Org. Lett.*, 2011, **13**, 1820; (*b*) H. Fuwa, N. Ichinokawa, K. Noto and M. Sasaki, *J. Org. Chem.*, 2012, **77**, 2588.

15 See ESI† for details.

16 T. A. Halgren, *J. Comput. Chem.*, 1996, **17**, 490.

17 (*a*) A. D. Becke, *Phys. Rev. A: At., Mol., Opt. Phys.*, 1988, **38**, 3098; (*b*) C. Lee, W. Yang and R. G. Parr, *Phys. Rev. B*, 1988, **37**, 785.

18 (*a*) R. Krishnan, J. S. Binkley, R. Seeger and J. A. Pople, *J. Chem. Phys.*, 1980, **72**, 650; (*b*) P. M. W. Gill, B. G. Johnson, J. A. Pople and M. J. Frisch, *Chem. Phys. Lett.*, 1992, **197**, 499.

19 (*a*) D. J. Tannor, B. Marten, R. Murphy, R. A. Friesner, D. Sitkoff, A. Nicholls, M. Ringnalda, W. A. Goddard III and B. Honig, *J. Am. Chem. Soc.*, 1994, **116**, 11875; (*b*) B. Marten, K. Kim, C. Cortis, R. A. Friesner, R. B. Murphy, M. N. Ringnalda, D. Sitkoff and B. Honig, *J. Phys. Chem.*, 1996, **100**, 11775.

20 M. Pellicena, K. Krämer, P. Romea and F. Urpí, *Org. Lett.*, 2011, **13**, 5350.

21 I. Paterson and G. W. Haslett, *Org. Lett.*, 2013, **15**, 1338.

22 F. G. Bordwell and H. E. Fried, *J. Org. Chem.*, 1991, **56**, 4218.

23 H. Fuwa, *Heterocycles*, 2012, **85**, 1255.

24 Thioesters have previously been shown to exhibit characteristics similar to ketones: A. M. M. El-Asar, C. P. Nash and L. L. Ingraham, *Biochemistry*, 1982, **21**, 1972.

25 (*a*) K. B. Sawant and M. P. Jennings, *J. Org. Chem.*, 2006, **71**, 7911; (*b*) S. Chandrasekhar, T. Shyamsunder, S. J. Prakash, A. Prabhakar and B. Jagadeesh, *Tetrahedron Lett.*, 2006, **47**, 47; (*c*) C. Bressy, F. Allais and J. Cossy, *Synlett*, 2006, 3455; (*d*) R. W. Bates and P. Song, *Tetrahedron*, 2007, **63**, 4497; (*e*) M.-A. Hiebel, B. Pelotier and O. Piva, *Tetrahedron*, 2007, **63**, 7874; (*f*) N. Kawai, S. M. Hande and J. Uenishi, *Tetrahedron*, 2007, **63**, 9049; (*g*) J. S. Yadav, B. Padmavani, B. V. S. Reddy, C. Venugopal and A. B. Rao, *Synlett*, 2007, 2045; (*h*) H. Wang, B. J. Shuhler and M. Xian, *Synlett*, 2008, 2651; (*i*) G. Sabitha, P. Padmaja and J. S. Yadav, *Helv. Chim. Acta*, 2008, **91**, 2235; (*j*) K. Lee, K. H. Kim and J. Hong, *Org. Lett.*, 2009, **11**, 5202; (*k*) G. Kumaraswamy, G. Ramakrishna, P. Naresh, B. Jagadeesh and B. Sridhar, *J. Org. Chem.*, 2009, **74**, 8468; (*l*) J. D. More, *Synthesis*, 2010, 2419; (*m*) R. N. Kumar and H. M. Meshram, *Tetrahedron Lett.*, 2011, **52**, 1003; (*n*) T.-L. Ho, B. Tang, G. Ma and

P. Xu, *J. Chin. Chem. Soc.*, 2012, **59**, 455; (*o*) E. Stefan, A. P. Nalin and R. E. Taylor, *Tetrahedron*, 2013, **69**, 7706; (*p*) H. Yao, J. Ren and R. Tong, *Chem. Commun.*, 2013, **49**, 193; (*q*) S. B. Meruva, R. Mekala, A. Raghunadh, K. Raghavendra Rao, V. H. Dahanukar., T. V. Pratap, U. K. Syam Kumar and P. K. Dubey, *Tetrahedron Lett.*, 2014, **55**, 4739; (*r*) T. Rybak and D. G. Hall, *Org. Lett.*, 2015, **17**, 4156; (*s*) P. A. Clarke, N. M. Nasir, P. B. Sellars, A. M. Peter, C. A. Lawson and J. L. Burroughs, *Org. Biomol. Chem.*, 2016, **14**, 6840.

26 L. S. Liebeskind and J. Srogl, *J. Am. Chem. Soc.*, 2000, **122**, 11260.

27 R. Wittenberg, J. Srogl, M. Egi and L. S. Liebeskind, *Org. Lett.*, 2003, **5**, 3033.

6. Abbreviations

Ac	Acetyl
aq.	Aqueous
Ar (in NMR)	Aromatic proton signal
BHT	Butylated hydroxytoluene
Bn	Benzyl
BPTPI	benzene-fused-phthaloyl-piperidinonate
br	Broad
Bu	Butyl
cm^{-1}	Wavenumber
COSY	Correlation spectroscopy
CSA	Camphorsulfonic acid
CuDPP	Cu(I) diphenylphosphinate
CuTC	Copper(I)-thiophene-2-carboxylate
d	Doublet
d.r.	Diastereomeric ratio
DBU	1,8-Diazabicycloundec-7-ene
DCE	1,1-Dichloroethene
DCM	Dichloromethane
DEAD	Diethyl diazenedicarboxylate
DEPT	Distortionless enhancement by polarisation transfer
DFT	Density functional theory
DIBAL-H	Diisobutylaluminium hydride
DMAP	4-Dimethylaminopyridine
DMF	Dimethylformamide

DMP	Dess-Martin periodinane
DMSO	Dimethylsulfoxide
E^+	Electrophile
ee	Enantiomeric excess
eq.	Equivalents
ESI	Electrospray ionisation
Et	Ethyl
g	Gram (s)
GI_{50}	50% growth inhibition
h	Hour (s)
HDA	hetero-Diels–Alder
HFIP	Hexafluoro-2-propanol
HMBC	Heteronuclear multiple bond correlation
HMQC	Heteronuclear multiple quantum correlation
HPLC	High-performance liquid chromatography
Hz	Hertz
i-Pr	Isopropyl
IR	Infrared
J	Coupling constant in Hz
L	Literature
LC_{50}	Lethal Concentration, 50%
LDA	Lithium diisopropylamide
LHMDS	Lithium bis(trimethylsilyl)amide
LUMO	Lowest unoccupied molecular orbital
M	Molar

m	Multiplet
m/z	Mass to charge ratio
M^+	Molecular ion
Me	Methyl
mg	Milligram(s)
MHz	Mega Hertz
min	Minutes (s)
mL	Millilitre (s)
mmol	Millimole (s)
mol	Mole (s)
MOM	Methoxymethyl ether
MS	Mass spectrometry
Ms	Methanesulfonyl
MS	Molecular sieves (4Å)
MW	Microwave irradiation
n	Nano
*n*Bu	Normal-butyl
NMO	4-Methylmorpholine *N*-oxide
NMR	Nuclear magnetic resonance spectroscopy
NOE	Nuclear overhauser effect
p	Pentet
ppm	Parts per million
Py	Pyridine
q	Quartet
R	Undefined group

Rf	Retention factor
rt	Room temperature
s	Singlet
SAR	Structure–activity relationship
sat.	Saturated
t	Triplet
TBAF	Tetrabutylammonium fluoride
TBDPS	Tertiary-butyl(chloro)diphenylsilane
TBS	Tertiary-butyldimethylsilyl
*t*Bu	Tertiary-butyl
TEMPO	2,2,6,6-Tetramethyl-1-piperidinyloxy
TES	Triethylsilyl
Tf	Trifluoromethanesulfonyl
TFA	Trifluoroacetic acid
TFP	Tri(2-furyl)phosphine
THF	Tetrahydrofuran
TIPS	Triisopropylsilyl
TLC	Thin layer chromatography
TMEDA	N,N, N',N'-tetramethylethylenediamine
Ts	*p*-Toluenesulfonyl
UV	Ultraviolet
δ	Chemical shift
μ	Micro
*μ*L	Micro Liters
v	Vibration frequency (cm^{-1})

7. References

1. P. A. Searle and T. F. Molinski, *J. Am. Chem. Soc.*, 1995, **117**, 8126-8131.
2. J. Yin, K. Kouda, Y. Tezuka, Q. Le Tran, T. Miyahara, Y. J. Chen and S. Kadota, *Planta Med.*, 2004, **70**, 54-58.
3. T. F. Molinski, *Tetrahedron Lett.*, 1996, **37**, 7879-7880.
4. M. R. Gesinski and S. D. Rychnovsky, *J. Am. Chem. Soc.*, 2011, **133**, 9727-9729.
5. K. Lee, H. Kim and J. Hong, *Org. Lett.*, 2011, **13**, 2722-2725.
6. S. S. Palimkar, J. i. Uenishi and H. Ii, *J. Org. Chem.*, 2012, **77**, 388-399.
7. J.-F. Brazeau, A.-A. Guilbault, J. Kochuparampil, P. Mochirian and Y. Guindon, *Org. Lett.*, 2010, **12**, 36-39.
8. S. Raghavan and P. K. Samanta, *Org. Lett.*, 2012, **14**, 2346-2349.
9. P. A. Clarke and K. Ermanis, *Org. Lett.*, 2012, **14**, 5550-5553.
10. S. Chandrasekhar, T. Shyamsunder, S. J. Prakash, A. Prabhakar and B. Jagadeesh, *Tetrahedron Lett.*, 2006, **47**, 47-49.
11. C. Bressy, F. Allais and J. Cossy, *Synlett*, 2006, 3455-3456.
12. K. B. Sawant and M. P. Jennings, *J. Org. Chem.*, 2006, **71**, 7911-7914.
13. R. W. Bates and P. Song, *Tetrahedron*, 2007, **63**, 4497-4499.
14. J. S. Yadav, B. Padmavani, B. V. S. Reddy, C. Venugopal and A. B. Rao, *Synlett*, 2007, 2045-2048.
15. M.-A. Hiebel, B. Pelotier and O. Piva, *Tetrahedron*, 2007, **63**, 7874-7878.
16. N. Kawai, S. Mahadeo Hande and J. i. Uenishi, *Tetrahedron*, 2007, **63**, 9049-9056.
17. G. Sabitha, P. Padmaja and J. S. Yadav, *Helv. Chim. Acta*, 2008, **91**, 2235-2239.
18. H. Wang, B. J. Shuhler and M. Xian, *Synlett*, 2008, 2651-2654.
19. G. Kumaraswamy, G. Ramakrishna, P. Naresh, B. Jagadeesh and B. Sridhar, *J.*

Org. Chem., 2009, **74**, 8468-8471.

20. K. Lee, H. Kim and J. Hong, *Org. Lett.*, 2009, **11**, 5202-5205.
21. J. D. More, *s-Stuttgart*, 2010, 2419-2423.
22. M. Anada, T. Washio, Y. Watanabe, K. Takeda and S. Hashimoto, *Eur. J. Org. Chem.*, 2010, 6850-6854.
23. O. g. Karlubíková, M. Babjak and T. Gracza, *Tetrahedron*, 2011, **67**, 4980-4987.
24. L. Raffier, F. Izquierdo and O. Piva, *Synthesis-Stuttgart*, 2011, 4037-4044.
25. T. L. Ho, B. Tang, G. H. Ma and P. F. Xu, *J. Chin. Chem. Soc.*, 2012, **59**, 455-458.
26. R. N. Kumar and H. M. Meshram, *Tetrahedron Lett.*, 2011, **52**, 1003-1007.
27. H. Yao, J. Ren and R. Tong, *Chem. Commun.*, 2013, **49**, 193-195.
28. E. Stefan, A. P. Nalin and R. E. Taylor, *Tetrahedron*, 2013, **69**, 7706-7712.
29. J. Merad, P. Borkar, T. Bouyon Yenda, C. Roux, J.-M. Pons, J.-L. Parrain, O. Chuzel and C. Bressy, *Org. Lett.*, 2015, **17**, 2118-2121.
30. A. Zúñiga, M. Pérez, G. Zoila, A. Fall, G. Gómez and Y. Fall, *Synthesis of diospongin A, ent-diospongin A and C-5 epimer of diospongin B from tri-O-acetyl-D-glucal*, 2015.
31. T. Rybak and D. G. Hall, *Org. Lett.*, 2015, **17**, 4156-4159.
32. P. A. Clarke, N. M. Nasir, P. B. Sellars, A. M. Peter, C. A. Lawson and J. L. Burroughs, *Org. Biomol. Chem.*, 2016, **14**, 6840-6852.
33. Z. L. Li and R. B. Tong, *Synthesis-Stuttgart*, 2016, **48**, 1630-1636.
34. S. J. Gharpure, S. P. Mane, L. N. Nanda and M. K. Shukla, *Isr. J. Chem.*, 2016, **56**, 553-557.
35. J. i. Uenishi, M. Ohmi and A. Ueda, *Tetrahedron: Asymmetry*, 2005, **16**, 1299-1303.
36. N. Kawai, J.-M. Lagrange, M. Ohmi and J. i. Uenishi, *J. Org. Chem.*, 2006, **71**,

4530-4537.

37. N. Kawai, J.-M. Lagrange and J. i. Uenishi, *Eur. J. Org. Chem.*, 2007, 2808-2814.

38. J. i. Uenishi and M. Ohmi, *Angew. Chem. Int. Ed.*, 2005, **44**, 2756-2760.

39. J. K. Stille, *Angew. Chem. Int. Ed. (English)*, 1986, **25**, 508-524.

40. H. Fuwa, K. Noto and M. Sasaki, *Org. Lett.*, 2011, **13**, 1820-1823.

41. K. Ermanis, Y.-T. Hsiao, U. Kaya, A. Jeuken and P. A. Clarke, *Chem. Sci*, 2017, **8**, 482-490.

42. K. Ermanis, PhD thesis, University of York, 2014.

43. M. Pellicena, K. Krämer, P. Romea and F. Urpí, *Org. Lett.*, 2011, **13**, 5350-5353.

44. I. Paterson and G. W. Haslett, *Org. Lett.*, 2013, **15**, 1338-1341.

45. C. Einhorn and J.-L. Luche, *J. Organomet. Chem.*, 1987, **322**, 177-183.

46. G. Molle and P. Bauer, *J. Am. Chem. Soc.*, 1982, **104**, 3481-3487.

47. Y. Yu and L. S. Liebeskind, *J. Org. Chem.*, 2004, **69**, 3554-3557.

48. M. T. Crimmins and A. L. Choy, *J. Am. Chem. Soc.*, 1999, **121**, 5653-5660.

49. M. T. Crimmins, S. J. Kirincich, A. J. Wells and A. L. Choy, *Synth. Commun.*, 1998, **28**, 3675-3679.

50. P. Cazeau, F. Duboudin, F. Moulines, O. Babot and J. Dunogues, *Tetrahedron*, 1987, **43**, 2075-2088.

51. J.-M. Lin and B.-S. Liu, *Synth. Commun.*, 1997, **27**, 739-749.

52. H. O. House, L. J. Czuba, M. Gall and H. D. Olmstead, *J. Org. Chem.*, 1969, **34**, 2324-2336.

53. M. Teruaki, N. Koichi and B. Kazuo, *Chem. Lett.*, 1973, **2**, 1011-1014.

54. D. A. Evans, K. T. Chapman and E. M. Carreira, *J. Am. Chem. Soc.*, 1988, **110**, 3560-3578.

55. A. K. Saksena and P. Mangiaracina, *Tetrahedron Lett.*, 1983, **24**, 273-276.

56. D. A. Evans and K. T. Chapman, *Tetrahedron Lett.*, 1986, **27**, 5939-5942.

57. K.-M. Chen, G. E. Hardtmann, K. Prasad, O. Repič and M. J. Shapiro, *Tetrahedron Lett.*, 1987, **28**, 155-158.

58. K. Narasaka and F.-C. Pai, *Tetrahedron*, 1984, **40**, 2233-2238.

59. K. Voigtritter, S. Ghorai and B. H. Lipshutz, *J. Org. Chem.*, 2011, **76**, 4697-4702.

60. L. S. Liebeskind and J. Srogl, *J. Am. Chem. Soc.*, 2000, **122**, 11260-11261.

61. H. Fuwa, N. Ichinokawa, K. Noto and M. Sasaki, *J. Org. Chem.*, 2012, **77**, 2588-2607.

62. H. Tokuyama, S. Yokoshima, T. Yamashita, S. C. Lin, L. P. Li and T. Fukuyama, *J. Braz. Chem. Soc.*, 1998, **9**, 381-387.

63. R. Wittenberg, J. Srogl, M. Egi and L. S. Liebeskind, *Org. Lett.*, 2003, **5**, 3033-3035.

64. S. Hanessian, A. Tehim and P. Chen, *J. Org. Chem.*, 1993, **58**, 7768-7781.

65. A. M. M. El-Assar, C. P. Nash and L. L. Ingraham, *Biochemistry*, 1982, **21**, 1972-1976.

66. S. Chanthamath, S. Takaki, K. Shibatomi and S. Iwasa, *Angew. Chem. Int. Ed.*, 2013, **52**, 5818-5821.

67. R. H. Cichewicz, F. A. Valeriote and P. Crews, *Org. Lett.*, 2004, **6**, 1951-1954.

68. S. Sakemi, T. Ichiba, S. Kohmoto, G. Saucy and T. Higa, *J. Am. Chem. Soc.*, 1988, **110**, 4851-4853.

69. N. B. Perry, J. W. Blunt, M. H. G. Munro and L. K. Pannell, *J. Am. Chem. Soc.*, 1988, **110**, 4850-4851.

70. G. R. Pettit, J.-P. Xu, J.-C. Chapuis, R. K. Pettit, L. P. Tackett, D. L. Doubek, J. N. A. Hooper and J. M. Schmidt, *J. Med. Chem.*, 2004, **47**, 1149-1152.

71. X. Jiang, N. Williams and J. K. De Brabander, *Org. Lett.*, 2007, **9**, 227-230.

72. S. Kiren and L. J. Williams, *Org. Lett.*, 2005, **7**, 2905-2908.

73. X. Jiang, J. García-Fortanet and J. K. De Brabander, *J. Am. Chem. Soc.*, 2005, **127**, 11254-11255.

74. T. L. Simmons, E. Andrianasolo, K. McPhail, P. Flatt and W. H. Gerwick, *Mol. Cancer. Ther.*, 2005, **4**, 333-342.

75. S. Wan, F. Wu, J. C. Rech, M. E. Green, R. Balachandran, W. S. Horne, B. W. Day and P. E. Floreancig, *J. Am. Chem. Soc.*, 2011, **133**, 16668-16679.

76. X. Huang, N. Shao, A. Palani, R. Aslanian and A. Buevich, *Org. Lett.*, 2007, **9**, 2597-2600.

77. C. An, J. A. Jurica, S. P. Walsh, A. T. Hoye and A. B. Smith, *J. Org. Chem.*, 2013, **78**, 4278-4296.

78. L. E. Brown, Y. R. Landaverry, J. R. Davies, K. A. Milinkevich, S. Ast, J. S. Carlson, A. G. Oliver and J. P. Konopelski, *J. Org. Chem.*, 2009, **74**, 5405-5410.

79. M. T. Crimmins, J. M. Stevens and G. M. Schaaf, *Org. Lett.*, 2009, **11**, 3990-3993.

80. T. Watanabe, T. Imaizumi, T. Chinen, Y. Nagumo, M. Shibuya, T. Usui, N. Kanoh and Y. Iwabuchi, *Org. Lett.*, 2010, **12**, 1040-1043.

81. S. R. Byeon, H. Park, H. Kim and J. Hong, *Org. Lett.*, 2011, **13**, 5816-5819.

82. W. J. Buffham, N. A. Swain, S. L. Kostiuk, T. P. Gonçalves and D. C. Harrowven, *Eur. J. Org. Chem.*, 2012, 1217-1222.

83. J. C. Rech and P. E. Floreancig, *Org. Lett.*, 2005, **7**, 5175-5178.

84. M. Bielitza and J. Pietruszka, *Chem. Eur. J.*, 2013, **19**, 8300-8308.

85. A. B. Smith, J. A. Jurica and S. P. Walsh, *Org. Lett.*, 2008, **10**, 5625-5628.

86. S.-i. Uesugi, T. Watanabe, T. Imaizumi, Y. Ota, K. Yoshida, H. Ebisu, T. Chinen, Y. Nagumo, M. Shibuya, N. Kanoh, T. Usui and Y. Iwabuchi, *J. Org. Chem.*, 2015,

80, 12333-12350.

87. M. Bielitza and J. Pietruszka, *Synlett*, 2012, **23**, 1625-1628.

88. D. J. Kopecky and S. D. Rychnovsky, *J. Org. Chem.*, 2000, **65**, 191-198.

89. P. W. Erhardt and J. R. Proudfoot, in *Comprehensive Medicinal Chemistry II*, ed. D. J. Triggle, Elsevier, Oxford, 2007, pp. 29-96.

90. M. O. Faruk Khan, M. J. Deimling and A. Philip, *American Journal of Pharmaceutical Education*, 2011, **75**, 161.

91. X. Huang, N. Shao, A. Palani, R. Aslanian, A. Buevich, C. Seidel-Dugan and R. Huryk, *Tetrahedron Lett.*, 2008, **49**, 3592-3595.

92. X. Huang, N. Shao, R. Huryk, A. Palani, R. Aslanian and C. Seidel-Dugan, *Org. Lett.*, 2009, **11**, 867-870.

93. N. Shao, X. Huang, A. Palani, R. Aslanian, A. Buevich, J. Piwinski, R. Huryk and C. Seidel-Dugan, *Synthesis*, 2009, 2855-2872.

94. R. A. Mosey and P. E. Floreancig, *Nat. Prod. Rep.*, 2012, **29**, 980-995.

95. C.-Y. Wu, Y. Feng, E. R. Cardenas, N. Williams, P. E. Floreancig, J. K. De Brabander and M. G. Roth, *J. Am. Chem. Soc.*, 2012, **134**, 18998-19003.

96. Q. Liu, C. An, K. TenDyke, H. Cheng, Y. Y. Shen, A. T. Hoye and A. B. Smith, *J. Org. Chem.*, 2016, **81**, 1930-1942.

97. M. E. Green, J. C. Rech and P. E. Floreancig, *Org. Lett.*, 2005, **7**, 4117-4120.

98. H. Lachance, O. Marion and D. G. Hall, *Tetrahedron Lett.*, 2008, **49**, 6061-6064.

99. A. Pal, Z. Peng, P. T. Schuber Jr, B. A. Bhanu Prasad and W. G. Bornmann, *Tetrahedron Lett.*, 2013, **54**, 5555-5557.

100. N. Shangguan, S. Kiren and L. J. Williams, *Org. Lett.*, 2007, **9**, 1093-1096.

101. J. Dubac, A. Laporterie, H. Iloughmane, J. P. Pillot, G. Déléris and J. Dunoguès,

J. Organomet. Chem., 1985, **281**, 149-162.

102. D. Tzeng and W. P. Weber, *J. Org. Chem.*, 1981, **46**, 693-696.

103. E.-i. Negishi, F.-T. Luo and C. L. Rand, *Tetrahedron Lett.*, 1982, **23**, 27-30.

104. T. H. Chan and I. Fleming, *Synthesis*, 1979, 761-786.

105. N. Nishizono, Y. Akama, M. Agata, M. Sugo, Y. Yamaguchi and K. Oda, *Tetrahedron*, 2011, **67**, 358-363.

106. S. D. Rychnovsky and D. J. Skalitzky, *Tetrahedron Lett.*, 1990, **31**, 945-948.

107. D. A. Evans, D. L. Rieger and J. R. Gage, *Tetrahedron Lett.*, 1990, **31**, 7099-7100.

108. S. D. Rychnovsky, B. Rogers and G. Yang, *J. Org. Chem.*, 1993, **58**, 3511-3515.

109. G. Sabitha, C. Srinivas, T. R. Reddy, K. Yadagiri and J. S. Yadav, *Tetrahedron: Asymmetry*, 2011, **22**, 2124-2133.

110. A. K. Chatterjee, T.-L. Choi, D. P. Sanders and R. H. Grubbs, *J. Am. Chem. Soc.*, 2003, **125**, 11360-11370.

111. M. Sailer, K. I. Dubicki and J. L. Sorensen, *Synthesis*, 2015, **47**, 79-82.

112. G. Himbert and S. Kosack, *Chem. Ber.*, 1988, **121**, 2163-2170.

113. Z. Cai, N. Yongpruksa and M. Harmata, *Org. Lett.*, 2012, **14**, 1661-1663.

114. Y. Shen and J. Zheng, *J. Fluorine Chem.*, 1987, **35**, 513-521.

115. C. Palomo, M. Oiarbide and J. M. Garcia, *Chem. Soc. Rev.*, 2004, **33**, 65-75.

116. B. List, R. A. Lerner and C. F. Barbas, *J. Am. Chem. Soc.*, 2000, **122**, 2395-2396.

117. K. Sakthivel, W. Notz, T. Bui and C. F. Barbas, *J. Am. Chem. Soc.*, 2001, **123**, 5260-5267.

118. Z. G. Hajos and D. R. Parrish, *J. Org. Chem.*, 1974, **39**, 1615-1621.

119. U. Eder, G. Sauer and R. Wiechert, *Angew. Chem. Int. Ed. Engl.*, 1971, **10**, 496-497.

120. M. E. Jung, *Tetrahedron*, 1976, **32**, 3-31.

121. K. L. Brown, L. Damm, J. D. Dunitz, A. Eschenmoser, R. Hobi and C. Kratky, *Helv. Chim. Acta*, 1978, **61**, 3108-3135.

122. C. Puchot, O. Samuel, E. Dunach, S. Zhao, C. Agami and H. B. Kagan, *J. Am. Chem. Soc.*, 1986, **108**, 2353-2357.

123. D. Rajagopal, M. S. Moni, S. Subramanian and S. Swaminathan, *Tetrahedron: Asymmetry*, 1999, **10**, 1631-1634.

124. S. Bahmanyar and K. N. Houk, *J. Am. Chem. Soc.*, 2001, **123**, 11273-11283.

125. S. Bahmanyar, K. N. Houk, H. J. Martin and B. List, *J. Am. Chem. Soc.*, 2003, **125**, 2475-2479.

126. B. List, L. Hoang and H. J. Martin, *PNAS*, 2004, **101**, 5839-5842.

127. T. D. Machajewski and C.-H. Wong, *Angew. Chem. Int. Ed.*, 2000, **39**, 1352-1375.

128. S. Bahmanyar and K. N. Houk, *J. Am. Chem. Soc.*, 2001, **123**, 12911-12912.

129. D. C. Rideout and R. Breslow, *J. Am. Chem. Soc.*, 1980, **102**, 7816-7817.

130. R. Breslow, *Acc. Chem. Res.*, 1991, **24**, 159-164.

131. A. I. Nyberg, A. Usano and P. M. Pihko, *Synlett*, 2004, 1891-1896.

132. P. M. Pihko, K. M. Laurikainen, A. Usano, A. I. Nyberg and J. A. Kaavi, *Tetrahedron*, 2006, **62**, 317-328.

133. N. Zotova, A. Franzke, A. Armstrong and D. G. Blackmond, *J. Am. Chem. Soc.*, 2007, **129**, 15100-15101.

134. T. J. Dickerson and K. D. Janda, *J. Am. Chem. Soc.*, 2002, **124**, 3220-3221.

135. X. Zhu, F. Tanaka, Y. Hu, A. Heine, R. Fuller, G. Zhong, A. J. Olson, R. A. Lerner, C. F. Barbas and I. A. Wilson, *J. Mol. Biol.*, 2004, **343**, 1269-1280.

136. N. Mase, Y. Nakai, N. Ohara, H. Yoda, K. Takabe, F. Tanaka and C. F. Barbas, *J.*

Am. Chem. Soc., 2006, **128**, 734-735.

137. M. Nakadai, S. Saito and H. Yamamoto, *Tetrahedron*, 2002, **58**, 8167-8177.

138. N. Mase, F. Tanaka and C. F. Barbas, *Angew. Chem. Int. Ed.*, 2004, **43**, 2420-2423.

139. Y. Hayashi, T. Sumiya, J. Takahashi, H. Gotoh, T. Urushima and M. Shoji, *Angew. Chem. Int. Ed.*, 2006, **45**, 958-961.

140. Y. Hayashi, *Angew. Chem. Int. Ed.*, 2006, **45**, 8103-8104.

141. L. Burroughs, M. E. Vale, J. A. R. Gilks, H. Forintos, C. J. Hayes and P. A. Clarke, *Chem. Commun.*, 2010, **46**, 4776-4778.

142. L. Burroughs, P. A. Clarke, H. Forintos, J. A. R. Gilks, C. J. Hayes, M. E. Vale, W. Wade and M. Zbytniewski, *Org. Biomol. Chem.*, 2012, **10**, 1565-1570.

143. A. B. Northrup, I. K. Mangion, F. Hettche and D. W. C. MacMillan, *Angew. Chem. Int. Ed.*, 2004, **43**, 2152-2154.

144. A. B. Northrup and D. W. C. MacMillan, *Science*, 2004, **305**, 1752-1755.

145. A. Cordova, M. Engqvist, I. Ibrahem, J. Casas and H. Sunden, *Chem. Commun.*, 2005, 2047-2049.

146. S. Pizzarello and A. L. Weber, *Science*, 2004, **303**, 1151-1151.

147. A. Córdova, I. Ibrahem, J. Casas, H. Sundén, M. Engqvist and E. Reyes, *Chem. Eur. J.*, 2005, **11**, 4772-4784.

148. J. Kofoed, J.-L. Reymond and T. Darbre, *Org. Biomol. Chem.*, 2005, **3**, 1850-1855.

149. A. P. Brogan, T. J. Dickerson and K. D. Janda, *Angew. Chem. Int. Ed.*, 2006, **45**, 8100-8102.

150. L. Burroughs, PhD thesis, University of York, 2011.

151. R. Martinez, L. Berbegal, G. Guillena and D. J. Ramon, *Green Chem.*, 2016, **18**,

1724-1730.

152. W. Sharp, MSc thesis, University of York, 2014.

153. S. S. Chimni, S. Singh and A. Kumar, *Tetrahedron: Asymmetry*, 2009, **20**, 1722-1724.

154. C. J. Rogers, T. J. Dickerson, A. P. Brogan and K. D. Janda, *J. Org. Chem.*, 2005, **70**, 3705-3708.

155. E. Airiau, T. Spangenberg, N. Girard, B. Breit and A. Mann, *Org. Lett.*, 2010, **12**, 528-531.

156. I. Paterson, M. P. Housden, C. J. Cordier, P. M. Burton, F. A. Muhlthau and O. Loiseleur, *Org. Biomol. Chem.*, 2015, **13**, 5716-5733.

157. R. Haraguchi, Z. Ikeda, A. Ooguri and S. Matsubara, *Tetrahedron*, 2015, **71**, 8830-8837.

158. S. Ito, A. Hayashi, H. Komai, H. Yamaguchi, Y. Kubota and M. Asami, *Tetrahedron*, 2011, **67**, 2081-2089.

159. S. Masson, M. Saquet and A. Thuillier, *Tetrahedron*, 1977, **33**, 2949-2954.

160. T. Bach, *Liehigs Ann.* , 1995, 855-865.

161. C. M. Crudden and H. Alper, *J. Org. Chem.*, 1995, **60**, 5579-5587.

162. S. M. Soria-Castro and A. B. Peñéñory, *Beilstein J. Org. Chem.*, 2013, **9**, 467-475.

163. X. Wu, Z. Jiang, H.-M. Shen and Y. Lu, *Adv. Synth. Catal.*, 2007, **349**, 812-816.

164. H. Yang and R. G. Carter, *Org. Lett.*, 2008, **10**, 4649-4652.

165. S. Hu, J. Li, J. Xiang, J. Pan, S. Luo and J.-P. Cheng, *J. Am. Chem. Soc.*, 2010, **132**, 7216-7228.